# Genetic and environmental factors affecting Alzheimer's disease pathogenic mechanism: the role of sirtuins

## Thesis

# Genetic and environmental factors affecting Alzheimer's disease pathogenic mechanism: the role of sirtuins

**Letizia Polito**

Thesis submitted for the degree of Doctor of Philosophy at the Open University of London, UK

Discipline of Life and Biomolecular Sciences

Affiliated Research Centre:
Istituto di Ricerche Farmacologiche Mario Negri

**Submitted: September 2011**

Date of Submission: 30 September 2011
Date of Award: 28 February 2012

**ABSTRACT**

Alzheimer's disease (AD) is the leading cause of senile dementia and the current lack of effective treatments provides a strong incentive for an improved therapeutic strategy. In particular, non-pharmacological treatments, such as calorie restriction (CR), were shown to be useful in delaying or preventing AD onset. This has given insight into the molecular pathways involved.

Sirtuins (SIRT1-7) are evolutionary conserved enzymes that modulate life expectancy in simple organisms. In mammals, sirtuins are involved in pathways linked to age-related diseases, such as AD. In particular, they seem to be the molecular effectors of some beneficial effects mediated by external stimuli such as CR and physical activity.

This thesis aims at investigating, for the first time, the involvement of all 7 sirtuins in AD. The relevance of sirtuin gene variation to AD risk was assessed by a combined mutation screening and case-control genetic study design. Sirtuin expression levels were also assessed in a transgenic mouse model of AD (APP23 mice) and within the application of a non-pharmacological approach (environmental enrichment-EE). Finally, the possible role of SIRT1 in AD pathogenesis was better elucidated through *in vitro* studies.

Overall, *in vitro* studies confirmed the neuroprotective role of SIRT1 activator resveratrol in etiopathological contexts related to AD. Moreover, genetic studies have highlighted *SIRT2* could be involved in modulating AD etiology. In particular, a common polymorphism in *SIRT2* could be a weak genetic risk factor for AD. Finally, *in vivo* studies confirmed the beneficial effects of an EE protocol in delaying AD onset. However, despite sirtuin involvement in other environmental paradigms, no apparent modulation was registered under EE.

## PUBLICATIONS ARISING FROM THIS WORK

1: Albani D, Polito L, Forloni G. Sirtuins as novel targets for Alzheimer's disease and other neurodegenerative disorders: experimental and genetic evidence. *J Alzheimers Dis*. 2010; 19(1):11-26. Review.

2: Polito L, Kehoe PG, Forloni G, Albani D. The molecular genetics of sirtuins: association with human longevity and age-related diseases. *Int J Mol Epidemiol Genet*. 2010; 1(3):214-25. Review.

3: Albani D[1], Polito L[1], Batelli S, De Mauro S, Fracasso C, Martelli G, Colombo L, Manzoni C, Salmona M, Caccia S, Negro A, Forloni G. The SIRT1 activator resveratrol protects SK-N-BE cells from oxidative stress and against toxicity caused by alpha-synuclein or amyloid-beta (1-42) peptide. *J Neurochem*. 2009; 110(5):1445-56.

A manuscript comprising the results described in chapters 3 and 4 is in preparation.

**ACKNOWLEDGMENTS**

I owe my deepest gratitude to dr. Patrick Kehoe for his supervision, advice and guidance during my studies. He definitely enriched my growth as a student and a researcher. His involvement with his originality has triggered and nourished my intellectual maturity that I will benefit from, for a long time to come.

I thank dr. Gianluigi Forloni for giving me the freedom and flexibility to pursue what interested me in research, and enabling me of independent scientific thinking, research and writing.

I am grateful to Professor Silvio Garattini and dr. Enrico Garattini for providing me with an extraordinary opportunity to pursue my Ph.D in an enriched environment of diverse research fields.

I also thank dr. Diego Albani for the valuable suggestions that he gave me during my studies.

I am very grateful to all my lab-mates for providing their help and support; in particular to Alessandra Signorini, Marta Tunesi, Eleonora Ateri, Serena Rodilossi, Gloria Biella, Annalisa Davin, Ilaria Vitali, and Jessica Grigoletto. Their great companionship made these four years an easy sail for me.

Special thanks also to all my friends, especially to Stefania, Matteo, Melissa, Salvo, Irene, Fabio, Simona, Valeria and Elena, for their support in these four years and to have made this journey fun and memorable. At last, I thank my beloved Edoardo for the beautiful time spent together and for his love, understanding and endless support through the duration of my studies.

I owe my aspirations and my strength to pursue them, to the selfless love, support and encouragement from my parents. Thank you for everything.

## CONTENTS

## LIST OF THE MAIN ABBREVIATIONS

| | |
|---|---|
| 3-MA | 3-Methyladenine |
| ABCA7 | ATP-Binding Cassette sub-family A member 7 |
| AD | Alzheimer's Disease |
| AFM | Atomic Force Microscopy |
| ANOVA | Analysis of Variance |
| APOE | Apolipoprotein E |
| APP | Amyloid Precursor Protein |
| AU | Arbitrary Unit |
| Aβ | Amyloid β |
| BDNF | Brain Derived Neurotrophic Factor |
| BIN1 | Bridging Integrator Protein 1 |
| CAA | Cerebral Amyloid Angiopathy |
| CDK | Cyclin Dependent Kinase |
| CI | Confidence Interval |
| CLU | Clusterin |
| CR | Calorie Restriction |
| CR1 | Complement Receptor 1 |
| CT | Control |
| CVD | Cerebrovascular Disease |
| DCFH-DA | 2'-7'-Dichlorofluorescein Diacetate |
| dHPLC | denaturing High Performance Liquid Chromatography |
| DMEM | Dulbecco's Modified Eagle's Medium |
| DMSO | Dimethylsulfoxide |
| DSM | Diagnostic and Statistical Manual of Mental Disorders |
| EDTA | Ethylenediaminetetraacetic acid |
| EE | Environmental Enrichment |
| ELISA | Enzyme-Linked ImmunoSorbent Assay |
| EOAD | Early Onset Alzheimer's Disease |
| eQTL | expression Quantitative Trait Locus |
| FAD | Familiar Alzheimer's Disease |
| FTD | Frontotemporal Disease |
| GDH | Glutamate dehydrogenase |
| gDNA | Genomic Deoxyribonucleic Acid |
| GWAs | Genome Wide Association studies |

| | |
|---|---|
| $H_2O_2$ | Hydrogen Peroxyde |
| HDAC | Histone Deacetylase Enzymes |
| HMP | the International HapMap Project |
| HST | Homologues of SIR2 proteins |
| IC | Immunocitochemistry |
| ICD | International Classifications of Diseases |
| IH | Immunohistochemistry |
| KO | Knock-out |
| LC3 | microtubule-associated protein 1 Light Chain 3 |
| LD | Linkage Disequilibrium |
| LOAD | Late Onset Alzheimer's Disease |
| LTP | Long Term Potentiation |
| MAF | Minor Allele Frequency |
| MAPT | Microtubule-Associated Protein Tau |
| MCI | Mild Cognitive Impairment |
| MMSE | Mini Mental State Examination |
| MRI | Magnetic Resonance Imaging |
| MWM | Morris Water Maze |
| NAD | Nicotinamide Adenine Dinucleotide |
| NAM | Nicotinamide |
| NCBI | the National Centre of Biotechnology Information |
| NFTs | Neurofibrillary Tangles |
| NF-κB | Nuclear Factor Kappa β |
| NINCDS-ADRDA | National Institute of Neurological and Communicative Disorders and Stroke and Alzheimer 's disease and Related Disorders Association |
| NMDA | N-Methyl-D-aspartate |
| NO | nitric oxygen |
| OAADPr | O-acetyl-ADP ribose |
| OR | Odds ratio |
| PA | Physical Activity |
| PBS | Phosphate Buffer Saline |
| PCR | Polymerase Chain Reaction |
| PET | Positron Emission Tomography |
| PHFs | Paired Helical Filaments |
| PICALM | Phosphatidyl Inositol-binding Clathrin Assembly Protein |
| PSEN | Presenilin |

| | |
|---|---|
| p-tau | phosphorylated tau |
| RA | Retinoic Acid |
| rDNA | ribosomal DNA |
| RES | Resveratrol |
| ROS | Reactive Oxygen Species |
| RT-PCR | Real Time-PCR |
| SAD | Sporadic Alzheimer's Disease |
| SEM | Standard Error of the Mean |
| SF | straight filament |
| SIR2 | Silent mating type Information Regulation 2 |
| siRNA | small interfering RNA |
| SNP | Single Nucleotide Polymorphism |
| SPs | Senile Plaques |
| STACs | Sirtuin Activating Compounds |
| T2D | Type 2 Diabetes |
| tagSNP | tagging SNP |
| TBI | Traumatic Brain Injury |
| TG-EEs | Transgenic mice in enriched cages |
| TG-SHs | Transgenic mice in standard cages |
| TSI | Toscani in Italia |
| VaD | Vascular Dementia |
| vORT | visual Object Recognition Test |
| WB | Western Blotting |
| WT-EEs | Wild-type mice in enriched cages |
| WT-SHs | Wild-type mice in standard cages |

## LIST OF TABLES

## LIST OF FIGURES

# *CHAPTER 1:*

# *GENERAL INTRODUCTION*

# 1.1. ALZHEIMER'S DISEASE

Alzheimer's disease (AD) is the most common cause of senile dementia accounting for 60-70% of all dementia cases (Barker et al., 2002). AD bears the name of the Bavarian psychiatrist Alois Alzheimer who reported the first description of this dementing illness in 1906. He documented a case of a woman in her fifties who had shown progressive cognitive impairment pertaining to memory, language, and social interaction. After her death, Alzheimer stained sections from the autopsied brain and discovered the presence of "miliar foci, which are caused by deposition of a peculiar substance in the cortex" (now recognized as neuritic or senile plaques) and "very peculiar changes in the neurofibrils" (now recognized as neurofibrillary tangles) (Möller and Graeber, 1998). These two brain features are now core determinants of the gold standard of *post mortem* AD diagnosis. Although dr. Alzheimer's discovery, it was not until the 1970's, when neurological studies became more widespread and common, that AD became more formally accepted as a major disease in its own right and not just a general part of ageing as had been originally thought.

## *Global dementia prevalence*

The last estimate of global dementia prevalence published in the World Alzheimer Report released in 2009 (Alzheimer's Disease International, 2009), assessed that 35.6 million people worldwide would have been living with dementia in 2010 and that this number will almost double every 20 years, rising to 65.7 million in 2030 and 115.4 million in 2050. According to the report, much of the expected increase in the number of demented people will be attributed to low and middle income countries (LAMIC - parts of Asia, Africa and

South America). In 2010, 57.7% of all people with dementia lived in LAMIC, rising to 63.4% in 2030 and 70.5% in 2050. This expected increase can be explained by a longer life expectancy in these regions as a result of better healthcare. Also developed countries (HIC-high income countries) will continue to experience increases in the number of people with dementia. Over the next 20 years, it is forecast a 40% increase in demented people in Europe, 63% in North America, 77% in the southern Latin America, 89% in the developed Asia Pacific countries. This predicted growth compares with 117% growth in east Asia, 107% in south Asia, 134-146% in the rest of Latin America, and 125% in North Africa and the Middle East (Alzheimer's Disease International, 2009).

Alongside the anticipated rises in the number of patients, there is and will continue to be a natural escalation in the cost of caring for this increasing number of demented people. As such dementia will be declared a global health priority. A World Health Organization (WHO) report estimated that dementia contributed 11.2% of years spent living with a disability in people over 60 years old, more than stroke, cardiovascular disease, and cancer (World Health Organization, 2003). Due to the prevalence of AD amongst other forms of dementia, AD in its own right is likely to become one of the most important global public health issues for the foreseeable future.

## 1.1.1. CLINICAL FEATURES OF ALZHEIMER'S DISEASE

### *1.1.1.1. Symptomatology*

Although AD is recognised to have a number of pathological facets including the involvement of numerous biochemical pathways, common clinical features are recognised during the progress of the disease. AD typically begins with deterioration of episodic memory. At this stage the patients suffer from forgetfulness or confusion and have difficulties to remember recently learned tasks. Apathy and depression are also common early symptoms of the disease. Normally these symptoms are very mild and the presence of the disease may neither be apparent to the person experiencing the symptoms nor to his relatives or the difficulties experienced are thought to be the result of some other causes. Later symptoms include impaired judgment, disorientation, behaviour changes and difficulty in speaking, swallowing and walking (Isik, 2010). In the latest stages of the disease, people become bed-bound and wholly reliant on caregivers. On average, people with AD generally live for 8 to 10 years after diagnosis, and in some cases AD can last as long as 20 years or more. Death is usually caused by secondary pathologies; in fact AD makes people more vulnerable to infections such as pneumonia.

### *1.1.1.2. Diagnosis*

There are two stages to the diagnosis of AD: what is often termed the clinical diagnosis, usually referring to while people are still alive, and the *post mortem* diagnosis which does not always occur but is the only means to definitely confirm the presence of AD for the dementia in question. The clinical diagnosis is often based on international criteria such as the NINCDS-ADRDA criteria (National Institute of Neurological and Communicative Disorders and Stroke and Alzheimer 's disease and Related Disorders Association) (McKhann et al., 1984). These criteria are actually research-based criteria and link clinical features to neuropathology and provide a diagnosis that distinguishes patients who have possible, probable and eventually definite AD (McKhann et al., 1984). As mentioned, definite AD diagnosis is only attributable *post mortem* requiring also neuropathological evidence.

A diagnosis of probable AD is made by clinical examination and confirmed by neuropsychological tests. A detailed history of the type and course of symptoms is taken from the patient or another source (e.g. care giver) to assess whether there is cognitive impairment. Supportive features of AD include progressive deterioration of language, praxis and visual recognition, with impaired activities of daily living (social, occupational, or other instrumental functions) or a positive family history of AD. Neuropsychological testing can help to highlight objective signs of memory disturbance in early cases.

NINCDS-ADRDA criteria, written 27 years ago, have been revised over time. In particular, there are ongoing efforts to address two crucial shortcomings in AD diagnosis: 1) to improve sensitivity and specificity in distinguishing between AD and other forms of dementia, 2) to detect AD in a presymptomatic stage.

Diagnosis of AD at the preclinical stage will be vital towards the successful discovery of disease-modifying treatments. Currently there is a large effort to discover biomarkers that can be measured in for example, blood or cerebrospinal fluid that will allow the detection

of early stages of the disease. Such biomarkers could also offer valuable tools in clinical trials and potentially in clinical practice as they could allow better monitoring of disease progression and the effectiveness of therapeutic intervention and reduce the likelihood of misdiagnosis of the disease (Aluise et al., 2008). New criteria for earlier diagnosis of AD, developed in 2007 which are now being validated, retain the requirement for the presence of objective memory deficits but do not include a requirement that disability must already be present (Dubois et al., 2007). These new criteria also require evidence of at least one biomarker consistent with an AD diagnosis [e.g. brain atrophy detected by high-resolution magnetic resonance imaging (MRI), functional alterations such as temporoparietal cortical hypometabolism detected by positron emission tomography (PET) and/or abnormality of cerebrospinal fluid markers] to support the clinical diagnosis of preclinical AD (Dubois et al., 2007).

PAGE 21 HAS BEEN EXCLUDED ON INSTRUCTION FROM THE UNIVERSITY

### *1.1.1.3. Stages of AD*

In addition to the attempts to identify preclinical forms of AD, newly proposed criteria also suggest a revision to the possible diagnostic categories of AD from the possible, probable and definite categories proposed through the NINCDS-ADRDA criteria. Furthermore, these new proposed guidelines for AD diagnosis also involved three stages of AD but in this case they are preclinical, mild cognitive impairment (MCI), and clinical AD (Dubois et al., 2007).

The term MCI was introduced in the 1990s and is used to refer to patients with early clinical signs of AD who did not yet fulfil the criteria of dementia. MCI is often subdivided into different subtypes: the amnestic variant, characterized by dysfunction in memory with retention of normal cognitive abilities in judgment, reasoning, and perception; the non-amnestic MCI, which involves impairment in cognitive functions related to attention, perception, and language, predominates over deficits in memory. Amnestic MCI has been suggested to constitute a transitional stage between normal ageing and AD (Petersen, 2004). About two-third of all patients with amnestic MCI harbour the pathological features of AD and develop the clinical syndrome of AD within 5 years, whereas the remaining one-third have non-progressive or very slowly progressive causes of cognitive impairment (e.g. depression, age-related cognitive impairment) (Petersen, 2004; Visser et al., 2005).

Current thinking is that the earliest manifestations of AD-related changes in the brain begin years, perhaps decades, before any obvious symptoms occur. It is hoped that these earliest changes and this long preclinical stage could be identified and characterized by measurable changes in biomarkers before any observable disruptions in memory, thinking or behaviour. However, as yet no biomarkers fulfil the necessary requirements in such a context and as such the proposed diagnostic criteria have yet to be validated.

Until this is resolved, the use of NINCDS-ADRDA criteria is likely to continue for many specialist memory centres; however, in primary care, where there is arguably less specialist

knowledge, diagnosis of AD is also done using standard criteria for the classification of mental disorders such as DSM-IV and the international classification of diseases (ICD-10) diagnostic criteria.

## 1.1.2. NEUROPATHOLOGY

The neuropathology of AD is characterized by a number of features; however, the two main hallmarks, which figure heavily in the *post mortem* diagnosis of AD, are: senile plaques (SPs) and neurofibrillary tangles (NFTs).

### *1.1.2.1. Senile plaques*

SPs are spherical lesions found in the neocortex, hippocampus and other subcortical regions, measuring up to 100 μm. SPs, also known as neuritic plaques (NPs), have a central core of extracellular amyloid surrounded by a halo of dystrophic neuronal processes with neurofibrillary degeneration. The amyloid core of these plaques has a fibrillary fine structure with a β-sheet conformation as identified by electron microscopy. NPs can also be recognized by light microscopy with stains such as Congo Red and Thioflavin-S, like other amyloids. Furthermore, in areas surrounding NPs, there is also gliosis with hypertrophy and alteration of the morphology, as well the proliferation of astrocytes and microglia (Heneka and O'Banion, 2007).

In mid-1980s researchers succeeded in purifying plaque cores and identified a small peptide called β-amyloid peptide (Aβ), the major amyloid component of SPs (Masters et al., 1985). This peptide was later found to be derived from a larger protein called amyloid precursor protein (APP), which is a normal component of neurons (McKenzie et al., 1996). Besides NPs, Aβ can be deposited and aggregated in a non-β-sheet (non fibrillar) conformation, in diffuse non-fibrillar deposits (i.e. diffuse plaques). Moreover, Aβ aggregates are found in blood vessels walls independently of deposition in the neuropil (which occurs in many cases of AD) in what are called cerebrovascular plaques or cerebral amyloid angiopathy (CAA) (Smith and Greenberg, 2009).

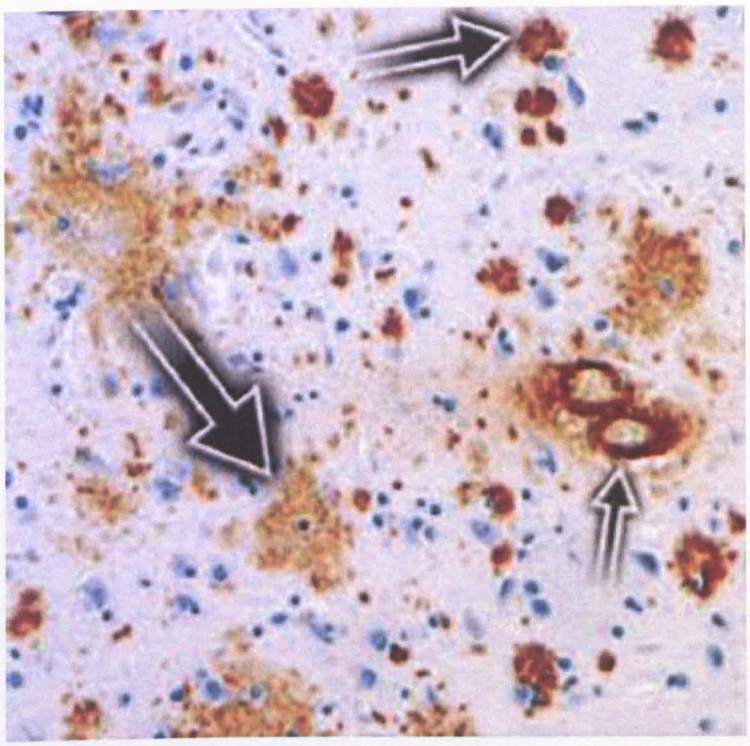

**FIGURE 1.2. Senile plaques.**

*Taken from* (Holtzman et al., 2011).

*Anti-Aβ antibody immunohistochemical staining of sections of brain tissue taken from an AD brain shows diffuse plaques containing Aβ (large arrow), compact plaques (medium size arrow), and CAA (smallest arrow) (100X magnification).*

### *1.1.2.2. Neurofibrillary tangles*

NFTs are deposits of protein filaments in the neuronal cell body. Similar deposits are present in the dystrophic processes that surround the amyloid core of SPs and in dendrites (i.e. neuropil threads). These aggregates have a high β-sheet content and ultrastructurally appear as paired helical filaments (PHFs) (Lee et al., 1991).

The discovery that the protein component of NFTs and neuropil threads was a hyperphosphorylated, aggregated form of the microtubule-binding protein tau was made

during the 1980s (Kosik et al., 1986; Grundke-Iqbal et al., 1986). NFTs appear first in the entorhinal cortex and hippocampus and then spread to the neocortex.

Most cases of AD show a combination of SPs and NFTs, but there are rarer collections of cases where there have been reports of a predominance of one or the other marker. NFTs are also found in other neurodegenerative diseases besides AD, particularly in frontotemporal dementia (FTD).

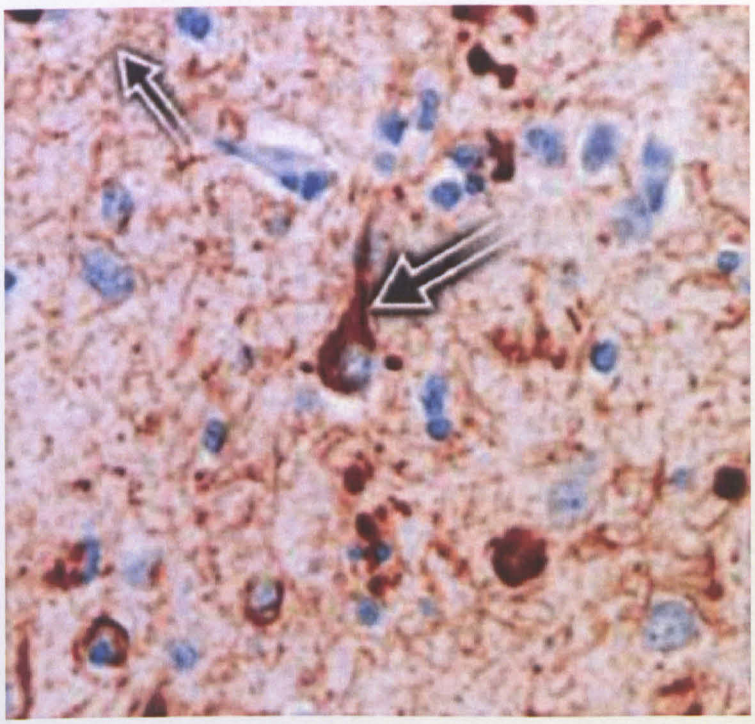

**FIGURE 1.3. Neurofibrillary tangles.**

*Taken from* (Holtzman et al., 2011).

*Anti–phospho-tau antibody immunohistochemical staining reveals hyperphosphorylated tau accumulation in neuronal cell bodies (large arrow) and throughout the neuropil in neuronal processes called neuropil threads (smaller arrow; 200X magnification).*

### *1.1.2.3. Other neuropathological hallmarks*

In addition to SPs and NFTs, other neuropathological hallmarks of AD include loss of synapses and selective neuronal cell death.

Neurons that are particularly vulnerable in AD include those in layer II of the entorhinal cortex, the pyramidal layers of the hippocampus, and certain areas of the temporal, parietal, and frontal neocortex (Geula, 1998). AD brain tissue from patients with an advanced form of the disease display high levels of atrophy of both neocortex and subcortical regions (in particular atrophy of the hippocampus), as well as enlargement of the ventricles.

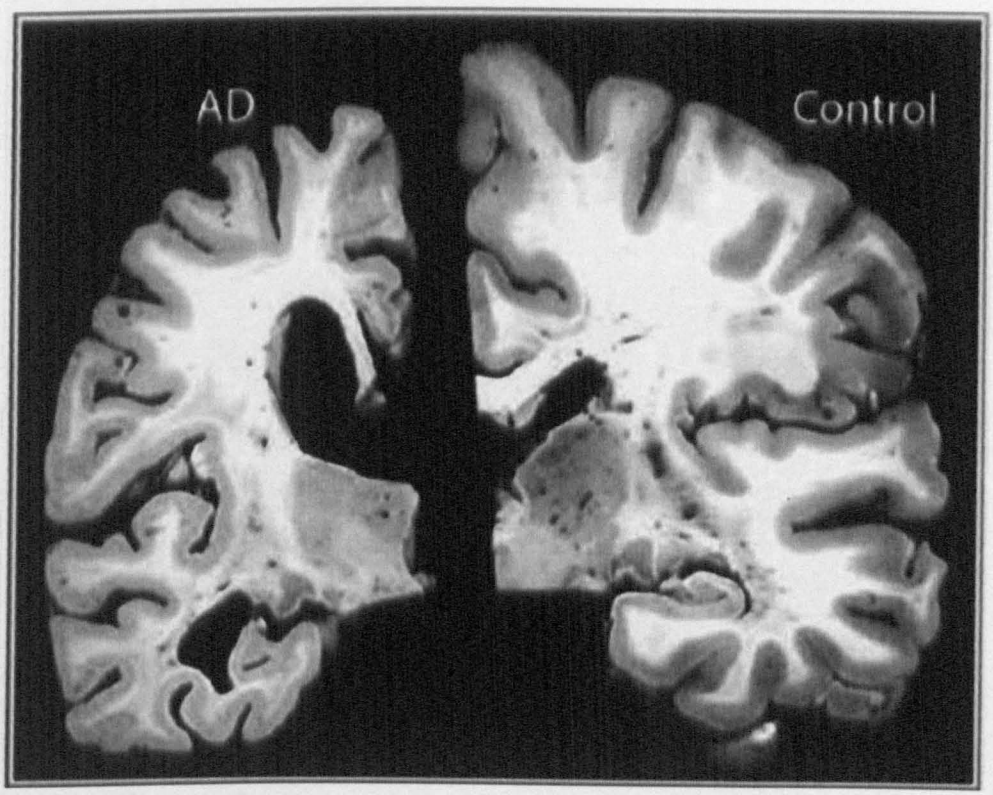


**FIGURE 1.4. Brain atrophy.**

*Taken from* (Holtzman et al., 2011).

*Coronal slices of a post mortem brain taken from an AD case (left) compared with that of cognitively normal individual (right) reveal severe brain atrophy in AD.*

Inflammation is another pathological feature of AD. Indeed, in AD there is evidence of a chronic neuroinflammatory process and the inflammatory mediators IL-1, IL-6, IL-10 and TNFα have all been implicated (Glass et al., 2010; McGeer and McGeer, 1996).

Another important but often-overlooked facet of AD is the occurrence of cerebrovascular diseases (CVDs), some of which are thought to occur as some of the earliest pathologies of AD (Murray et al., 2011). Indeed, high levels of co-morbidity of CVD often produce other symptoms which are more typically seen in forms of vascular dementia (VaD). As such these co-morbidities complicate the diagnosis of AD and commonly result in a diagnosis of a mixed dementia (Jellinger, 2008).

### 1.1.3. EPIDEMIOLOGY

Most often, AD is diagnosed amongst people over 65 years of age and thus it is commonly known as late onset AD (LOAD). LOAD is also referred as "sporadic" (SAD) because there is no evidence of a genetic underpinning or of a known family history of the disease. For LOAD no causal factors have still been found but a number of factors that can increase the risk of developing the disease (i.e. risk factors) have now been identified. In addition to LOAD, a small percentage of AD cases (less than 5%) occurs within families (FAD) and is inherited in an autosomal dominant fashion. In these families, dementia onset is usually between the ages of 30 and 60 years (early onset AD, EOAD) and can occur in multiple members of the same family and across numerous generations. Despite the different clinical presentations and the often more rapid form of progression seen in FAD (Lippa et al., 1996), brain tissue from both FAD and SAD are almost indistinguishable when examined *post mortem* for distributions of the various pathologic features of AD (e.g. SPs, NFTs, neuronal loss). The similarity in end-stage neuropathology provides evidence for a final common pathophysiologic pathway in AD.

#### *1.1.3.1. Non genetic risk factors*

Although the etiology of SAD is still uncertain, several risk factors have been proposed.

- Age - ageing is the well-accepted risk factor for AD. Indeed, AD prevalence increase almost exponentially in elderly people, being below 1% in individuals aged 60-64 years and between 24% and 33% in people older than 85 years, in the Western world (Ferri et al., 2006). As we age, repair mechanisms that counteract

insults are less efficient and clinical conditions that are risk factors for the disease tend to increase (such as diabetes, elevated cholesterol and being overweight);

- Vascular risk factors - midlife hypertension (Qiu et al., 2005), hypercholesterolemia (Anstey et al., 2008), obesity (Beydoun et al., 2008) and smoking (Lee et al., 2010) have been reported to increase the risk of AD. Moreover, strokes and small haemorrhages in the brain (Pendlebury and Rothwell, 2009) are also well-accepted risk factor for AD and for VaD.
- Traumatic brain injury (TBI) (Sundström et al., 2007) – TBI at any age, and especially repeated concussions, is a risk factor for AD. Interestingly, both in stroke and TBI, increased Aβ production and deposition have been shown (Loane et al., 2009).
- Type 2 Diabetes (T2D) (Lu et al., 2009) – T2D is another risk factor for AD. Recent experimental evidence have shown that impaired insulin signal may be implicated in AD suggesting that the AD brain has a diabetes-like condition that some are calling type 3 diabetes (de la Monte and Wands, 2008).
- Down's syndrome - most of the individuals with Down's syndrome who live into their forties and beyond develop neuropathological changes characteristic of AD (SPs and NTFs) and eventually dementia (Menéndez, 2005).
- Others - in addition to the risk factors described above, all of the following have been documented as risk factors for AD: chronic inflammatory conditions such as certain forms of arthritis, a history of episodes of clinical depression, stress and the post-menopausal state in women because of the decline in the hormone estrogen.

## *1.1.3.2. Genetic risk factors*

**Genetics of FAD**

The etiology of EOAD, which has an onset before 65 years, has a strong genetic component. As already mentioned there are autosomal dominant mutations causing FAD. These mutations have been identified in three genes: *APP* on chromosome 21, presenilin 1 *(PSEN1)* on chromosome 14 and presenilin 2 (*PSEN2)* on chromosome 1. Currently 32 mutations in *APP*, 182 in *PSEN1*, and 14 in *PSEN2* are reported, which have been identified in 86, 401, and 23 families, respectively (Alzheimer Disease & Frontotemporal Dementia Mutation Database, http://www.molgen.ua.ac.be/ADMutations/). AD-linked mutations in these three genes exhibit high penetrance (>85%) and in most of the cases show autosomal dominant inheritance. These mutations are thought to be the direct cause of the disease in FAD patients hence they can be used as 'diagnostic biomarkers' of the disease. However, these mutations only account for <5% of all AD cases.

**Genetics of SAD**

Although there are no reported genes that cause SAD, a genetic contribution exists also for this disease. First-degree relatives of patients with LOAD have twice the expected lifetime risk of developing the disease in comparison with people who do not have an AD-affected first-degree relative (Green et al., 2002). Moreover, twin studies have demonstrated a heritability of 58%-79% for LOAD (Gatz et al., 2006), which is consistent with a genetic contribution. In the last two decades, numerous genetic factors have been proposed for SAD.

*APOE*, which is the gene that encodes for apolipoprotein E (APOE), is the only established susceptibility gene for LOAD. APOE is a lipid-binding protein that is expressed in humans as one of three common isoforms (APOE E2, E3, and E4), which are encoded by three different alleles (i.e. *APOE* ε2, *APOE* ε3, *APOE* ε4), and that only differ in sequence by

one amino acid at either position 112 or 158. Having at least one copy of *APOE* ε4 increases risk of AD by ~ 3-fold whereas two copies ~ 12-fold. Moreover each inherited *APOE* ε4 allele lowers the age of AD onset by ~ 5-6 years (Corder et al., 1993; Kurz et al., 1996; Poirier et al., 1993). The *APOE* ε4 allele has also been shown to be associated with memory impairment, MCI and progression from MCI to dementia (Farlow et al., 2004). *APOE* ε4 has been suggested to account for 50% of the genetic risk of SAD (Saunders et al., 1993). Hence other genetic factors could explain the remaining genetic contribution in SAD. However, despite hundreds of genetic association studies during the last 15 years, few reported genetic associations have been replicated across studies (see http://www.alzgene.org) (Bertram et al., 2010). More recent Genome Wide Association studies (GWAs), evaluating millions of single nucleotide polymorphisms (SNPs) in thousands of samples have resulted in evidence for a number of new genetic risk factors including bridging integrator protein 1 (*BIN1*), clusterin (*CLU*), ATP-binding cassette sub-family A member 7 (*ABCA7*), complement receptor 1 (*CR1*), phosphatidylinositol-binding clathrin assembly protein (*PICALM*) and others (Hollingworth et al., 2011; Naj et al., 2011). However, the common SNPs identified in these GWAS have low odds ratios. It still seems that *APOE* ε4 remains the most important genetic risk factor in modulating AD risk. Nevertheless, these new gene discoveries provide new impetus for focused studies aimed at improved understanding of the pathogenesis of AD. Indeed, some of these new genes appear to be involved in Aβ metabolism (for example, *CLU*), whilst several others may highlight new pathological pathways involving inflammation, endocytosis, and lipid biology.

### *1.1.3.3. Protective factors*

Over the last decade or so, research has also uncovered factors that may offer some protection against this currently uncurable disease. A lifestyle including healthy eating, maintaining a healthy weight, taking part in regular physical activity, maintaining normal blood pressure and cholesterol levels and participating in activities that involve socializing and stimulating brain have all been suggested to reduce the personal overall risk of developing AD.

**Diet**

Mediterranean diet, a diet characterized by a high intake of plant foods, high consumption of olive oil and fish, a moderate intake of wine and a low intake of red meat and poultry reduces the incidence of AD and slows Mini Mental State Examination (MMSE) cognitive decline (Féart et al., 2009; Scarmeas et al., 2006). Omega 3-fatty acids, present in high amounts in fish, were shown to limit AD pathology by reducing Aβ deposition by increasing its clearance (Cole et al., 2005; Fotuhi et al., 2009). Furthermore, a moderate intake of red wine was associated with a reduction in the risk of AD and dementia in a meta-analysis of 15 prospective studies exploring the effect of alcohol on dementia risk (Anstey et al., 2009) and this might be attributed to some extent to alcohol-induced elevations in high density lipoprotein cholesterol and reduction in thrombotic factors (Rimm et al., 1999). In addition, the Mediterranean diet includes foods that are rich in antioxidants and vitamins, like berries and dark green leafy vegetables. Moreover, other beneficial effects of fruit and vegetable juice was reported (at least three glasses weekly); this effect appears to be more related to the presence of antioxidants called polyphenols, rather than vitamins such as E or C (Dai et al., 2006). However it is of note that there is also evidence that reduced blood levels of folate (which can be supplemented through diet) and increased levels of homocysteine have been associated with increased incidence of

dementia (Kim et al., 2008). As it remains unclear if supplementation with folate and other associated vitamins can offer some levels of protection against AD.

**Physical exercise**

Epidemiological and experimental data suggest that physical activity (PA) may promote brain health. A recent meta-analysis that included 13 prospective studies focused on AD, dementia or both, capturing data from at least 150 000 participants found that PA produced beneficial effects both in dementia and AD patients (Hamer and Chida, 2009). Several molecular mechanisms have been proposed to explain these beneficial effects including alterations of neurotrophins, oxidative stress, inflammation, Aβ degrading enzymes, blood flow, and metabolism (Radak et al., 2010). Several studies have shown that PA results in increased levels of brain derived neurotrophic factor (BDNF) (Macias et al., 2007), glial cell derived neurotrophic factor (Kleim et al., 2003), and nerve growth factor (Neeper et al., 1996), three neurotrophic factors that play an important role in cell survival and brain plasticity-enhancing properties of neurons, thus resulting in enhanced cognitive functions. Moreover PA is widely recognised for reducing reactive oxygen species (ROS) production and increase the level/activity of antioxidant enzymes in rat brain (Radák et al., 2001). It is also documented that a regular exercise decreases the level of lipid peroxidation and protein oxidation (Radák et al., 2001). Perhaps of more interest is the experimental evidence that PA decreases cortical Aβ accumulation in a transgenic mouse model of AD (Adlard et al., 2005). In addition, PA significantly increases both the cerebral blood flow (Ogoh and Ainslie, 2009) and cerebral metabolism in humans (Quistorff et al., 2008), both of which are compromised in AD patients. Increased oxygen supply to the brain resulting from PA is also important because hypoxia, which results from a reduced oxygen supply, promotes the production of Aβ (Li et al., 2009).

**Cognitive activity**

Epidemiological studies have demonstrated that higher levels of education or a lifetime of mental activity, which can increase brain reserve, reduced AD incidence (Stern et al., 1994). Similarly, higher levels of cognitive activity decrease the risk of cognitive decline (Fratiglioni and Wang, 2007). Several prospective studies have found that both young (Carlson et al., 2008) and old (Fratiglioni and Wang, 2007) people who were engaged in cognitive activity, such as learning, reading or playing games, were less likely to develop dementia than individuals who did not engage in these activities. Another study, on 107 same-gender twin pairs, have shed light on gender-specificity in taking advantage from stimulating activities; indeed, greater participation in intellectual activities was associated with lower risk of AD for women, but not for men (Crowe et al., 2003). Overall, the effect of cognitive activity on the risk of dementia is unclear.

**Social interaction**

Data from several independent time points from a large Swedish epidemiological study have suggested that better social networks and social activities might be associated with reduced incidence of AD (Fratiglioni et al., 2004), but this has not been examined systematically in large epidemiological cohorts. Whilst interesting, studies to properly explore this, particularly in the context of gold standard controlled trials, would be very problematic to design and so widespread study of this potential protective factor is unlikely.

## 1.1.4. PATHOGENESIS

### *1.1.4.1. Biology of AD*

#### β-amyloid

β-amyloid (Aβ) is the major constituent of amyloid plaques. Aβ peptides (consisting of 36 to 43 amino acids) are cleavage products of APP following the sequential enzymatic actions of β-secretase and γ-secretase (figure 1.5).

The physiological function of APP is still undetermined. A role for APP has been suggested in neurite outgrowth and synaptogenesis, neuronal protein trafficking along the axon, transmembrane signal transduction, cell adhesion, calcium metabolism, and others, all requiring additional *in vivo* evidence (Zheng and Koo, 2006).

The most abundant Aβ species produced in the brain and found in the cerebrospinal fluid (CSF) is Aβ40 (where 40 denotes the number of amino acids). Aβ42 is generally present in tissues and body fluids at levels from 5 to 10% of those of Aβ40, and it appears to be central to initiating Aβ aggregation because it is more hydrophobic and prone to aggregate (Kim and Hecht, 2005). An imbalance between production, clearance and aggregation of Aβ peptides, has been proposed as the initiating event in AD (cfr. "amyloid cascade hypothesis"). Aβ spontaneously self-aggregates in multiple coexisting physical forms; one of these consists of oligomers (2-6 peptides) that are currently considered the most neurotoxic form (Lambert et al., 1998).

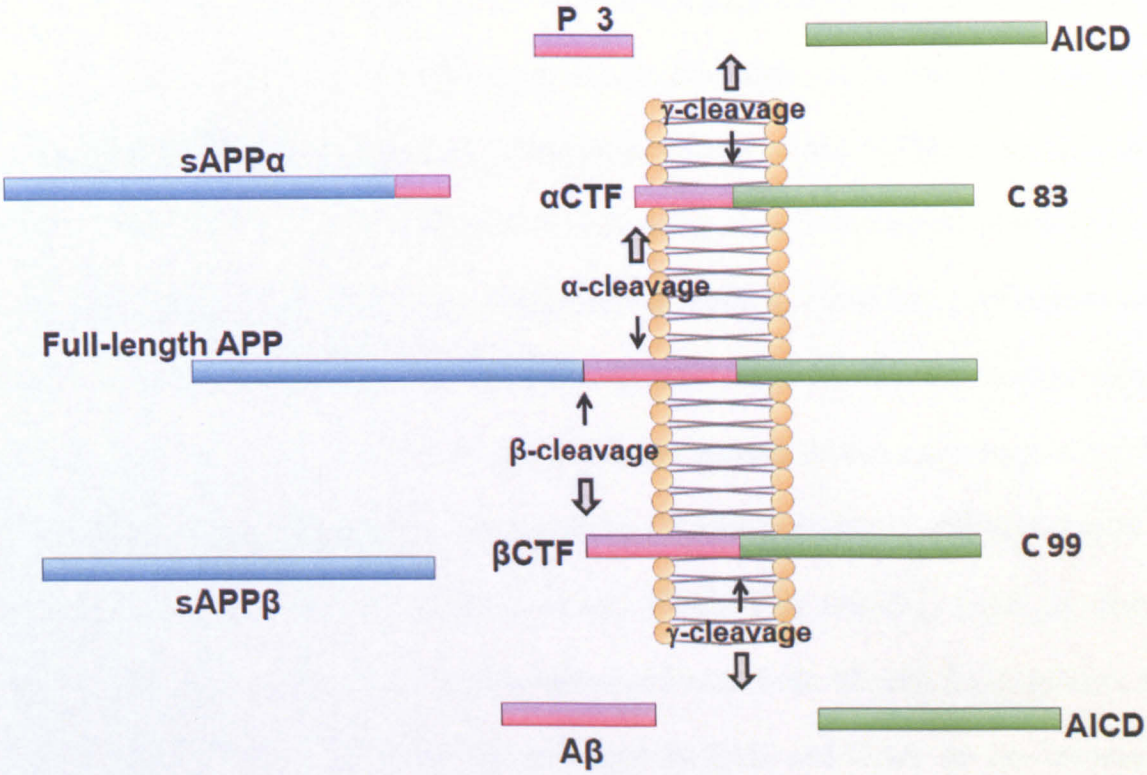


**FIGURE 1.5. Schematic diagram of APP processing.**

*Revised from* (Zhang et al., 2011).

*Abbreviations: sAPP, soluble APP; CTF, C-terminal fragment;AICD, APP intracellular domain.*

*APP is a transmembrane protein with a large N-terminal extracellular tail and a domain termed "Aβ" which is partly embedded in the plasma membrane. APP can be processed along two main pathways. In the α-secretase pathway, α-secretase cleaves APP within the Aβ domain, releasing sAPPα. The remaining α-CTF, or C83, is cleaved by the γ-secretase complex releasing the p3. The remaining AICD is metabolised in the cytoplasm. Since APP cleavage by α-secretase is within the Aβ domain this precludes Aβ generation. In the β-secretase pathway, β-secretase cleaves APP just before the Aβ domain, releasing soluble sAPPβ. The remaining β-CTF, or C99 is cleaved by the γ-secretase complex releasing the 40 or 42 aminoacid Aβ peptide. The remaining AICD is metabolised in the cytoplasm.*

**Familial missense mutations in APP and PSEN genes**

As mentioned, missense mutations occur in *APP* and these are thought to cause the disease because they lead to amino acid changes which are located at or near the sites of APP endoproteolysis by β-secretase and γ-secretase (Goate et al., 1991) or a rare familial disease with CAA and cerebral haemorrhage (Levy et al., 1990). Mutations adjacent to the γ-secretase site, lead to an increase in the ratio of Aβ42 to Aβ40 being produced without having a significant effect on total Aβ levels (Haass et al., 1994) however over time this increased Aβ42 is likely to be central to AD pathogenesis. In contrast, another mutation, the APP Swedish FAD mutation (identified in a Swedish family with FAD), occurs near the β-secretase cleavage site (Mullan et al., 1992). This mutation leads to increased production of all species of Aβ and is associated with both AD and CAA (Citron et al., 1992). Some of the *APP* mutations that lead to FAD and CAA do not increase Aβ production and are located within the Aβ peptide itself. These mutations are C-terminal to the α-secretase cleavage site in APP and change the sequence of Aβ such that it increases the propensity of Aβ to oligomerize, fibrillize, or be cleared less effectively (Nilsberth et al., 2001). Another recently described APP mutation exhibits autosomal recessive inheritance of AD and results in the deletion of one amino acid at position 22 in Aβ producing a peptide that is markedly fibrillogenic (Tomiyama et al., 2008).

In addition to the *APP* mutations, those that have also been described to occur in *PSEN1* (Sherrington et al., 1995; Levy-Lahad et al., 1995) and *PSEN2* (Sherrington et al., 1995) also contribute to Aβ production. The presenilin genes encode for constituent parts of the γ-secretase complex which also involve three other proteins: APH-1, PEN2, and nicastrin (Takasugi et al., 2003). Similar to what is observed with many *APP* mutations, a selective and significant increase in the total level of Aβ42 or the ratio of Aβ42 to Aβ40 is found in the plasma, and in the media of cultured fibroblasts, from patients with *PSEN* mutations (Scheuner et al., 1996).

## Tau

Besides amyloid plaques, the major component of NFTs is the abnormally hyperphosphorylated and aggregated form of tau. Tau is the major neuronal microtubule-associated protein, prevalently localized in the axons, which promotes assembly and stability of microtubules (Weingarten et al., 1975). Tau is actively phosphorylated in normal individuals regulated by the balance between multiple kinases [glycogen synthase kinase-3 (GSK-3), cyclin dependent protein kinase-5 (CDK5), protein kinase A (PKA), calcium and calmodulin-dependent protein kinase-II (CaMKII), casein kinase-1 (CK-1), mitogen-activated protein (MAP) kinase ERK 1/2, and stress-activated protein kinases (SAPKs)] and phosphatases (protein phosphatase PP-2A and PP-1) (Iqbal et al., 2009). In AD brain, tau is at least three- to four-fold more hyperphosphorylated (Iqbal et al., 1986; Köpke et al., 1993). Hyperphosphorylated tau is insoluble, lacks affinity for microtubules, self-associates into PHFs and accumulates in the somato-dendritic compartment (Alonso et al., 2001; Iqbal et al., 2010).

## *1.1.4.2. Pathogenic hypothesis*

**Amyloid hypothesis**

A major advance in the study of AD came with the sequencing of the main constituent of SPs (i.e. the Aβ peptide) (Glenner and Wong, 1984; Masters et al., 1985). This led in rapid sequence to four key discoveries:

- Aβ peptide is a part of the large type I membrane protein APP (Kang et al., 1987);
- *APP* is mutated in a significant fraction of the cases of FAD (Goate et al., 1991);
- Individuals with Down's syndrome, who have three copies of chromosome 21 and hence three copies of *APP*, develop clinical and pathological signs of early-onset AD (Delabar et al., 1987; Olson and Shaw, 1969);
- Mutations in *PSEN1* and *PSEN2*, encoding the catalytic subunit of the γ-secretase activity that liberates the Aβ peptide from the C-terminus of APP, can behave as dominant familial AD genes (Scheuner et al., 1996).

Collectively these findings formed the cornerstones of the "amyloid cascade hypothesis". This hypothesis suggests that Aβ deposition, due to an imbalance between the production and clearance of Aβ in the brain is the initiating event of a number of downstream consequences ranging from synapse loss to inflammation, triggering of tau hyperphosphorylation, and the death of susceptible neurons (Hardy and Selkoe, 2002).

The amyloid hypothesis has prevailed for over two decades. Initially, it was thought that Aβ deposited in SPs was the primary source of neurotoxicity. However, more recent findings have pointed to unpleated Aβ oligomers being responsible for inhibiting hippocampal long-term potentiation and disrupting synaptic plasticity well before the accumulation of fibrillary Aβ (Ferreira et al., 2007). In particular, Aβ*56, a specific form of Aβ oligomer (56 kDa), was demonstrated to be associated with cognitive decline (Morris and Mucke, 2006).

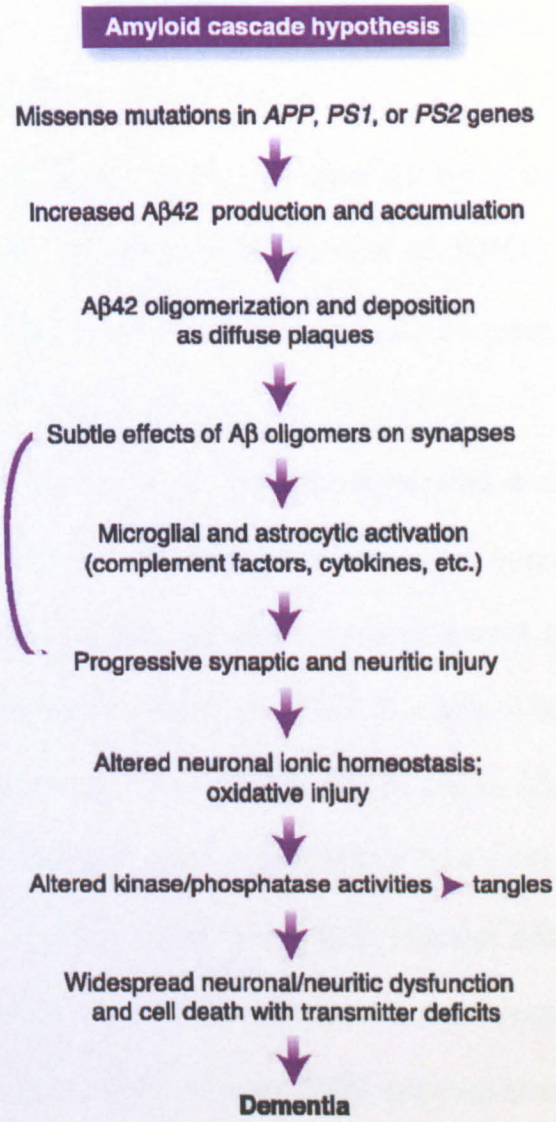


**FIGURE 1.6. The amyloid cascade hypothesis.**

*Taken from* (Hardy and Selkoe, 2002).

*The violet arrows indicate the proposed sequential events that lead to dementia in FAD patients. Noteworthy, Aβ oligomers may directly injure the synapses and neurites of brain neurons (curved arrow), or indirectly through the activation of microglia and astrocytes.*

**Tau hypothesis**

The tau hypothesis is supported by several observations:

- AD severity correlates well with the increasing accumulation of NFTs in the brain (Ghoshal et al., 2002);
- Phosphorylated forms of tau, in the CSF from AD brain, are highly correlated with the extent of cognitive impairment (Maccioni et al., 2006);
- Drugs that decrease tau filaments alleviate cognitive impairment (Duff et al., 2010).

The tau hypothesis states that in AD tau hyperphosphorylation starts intracellularly, and leads to sequestration of normal tau and other microtubule-associated proteins, which causes disassembly of microtubules and thus impaired axonal transport, compromising neuronal and synaptic functions (Iqbal et al., 2005). Recently it has been proposed that as much as 40% of the abnormally hyperphosphorylated tau in AD brain is present in the cytosol and not polymerized into PHFs/NFTs. The AD cytosolic abnormally phosphorylated tau (p-tau) does not bind to tubulin to promote microtubule assembly, but it inhibits microtubule assembly and sequesters normal tau generating oligomeric species that self-assemble into PHFs and straight filament (SFs) and then form NFTs. The current idea is that, like Aβ oligomers, intermediate aggregates of abnormal tau molecules are cytotoxic and are reported to impair cognitions (Iqbal et al., 2010). As a result of neuronal death, oligomeric forms and tau filaments are released to the extracellular environment, contributing to activation of microglial cells and stimulating the deleterious cycle leading to progressive neuronal degeneration (Herrup, 2010).

According to the updated tau hypothesis, tau hyperphosphorylation constitutes a final common pathway in AD pathogenesis, upon which a host of signalling mechanisms converge, and this phenomenon precedes widespread neuronal degeneration (Fernández et al., 2008).

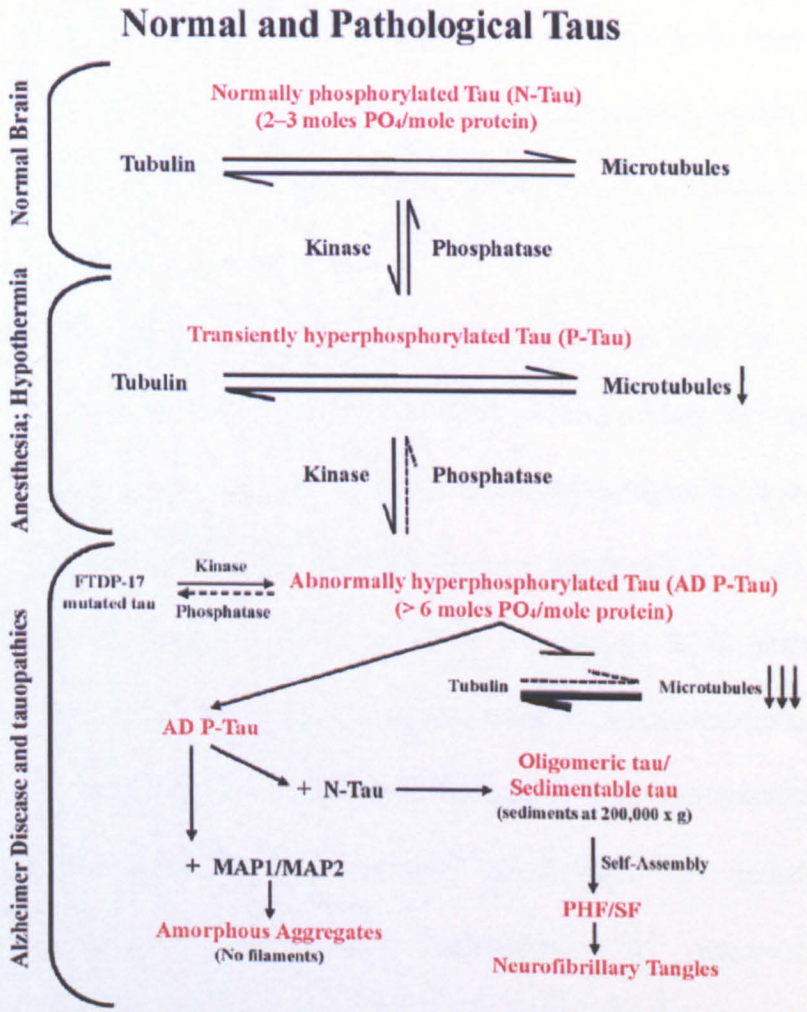


**FIGURE 1.7. The tau hypothesis.**

*Taken from* (Iqbal et al., 2010).

*In AD brain a phosphorylation/dephosphorylation imbalance leads to abnormal hyperphosphorylation of tau. This AD p-tau on one hand sequesters normal MAPs from microtubules and causes inhibition and disruption of microtubules. On the other hand, while the binding of AD p-tau to MAP1 or MAP2 results in amorphous aggregates, the binding to normal tau forms oligomers. Unlike normal tau, which is highly soluble, the tau oligomers formed with AD p-tau self-assemble into PHFs/SFs in the form of NFTs.*

**Other hypotheses**

Several other hypotheses of disease mechanisms have been proposed to explain specific features of AD pathogenesis, including inflammatory mechanisms, oxidative stress, altered vasoactive pathways (Kehoe et al., 2009) and mitochondrial dysfunction with disruption in neuronal energy metabolism.

Mitochondrial dysfunction has an established role in age-related neurodegenerative diseases, such as AD (Beal, 1998). Mitochondria sustain the activity of neurons by producing ATP via the electron transport system by coupling electron transfer to the pumping of protons across the inner mitochondrial membrane. However, electrons can escape the electron transport chain and reduce ROS. Oxidative damage results from a disturbance in the ROS-antioxidant balance that promotes oxidation. Oxidative damage to mitochondria may be especially relevant in neurodegenerative diseases since mitochondria are regulators of both cellular metabolism and apoptosis (Sullivan et al. 2005). Mitochondria also maintain intracellular $Ca^{2+}$ homeostasis and alterations in $Ca^{2+}$ homeostasis in SAD patients was firstly reported in the middle of the 1980s (Peterson et al., 1986). Increased mitochondrial $Ca^{2+}$ overload as a result of excitotoxicity has been associated with the generation of superoxide and may induce the release of pro-apoptotic mitochondrial proteins, proceeding through DNA fragmentation/condensation and culminating in cell demise by apoptosis and/or necrosis (Rego and Oliveira, 2003).

To date, an unifying hypothesis takes into account previously formulated hypotheses (Herrup, 2010). Three main stages can be identified:

1) A precipitating injury begins the pathogenic process (e.g. Aβ oligomers, oxygen free radicals, iron overload, disorders of lipid metabolism, hyperglycaemia, deregulation of insulin levels, chronic infections, head trauma, and others),

2) The injury triggers a chronic inflammatory process that adds additional relentless stress to brain cells already weakened by age [i.e. activated glial cells respond by releasing

Nuclear Factor Kappa β (NF-κB) and overproduce proinflammatory cytokines which contribute to brain inflammation and alterations in neuron-glia interaction pattern],

3) Eventually there is a major shift in the cellular physiology of brain cells (e.g. synaptic dysfunction and neuronal death).

## 1.1.5. TREATMENTS

### *1.1.5.1. Symptomatic drugs*

Currently, there are only 5 drugs approved by the Food and Drug Administration (FDA) to treat AD. These are all symptomatic treatments, addressing the cognitive impairments of the AD patients, but do not target the underlying pathology.

**Acetylcholinesterase inhibitors**

Although most of the vulnerable neurons in AD use glutamate, the major neurotransmitter in the brain, there is also loss/dysfunction of certain subcortical projection neurons such as basal forebrain cholinergic neurons and noradrenergic neurons in the locus coeruleus (Coyle et al., 1983). The cholinergic hypothesis in AD states that cholinergic system in the basal forebrain nuclei is affected early in the disease process causing disturbances in presynaptic cholinergic terminals in the hippocampus and neocortex, resulting in memory disturbances as well as deterioration of other cognitive and non-cognitive functions such as neuropsychiatric symptoms (Terry and Buccafusco, 2003; Bartus et al., 1982). Drugs inhibiting acetylcholinesterase, increase the availability of acetylcholine (ACh) and enhance cholinergic neurotransmission. Four Acetylcholinesterase inhibitors were originally approved by FDA for clinical use in AD: tacrine (1993), donepezil (1996), rivastigmine (2000) and galantamine (2001). Persistent treatment with cholinesterase inhibitors slows clinical progression of AD in early to moderate AD patients (Rountree et al., 2009). However, in most of the cases the therapeutic efficacy of these drugs is moderate and sometimes wears off after a short treatment period (~ 6 months) although other patients can benefit for a number of years. Tacrine is no longer used because of its high prevalence of hepatotoxicity (Ames et al., 1988).

**Memantine**

A dysfunction of glutamatergic neurotransmission, causing neuronal excitotoxicity, is also known to be involved in the etiology of AD (Areosa et al., 2005). Targeting the glutamatergic system, specifically N-Methyl-D-aspartate (NMDA) receptors, has served as one current important therapeutic strategy. Indeed, NMDA receptors control synaptic plasticity and memory function in the brain (Li and Tsien, 2009) while Aβ disturb the function of postsynaptic NMDA receptors causing excessive $Ca^{2+}$ influx into neurons and activation of NMDA-dependent downstream pathways. The cytosolic and mitochondrial $Ca^{2+}$ overload that in turn initiates a cascade of oxidative citotoxicity and apoptosis (Hynd et al., 2004).

Memantine is a non-competitive NMDA-receptor antagonist that is believed to protect neurons from excitotoxicity without preventing the physiological NMDA-receptor activation needed for cognitive functioning (Wilcock, 2003). It was approved by FDA in 2003 for the treatment of patients with moderate to severe AD. Combination use of memantine and donepezil have proved a significant benefit in cognitive function compared to treatment with memantine alone in patients with moderate to severe AD (Tariot et al., 2004).

### *1.1.5.2. Disease-modifying drugs*

Unlike treatments that target symptoms of cognitive dysfunction, disease-modifying therapies could slow or arrest AD progression by interrupting underlying pathophysiologic processes (Mangialasche et al., 2010). For example drugs targeting Aβ production (e.g. γ-secretase inhibitors), clearance (e.g. immunotherapy) or aggregation to avoid the generation of toxic Aβ oligomers may show potential benefit for AD treatment in mild to moderate AD (Mangialasche et al., 2010). Besides drugs aimed to interfere with Aβ metabolism, treatments that could target abnormal tau protein are also being investigated

(e.g. inhibitors of tau-phosphorylating kinases and compounds that inhibit tau aggregation and/or promote aggregate disassembly) (Gong and Iqbal, 2008). Other promising strategies target mitochondrial dysfunction or increase neurotrophic agents to rescue cholinergic cell death. To this concern, Cerebrolysin, a peptidergic drug that exerts nerve growth factor like activities on neurons is currently approved and marketed in several countries worldwide for the treatment of AD.

# 1.2. SIRTUINS IN AGEING AND AGE-RELATED DISEASES

## 1.2.1. GENERAL INTRODUCTION ON SIRTUINS

### *1.2.1.1. The sirtuin protein family*

The Sir2-related proteins (HST - homologues of *SIR2*), also known as sirtuins, are evolutionary conserved enzymes found in all domains of life (Brachmann et al., 1995). In the last decade, a growing interest in resolving the function of mammalian sirtuins has arisen after the discovery that this protein family regulates ageing and longevity in lower organisms such as yeast, worms and flies (Fontana et al., 2010).

Sir2p (silent mating type information regulation 2), of the budding yeast *Saccharomyces cerevisiae* (S.c.), was the first member of this family to be discovered by Klar and colleagues in the late 1970s (Klar et al., 1979). Sir2p was later shown to be essential for genome integrity by regulating gene silencing at three genetic *loci*: mating-type loci, ribosomal DNA (rDNA), and telomeres (Bryk et al., 1997; Gottschling et al., 1990; Rine and Herskowitz, 1987; Smith and Boeke, 1997). In particular, silencing at the rDNA seems to be the mechanism through which Sir2p promotes longevity in yeast, by preventing accumulation of extrachromosomal rDNA circles, a yeast specific cause of ageing. The first identified protein substrates of yeast Sir2p were histones (Blander and Guarente, 2004), indeed it was shown that Sir2 exerted its function through deacetylation of specific lysine residues in the amino-terminal tail of histones H3 and H4.

The alignment between sirtuin protein sequences, ranging from bacteria to humans, revealed that these proteins are ~30-65% identical to yeast Sir2p overall (Sherman et al., 1999). In particular sirtuins all contain a characteristic core domain (~ 260 amino acid long), highly conserved (up to 84% identical to Sir2p), relevant for sirtuin catalytic activity

(Sherman et al., 1999). Based on sequence similarity in this conserved domain, the eukaryotic HST proteins were grouped into four main classes (class I-IV). Yeast Sir2p belongs to class I, while the 7 human sirtuins are represented across all four classes: SIRT1, SIRT2, and SIRT3 (class I); SIRT4 (class II) SIRT5 (class III); and SIRT6 and SIRT7 (class IV). A fifth class also exists (class U) found only in Gram-positive bacteria (Frye, 2000).

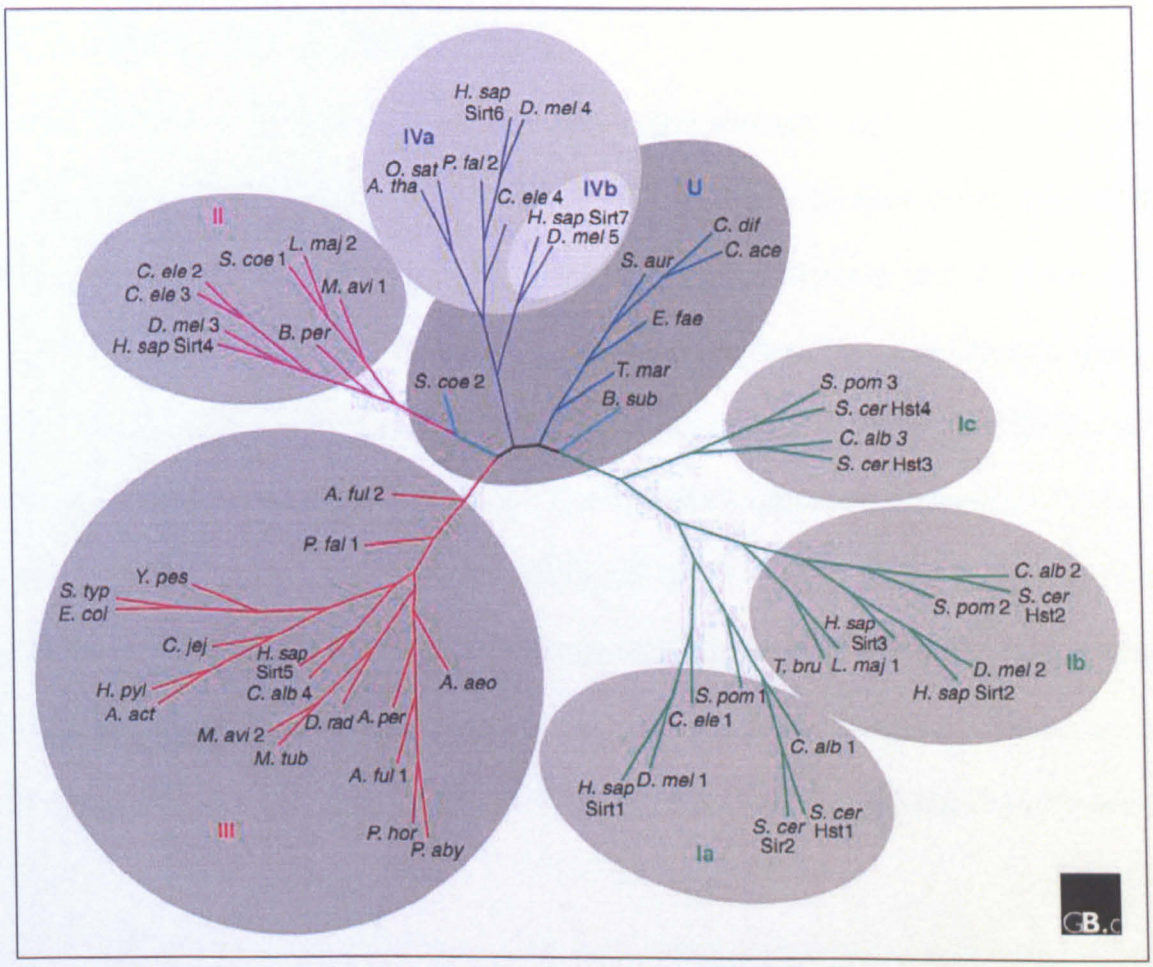


**FIGURE 1.8. Phylogenetic tree of class I, II, III, IV and U sirtuins.**

*Taken from* (North and Verdin, 2004).

*Abbreviations: A. act, Actinobacillus actinomycetemcomitans; A. aeo, Aquifex aeolicus; A. ful, Archaeoglobus fulgidus; A. per, Aeropyrum pernix; A. tha, Arabidopsis thaliana; B. per, Bordetella pertussis; B. sub, Bacillus subtilis; C. ace, Clostridium acetabutylicum; C. alb, Candida albicans; C. dif, Clostridium difficile; C. ele, Caenorhabditis elegans; C. jej, Campylobacter jejuni; D. mel, Drosophila melanogaster; D. rad, Deinococcus radiodurans; E. col, Escherichia coli; E. fae, Enterococcus faecalis; H. sap, Homo sapiens; H. pyl, Helicobacter pylori; L. maj, Leishmania major; M. avi, Mycobacterium avium; M. tub, Mycobacterium tuberculosis; O. sat, Oryza sativa; P. aby, Pyrococcus abyssi; P. fal, Plasmodium falciparum; P. hor, Pyrococcus horikoshii; S. aur, Staphylococcus aureus; S. coe, Streptomyces coelicolor; S. pom, Schizosaccharomyces pombe, S. typ, Salmonella typhimurium; S. cer, Saccharomyces cerevisiae; T. bru, Trypanosoma brucei; T. mar, Thermotoga maritima; Y. pes, Yersinia pestis.*

### *1.2.1.2. Sirtuin mechanism of action*

The first reaction characterized for sirtuins was a ribosyltransfer reaction catalysed by the Sir2 homolog CobB in *Salmonella typhimurium* (Tsang and Escalante-Semerena, 1998). More recently, sirtuins were discovered to act as deacetylases and/or mono-ADP-ribosyltransferases a function found to be dependent on oxidized nicotinamide adenine dinucleotide (NAD+). Sirtuins are histone deacetylase enzymes (HDACs). HDACs occur in four groups (HDAC I-IV) based on function and DNA sequence similarity. Sirtuins are unconventional HDACs and alone constitute Class III due to their unique enzymatic mechanism. Their main peculiarities are the use of NAD+ instead of zinc as a co-factor and the lack of production of acetate (Hernick and Fierke, 2005). Moreover sirtuins are not affected by Trichostatin A (TSA) and sodium butyrate (SB), two inhibitors of "classical" HDACs.

Landry et al. in 1999 elucidated the mechanism of Sir2p-mediated deacetylation showing that the deacetylase reaction is tightly coupled to the formation of a novel product (O-acetyl-ADP ribose, OAADPr). One molecule of NAD+ and one molecule of acetyl-lysine of the target protein are readily catalysed to one molecule of deacetylated lysine, nicotinamide (NAM), and OAADPr (Tanner et al., 2000) as shown in figure 1.9. The unique product OAADPr was proposed to have an important signalling role as a cofactor for SIR2 catalytic activity (Tanner et al., 2000).

Besides deacetylation, some sirtuins possess mono-ribosyltransferase activity. Sirtuin-mediated mono-ribosyltransferase reaction transfers the ADP-ribose group from NAD+ to acceptor proteins in a post-translational modification called ADP-ribosylation. This reaction produces mono-ADP-ribosylated proteins and, similiar to the deacetylation reactions, also yields NAM (Sauve, 2010). The requirement of NAD+ for sirtuin catalyses, which is different to HDAC I/II mediated reactions that simply hydrolyse acetyl-lysine, suggests that sirtuins may have evolved as sensors of cellular energy and redox state

coupled to the metabolic status of the cell (Sinclair and Guarente, 2006). Indeed, sirtuins respond to changes in the concentrations of NAD+, NADH and NAM (NADH and NAM are inhibitors of sirtuins) (Sauve, 2010).

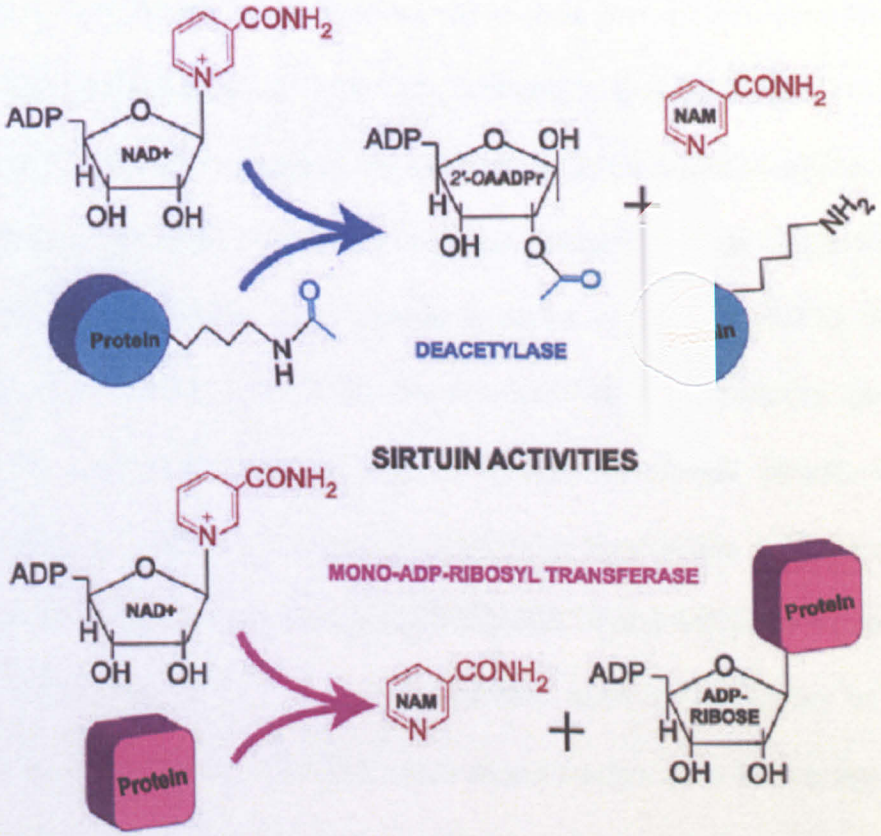


**FIGURE 1.9. Sirtuin enzymatic activities.**

*Taken from* (Michan and Sinclair, 2007)

*Sirtuins catalyse two reactions that are NAD+-dependent: A. DEACETYLATION. The amide cleavage of NAD+ is the driving force that cleaves an acetyl group from an acetyl-lysine residue of a target protein generating OAADPr and NAM; B. ADP-RIBOSYL TRANSFER. An ADP-ribose from one NAD+ molecule is transferred to an uncoupled protein generating NAM.*

### *1.2.1.3. Mammalian sirtuins*

As mentioned, the mammalian sirtuin family so far consists of 7 sirtuins (SIRT1-7) discovered in humans (Michishita et al., 2005). These proteins are involved in a variety of cellular functions such as stress resistance and apoptosis, genomic integrity and cellular metabolism (Michan and Sinclair, 2007).

Mammalian sirtuins share, as well as all the other HST proteins, the sirtuin core domain. Although mammalian sirtuins are well conserved in their core domain, they vary in length in the N- and C-terminal flanking sequences. Moreover, they have different patterns of subcellular localization and expression, unique binding partners and substrates and display different enzymatic activities. Indeed, sirtuins act preferentially as deacetylases and/or mono-ADP-ribosyl transferases. For example in terms of activity, SIRT1 has a robust deacetylase activity, SIRT4, only shows a mono-ADP-ribosyl transferase activity, while SIRT3 performs both deacetylase as well as mono-ADP-ribosyl transferase activities (Michan and Sinclair, 2007). In terms of subcellular localization differences SIRT2 is predominantly localized in the cytoplasm; SIRT3, SIRT4 and SIRT5 in the mitochondria and SIRT1, SIRT6 and SIRT7 are predominantly nuclear (Michishita et al., 2005). Although this classification is still valid, more recent studies have shown that sirtuins are distributed among multiple compartments of the cell and their localization may be dynamic, depending on tissue/cell type and physiologic condition. For example SIRT1 and SIRT2 were found to localize in both the nucleus and the cytoplasm and to interact with both nuclear and cytosolic proteins (North and Verdin, 2007; Tanno et al., 2007). Consistently, SIRT1 was shown to possess two nuclear import signals and two nuclear export signals in its sequence (Tanno et al., 2007). Also SIRT2 was shown to possess a nuclear localization signal (North and Verdin, 2007).

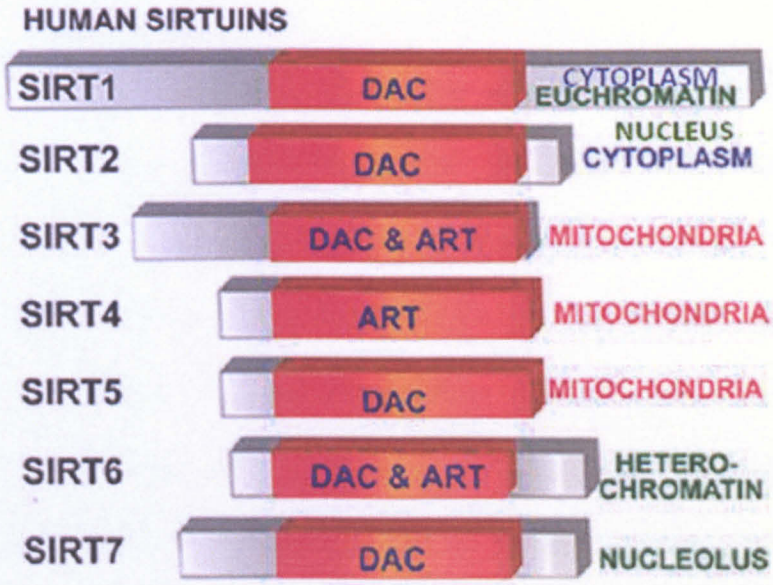


**FIGURE 1.10. Mammalian Sirtuins.**

*Revised from* (Michan and Sinclair, 2007)

*Mammals have 7 sirtuins, SIRT1–7. All have a NAD+-dependent catalytic core domain that may act preferentially as a mono-ADP-ribosyl transferase (ART) and/or NAD+-dependent deacetylase (DAC). Additional N-terminal and/or C-terminal sequences of variable length may flank this core domain. The 7 sirtuins show different cellular localizations.*

Besides cellular localization, post-translational modifications regulate sirtuin function. For example SIRT2 activity was shown to be regulated by phosphorylation at multiple sites. Phosphorylation at Ser 331 mediated by CDK2 and CDK5 is predicted to inhibit the deacetylase activity of SIRT2 (Pandithage et al., 2008) while phosphorylation at Ser 368 by CDK1 inhibited SIRT2 degradation through the 26S proteasome (Dryden et al., 2003). SIRT1 was shown to be positively regulated by phosphorylation by different kinases among which JNK1 and CDK1 (Sasaki et al., 2008; Nasrin et al., 2009) and its deacetylase

activity was also reported to be positively regulated by sumoylation at Lys 734 (Yang et al., 2007b).

Recent reports showed that SIRT1 function is also regulated by other proteins including the activators AROS, necdin and DBC1. Both DBC1 and AROS bind to the N-terminus of SIRT1, the same region to which SIRT1 small-molecule activators bind, raising the possibility of a common mechanism of control (Haigis and Sinclair, 2010). Moreover, despite their different targets and cellular localization, perturbation of the activity of one sirtuin has been shown to impact the activities of other sirtuin members. For example SIRT1 can regulate SIRT6 expression (Kim et al., 2010). Intensive crosstalk between nuclear and mitochondrial sirtuins have also been implied in the literature (Kong et al., 2010; Nasrin et al., 2010).

### *1.2.1.4. Pharmacological activators and inhibitors of sirtuins*

**Activators**

In an initial screening of chemical libraries, a series of naturally occurring plant polyphenols were identified as SIRT1 activators, in particular quercitin and resveratrol (RES) (Howitz et al., 2003). More recently, several isoflavones were observed either to activate SIRT1 or increase its expression or do both (Rasbach and Schnellmann, 2008). These compounds are collectively called Sirtuin Activating Compounds (STACs).

RES was reported to be the most potent naturally available SIRT1 activator, and numerous studies showed that RES treatment *in vivo* and *in vitro* recapitulates biochemical effects exerted by SIRT1 genetic overexpression. However, controversial data about SIRT1 activation still exist and some authors have suggested that RES may activate sirtuins indirectly or even not activate it (Hu et al., 2011). Despite the SIRT1 ambiguities RES was also shown to activate other sirtuins *in vitro*; for example exposure of cardiomyocyte cells to RES caused rapid activation of SIRT1\3\4 and 7 (Yu et al., 2009).

Other SIRT1 activators also exist but to date there are currently few published examples of compounds that have a higher specificity for SIRT2-SIRT7. In 2007 Sirtris Pharmaceuticals identified three compounds to serve as novel SIRT1 activators containing an imidazothiazole scaffold and which did not resemble RES structure. They named these compounts SRTs (Milne et al., 2007). Among these SRT1720 and SRT2183 were reported to be the most potent activators of SIRT1. Like RES, no clear data are yet available about SIRT1 effective activation by SRTs. Although the exact mechanisms of activation are not yet clear, some authors have proposed that sirtuin activators bind to the N-terminus of SIRT1, lower the Km for the substrate and for NAD+ and in a lesser extent, increase the maximum enzyme velocity (Vmax).

**Inhibitors**

The first step in sirtuin catalysis is the formation of a ternary complex of the enzyme, NAD+, and acetylated peptide, followed by the expulsion of NAM to form an AD-ribose-peptidyl imidate intermediate. This intermediate can proceed in the forward reaction steps leading to production of deacetylated peptide and OAADP and reverse reaction steps with reincorporation of NAM and synthesis of substrates. NAM, produced by sirtuin catalysis, is a naturally occurring potent inhibitor of sirtuins' activity (particularly Sir2p, SIRT1 and SIRT2). In fact, excess NAM is thought to promote the reverse reaction (Blum et al., 2010).

Although NAM is not specific for any particular sirtuin, its analogue 2-anilinobenzamine was identified to be a potent SIRT1 inhibitor (Suzuki et al., 2009). Also NAD+ analogues, such as carbamido-NAD, were shown to inhibit sirtuins. While NAM is a non-competitive allosteric inhibitor, carbamido-NAD acts by competing for the NAD+ binding site within the active site.

In a high-throughput screening, indole-based compounds were identified as sirtuin inhibitors (Napper et al., 2005). These compounds were hypothesized to bind close to or in

conjunction with the NAM binding site. Among these, EX527 was reported to be the highest specific inhibitor of SIRT1, approximately 1000 fold more potent than NAM.

One of the first commercially available sirtuin inhibitors was sirtinol. This compound, shown to inhibit SIRT1, SIRT2 and Sir2p, was widely employed and a number of more potent analogues were developed rationally designed to improve SIRT1 activation, such as salermide.

A specific reversible inhibitor for SIRT2 is also available, named AGK2.

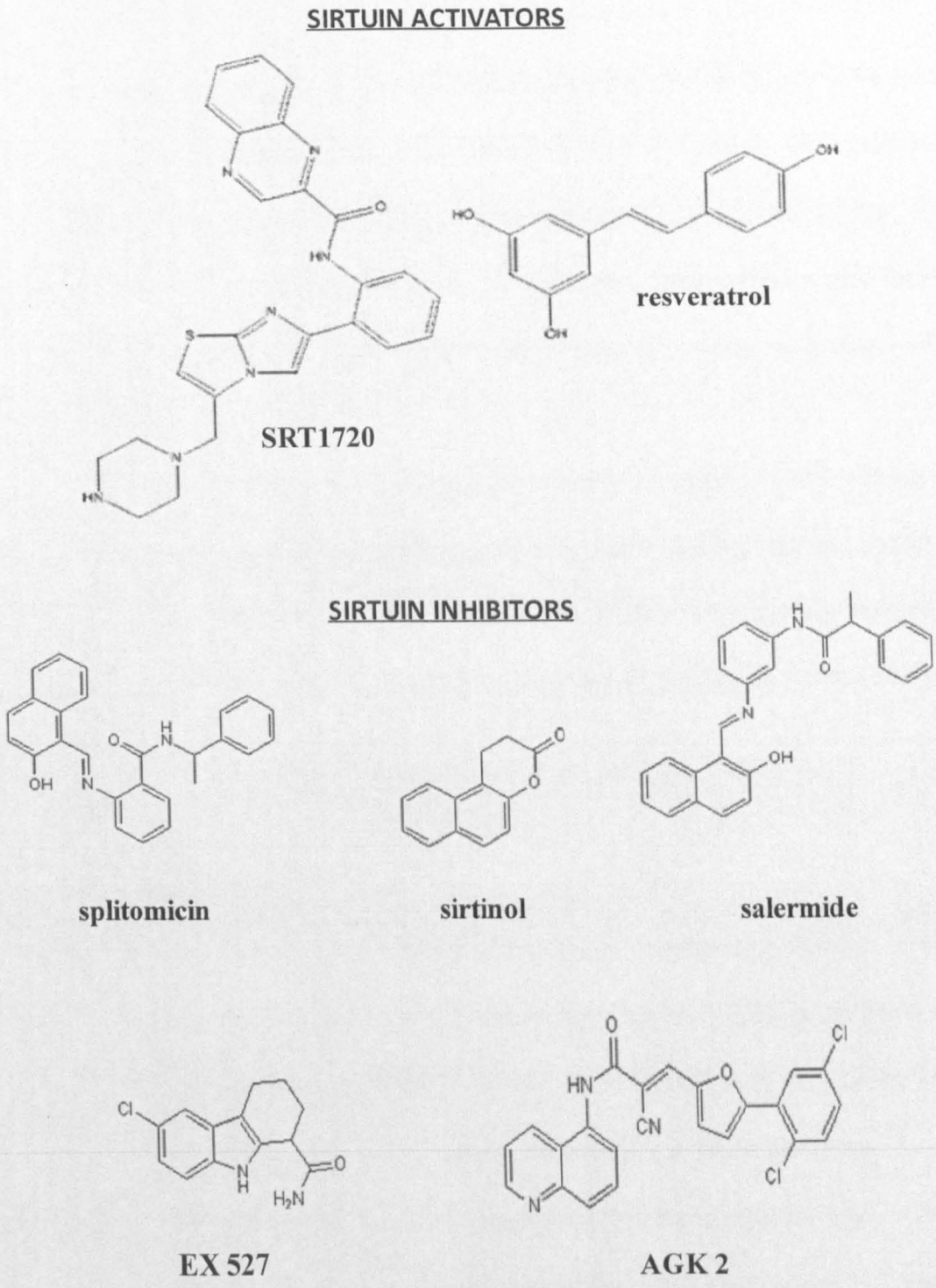


**FIGURE 1.11. Chemical structure of sirtuin activators and inhibitors.**

## *1.2.1.5. Function of the mammalian sirtuins*

### SIRT1

SIRT1 is the most extensively studied mammalian sirtuin and it is implicated in the regulation of multiple biological phenomena including DNA damage repair, mitochondrial biogenesis, insulin secretion, stress response, apoptosis as well as genome stability. SIRT1 is highly expressed in several brain regions including the hypothalamus, and has been found in the heart, kidney, liver, pancreas, skeletal muscle, spleen, and white adipose (Michishita et al., 2005).

SIRT1, similar to yeast Sir2p, induces heterochromatin formation, which generally is associated with hypoacetylation and gene repression by deacetylating various histones (e.g. histone H1) (Vaquero et al., 2004). However, although sirtuins were initially thought to be exclusively histone deacetylases, more recently a variety of non-histone targets have been identified.

#### SIRT1 and energy metabolism

SIRT1 plays a critical role in the regulation of metabolic responses to changes in nutrient availability in multiple tissues. Calorie restriction upregulates SIRT1 in different tissues including liver, skeletal muscle and white adipose tissue (Haigis et al., 2006). In these tissues, through different targets, SIRT1 exerts important metabolic functions. In skeletal muscle, SIRT1 deacetylates PGC-1α thus upregulating the transcription of genes involved in mitochondrial biogenesis, muscle oxidative capacity, fatty acid oxidation and energy expenditure (Gerhart-Hines et al., 2007).

In liver, during short-term fasting, SIRT1 inhibits TORC2, a key mediator of early phase gluconeogenesis, and prolonged fasting leads to increased SIRT1 deacetylation and activation of PGC-1α, an essential co-activator for a number of transcription factors, resulting in increased fatty acid oxidation and improved glucose homeostasis

(Purushotham et al., 2009; Rodgers et al., 2005). In conjunction, SIRT1-mediated deacetylation of FOXO1, that causes its retention in the nucleus, promotes FOXO1-mediated transcription of genes involved in gluconeogenesis (Frescas et al., 2005). Moreover, during fasting, SIRT1 deacetylates SREBP-1c thus inhibiting its transcriptional activity responsible for liver lipogenesis and thus attenuating liver steatosis in diet-induced and genetically obese mice (Ponugoti et al., 2010). SIRT1 also regulates hepatic cholesterol and bile acid homeostasis through direct modulation of the liver X receptor and farnesoid X receptor (Kemper et al., 2009; Li et al., 2007).

In white adipose tissue, SIRT1 interacts with PPARγ, a nuclear transcription factor receptor that controls adipogenesis. SIRT1 deacetylation was proposed to repress PPARγ activity and promote free fatty acid mobilization in adipocytes (Picard et al., 2004). In addition, in adipocytes SIRT1-catalyzed deacetylation/activation of FOXO1 increases the transcription of the adiponectin gene (Qiao and Shao, 2006). Furthermore SIRT1 was shown to positively regulate insulin secretion in pancreatic β cells repressing the uncoupling protein 2 (UCP2) (Bordone et al., 2006).

SIRT1 and DNA damage repair

Recent experimental evidence suggests that SIRT1 is involved in response to DNA damage and in the maintenance of genomic stability. SIRT1 overexpression was shown to enhance repair of DNA strand breakages produced by radiation through deacetylation of Ku70 (Jeong et al., 2007). Moreover, SIRT1 plays an important role in the regulation of both the nucleotide excision repair pathway, through modulation of XPA acetylation status (Fan and Luo, 2010), and the DNA double-strand break repair maintaining NBS1 in a hypoacetylated state (Yuan et al., 2007).

Stress resistance and apoptosis

SIRT1 has a role in control cell survival and apoptosis. In β-pancreatic cells overexpression of SIRT1 counteracted cytokine toxicity and reduced induction of nitic oxygen (NO) synthetase by suppressing NF-κb signalling pathway (Lee et al., 2009). On the other hand, SIRT1 was shown to bind and deacetylate the tumor suppressor protein p53 at lysine 382 causing the accumulation of p53 in the cytoplasm rather than in the nucleus. Under ROS stimulation, cytoplasmic p53 translocates into mitochondria and enhances apoptosis (Han et al., 2008).

## SIRT2

SIRT2 is localized in both the cytoplasm and in the nucleus. SIRT2 is reported to be the most abundant sirtuin in adipocytes, found in white and brown adipose tissue. It is also highly expressed in the brain and nervous system (Kelly, 2010). SIRT2 was proposed to have a role in cell cycle regulation. In Saos2 cells, SIRT2 overexpression delayed the progression through the mitotic phase of the cell cycle and in synchronized cells SIRT2 accumulates in mitosis particularly at the G2/M transition, delaying exit from mitosis (Dryden et al., 2003). One proposed mechanism through which SIRT2 may regulate the cell cycle is that H4K16 deacetylation during mitosis could affect chromatin packaging (Vaquero et al., 2006).

FOXO1 and FOXO3a are two transcriptional factor targets of SIRT2. SIRT2-dependent deacetylation of FOXO1 enhances localization of FOXO1 to the nucleus by altering its level of phosphorylation, a post-translational modification that normally causes FOXOs to localize to the cytosol where it is inactive (Jing et al., 2007). FOXO1 is an inhibitor of adipocyte differentiation and inhibiting SIRT2 was reported to accelerate adipocyte differentiation (Jing et al., 2007). Hypoacetylation of FOXO3a by SIRT2 overexpression in kidney cells provided resistance to ROS through increased transcription of FOXO3a genes (e.g. Bim, Mn SOD) (Wang et al., 2007).

## SIRT3

SIRT3 is a mitochondrial protein expressed in various tissues, at especially high levels in brain, kidney, brown adipose tissue, heart, liver and muscle (Shi et al., 2005). SIRT3 is a major mitochondrial deacetylase, indeed SIRT3 knock-out (KO) mice exhibit striking mitochondrial protein hyperacetylation, differently from KO mice of the other two mitochondrial sirtuins, SIRT4 and SIRT5 (Lombard et al., 2007).

The first biological role identified for SIRT3 was its involvement in the activation of thermogenesis in brown adipocytes by enhancing expression of PGC1α and UCP1 (Shi et al., 2005). More recently, a feedback loop has been proposed between SIRT3 and PGC1α since PGC1α was shown to stimulate SIRT3 expression (Kong et al., 2010). AceCS2 is another target of SIRT3-mediated deacetylation. Deacetylated AceCS2 accelerates conversion of mitochondrial acetate to acetyl-CoA in the presence of ATP (Schlicker et al., 2008). Moreover the discovery that glutamate dehydrogenase (GDH) and isocitrate dehydrogenase are substrates of SIRT3, has shed light on the putative role of SIRT3 in regulating citric acid cycle and in mitochondrial energy metabolism. Moreover, complex II and succinate dehydrogenase flavoprotein are other probable targets of SIRT3 that explain why SIRT3 deficiency is associated with mitochondrial loss of performance in electron transport and weak ATP production (Cimen et al., 2010). Decrease in SIRT3 is also associated with increased ROS formation and hepatocyte death (Bao et al., 2010).

With its central role in mitochondrial biology, SIRT3 contributes to cell survival by modulating oxidative stress pathways. Benigni et al. demonstrated that KO mice of the angiotensin II type 1 receptor, a gene responsible for promoting high blood pressure and various pathological conditions, such as heart, kidney and brain diseases, promoted longevity in mice. The lack of this receptor was associated with increased numbers of mitochondria, attenuation of oxidative stress, and upregulation of Nampt and SIRT3 levels. SIRT3 protects cardiomyocytes and HeLa cells from genotoxic and oxidative stress-mediated cell death. By binding to and deacetylating Ku70, SIRT3 augments Ku70–Bax

interactions, which in turn prevents Bax translocation to the mitochondria, and prevents apoptosis during stress-mediated conditions (Benigni et al., 2009). SIRT3 has also a role in lipid metabolism regulation. During fasting, livers from SIRT3 KO mice experienced increased fat accumulation versus wild-type, suggesting a deficiency in fat processing (Hirschey et al., 2010).

**SIRT4**

SIRT4 is another mitochondrial protein highly expressed in kidney, heart, liver and brain (Michishita et al., 2005; Haigis et al., 2006). The only known substrate of SIRT4 is GDH, an enzyme that regulates the usage of amino acids into energy production (Haigis et al., 2006). In early work, it was shown that SIRT4 interacts with GDH and suppresses its activity via ADP-ribosylation (Haigis et al., 2006). GDH promotes the metabolism of glutamate and glutamine, generating ATP, which promotes insulin secretion. Consistently, loss of SIRT4 in insulinoma cells activates GDH, thereby upregulating amino acid-stimulated insulin secretion. Furthermore, isolated pancreatic islets from SIRT4 KO mice have higher GDH activity than wild-type mice and treatment of wild-type mitochondrial lysates with phosphodiesterase, which cleaves the AMP moiety of ADP-ribosylated proteins, increases GDH activity to the level of SIRT4 KO lysates (Haigis et al., 2006). Moreover, in SIRT4 KO mice increased insulin secretion was observed in response to glucose and glutamine (Haigis et al., 2006). In another study, depletion of SIRT4 from insulin-producing INS-1E cells resulted in increased insulin secretion in response to glucose, while overexpression of SIRT4 in the same cultured cells suppresses insulin secretion (Ahuja et al., 2007). Recently, SIRT4 inhibition was also shown to increase fatty acid oxidation in liver and mitochondrial gene expression in muscle cells, although the mechanisms underlying these phenotypes are still unclear (Nasrin et al., 2010).

## SIRT5

SIRT5 is a mitochondrial protein with few known substrates. SIRT5 is expressed predominantly in brain, heart, liver and kidney (Michishita et al., 2005; Nakagawa et al., 2009). One putative *in vitro* target of SIRT5 is cytochrome c but the interaction currently requires verification *in vivo* (Nakagawa et al., 2009). Recently, SIRT5 was shown to deacetylate carbamoyl phosphate synthetase 1 (CPS1), a regulated enzyme that commits ammonia and bicarbonate to the first step of the urea cycle forming carbamoyl phosphate. SIRT5-mediated CPS1 deacetylation, without any change in protein level, enhances CPS1 function. Further evidence has corroborated the hypothesis that SIRT5 could have a role in nitrogen metabolism during fasting. Indeed the protein under fasting is upregulated in liver (Ogura et al., 2010), acetylation of CPS1 decreases, and CPS1 activity increases. Under fasting increased amino acid catabolism increases ammonia production that could be poorly compensated in SIRT5 KO mice (Nakagawa et al., 2009). Consistently, SIRT5 KO mice under fasting became hyperammonemic. On the other hand, CPS1 was hypoacetylated and CPS1 activity and urea production were significantly higher than control mice, in livers of transgenic mice overexpressing SIRT5 (Ogura et al., 2010). Although these findings provide some possible insights into SIRT5 function, further studies should better elucidate this mechanism whilst also evaluating the involvement of NAD+ that is also increased during fasting (Yang et al., 2007a).

## SIRT6

SIRT6 is located in the nuclear compartment and is associated with chromatin. SIRT6 is broadly expressed, with the highest levels in adipose tissue, skeletal muscle, brain and heart (Kelly, 2010). SIRT6 KO mice have a phenotype that involves instability of the genome suggesting that SIRT6 functions in DNA repair pathways. SIRT6 -/- (i.e. knocked out) cells were found to be deficient in base excision repair pathways (Mostoslavsky et al., 2006). SIRT6 -/- cells also displayed abnormalities to the telomeres such as sequence loss,

and shortening of telomeres can limit replicative lifespan in mammals. Consistently, SIRT6 -/- cells undergo premature senescence in culture (Michishita et al., 2008). SIRT6 have also been implicated in regulation of double strand breaks. SIRT6 KO cells have higher levels of broken DNA upon neocarzinostatin treatment versus control cells (McCord et al., 2009).

SIRT6 also has a role in metabolism. SIRT6 downregulates a subset of PPARγ target genes suppressing fat synthesis (Kanfi et al., 2010). SIRT6 also deacetylates histone H3K9(Ac) at chromatin promoter sites recognized by HIF1α, represses HIF1α signalling (Zhong et al., 2010). HIF1α is a known positive regulator of cell survival in low oxygen stress, which generally causes cells to shift to a glycolytic metabolism. Consistently SIRT6 KO mice have a hypoglycaemic phenotype although SIRT6 also showed a role in inflammatory signalling by suppressing NFkB transcriptional activities (Kawahara et al., 2009).

**SIRT7**

SIRT7 is found in many cells including adipocytes and cardiomyocytes (Kelly, 2010). SIRT7 is located in the nucleolus where it has been reported to activate RNA polymerase I (RNA Pol I) transcription. SIRT7 overexpression led to increased transcription of rDNA stimulating PolI association with DNA (Ford et al., 2006). In a more recent work, the interaction between SIRT7 and PolI was shown to be important for the resumption of rDNA transcription after exit from mitosis (Grob et al., 2009). In this work, it has also been observed that SIRT7 is finely regulated by phosphorylation during mitosis. Further studies should elucidate SIRT7 physiological function, in particular in the heart, since SIRT7 KO mice have a shorter life span due to cardiac hypertrophy.

| PROTEIN | LOCALIZATION | ACTIVITY | TARGET | BIOLOGICAL EFFECT |
|---|---|---|---|---|
| SIRT1 | Nucleus, cytosol | Deacetylase | PPAR-γ, PGC-1α, FOXOs, AMPK, SREBP-1, UCP2, p53, NF-κB, | Metabolism Stress resistance apoptosis DNA repair |
| SIRT2 | Cytosol, nucleus | Deacetylase | H4K16, TUBULIN, FOXOs | Cell cycle metabolism |
| SIRT3 | Mitochondria | Deacetylase, ART | PGC1α, ACS2, GDH, Complex I | Thermogenesis, Mitochondrial biogenesis and metabolism |
| SIRT4 | Mitochondria | ART | GDH | Insulin secretion |
| SIRT5 | Mitochondria | Deacetylase | CPS1 | Urea cycle |
| SIRT6 | Nucleus | Deacetylase, ART | H3, NF-κB | Base excision repair Metabolism |
| SIRT7 | Nucleolus | Deacetylase | Pol I | rDNA transcription |

**TABLE 1.1. Function and tissue localization of mammalian sirtuins.**

*Abbreviations: ART, ADP-ribosyltransferase; PPAR-γ, peroxisome proliferator-activated receptor γ; PGC-1α, peroxisome proliferator-activated receptor γ coactivator 1 α; FOXO, forkhead box O; AMPK, AMP-activated protein kinases; SREBP-1, sterol regulatory element–binding protein gene; UCP2, uncoupling protein 2; NF-κB, nuclear factor kappa B; ACS2, acetyl-CoA synthetase; GDH, glutamate dehydrogenase; CPS1, carbamoyl phosphate synthetase 1; Pol, DNA polymerase I.*

| PROTEIN | VIABILITY | PHENOTYPE | REF. |
|---|---|---|---|
| SIRT1 | Lethal on inbred background (129/J), viable on outbred genetic background. | - Are smaller and often sterile<br>- Frequently have craniofacial abnormalities, and develop an eyelid inflammatory condition<br>- Some develop a disease resembling diabetes insipidus at 2 years of age. | (Sequeira et al., 2008; McBurney et al., 2003) |
| SIRT2 | NA | Normal | (Vaquero et al., 2006) |
| SIRT3 | NA | - No metabolic relevant problems (reduced ATP production, decreased rates of fatty acid oxidation and ketone body production, and fatty liver.<br>- Show signs of cardiac hypertrophy and interstitial fibrosis at 8 weeks of age | (Lombard et al., 2007; Sundaresan et al., 2009) |
| SIRT4 | NA | - No phenotypic abnormalities, higher circulating insulin levels | (Nasrin et al., 2010) |
| SIRT5 | NA | - Hyperammonemia under fasting | (Nakagawa et al., 2009) |
| SIRT6 | Die during the early postnatal period | - Premature ageing including lipodystrophy, bone defects, colitis and severe apoptosis in lymphocytes.<br>- Metabolic defects such as low serum IGF-1 levels and hepatic steatosis in the liver | (Mostoslavsky et al., 2006) |
| SIRT7 | 7.5 month (mean lifetime) | - Cardiac dysfunction in the form of degenerative cardiac hypertrophy accompanied by cardiac myocyte enlargement and cardiac fibrosis,<br>- 200% increased apoptosis in the myocardium. | (Vakhrusheva et al., 2008b) |

**TABLE 1.2. Summary of phenotypes of sirtuin full body knockout mice.**

*Abbreviations: NA, not available (i.e. no visible defect).*

## 1.2.2. SIRTUINS INVOLVEMENT IN AGEING AND AGE-RELATED DISEASES

### *1.2.2.1. Sirtuins involvement in ageing*

The role of sirtuins in ageing was initially discovered in yeast. Sir2p in *S. cerevisiae* was shown to extend the life span of the budding yeast by repressing genome instability (Kaeberlein et al., 1999). Experimental evidence showed that the addition of an extra copy of the *SIR2* gene extended replicative life span (the number of cell divisions undergone by a mother cell before it stops dividing) by ~30% while deleting SIR2 resulted in a much shorter life span (approximately 50% of the control) (Kaeberlein et al., 1999). Starting from this finding, the conserved functional role of SIR2 homologues in ageing has become evident from studies involving more complex laboratory organisms, such as *Caenorhabditis elegans* (Tissenbaum and Guarente, 2001) and *Drosophila melanogaster* (Rogina and Helfand, 2004). Some experimental evidence has suggested that the activation of sirtuins, either by restricting calories or by pharmacological means, extends the life span and promotes the health of a wide variety of organisms from yeast to mammals (Westphal et al., 2007).

To date, knock-out mice for all the 7 sirtuins have been developed. Interestingly, amongst these, SIRT6 KO mice present an ageing phenotype. SIRT6-deficient mice are smaller and at 2-3 weeks of age develop abnormalities that include profound lymphopenia, loss of subcutaneous fat, lordokyphosis, and severe metabolic defects, eventually dying at about 4 weeks (Mostoslavsky et al., 2006). Although having different phenotypes, SIRT1 and SIRT7 KO mice also display a shortened lifespan. Conversely mice that overexpress SIRT1 have an extended lifespan and maintain lower cholesterol, blood glucose, and insulin levels (Vinciguerra et al., 2010).

**Sirtuin, calorie restriction and life span promotion**

Calorie restriction (CR), a dietary regimen that restricts calorie intake without malnutrition, was shown to extend the life span in a wide range of organisms, including rotifers, spiders, worms, fish, mice and rats (Weindruch, 1996). The role of CR in lifespan in such a diverse group of organisms suggests that the mechanism by which CR regulates longevity is an ancient and well conserved pathway. However, although CR has also proved to be beneficial in non-human primates (Colman et al., 2009), a CR protocol would not be easily applicable to humans because of its physical and psychological side effect (Dirks and Leeuwenburgh, 2006). A major interest has arisen in studying CR molecular mechanisms and finding CR mimetics, molecules that could produce the same pro-longevity effects that CR provides, but without reducing calorie intake.

CR was hypothesized to be a stress stimulus that causes an adaptive response in different tissues which in turn induces changes in gene expression. Several studies have shown that CR primarily affects metabolic pathways such as insulin/insulin-like growth factor 1 (IGF-1) and the target of rapamycin (TOR) pathways (Fontana et al., 2010). Besides these pathways, increasing evidence supports the involvement of sirtuins in mediating CR effects. Indeed, in yeast, life span extension by moderate CR requires *SIR2* (Fabrizio et al., 2005). In mammals, although the scenario is much more complex, preliminary evidence also suggests the involvement of sirtuins. Different authors reported that CR modulates SIRT1 expression levels in a variety of tissues. For example, Rodgers and colleagues showed that under fasting conditions such as CR, murine SIRT1 protein level is increased in liver where this enzyme interacts and deacetylates the transcriptional coactivator PGC-1α inducing gluconeogenic genes and repressing glycolytic genes (Rodgers et al., 2005). Overall, it seems that in mice CR-mediated regulation of SIRT1 expression could be tissue and brain region specific (Chen et al., 2008). In humans SIRT1 gene expression also appears to be responsive to caloric intake (Kelly, 2010). CR also was shown to induce the mammalian SIRT2, SIRT3 and SIRT5 in some tissues (Kelly, 2010) (table 1.3). Moreover,

sirtuin activation could be critically affected by changes in NAD+/NAM ratio in tissues and CR has also been shown to increase NAD+ levels (e.g. in the liver) (Kelly, 2010).

| GENE | Up-regulation | Down-regulation |
|---|---|---|
| *SIRT1* | Liver, kidney, intestines, skeletal muscle, white adipose | Hypothalamus |
| *SIRT2* | Adipose tissue | NA |
| *SIRT3* | Liver, skeletal muscle | NA |
| *SIRT5* | Liver | NA |

**TABLE 1.3. Regulation of sirtuin expression levels under calorie restriction.**

*Taken from* (Kelly, 2010).

Further evidence of SIRT1 involvement in CR came from transgenic mice that moderately overexpressed mouse SIRT1 in several tissues including white and brown adipose tissues. These mice displayed phenotypes that mimic some of the physiological changes in response to CR (i.e. they are leaner than littermate controls; more metabolically active; display reductions in blood cholesterol, adipokines, insulin and fasted glucose; exhibited more glucose tolerance; perform better on a rotaroad challenge, and display delayed reproduction) (Bordone et al., 2007). In another study, in a SIRT1-deficient mouse model, it was shown that at least the CR-induced increase in physical activity (PA) requires SIRT1 (Chen et al., 2005a). However, in the same study, SIRT1 deficiency did not prevent the reduction in blood of triglycerides, insulin-like growth factor1 and glucose levels observed in response to CR (Chen et al., 2005a). In another study, CR did not extend lifespan of SIRT1-deficient mice (Kelly, 2010).

Given these and other experimental findings, STACs were proposed as calorie restriction mimetics (Baur, 2010). Pathway analysis of genome-wide expression profiles revealed that

about half of pathways altered by CR overlapped with the pathways modulated by RES in the livers of mice (Baur et al., 2006). Furthermore, gene expression data from hearts, skeletal muscles, and brains of mice indicated that RES mirrors CR in terms of alteration of gene transcriptions *in vivo* (Barger et al., 2008; Pearson et al., 2008). Overall, although SIRT1 overexpression or its pharmacological activation by STACs were proved to mimic CR, the life prolonging effect of CR was not recapitulated in these models (Pearson et al., 2008). However, although RES did not extend mice lifespan in a standard-chow diet, under a high-fat diet was reported to increase life expectancy probably protecting mice against some of the deleterious physiological effects of a high-fat diet.

### *1.2.2.2. Sirtuins and age-related diseases*

Ageing increases susceptibility to a variety of diseases, such as diabetes, cardiovascular diseases, cancer, neurodegenerative diseases, and inflammation. Sirtuins are emerging as therapeutic targets to treat age-related diseases.

Metabolic imbalance, such as insulin resistance, is observed with increasing frequency during ageing. Abnormal metabolic homeostasis can have severe consequences and often manifests as syndromes such as obesity and T2D. By virtue of their NAD+-dependency, sirtuins were hypothesized to be sensors of nutrient availability. Moreover, increasing evidence shows that sirtuins could have an evolutionary conserved role in metabolic homeostasis under fasting and calorie restriction (cfr. 1.2.2.1).

Several studies have implicated SIRT1 in glucose homeostasis and lipid metabolism in various tissues including adipose tissues, liver, pancreas, and skeletal muscle (Kelly, 2010) while SIRT1 also affects insulin signalling and is involved in insulin secretion. In *vivo* evidence showed that SIRT1-transgenic mice display some phenotypic similarities to littermate control mice on CR, they are leaner and more metabolically active. They also have lower blood cholesterol, adipokine levels, insulin, and fasting glucose, and are more glucose tolerant (Bordone et al., 2007). Moreover, mice with moderate overexpression of

SIRT1 exhibit fat mass gain similar to wild-type controls when exposed to a high-fat diet due to a higher energy expenditure and also show lower lipid-induced inflammation as well as better glucose tolerance, and are almost entirely protected from hepatic steatosis (Feige et al., 2008; Pfluger et al., 2008). In a recent study, SIRT1 and SIRT4 have been confirmed to be associated with homeostasis of glucose/lipid metabolism in humans. Indeed, the expression of SIRT1 and SIRT4 was lower in peripheral blood leukocytes from T2D patients than in normal control group. Moreover a negative correlation was found between SIRT1 and SIRT4 mRNA levels and fasting plasma glucose (Song et al., 2011).

Sirtuins are also being investigated in relation to cancer. SIRT1 and SIRT3, by virtue of their role in regulating both cell death and survival, have been focused upon and there has emerged in the literature interesting debate about their roles as tumor promoters and/or tumor suppressors. In tumor samples, heterogeneous SIRT1 and SIRT3 levels have been observed in subsets of tumours, and therefore, the stage of the tumor, the type of tumor, and the varying cellular environments and signals might all contribute to whether sirtuin has tumor suppressor or oncogenic functions. For example SIRT3 was found to be upregulated in oral cancer and in anoikis-resistant oral squamous cell carcinoma cells, whereas SIRT3 was downregulated in human breast cancer cells compared to normal controls breast tissue. Indeed SIRT3−/− mice developed mammary tumours over a 24-month period (Alhazzazi et al., 2011).

A potential involvement in cardiovascular diseases is also emerging with interesting findings. Alcendor et al. reported that increasing SIRT1 activity could retard ageing and confer stress resistance to the heart *in vivo*, but this beneficial effect can be observed only at low to moderate increases in SIRT1 (2.5-7.5 fold) expression (Alcendor et al., 2007). SIRT7 was also shown to increase stress resistance of cardiomyocytes and prevent apoptosis and inflammatory cardiomyopathy in mice. Consistently, SIRT7-deficient mice developed hypertrophy of the heart and inflammatory cardiomyopathy with extensive fibrosis in the heart (Vakhrusheva et al., 2008a). SIRT3 was reported to have a role in

cardiac hypertrophy by augmenting FOXO3a-dependent antioxidant mechanisms. In fact, SIRT3-deficient mice showed signs of cardiac hypertrophy and interstitial fibrosis. Application of hypertrophic stimuli to these mice produced severe cardiac hypertrophy, whereas SIRT3-expressing transgenic mice were protected from similar stimuli (Sundaresan et al., 2009).

Increasing evidence has shed light on the role of sirtuins in inflammation. Inflammation is an important factor in the pathogenesis of several age-related degenerative diseases. NFκB has a central role in the innate immunity (Salminen et al., 2008). Two different sirtuins, SIRT1 and SIRT6, inhibit transcription of genes by NFκB. By damping the activation of NFκB, SIRT1 augmented apoptosis in response to the pro-inflammatory factor TNFα (Yeung et al., 2004), and protected pancreatic β cells against cytokine toxicity, NO production and iNOS expression (Lee et al., 2009). SIRT6 attenuates NFκB signalling by deacetylating histone H3k9 at NFκB promoter (Kawahara et al., 2009). Blockade of NFκB may protect against pro-inflammatory diseases.

**Sirtuins and neurodegeneration**

Sirtuins appear to play very different roles and respond in different ways to stress and toxicity. Growing evidence suggests that sirtuins are involved with opposing effects in the regulation of neuronal survival. For example, Pfister et al. reported that in cerebellar granule neurons SIRT1 had a protective effect against apoptosis induced by low potassium treatment while SIRT2, SIRT3, and SIRT6 induced apoptosis in otherwise healthy neurons. SIRT5 has a dual role depending on the subcellular localization. Moreover, in the same study SIRT6 was modestly protective in HT-22 neuroblastoma cells treated with homocysteic acid toxicity (Pfister et al., 2008).

At present, most research is focused on SIRT1 and SIRT2. SIRT1 is ubiquitously present in areas of the brain that are especially susceptible to age-related neurodegenerative states (e.g., the prefrontal cortex, hippocampus, and basal ganglia) (Zakhary et al., 2010).

Moreover, SIRT1 KO mice exhibit decreases in dendritic branching, branch length and complexity of dendritic arbours, and these mice show impaired cognitive abilities (Michan et al., 2010). The first evidence of SIRT1 neuroprotective role was seen in primary dorsal root ganglion neurons infected with lentivirus expressing slow Wallerian degeneration ($Wld^S$) protein. This protein is a chimeric nuclear protein spontaneously generated by an autosomic dominant mutation in what are called the $Wld^S$ mice that resulted in delayed axonal degeneration. Axonopathy is a critical feature of peripheral neuropathies as well as neurodegenerative disorders (Raff et al., 2002). Akari and colleagues found that $Wld^S$ protein increases Nmnat activity, an enzyme involved in NAD biosynthesis, leading to axonal protection and that SIRT1 is the downstream effector of this phenomenon (Araki et al., 2004). In a more recent study in *C.elegans*, the genetic overexpression or pharmacological activation by RES of the homologous of SIRT1, rescued early neuronal dysfunction phenotypes induced by the expression of the polyglutamine (polyQ) fragment of the Huntington disease–associated protein huntingtin (htt) in *C. elegans*. Moreover RES, in neuronal cell lines derived from the striatum of HdhQ111 KO mice, decreased cell death due to the expression of mutant htt (109Q). This effect appears to have been mediated by sirtuins since the effect was prevented by sirtinol or NAM (Parker et al., 2005). SIRT1 was also shown to protect neurons expressing mutant SOD1-G37R, a model of amyotrophic lateral sclerosis (Lee et al., 2010).

SIRT2 is highly expressed in the brain, particularly in oligodendrocytes, post-mitotic neurons and glial cells (Tang and Chua, 2008). SIRT2 downregulation in neurons by pharmacological treatment (with AK-1 and AGK2), rescued primary midbrain cultures from cell death caused by a mutant α-synuclein (A53T) (Outeiro et al., 2007). More recently, SIRT2 inhibition was shown to provide protection in a Huntington's disease model. As observed in Parkinson's disease models, SIRT2 inhibitors were neuroprotective in a *D. melanogaster* transgenic model expressing a Q93 repeat of the pathogenic human Htt and in a *C. elegans* Huntington's disease model (Luthi-Carter et al., 2010).

SIRT1 and APP metabolism

SIRT1 is upregulated in the brain in a mouse model of AD (Kim et al., 2007). However, in another model of AD reductions of cortical levels of SIRT1 coincided with the accumulation of tau (Julien et al., 2009). In humans with AD, SIRT1 levels are reportedly decreased in the parietal cortex which is affected by AD pathology but not in the cerebellum which is generally spared of AD pathology. Moreover, lower cortical levels of SIRT1 were found to be correlated with the duration of symptoms, lower global cognition scores, and accumulation of Aβ and tau in the cerebral cortex (Julien et al., 2009).

SIRT1 involvement in AD has been initially investigated in the context of CR. Epidemiological evidence suggests that individuals who maintain a low calorific diet have a reduced risk of developing AD (Luchsinger et al., 2002). Moreover it has been demonstrated that CR prevents Aβ neuropathology in an AD-like mouse model (Wang et al., 2005b). Pasinetti's group explored the involvement of SIRT1 in CR-mediated prevention of Aβ generation and deposition in SPs. Pharmacologically activating SIRT1 in neuronal cultures by NAD+ and RES treatment, reflected by reduced content of H4-k16ac, the accumulation of Aβ40 and Aβ42 peptides was prevented thus reproducing what they had previously found with CR (Wang et al., 2005b; Qin et al., 2006b). The mechanism proposed involved the regulation of the serine/threonine Rho kinase ROCK1, known in part for its role in the inhibition of the non-amyloidogenic α-secretase processing of APP. The same group found that under CR, FOXO3a was hyperphosphorylated and excluded from the nucleus and that nuclear FOXO3a was deacetylated by SIRT1 and its activity is inhibited. FOXO3a is a transcription factor, these two events lead to the repression of ROCK1 expression (Qin et al., 2008). Also in a non-human primate model, CR decreased cortical Aβ40 and Aβ42 and this reduction was inversely correlated to an increase in

SIRT1 and α-secretase in the same brain regions. These were associated with a reduction in ROCK1 (Qin et al., 2006a).

More recently, it was also demonstrated by Guarente's group that SIRT1 overexpression *in vivo* activates the transcription of ADAM10, the gene encoding α-secretase, through a mechanism involving deacetylation of the retinoic acid receptor β, a known regulator of ADAM transcription. ADAM10 activation by SIRT1 results in reduced production of Aβ and plaques in AD-like mouse model. Moreover increased α-secretase activity induced the Notch pathway, which is known to repair neuronal damage in the brain (Donmez et al., 2010; Qin et al., 2008).

SIRT1 and Aβ-induced inflammation

In mixed cortical cultures, Aβ exposure was shown to cause microglia-dependent toxicity through strong activation of NFκB signalling that was proposed to activate target genes, including cathepsin B and iNOS that are directly responsible for causing neuronal injury. In this model Aβ42 exposure was proposed to increase acetylation of RelA/p65 resulting in NFκB transcriptional activation in microglia. SIRT1 overexpression with lentivirus or its pharmacological activation by RES treatment, specifically deacetylated Lys 310 of RelA/p65 thus preventing NFκB activation and counteracting neuronal death induced by Aβ42 challenge (Chen et al., 2005b).

SIRT1 and Tau

In a recent study tau protein was found to be acetylated in primary neuronal cultures treated with low level of oligomeric Aβ. Tau acetylation was shown to be mediated by p300 while SIRT1 has been proposed to deacetylate tau *in vitro*. Furthermore, SIRT1 inhibition increases tau acetylation and this event blocks tau polyubiquitination and its degradation via the ubiquitin-proteasome system, resulting in p-tau accumulation (Min et

al., 2010). SIRT1 deacetylation of tau, although not yet demonstrated *in vivo*, could be an additional mechanism through which SIRT1 could counteract AD pathology.

# 1.3. AIMS OF THE STUDY

The overall purpose of this research was to investigate, for the first time, the involvement of all 7 known sirtuins (SIRT1-7) in AD through a number of complementary experimental approaches. These included gene mutation analysis and genetic association studies; the application of a non-pharmacological therapeutic protocol *in vivo* to the APP23 mouse model of AD and the use of *in vitro* analyses to explore the potential role of SIRT1 in the pathogenesis of AD.

## Specific aims

GENETIC STUDIES SECTION

I. To conduct a mutational analysis of coding regions of sirtuin genes in relation to possible association with AD susceptibility. (chapter 3)

II. To test using a case-control cross-sectional approach the extent of the association between sirtuin gene common variants (previously known and newly identified) and AD risk. (chapter 4)

*IN VIVO* SECTION

III. To investigate the effectiveness of an environmental enrichment protocol in delaying progression of AD-like pathology in a mouse model (APP23) of AD and in turn

assess sirtuin expression levels, in relevant regions of the brain affected by AD pathology. (chapter 5)

*IN VITRO* SECTION

IV. To investigate the potential role of SIRT1 in promoting cell survival response against exposure of SK-N-BE(2) cells to different stress stimuli that are commonly linked to AD etiopathogenesis. (chapter 6)

# *CHAPTER 2:*

# *GENERAL MATERIALS AND METHODS*

In this section I will describe the general materials and methods I have used during my experiments. Specific methods will be discussed in detail in subsequent associated chapters.

## 2.1. SUPPLIERS

Abcam (Cambridge, UK)

Abnova (Taipei, Taiwan)

Ambion (Austin, Texas, USA)

Applied Biosystems (Foster City, California, USA)

Asahi Techno Glass (Funabashi City, Chiba)

Axxora Life Sciences (San Diego, California, USA)

Bio-Rad Laboratories (Hercules, California, USA)

Biotium (Hayward, California, USA)

Charles River Laboratories (Wilmington, Massachusetts, USA)

Chemicon (Temecula, California, USA)

Eppendorf (Hamburg, Germany)

Immuno-Biological Laboratories (Fujioka, Japan)

Invitrogen (Carlsbad, California, USA)

Leica Microsystems (Wetzlar, Germany)

Lillico Biotechnology (Surrey, UK)

MBL (Woburn, Massachusetts, USA)

Millipore (Billerica, Massachusetts, USA)

MityFlex (ANKO, Bradenton, Florida, USA)

Molecular Devices (Sunnyvale, California, USA)

Olympus (Tokyo, Japan)

Pierce-Thermo Scientific (Waltham, Massachusetts, USA)

Promega (Madison, Wisconsin, USA)

Sigma-Aldrich (St. Louis, Missouri, USA)

Signet Covance (Princeton, New Jersey, USA)

Termo Fisher Scientific (Waltham, Massachusetts, USA)

Transgenomic (Omaha, Nebraska, USA)

Upstate (Charlottesville, Virginia, USA)

Vector Laboratories (Burlingame, California, USA)

Veeco Instruments (Plainview, New York, USA)

Waters (Milford, Massachusetts, USA)

# 2.2. GENETIC STUDIES SECTION

## 2.2.1. RECRUITMENT OF AD PATIENTS AND CONTROLS

All the subjects involved in this work were recruited from the Northern Italy and Italian Canton of Switzerland. Briefly they derived from "Luigi Sacco" hospital in Milan (Italy), "Beata Vergine" hospital in Mendrisio (Italian-speaking canton of Switzerland), "S. Antonio Abate" hospital in Gallarate (Italy) and "Centro S.Giovanni di Dio-Fatebenefratelli" hospital in Brescia (Italy). The demographics of each cohort are described in the materials and methods sections of chapters 3 and 4. Informed consent was obtained from all subjects.

Patients were diagnosed according to DSM-IV, and National Institute of Neurologic and Communicative Disorders and Stroke–AD and Related Disorders Association (NINCDS–ADRDA) criteria for probable AD (McKhann et al., 1984), and had an age at onset greater than 60 years. Control subjects (CT) were recruited including elderly subjects cognitively healthy.

MMSE was employed both in AD and CT groups to confirm or exclude the presence of cognitive decline. CT subjects were selected with a MMSE score higher than 23 points.

## 2.2.2. GENOMIC DNA ISOLATION FROM PERIPHERAL BLOOD SAMPLES

For each subject included in the study 5 mL of peripheral blood was collected in tubes with ethylenediaminetetraacetic acid (EDTA) and stored on ice. The blood was then sub-aliquoted into smaller volumes of 200 µL and stored at -20 °C until it was necessary. Genomic DNA (gDNA) from 150 µL of blood was extracted using standard procedures by

a semi-automated vacuum-based nucleic acid extractor ABI PRISM® 6100 Nucleic Acid PrepStation (Applied Byosistems). Then, it was eluted in 200 µL of nuclease free water and the sample concentration determined by Nanodrop 1000 (Thermo Fisher Scientific). The resultant DNA samples were then stored at 4 °C.

### 2.2.3. POLYMERASE CHAIN REACTION

Polymerase chain reaction (PCR) was used to amplify gDNA for further analysis. PCR amplification was usually carried out in a reaction volume of 20 µL containing:

- 1 µL template DNA ~ 40 ng/µL
- 1 µL of both forward and reverse primer 10 µM (Invitrogen)
- 2 µL dTNPs 2.5 mM (Thermo Fisher Scientific)
- 0.2 µL Taq polymerase 5 U/µL (Thermo Fisher Scientific)
- 2 µL PCR buffer 200 mM Tris-HCl, 500 mM KCl (Thermo Fisher Scientific)
- 0.6 µL $MgCl_2$ 25 mM (Thermo Fisher Scientific)
- 12.2 µL deionised water

The following PCR programs were employed for PCR reactions on thermocyclers (Eppendorf). In most of the cases, the conventional 3 step PCR protocol was applied whereas, when the difference between the annealing temperatures of the two primers was higher than 3 °C, the touchdown PCR protocol was used to reduce non-specific PCR products.

The standard PCR cycle consisted of 1 cycle at 95 °C for 5 min, followed by 30-35 cycles of 30 s at 95 °C (denaturation), 30 s at 50-68 °C (annealing) and 45-120 s at 72 °C (extension), and finished with 10 min at 72 °C.

The touchdown PCR protocol consisted of a denaturation step at 95 °C for 5 min, followed by 14 cycles at 95 °C for 30 s, 50-68 °C for 30 s and 72 °C for 30 s. The annealing temperature was dropped by 0.5 degrees each cycle, then samples underwent 19 cycles at 95 °C for 30 s, 50-68 °C for 30 s and 72 °C for 1 min. Finally, 10 min at 72 °C.

The PCR protocols used were issued from free online software Optimase ProtocolWriter™, provided by Transgenomic® at http://www.mutationdiscovery.com/md/MD.com/home_page.jsp.
The specific annealing temperatures and extension time, for each DNA sequence amplified in this thesis, will be reported in the relevant results chapters.

**Primer design and synthesis** Oligonucleotide primers for PCR were designed to amplify DNA from regions of interest. Starting from gene sequences obtained from the Entrez Nucleotide database at the National Centre of Biotechnology Information website (http://www.ncbi.nlm.nih.gov/nuccore), sense and antisense primer sequences were designed with the free online primer design software 'Primer 3' at http://frodo.wi.mit.edu/cgi-bin/primer3/primer3. Primer lengths ranged from 20 to 25 nucleotides. Primers were provided lyophilised by Invitrogen and were resuspended in DNase free water to a final concentration of 100 µM before use.

### 2.2.4. AGAROSE GEL ELECROPHORESIS OF DNA

gDNAs and PCR products were resolved on agarose gels at 0.6% and 1%, respectively. Agarose (Thermo Fisher Scientific) was melted in 1x TAE buffer from 50x stock solution (242 g Trizma base, 100 mL 0.5 mM EDTA, 57.1 mL glacial acetic acid) in a microwave.

The gel mixture was left to cool for 10 min and then Gel Red (Biotium) was added to the agarose solution at 1:30 dilution for DNA labelling. Gel mixture was then poured into the gel tray and the combs inserted. The gel was left to set for 20 min before being placed into the electrophoresis tank (Bio-Rad Laboratories). The tank was filled with 1x TAE buffer. DNA size standard ladder and the samples for genotyping were loaded and the gel was run at 10 V/cm (interelectrode distance), while the electrophoresis time was dependent on the size of the fragments to be resolved. The gel was then viewed using a UV box (Thermo Fisher Scientific) and photographed.

Individual samples to be loaded were prepared by mixing 5 μL of DNA sample with 1 μL loading buffer starting from 10x stock solution (500 μL glycerol, 40 μL bromophenol blue or xylene cyanol 10%, 418 μL $H_2O_2$).

The DNA size standard ladder comprised 100 bp (fragments ranging in length from 100 to 1.5 kbp) or 1 kbp DNA ladder (fragments ranging in length from 250 to 10 kbp) (Promega) and was used to decipher the size of DNA bands visualised on agarose gels.

### 2.2.5. dHPLC ANALYSIS

dHPLC was used to identify polymorphisms within PCR-amplified DNA fragments. In this technique the PCR amplified fragments (i.e. amplicons) were denatured (95 °C for 10 min) and slowly cooled to allow the formation of homoduplexes and, if a polymorphism was present heteroduplexes. The renatured PCR products (5-8 μL) were then injected into a HPLC column that contained a DNASep (Transgenomic) cartridge and triethylammonium acetate buffer. The DNASep cartridge is based on ion-pair-reversed phase HPLC methodology. The positive charges on the triethylammonium ions interact with the negative charges on the phosphodiester backbone of the DNA giving the DNA molecules a

hydrophobic coating. These hydrophobic trialkyl groups interact with the hydrophobic surface of the DNASep matrix and immobilize the DNA in a size-dependent manner. During the experiment the concentration of acetonitrile running through the column was gradually increased and the DNA was eluted from the column in a size-dependent manner. The DNASep cartridge also has the abililty to resolve two fragments of the same size but different helical content. A UV sensor then detects eluted samples. At a given melting temperature, samples containing heteroduplexes will denature before homoduplexes and will therefore elute from the column first (figure 2.1). Chromatographic profiles are generated for each fragment based on the time it eluted from the column and its absorption, allowing the detection of samples containing polymorphisms. The presence of a polymorphism was then confirmed and characterised by direct sequencing.

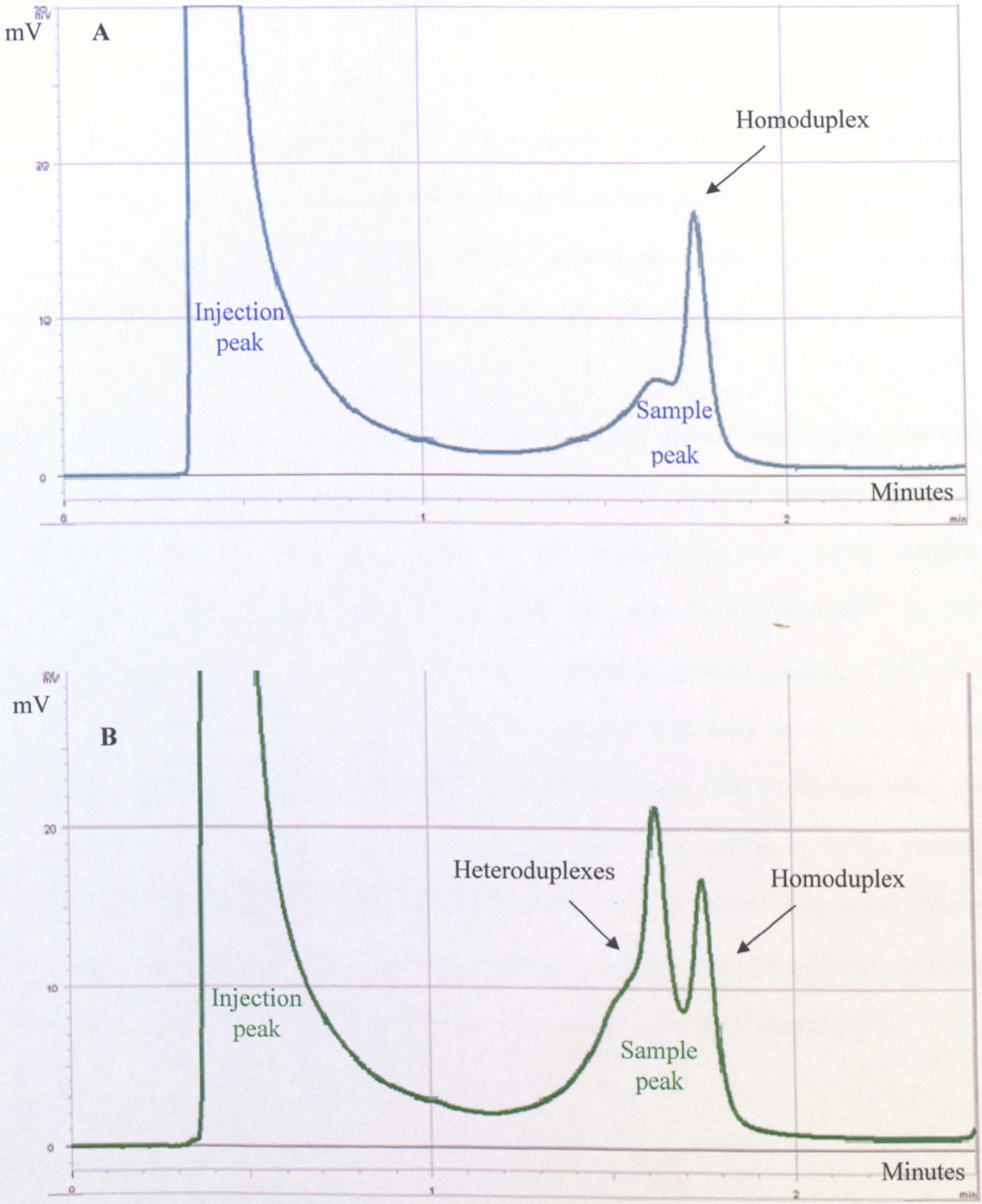


**FIGURE 2.1. Examples of dHPLC chromatographic profiles.**

***A.*** *Single-peak dHPLC profile;* ***B.*** *Aberrant dHPLC profile.*

The dHPLC machine uses four buffers: Buffer A (5 mM triethylammonium acetate [TEAA][Transgenomic], 0.25% acetonitrile [ACN][BDH] in $H_2O$), Buffer B (5 mM TEAA, 25% ACN in $H_2O$), Buffer C (75% ACN in $H_2O$) and Buffer D (8% ACN in $H_2O$). Buffers A and B were used in fragment analysis and throughout the run the ratio of buffer B to buffer A is increased to elute the DNA from the column. Buffer C is used to clean the system after use and Buffer D to wash the syringe before use. Before each run the system was equilibrated for 10-20 min by washing the column at 0.9 mL/min with Buffer A.

**Setting of melting temperature.** Amplicons analysed by dHPLC were shorter than 600 bp. Prior to the sample injection of each DNA fragment, the expected 'wild-type' sequence (usually uploaded from the Entrez Gene database at the NCBI website (http://www.ncbi.nlm.nih.gov/gene), was analysed using WAVEMAKER™ v. 3.4 (Transgenomic). This software identifies the temperature at which domains within the fragment were approximately 75% helical. A sequence may have one or a number of domains, each with different temperatures at which this helical state is achieved. All of the temperatures determined by the programs were used. The setting up of the melting temperature was determined by running the renatured PCR product with a temperature gradient around the theoretical melting temperature suggested by the software. Analysis methods for each melting temperature were then created using WAVEMAKER™.

## 2.2.6. DIRECT SEQUENCING

PCR products were purified using a commercial kit (PCR clean up system) according to the customer indications. DNA samples were resuspended in 50 μL nuclease-free water (Promega). The amount of DNA was quantified by spettrophotometric analysis (Nanodrop 1000, Thermo Fisher Scientific). A concentration of gDNA (10 ng for each 100 bases

transcript to be sequenced) and 12.8 µL of the specific primer (10 µM) were outsourced to a sequencing facility (Primm, http://www.primmbiotech.com). After having received raw data, chromatograms were analysed using Chromas Lite software (freely available at http://www.technelysium.com.au/chromas_lite.html). The presence of overlapping peaks in resultant chromatograms identifies heterozygous substitution at individual base locations (figure 2.2). Identified substitutions were later characterized referring to NCBI reference sequences (chromosome position, nucleotide position along the gene and eventual codon change for substitution in the coding regions).

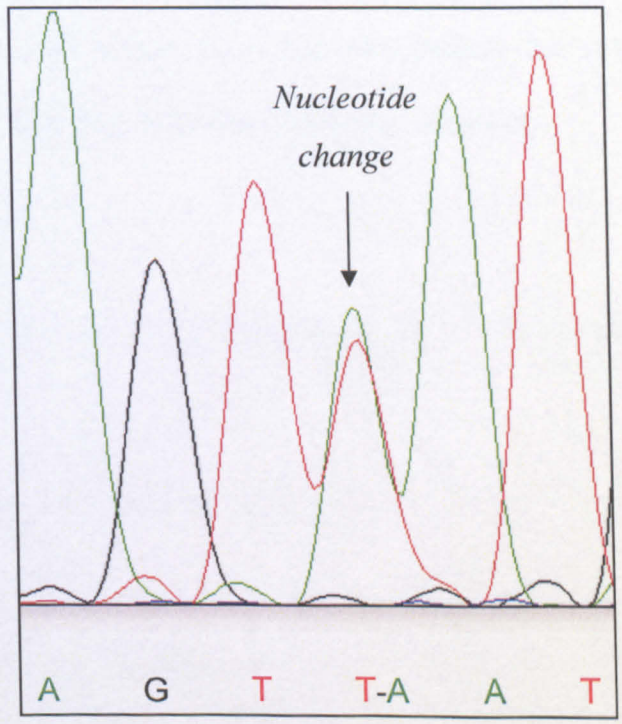


**FIGURE 2.2. Sequencing chromatogram of a heterozygote sample.**

*Example of a PCR amplicon with a heterozygous SNP highlighted by the presence of two overlapping peaks. In this case, one allele carries a T, while the other has an A. Both peaks are present, but at roughly half the height they would ordinarily be at if they were homozygous.*

### 2.2.7. SEQUENOM MassARRAY™

Sequenom MassARRAY™ platform (Sequenom) allows the high-throughput SNP genotyping of up to 40 SNPs simultaneously within a single well of a 384-well plate. The principle of the MassARRAY system is the extension of an oligonucleotide probe over a SNP site in a PCR product, with a mixture of deoxynucleotides and dideoxynucleotides, to produce different size products for each allele of a SNP. The extended products are analyzed by Sequenom with matrix assisted laser desorption/ionization-Time-of-Flight mass spectrometry (MALDI-TOF), and the time-of-flight is proportional to mass, thereby allowing precise determination of the size of products generated, which can be converted into genotype information (figure 2.3). For this project the sequenom analysis was performed by dr. Mayhaus from Saarland University, Germany.

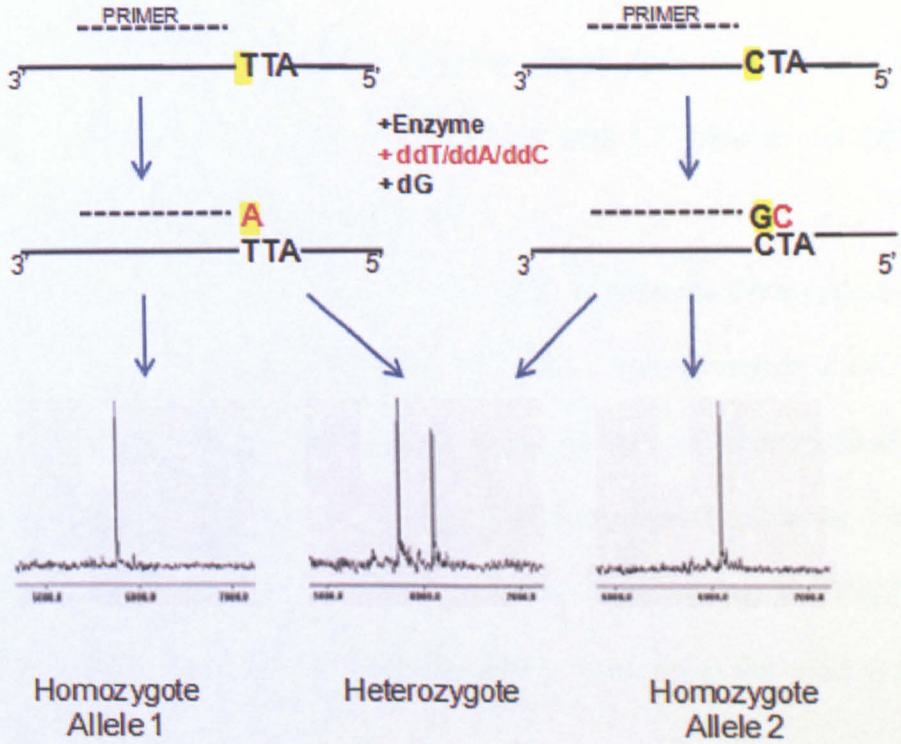


**FIGURE 2.3. Sequenom MassARRAY™.**

*Revised from www.currentprotocols.com*

*The assay consists of the initial annealing of an oligonucleotide primer immediately upstream of the polymorphic site of interest. This step is followed by single base extension using mass-modified dideoxynucleotide terminators. Only the complementary base to the polymorphic nucleotide (Allele 2) will allow primer extention. Using MALDI-TOF mass spectrometry, the distinct mass of the extended primer identifies the SNP allele.*

## 2.2.8. ALLELIC DISCRIMINATION BY REAL TIME-PCR

Allelic discrimination genotyping was performed by Real Time-PCR (RT-PCR) (7300 RT-PCR system, Applied Biosystems). Pre-developed TaqMan® MGB probes [C_71547 for *SIRT2* rs10410544 or C_904973 and C_3084793 for *APOE* rs7412 and rs429358, respectively], along with TaqMan® Genotyping Master mix (Applied Byosistem) were used. Custom TaqMan® MGB probes were labelled with a 5' reporter dye (allele 1 FAM, allele 2 VIC) and a 3' non-fluorescent quencher.

PCR reactions were carried out under the following conditions: denaturation at 95 °C for 10 min followed by a 15 s annealing at 92 °C and a 1 min extention at 60 °C that were repeated for 40 cycles. We performed a pre-read (background fluorescence) and a post-read after the PCR run, according to customer instructions outlined in the ABI 7300 User Manual. Each sample was characterized as either homozygote for FAM or VIC or heterozygote. A positive control for each genotype was run in the plate together with a blank.

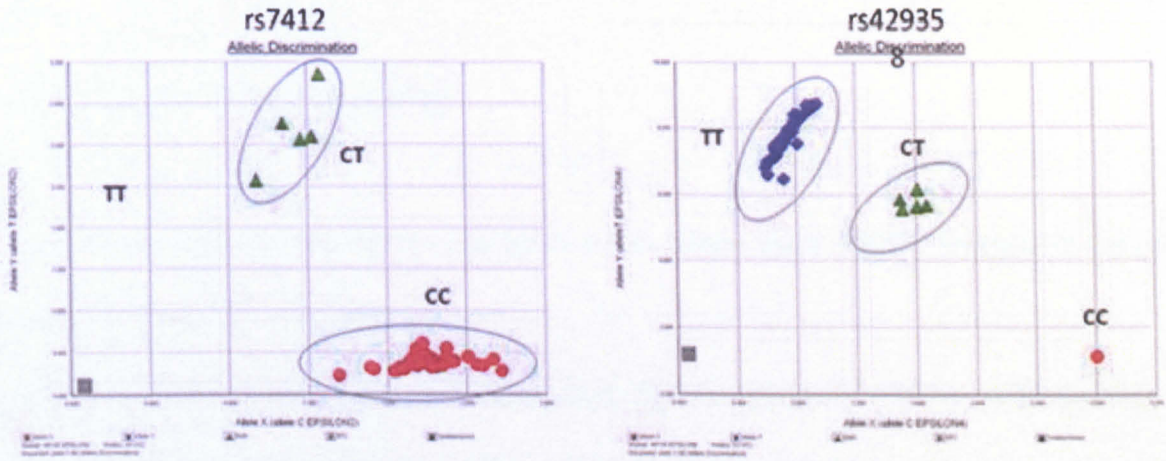


| Rs7412 | Rs429358 | *APOE* Genotype |
|---|---|---|
| TT | TT | ε2//ε2 |
| CT | TT | ε2//ε3 |
| CT | CT | ε2//ε4 |
| CC | TT | ε3//ε3 |
| CC | CT | ε3//ε4 |
| CC | CC | ε4//ε4 |

**FIGURE 2.4. RT-PCR Allelic Discrimination assay for genotyping *APOE*.**

*Allelic discrimination cluster plots of the two SNPs that together determine the three main genetic variants of APOE. In the table, to the way in which APOE genotypes are determined from the two different assays are illustrated.*

# 2.3. *IN VIVO* STUDIES

## 2.3.1. MOUSE MODEL: APP23

The animals used for the *in vivo* section of this thesis were APP23 transgenic mice and their wild-type (WT) littermates.

APP23 mice are hemizygous for the human full length *APP* ($APP_{751}$), harbouring the "Swedish" double mutation at position 670/671 (KM → NL), under the murine Thy-1 promoter (figure 2.5.A). These mice display a 7-fold overexpression of the transgene in the neocortex and hippocampus (figure 2.5.B) (Sturchler-Pierrat et al., 1997). These mice were kindly provided by dr. Matthias Staufenbiel (Novartis Pharma).

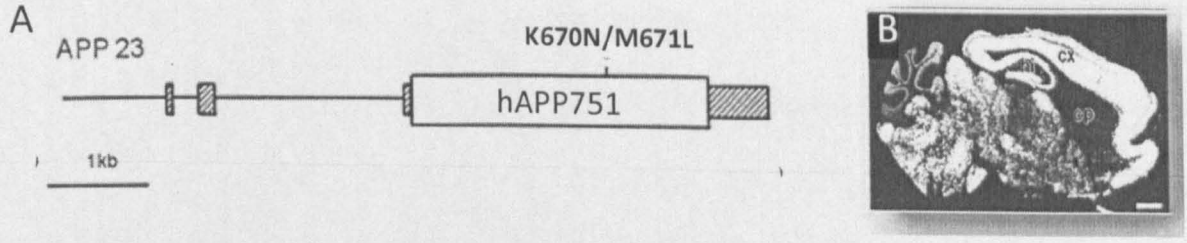


**FIGURE 2.5. Transgenic transcription unit and expression in APP23 transgene mice**

***A**. Transcription unit for APP23 transgenic mice. Hatched boxes represent the murine Thy-1 exons. hAPP751 cDNA is shown as open box with vertical line marking the position of the "Swedish" mutation (K670N/M671L).* ***B**. Expression of APP mRNA assessed by* in situ *hybridization in 24-month-old APP23 mice. Figure modified from* (Sturchler-Pierrat et al., 1997).

APP23 transgenic mice, originally established in a C57BL/6xDBA2 background (Sturchler-Pierrat et al., 1997), were back-crossed into the C57BL/6N genetic background, by crossing APP23 with C57BL/6N purchased from Charles River Laboratories, for more than six generations.

Procedures involving animals and their care were conducted and conformed with the institutional guidelines in compliance with national (D.L. n. 116, G.U., suppl. 40, Feb. 18, 1992) and international laws and policies (EEC Council Directive 86/609, OJ L 358, 1, Dec.12, 1987; Guide for the Care and Use of Laboratory Animals, U.S. National Research Council, 1996).

### 2.3.2. MOUSE GENOTYPING

Genotyping was performed on genomic DNA (gDNA) obtained from tail biopsies of mice at weaning age. A small terminal portion of the mouse tail was completely digested by overnight incubation at 55 °C with a lysis buffer containing 0.1 mg/mL Proteinase K (Promega). gDNA was then extracted with WizardR SV Genomic DNA Purification System (Promega), according to the manufacturer's instructions. The presence of the human APP transgene was verified by PCR analysis (cfr. 2.2.3). Mice β-globin gene was also amplified a control of DNA quality.

The primer sequences used are reported in table A.6. in the appendix.

## 2.3.3. ENVIRONMENTAL ENRICHMENT PROTOCOL

Mice were weaned at 1 month of age and caged in standard housing conditions. At 3 months of age, mice were moved to enriched cages. Enrichment cages (44 x 52 x 28 cm) were approximately double the dimension of standard cages (26 x 42 x 18 cm). They were furnished with a variety of different coloured plastic objects (e.g. crawling balls, igloos, tunnels purchased from Lillico Biotechnology) and hydraulic tubes. The objects were combined together to provide a more complex environment and were re-positioned or changed twice per week to provide novel stimulation. Environmental enrichment lasted till the end of the experiment (i.e. mice sacrifice).

Mice which has experienced the enriched environment 'enriched mice' were compared to mice housed under standard conditions for the duration of the experiment.

Standard and enriched cages each housed a maximum of 4 mice. All cages were kept in the same room, were maintained on the same 12:12 h light:dark cycle, and were exposed to the same level of intrusions from experimenter and the presence of caretaker in the room. Food and water were provided ad libitum.

## 2.3.4. BEHAVIORAL TESTS

### *2.3.4.1. Morris Water Maze*

Animals were trained in a circular water tank (1.5 m in diameter and 0.5 m high) which was filled with water that was maintained at 22 °C. Four points on the perimeter of the pool were designated north (N), east (E), south (S) and west (W), thus dividing the pool

into four quadrants (NW, NE, SE, SW). A 10x10 cm white platform was hidden in the centre of SW quadrant with the top of the platform submerged 1 cm below the surface of the water. A nontoxic white powder was added to the water to facilitate tracking the black mice and to obscure the platform. The pool was in the centre of a room containing various salient visual cues. Illumination was held constant. A tracking system was used to record mouse behaviour (EthoVision® XT, Noldus). The camera was mounted directly over the centre of the maze.

All animals were initially trained in the Morris maze for 10 days. Each day consisted of four trials with an approximate 30 min inter-trial interval. During training trials, the submerged platform remained at a fixed position. Each day of training, the direction from which the animal started was varied during the 4 training trials (i.e. N, S, W and E) to prevent the association of the platform location with a single constellation of cues. Latency from immersion into the pool to escape onto the platform was recorded automatically by the tracking system. If the animal located the platform during the 1 min trial, it was allowed to remain on the platform for an additional 10 s. If the animal did not find the platform within the allotted 1 min, then the animal was guided to the platform, where it remained for 10 s before being removed from the pool.

The probe trial was performed at the $11^{th}$ day (24 h after the last training trial) by removing the platform and measuring the time spent in the four quadrants within 1 min trial. Learning (acquisition) was infered by plotting escape latencies against day of training. Memory (retention) was expressed as the percentage of time spent in the correct quadrant (SW) in the probe trial.

### *2.3.4.2. Object recognition test*

Mice were tested in an open-square gray arena (40 × 40 cm), 30 cm high, with the floor divided into 25 squares by black lines. The following objects were used: a black plastic cylinder (4 × 5 cm), a glass vial with a white cup (3 × 6 cm), and a metal cube (3 × 5 cm). The task started with a habituation trial during which the animals were placed in the empty arena in the absence of any specific stimulus for 5 min, and their movements were recorded as the number of line crossings. Outer quadrant (anxious behaviour) and inner quadrant (self-confident behaviour) crossing were counted separately.

The next day, mice were again placed in the same arena containing two identical objects (familiarization phase). Exploration was recorded in a 10-min trial. Sniffing, touching, and stretching the head toward the object at a distance not more than 2 cm were scored as object investigation.

Twenty-four h later (test phase) mice were again placed in the arena containing two objects: one identical to one of the objects presented during the familiarization phase (familiar object), and a new, different one (novel object), and the time spent exploring the two objects was recorded for 10 min. Memory was expressed as a discrimination index (IE = (seconds on novel – seconds on familiar object)/(seconds on novel + seconds on familiar object).

The positions of the objects were randomly permuted for each animal from an experimental group and the arena was cleaned between trials with EtOH diluted in water.

## 2.3.5. DISSECTION OF MOUSE CORTICES AND HIPPOCAMPI FOR BIOCHEMICAL ANALYSES

Mice were anaesthetized by intraperitoneal injection of avertin 2.5% (400 mg/kg) and sacrificed by decapitation. The brains were removed from the skull and laid on an ice-chilled dish; the cerebellum was removed and discarded. The brain was cut along the sagittal line. The two hippocampi and the two cortices were dissected and weighted. Tissue samples were also taken and homogenized for biochemical analyses.

## 2.3.6. RNA EXTRACTION AND RELATIVE QUANTITATIVE RT-PCR

Total RNA was extracted from tissue lysates with SV Total RNA Isolation System (Promega).

Tissues (~ 10 mg weight) were resuspended in 175 µL lysis buffer and homogenated by a syringe needle. Lysates were then cleared by centrifugation at 14 000 rpm for 15 min at 4 °C. Supernatants were processed to obtain RNA according to the manufacturer's instructions.

RNA concentration was measured by capillary electrophoresis and sample purity was determined by 260 nm/280 nm absorbance ratio readings. RNA was aliquoted and stored at -80 °C until use.

All steps were carried out at room temperature with RNase-Zap (Ambion).

A total of 1 µg RNA was reversed transcribed into cDNA in a 20 µL reaction mixture with High-Capacity cDNA Reverse Transcription Kit (Applied Biosystems) according to the manufacturer's instructions.

RT-PCR assays were run on the Applied Biosystems 7300 RT-PCR System under the following thermal conditions: 10 min at 95 °C once, and 40 cycles of 15 s at 95 °C and 1 min at 60 °C.

RT-PCR were prepared using 50 ng of cDNA, 2x TaqMan® Master mix and 20x TaqMan® gene expression assays (Applied Biosystems, cfr table A.4.in the appendix).

The fluorescence emitted after each cycle was measured and plotted (in log scale) against the cycle number. *A posteriori* the threshold was determined and the raw data (threshold cycle, $C_T$) were used for the analysis of mRNA expression. The relative expression of each gene was calculated by the delta delta $C_T$ method ($\Delta\Delta C_T$) (Livak and Schmittgen, 2001) according to the following formula:

$$\text{Amount of target} = 2^{-\Delta\Delta C_T}$$

Where $\Delta\Delta C_T = [(C_{T,\text{target gene}} - C_{T,\text{reference gene}})_Q - (C_{T,\text{target gene}} - C_{T,\text{reference gene}})_{CB}]$

Q= any sample (e.g. treated cells) and CB= calibrator (i.e. control condition).

All samples were run in triplicate in the same 96-well plate.

## 2.3.7. PROTEIN ANALYSES

### *2.3.7.1. Protein extraction from tissues.*

Ice-cold Lysis Buffer pH 7.4 (50 mM Tris/HCl, 150 mM NaCl, 0.5 mM EDTA and 1% Triton X-100) was prepared. A further 1% of a broad-range protease inhibitor cocktail and

1 mM Sodium Butyrate (inhibitor of class I and II deacetylase) (Sigma-Aldrich) was also added.

Tissues were homogenated by a Teflon-on-glass homogeniser with 1 mL/g of tissue ice-cold lysis buffer. Lysates were then cleared by centrifugation at 14 000 rpm for 15 min at 4 °C. Supernatants were sub-aliquoted and stored at -80°. Small aliquots were taken for protein quantification.

Protein concentration of supernatants was measured by BCA protein assay (Pierce-Thermo Scientific) according to the manufacturer's instructions.

### *2.3.7.2. SDS-polyacrylamide gel electrophoresis and western blotting*

Sample preparation - 10 µg of tissue lysates were denatured by boiling in SDS sample buffer (125 mM Tris-HCl pH 6.8, SDS 10%, glycerol 10%, bromophenol blue 0.006 %) added with 0.1 M DTT at 95 °C for 5 min.

Electrophoresis and western blotting (WB) - Proteins were electrophoresed on 6-12% polyacrylamide gels using the Mini-PROTEAN® gel electrophoresis system (Bio-Rad Laboratories). Gel electrophoresis was carried out in 1x running buffer for about 1.5 h at 25 mA. Bio-Rad Dual Color standard ladder (Bio-Rad Laboratories) was also loaded to confirm the sizes of the proteins being investigated.

Proteins were electroblotted onto a 0.2 µM nitrocellulose membrane using a Mini-Transblot® apparatus (Bio-Rad Laboratories) in 1x transfer buffer for 1.5 h at 350 mA.

### *2.3.7.3. Slot blot*

A total of 5 µg of tissue lysates were diluted in TBS at a final volume of 200 µL. Samples were loaded onto a 0.2 µM nitrocellulose membrane using a Bio-Dot® (slot format, SB) apparatus (Bio-Rad Laboratories) integrated with a vacuum pump.

### *2.3.7.4. Immunodetection*

The nitrocellulose membranes after WB or SB were blocked with 5% skim milk powder (Sigma-Aldrich) in 1x TBS supplemented with 0.1% Tween-20 (TBS-T) for 1 h with gentle shaking. Membranes were then incubated with the specific primary antibody in 5% skimmed milk/TBS-T solution overnight at 4 °C with gentle shaking. The following day, membranes were washed 3 x 5 min in TBS-T and probed with the appropriate secondary antibody (HRP-conjugated Ig antibody) for 1 h at room temperature with gentle shaking. Membranes were washed 2 x 15 min in TBS-T and placed in ECL substrate reagent (Millipore) for 4 min. Membranes were exposed to a Kodakon film in a dark room.

Films were scanned on an Epson scanner and band intensities measured using Image J (National Institutes of Health). The obtained values were normalized to the corresponding β–globin band intensity and expressed as percentage of the basal value registered in the control sample.

### *2.3.7.5. Enzyme-linked immunosorbent assay*

Human Amyloidβ (1-40) (N) and Human Amyloidβ (1-42) (N) Enzyme-Linked ImmunoSorbent Assay (ELISA) (IBL) were used to measure Aβ40 and Aβ42 amyloid

peptides. A pilot experiment was carried out on two samples at four different dilutions ranging from 1:10 to 1:100 to estimate the appropriate dilution of tissue protein homogenates for the final experiment.

The ELISA assays were performed on tissue homogenates according to manufacturer's instructions.

### 2.3.8. INTRACARDIAC BRAIN PERFUSION

For mice for which the brain was processed for immunohistochemistry (IH) they were perfused as follows. Mice were anaesthetized by intraperitoneal injection of avertin 2.5% (400 mg/kg) and, after mice were unresponsive to a foot pinch, secured on a silicon support. The chest cavity was opened by cutting across the abdomen just below the sternum and then the diaphragm was carefully cut. The body cavity was exposed by clamping the ribs on each side and, where necessary, connective tissue was cut to free the heart from the chest cavity. A butterfly needle (25 gauge) was inserted into the left ventricle, the right auricle was cut and the animal was slowly perfused. The needle was connected, by a plastic tube, to a peristaltic pump (Mityflex) that allows a controlled-speed efflux of the perfusion solutions into the whole body. Ice-cold Phosphate Buffer Saline (PBS) was first delivered for 2 min to wash out blood and then 4% paraformaldehyde (PFA) for 4 min allowed the cross-linking of tissues, therefore their preservation. After perfusion was completed, the animal was decapitated and the brain quickly explanted and placed in 4% PFA for 2-3 h in post-fixation. The tissue was finally placed overnight in a solution of 20% sucrose and then for a second overnight incubation in a solution of 30% sucrose to ensure cryoprotection and quickly frozen in-pentan at – 45 °C.

## 2.3.9. IMMUNOHISTOCHEMISTRY

Sagittal sections (30 µm) of the whole frozen brain (cfr. 2.2.4) were cut using a cryostat (Leica Microsystems) and dipped in 24-well plates containing PBS. Free-floating sections were incubated in 0.6% $H_2O_2$ solution in PBS for 10 min to inactivate the endogenous peroxidases. After washing in PBS, the slices were incubated for 30 min in 0.1% Triton X-100, 3% normal goat serum (Vector Laboratories). Then, the slices were incubated overnight at 4 °C with 6E10 primary antibody (diluted 1:200, Chemicon). The next day, after three washes in PBS, the sections were incubated with the secondary biotinylated goat anti-mouse antibody (1:400, Vector Laboratories) for 1 h at room temperature. Then, 1% avidin-biotin horseradish peroxidase complex (Vector Laboratories) was added for 1 h. Peroxidase activity was determined by reaction with a solution containing Diaminobenzidine (Sigma-Aldrich) and nickel ammonium sulfate (Sigma-Aldrich).
The sections were mounted on slides, dried, dehydrated and covered with mounting medium (Thermo Fisher Scientific).

Briefly, using a light microscope (BX51, Olympus), 10X images (219×164 µm size) were captured with a video camera (Olympus), and projected onto a computer monitor. Plaque load quantification was performed with ImageJ (National Institutes of Health) by executing a macro specifically written in our laboratory. Four sections per animal were counted and averaged to obtain the mean ± standard error of the mean (SEM) for each animal.

# 2.4. *IN VITRO* CELLULAR SECTION

## 2.4.1. CELL CULTURE: SK-N-BE(2)

SK-N-BE(2) (ECACC 95011815) cell line is established from a bone marrow biopsy of a 22-month-old Caucasian male with disseminated neuroblastoma. SK-N-BE(2) cells were cultured in Dulbecco's Modified Eagle's Medium (DMEM) supplemented with 10% Foetal Bovine Serum, 2 mM L-glutamine, 100 U\mL penicillin and 100 µg\mL streptomycin (Invitrogen).

SK-N-BE(2) cells were grown as monolayer in flask. Cells were incubated at 37 °C in 5% $CO_2$ humified atmosphere. SK-N-BE(2) cells were routinely split by removing medium from confluent flasks. After washing with PBS (Invitrogen), to remove any trace of serum. cells were incubated with a minimal volume (500 µL\25 $cm^2$ flask) of trypsin\EDTA solution (0.05% trypsin and 0.02% EDTA in PBS) for 1 min at 37 °C. Trypsin was inhibited by adding 2.5 mL of fresh medium and cells were seeded in the appropriate flasks.

SK-N-BE(2) cells were differentiated into a neuronal-like phenotype with retinoic acid (RA) (Sigma-Aldrich).

Cells were seeded in multi-well plates (Asahi Techno Glass) in complete medium. After 4 h, the medium was removed and 200 µL of freshly prepared medium without serum and supplemented with 10 µM RA was added. After 4-5 days cells showed a differentiated phenotype (figure 2.6.). All specific treatments started on the $5^{th}$ day after RA supplementation. RA was renewed 2 days after cell seeding, and just before the starting of cell treatments.

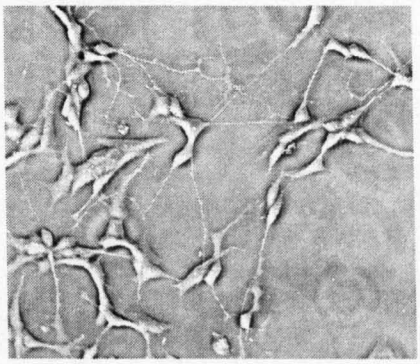

**FIGURE 2.6. Differentiated SK-N-BE(2) by retinoic acid treatment.**

## 2.4.2. CELL VIABILITY ASSAY

Cell viability was assessed with the CellTiter 96® Aqueous One Solution Cell Proliferation Assay (Promega) that contains a tetrazolium compound [3-(4,5-dimethylthiazol-2-yl)-5-(3-carboxymethoxyphenyl)-2-(4-sulfophenyl)-2H-tetrazolium, inner salt; (MTS)] and an electron coupling reagent (phenazine ethosulfate; PES) in a unique aqueous reagent. Cell viability was assessed by measuring the level of cellular conversion of MTS into a water-soluble colored formazan product. The assay was performed by adding the reagent (10%) directly to culture medium, incubating for 4 h at 37 °C and then recording the absorbance at 490 nm with a plate reader (Molecular Devices). The absorbance recorded was directly proportional to the number of living cells in culture. Data were presented as the percentage of viable cells in the treated group with respect to untreated control cultures. All cell viability assays were performed in triplicate.

### 2.4.3. APOPTOTIC NUCLEAR STAINING

Apoptosis was revealed by nuclear fragmentation following DNA staining using the fluorescent dye Hoechst 33342 (Sigma-Aldrich). Apoptotic cells were counted under a fluorecence microscope and expressed as percentage of total nuclei count.

### 2.4.4. ASSESSMENT OF INTRACELLULAR ROS

Intracellular oxidative stress was measured using the nonfluorescent compound 2'-7'-dichlorofluorescein diacetate (DCFH-DA) (Sigma-Aldrich). Viable cells deacetylate DCFH-DA to 2'-7' -dichlorofluorescin, and in presence of ROS to the fluorescent dye 2'-7'-dichlorofluorescein, which remains trapped within the cell and can be measured with a fluorescence plate reader (excitation at 480 nm, emission at 530 nm). Cells were pre-loaded with 10 μM DCFH-DA 1 h before oxidative stress induction and 7'-dichlorofluorescein was measured after 24 h. ROS levels were expressed as percentage of the fluorescence intensity of the baseline ROS in the control group.

### 2.4.5. RESVERATROL UPTAKE

Resveratrol (RES) uptake was assessed in dr. Silvio Caccia's laboratory ("Mario Negri" Institute, Milano, Italy) by HPLC-MS-MS. A total of $3.5 \cdot 10^6$ SK-N-BE(2) cells were seeded and treated by RES as described in section 6.2.2. At 16, 20 and 44 h from the first RES treatment, RES intracellular content was measured. Cells were harvested, counted by erythrosine-dye exclusion assay and centrifuged. The washed pellet was frozen and then

resuspended in a solution containing 70% acetonitrile, 10% formic acid in presence of zeranol (10 μg/mL) as internal standard. After centrifugation at 15 000 g for 10 min, an aliquot of a 1:5 water dilution of the supernatant in presence of 0.05% acetic acid was injected into an HPLC-MS-MS system (Waters). RES content was quantified as described byWang et al. with minor modifications (Wang et al., 2005a). The limit of detection was 0.04 μg/mL and the assay was linear up to 2 μg/mL; coefficients of variation were between 10–20%.

### 2.4.6. Aβ42 SYNTHESIS

Aβ42 (DAEFRHDSGYEVHHQKLVFFAEDVGSNKGAIIGLMVGGVVIA) was synthesized in dr. Mario Salmona's laboratory ("Mario Negri" Institute, Milano, Italy) by solid-phase peptide synthesis (SPPS) and purified by reverse phase HPLC. Peptide identity was confirmed by MALDI-TOF analysis (Salmona et al., 2003). Aβ42 was stored at -80 °C as a powder.

### 2.4.7. FLUORIMETRIC BINDING ASSAY

Binding of RES to Aβ was examined by dr. Mario Salmona's laboratory ("Mario Negri" Institute, Milano, Italy) with a fluorimetric binding assay as described by Ahn et al. (Ahn et al., 2007) with minor modifications. This assay took advantage of RES intrinsic fluorescence (excitation at 320 nm, emission at 395 nm) and registered emission spectra between 300 and 600 nm. RES emission length was compared with and without incubation of the molecule with Aβ.

## 2.4.8. ATOMIC FORCE MICROSCOPY

Atomic force microscopy (AFM) was carried out by dr. Mario Salmona's laboratory ("Mario Negri" Institute, Milano, Italy).

Aβ42 was incubated in presence or absence of RES (ratio 1:1.5) at 37 °C for increasing time intervals (0.5, 6 and 24 h). Each sample was diluted to 1 μM with PBS 10 mM, pH 7.4 and incubated for 0.5 min on a freshly cleaved Muscovite mica disk. After the incubation time, the disk was washed with $H_2O$ and dried under gentle nitrogen stream. The sample was mounted onto a Multimode AFM with a NanoScope V system operating in Tapping Mode using standard phosphorus-doped silicon probes (T: 3.5–4.5 μm, L: 115–135 μm, W: 30–40 μm, K: 20–80 N/m) (Veeco Instruments).

## 2.4.9. RNA EXTRACTION AND RELATIVE QUANTITATIVE RT-PCR

Total RNA was extracted from cell lysates with SV Total RNA Isolation System (Promega).

Cells were cultured in multi-well plates and treated according to the specific experimental protocol. At the end of the experiment, cells were harvested by trypsinisation and lysed with 175 μL lysis buffer provided within the commercial kit used.

Tissues (~ 10 mg weight) were resuspended in 175 μL lysis buffer and homogenated by a syringe needle.

All steps were carried out at room temperature with RNase-Zap (Ambion).

A total of 1 μg RNA was reversed transcribed into cDNA and RT-PCR assays were run as described in section 2.3.6.2 using TaqMan® gene expression assays (Applied Biosystems, table A.4.).

## 2.4.10. PROTEIN ANALYSES

### *2.4.10.1. Protein extraction from cell line.*

Ice-cold Lysis Buffer pH 7.4 (50 mM Tris/HCl, 150 mM NaCl, 0.5 mM EDTA and 1% Triton X-100) was prepared. A further 1% of a broad-range protease inhibitor cocktail and 1 mM Sodium Butyrate (inhibitor of class I and II deacetylase) (Sigma-Aldrich) was also added.

Cells were cultured in multi-well plates and treated according to the specific experimental protocol. At the end of the experiment, supernatants were aspirated, cells were washed with PBS and subsequently incubated at 4 °C for 30 min with 100 µL/well of ice-cold lysis buffer. Cells were scraped on ice, and centrifuged at 14 000 rpm for 5 min at 4 °C.

Supernatants were sub-aliquoted and stored at -80 °C. Small aliquots were taken for protein quantification.

Protein concentration of supernatants was measured by BCA protein assay according to the manufacturer's instructions.

### *2.4.10.2. SDS-polyacrylamide gel electrophoresis and western blotting*

Sample preparation - 30 µg of cellular lysates, were denatured by boiling in SDS sample buffer (125 mM Tris-HCl pH 6.8, SDS 10%, glycerol 10%, bromophenol blue 0.006%) added with 0.1 M DTT at 95 °C for 5 min.

Proteins were electrophoresed and electroblotted onto a 0.2 µM nitrocellulose membrane as described in section 2.3.7.2.

Immunodetection was performed as described in section 2.3.7.4.

## 2.4.11. IMMUNOCYTOCHEMISTRY

Cells were cultured in a plastic chamber slide (Thermo Fisher Scientific) multi-well plates and treated according to the specific experimental protocol. At the end of the experiment, culture medium was removed and after 2 washes with PBS cells were fixed with 4% PFA and permeabilized using 0.5% Triton X-100. After 2 washes with PBS and 1 h block with 10% horse serum in PBS, cells were incubated overnight at 4 °C with the specific primary antibody at the appropriate dilution in PBS+1% horse serum. The next day, cells were incubated with Alexa Fluor ® 488-conjugated secondary antibody (Invitrogen) diluted 1:200 in PBS. Cells were then analyzed with a fluorescence microscope coupled to a digital camera (Olympus).

PAGE
NUMBERING
AS
ORIGINAL

As previously described, recent GWAs have identified over 40 candidate novel genetic loci related to AD, in addition to *APOE* ε4. However, only a few of these loci (e.g. near *CLU*, *CR1*, *PICALM* and *BIN1* genes) have shown consistent replication (Bertram, 2011) and these variants collectively do not entirely explain the genetic predisposition to all forms of SAD. Furthermore, since the role of interactions between genes and other factors are increasingly likely to contribute to AD risk and progression, investigations remain ongoing to find new genetic variants that could be implicated.

The 7 mammalian sirtuin proteins currently know in humans are each encoded by separate genes *SIRT1-7*. Increasing evidence has highlighted the involvement of mammalian sirtuins in ageing and age-associated disorders such as metabolic diseases, cancer, cardiovascular disease, neurodegeneration and inflammation. Thus it is possible, if not probable, that sirtuins are implicated in the various mechanisms and may also serve as therapeutic targets against age-linked pathologies. These findings have prompted a number of investigations into whether common allelic variations in some of the *SIRT* genes are associated with longevity and age-related diseases in humans. Interestingly, a silent variation on *SIRT3* gene was reported to be associated with survivorship in elderly males (Rose et al., 2003). This genetic variant was later found to be linked with a variable number of tandem repeats (VNTR) polymorphism, with a putative enhancer function revealed by functional studies. Consistently with the previous study, the allele lacking the enhancer activity was found to be absent in males older than 90 years (Bellizzi et al., 2005).

Genetic variants spanning the *SIRT1* gene, the most extensively studied sirtuin to date, were found to be associated with different aspects of human metabolism such as body mass index (BMI), LDL cholesterol levels basal energy expenditure and risk of obesity, and with

cardiovascular mortality (Kuningas et al., 2007; Weyrich et al., 2008; Zillikens et al., 2009a, 2009b). These genetic findings supported the involvement of SIRT1 in age-related metabolism homeostasis, which had already been suggested by substantial evidence from *in vitro* and *in vivo* studies. A weak genetic association was also found between *SIRT4* gene, encoding a mitochondrial sirtuin, and T2D (Reiling et al., 2009). Anyway, further studies could depict a relation between other genetic variants in mitochondrial sirtuins and metabolic parameters.

Sirtuins have been found to mediate disease-modifying effects in various models of neurodegeneration such as in AD, Parkinson's disease, Huntington's disease and amyotrophic lateral sclerosis. *SIRT1* in particular, has been proposed to be a putative risk factor in relation to AD because of its biological function and its location on chromosome 10 in a region that was previously reported in linkage studies to confer susceptibility for LOAD (Bertram et al., 2000). However, no evidence supporting an association between *SIRT1* variation and AD risk was found in studies derived from a British population and in another one in a Finnish cohort (Helisalmi et al., 2008; Morgan et al., 2007). Only a weak positive association with AD, that still requires replication, was reported in Finnish women older than 65 years (Helisalmi et al., 2008).

None of the other sirtuin genes (*SIRT2-SIRT7*) have been investigated in AD and given the increasing data showing the relevance of sirtuins in the brain and neurodegenerative diseases, a comprehensive study on sirtuin genetic variation and LOAD was deemed timely and worthwhile.

The overall aim of chapter 3 and 4 was to explore whether genetic variation in a number of sirtuins was associated with AD risk. To this concern, a three-stage study was designed including:

(i) A pilot dHPLC screening to investigate the presence of sirtuin variation in a population of Caucasians in relation to AD.

(ii) An initial case-control association study to quantify the extent, if any, of genetic association between identified sirtuin common polymorphisms and AD risk.

(iii) A replication case-control association study, in an independent cohort, to seek verification of the original association found and with the scope offered by increased sample size a better overview of the effect size of any observed association.

# *CHAPTER 3: POLYMORPHISM SCREENING IN SIRTUIN GENES BY dHPLC ANALYSIS*

# 3.1. SYNOPSIS

The aim of this study was to screen sirtuin common genetic variations in relation to AD. To achieve this, all 7 sirtuin genes were assessed to search for common polymorphisms (i.e. frequency higher than 20% in the population) rather than rare variants, in accordance with the idea that common diseases are more probably caused by common polymorphisms in the population (common disease-common variants theory) (Schork et al., 2009). As such, 96 subjects were screened (48 AD and 48 CT) for each of the 62 amplicons of interest.

The assessment of sirtuin variation was initially performed by dHPLC and suggested polymorphisms identified were then validated and characterised by direct DNA sequencing. To increase the likelihood of finding more functionally relevant SNPs dHPLC screening focused on the coding regions and small intronic flanking portions of all of the sirtuin genes (*SIRT1-7*).

Overall, 29 SNPs were identified across the 7 genes of which 18 resided in the intronic portions flanking the exons and 11 in protein coding regions (cSNPs) of the amplicons assessed. Among the cSNPs identified (3 novel SNPs and 8 already reported in the NCBI SNP database), 3 variants were silent SNPs, 1 was a nonsense SNP, leading to the premature truncation of SIRT5 protein and 7 were missense variants. In particular, 4 cSNPs lead to substitutions that could, at least locally, affect protein structure. However, in most instances, the cSNPs were of low frequency being restricted to one subject, and as such were more likely to be rare mutations than polymorphisms. Only 2 cSNPs were more frequent and interestingly one of these appeared to be have a slightly different genotype pattern between the ADs and CTs screened. Of the non-coding SNPs identified (8 novel SNPs and 10 already reported in the NCBI SNP database), many were frequent variants

and some of these were more present in one but not both of the two sample groups investigated thereby making them worthy of further investigations.

# 3.2. MATERIALS AND METHODS

## 3.2.1. SAMPLE POPULATION

As mentioned the population selected for the dHPLC screening was composed by 48 AD and 48 CT subjects. Both AD and CT were recruited at the "Luigi Sacco" Hospital in Milan (Italy) and at the "Beata Vergine" Hospital in Mendrisio (CH - Italian Canton). The sample size was such that it should identify variants in heterozygosis with a frequency higher than 1% (i.e. 1 in N=96 patient would correspond to 1%). The equal numbers of ADs and CTs also offered an initial screen to explore differences between the cases and controls for the most common variants identied.

The demographic data of AD and CT groups are summarized in table 3.1. AD and CT were gender-, and age-matched ($p > 0.5$ Student t-test for any comparison between AD and CT). Conversely, AD patients showed a MMSE score significantly lower than CT subjects ($p < 0.01$ t-test), highlighting a cognitive deficit.

| Cohorts | Diagnose (N°) | Gender M (%) | Mean age (years ± SD) | Mean MMSE (score ± SD) |
|---|---|---|---|---|
| "Luigi Sacco" Hospital | CT (24) | 29 | 78.3 ± 9.0 | 28.9 ± 1.5 |
| | AD (24) | 25 | 77.9 ± 5.3 | 15.1 ± 4.7 * |
| "Beata Vergine" Hospital | CT (24) | 30 | 79.4 ± 8.2 | 28.2 ± 1.5 |
| | AD (24) | 22 | 78.1 ± 6.0 | 16.0 ± 3.9 * |

**TABLE 3.1. Demographics of the cohorts included in the dHPLC analysis.**

*Abbreviations: AD, sporadic Alzheimer's disease; CT, healthy controls; M, males; SD, standard deviation; MMSE, Mini Mental State Examination; *p<0.01 vs. CT; Student t-test.*

### 3.2.2. dHPLC ANALYSIS

In the design stage of the study, a variable number of amplicons were defined for each *SIRT* gene. In the majority of the cases, amplicons included an exon and a small section of flanking intronic sequence taking into account intron/exon splicing sites. When an exon was too long and fell outside the optimal range for investigations by dHPLC (> 350 bp), and/or its melting profile was highly non-homogeneous, more than one overlapping amplicon was designed. For each amplicon a pair of primers was designed and the PCR amplification conditions were optimised. Each amplicon was amplified by PCR and the resultant product was analyzed by dHPLC with the appropriate melting temperature (table A.3. in the appendix)

| GENE NAME | NUMBER OF EXONS | NUMBER OF AMPLICONS |
|---|---|---|
| *SIRT1* | 9 | 10 |
| *SIRT2* | 16 | 16 |
| *SIRT3* | 7 | 7 |
| *SIRT4* | 3 | 3 |
| *SIRT5* | 8 | 8 |
| *SIRT6* | 8 | 8 |
| *SIRT7* | 10 | 10 |

**TABLE 3.2. Number of amplicons screened in the dHPLC study for *SIRT1-7* genes.**

*Summary of the number of exons and amplicons screened in the dHPLC study. Cfr. table A.3 in the appendix of the thesis for the extra detail on primer sequences, and condition of the dHPLC analysis.*

Samples with atypical chromatographic profiles, potentially indicative of the presence of polymorphism, were sequenced to identify if a substitution was present and characterise the nature of it. For the relevant regions, some samples with single-peak dHPLC profiles were also sequenced for comparison purposes.

### 3.2.3. *IN SILICO* ANALYSIS

Genetic variants were characterised by comparing genomic contiguous ('contig') sequences from the National Institute for Biotechnology website (NCBI) Entrez gene (NC reference sequences (table A.1. in the appendix) with the corresponding sequences obtained by direct sequencing. Chromosomal position and the position within the gene structure were defined taking advantage of Gene Table display setting. Protein reference sequences available were also examined for any coding SNPs found to determine if polymorphism resulted in any amino acid changes. The identification of SNPs already

published was performed using BLAST SNP. Sirtuin NCBI reference sequences are summarized in table A.1 in the appendix. Multiple alignment was performed by Clustal W software using the slow/accurate pairwise alignment method with a gap penalty of 10.00 and gap length of 0.10 and GONNET 250 as protein weight matrix.

# 3.3. RESULTS

## 3.3.1. IDENTIFICATION OF SINGLE NUCLEOTIDE POLYMORPHISMS

dHPLC screening of the 62 sirtuin amplicons designed, revealed several atypical profiles indicative of putative heterozygote substitutions within the sample population investigated (48 AD and 48 CT, cfr. chapter 3.2.1.). The subsequent direct sequencing of these gene regions, revealed 29 different SNPs. All the identified SNPs were verified to be absent in a subset of samples displaying single-peak dHPLC profiles for the relevant gene region which were sequenced at the same time.

The characterisation of the SNPs by *in silico* analysis elucidated the precise nature of the substitutions observed. In table 3.3, the identified SNPs are reported together with the corresponding chromosome position, exon/intron location across sirtuin genes, and the nucleotide change occurred. Previously described variants (18 out of the 29 SNPs) are denoted by the existing reference SNP (rs) number from NCBI Variation Database (dbSNP) (http://www.ncbi.nlm.nih.gov/projects/SNP/). Among the 29 identified SNPs, 11 resided in exons (cSNPs) whereas 18 were in the flanking intronic sequences.

| SNP (NCBI dbSNP) | Gene | Chromosome position | Exon/Intron | Nucleotide change |
|---|---|---|---|---|
| SNP 1 (rs2236318) | SIRT1 | 69648569 | IVS II -71 | T>A |
| SNP 2 (rs10823103) | | 69650969 | IVS III -191 | A>G |
| SNP 3 (rs7896005) | | 69651125 | IVS III -35 | A>G |
| SNP 4 (rs2273773) | | 69666598 | EXON V | T>C |
| SNP 5 (rs116040871) | | 69672479 | EXON VIII | G>A |
| SNP 6 | SIRT2 | 39374844 | IVS III +61 | G>A |
| SNP 7 | | 39374982 | IVS III -91 | C>T |
| SNP 8 | | 39378618 | IVS V -21 | C>T |
| SNP 9 | | 39378836 | IVS VI -21 | C>G |
| SNP 10 (rs11879010) | | 39379855 | IVS VII -60 | T>C |
| SNP 11 (rs45496398) | | 39370217 | IVS XIV | C>G |
| SNP 12 (rs11246020) | SIRT3 | 233067 | EXON III | G>A |
| SNP 13 (rs547025) | | 232855 | IVS III +128 | A>G |
| SNP 14 (rs61748606) | | 230474 | EXON IV | C>A |
| SNP 15 | | 224004 | IVS V +73 | G>A |
| SNP 16 (rs511744) | | 219089 | IVS V -48 | G>A |
| SNP 17 | | 219060 | IVS V -18 | C>T |
| SNP 18 (rs2261612) | SIRT4 | 120750239 | IVS I -20 | G>A |
| SNP 19 | SIRT5 | 13599900 | EXON I | C>T |
| SNP 20 (rs3734674) | | 13592135 | IVS III +9 | C>T |
| SNP 21 (rs34162626) | | 13612078 | EXON VIII | A>G |
| SNP 22 (rs34786277) | SIRT6 | 4180901 | EXON II | C>T |
| SNP 23 (rs352493) | | 4180836 | EXON II | A>G |
| SNP 24 (rs11554579) | | 4179250 | EXON III | A>G |
| SNP 25 | | 4179056 | EXON III | G>A |
| SNP 26 | | 4176044 | IVS III +17 | G>A |
| SNP 27 (rs7246235) | | 4175785 | IVS V -28 | C>A |
| SNP 28 | SIRT7 | 79870250 | IVS II -11 | C>T |
| SNP 29 | | 79870325 | EXON III | C>T |

**TABLE 3.3. List and description of the identified SNPs.**

*Abbreviations: SNP, single nucleotide polymorphism; IVS, intronic variance sequence.*

** Chromosome positions and the position of coding SNPs within sirtuin transcripts refer to NCBI reference sequences NC_ and NM_(full length isoform) respectively (table A.1. in the appendix).*

cSNPs were mapped with BlastX (http://blast.ncbi.nlm.nih.gov/Blast.cgi) to search for the corresponding amino acid substitution. We found that 3 of the 11 cSNPs where silent SNPs, since they caused a codon change that did not affect the resultant amino acid. A further 7 cSNPs were missense SNPs and the remaining SNP was a nonsense substitution leading to the insertion of a "stop" codon and should have resulted in the premature truncation of the *SIRT5* mRNA message. In table 3.4, the cSNPs in the sirtuin genes are reported with the amino acid change occurred and the biochemical feature of the substitution.

| *cSNP Rs code* | *PROTEIN (NP)* | *CODON CHANGE* | *AMINO CHANGE* | *CONVERSION* |
|---|---|---|---|---|
| *SNP 4 rs2273773* | *SIRT1* | *TTG > CTG* | *L332L* | *Synonymous* |
| *SNP 5 rs116040871* | *SIRT1* | *GAA > AAA* | *E536K* | *Negative charged > positive charged* |
| *SNP 12 rs11246020* | *SIRT3* | *GTC > ATC* | *V208I* | *Aliphatic* |
| *SNP 14 rs61748606* | *SIRT3* | *CCC > CAC* | *P262H* | *Small > positive charged* |
| *SNP 19 -* | *SIRT5* | *CAG > TAG* | *R10** | *Non sense* |
| *SNP 21 rs34162626* | *SIRT5* | *GAA > GGA* | *E305G* | *Negative charged > hydrophobic* |
| *SNP 22 rs34786277* | *SIRT6* | *TTC > TTT* | *F24F* | *Synonymous* |
| *SNP 23 rs352493* | *SIRT6* | *AGT > AAT* | *S46N* | *Small, polar* |
| *SNP 24 rs11554579* | *SIRT6* | *CGA > CGG* | *R76R* | *Synonymous* |
| *SNP 25 -* | *SIRT6* | *CGC > CAC* | *R121H* | *Positive charged* |
| *SNP 29 -* | *SIRT7* | *GCC > GTC* | *A99V* | *Small, hydrophobic* |

**TABLE 3.4. List of the cSNPs and related amino acid substitutions.**

*Abbreviations: cSNP, coding single nucleotide polymorphism; rs, reference SNP. Amino acid substitutions are referred to full length proteins NC reference sequences are listed in table A.1. in the appendix.*

PAGE
NUMBERING
AS
ORIGINAL


SIRT2
SIRT3 MAFWGWRAAAALRLWGRVVERVEAGGGVGPFQACGCRLVLGGRDDV 46
SIRT1 MADEAALALQPGGSPSAAGADREAASSPAGEPLRKRPRRDGPGLERSPGEPGGAAPEREV 60
Sir2p --MTIPHMKYAVSKTSENKVSNTVSPTQDKDAIRKQPDDIINNDEPSHKKIKVAQPDSLR 58
SIRT4
SIRT6
SIRT7 MAAGGLSRSERKAAERVRR 19
SIRT5
SIRT2 ----------MAEP-DPSHPLETQAG-KVQEAQDSDSDSEG------GAAGGEADMDFLR 42
SIRT3 SAGLRGSHGARGEPLDPARPLQRPPRPEVPRAFRRQPRAAAPSFFFSSIKGGRRSISFSV 106
SIRT1 PAAARGCPGAAAAALWREAEAEAAAAGGEQEAQATAAAGEGDN--GPGLQGPSREPPLAD 118
Sir2p ETNTTDPLGHTKAALGEVASMELKPTNDMDPLAVSAASVVSMSNDVLKPETPKGPIIISK 118
SIRT4 ----------MKMSFALTFRSAKGRWIANPSQ----------PCSKASIGLFV 33
SIRT6 ----------MSVNYAAGLSPYADKG----------KCGLPEIF 24
SIRT7 LREEQQRERLRQVSRILRKAAAERSAEEGRLLAESADLVTELQGRSRRREGLKRRQEEVC 79
SIRT5 ----------MRPLQIVPSRLISQLYCGLKP----------PASTRNQICLKM 33
SIRT2 NLFSQTLSLGSQKER- 57
SIRT3 GASSVVGSGGGSSDK- 120
SIRT1 NLYDEDDDDEGEEEEEAAAAAIGYRDNLLFGDEIITNGFHSCESDEEDRASHASSSDWTP 178
Sir2p NPSNGIFYGPSFTKRESLNARMFLKYYG------AHKFLDTYLPEDLNSLYIYYLIKLLG 172
SIRT4 PASPP- 38
SIRT6 DPPEE- 29
SIRT7 DDPEE- 84
SIRT5 ARPSS- 38
SIRT2 ----------LLDELTLEGVARYMQSE-------- 74
SIRT3 ----------GKLSLQDVAELIRAR-------- 135
SIRT1 RPRIGPYTFVQQHLMIGTDPRTILKDLLPETIPPPELDDMTLWQIVINILSEPPKR---- 234
Sir2p FEVKDQALIGTINSIVHINSQERVQDLGSAISVTNVEDPLAKKQTVRLIKDLQRAINKVL 232
SIRT4 ----------LDPEKVKELQRFITLS-------- 54
SIRT6 ----------LERKVWELARLVWQS-------- 44
SIRT7 ----------LRGKVRELASAVRNA-------- 99
SIRT5 ----------SMADFRKFFAKA-------- 50
SIRT2 ----------RCRRVICLVGAGISTSAGIPDFRSPSTGLYD--NLEKYHL 112
SIRT3 ----------ACQRVVVMVGAGISTPSGIPDFRSPGSGLYS--NLQQYDL 173
SIRT1 ---KKRKDINTIEDAVKLLQECKKIIVLTGAGVSVSCGIPDFRS-RDGIYARLAVDFPDL 290
Sir2p CTRLRLSNFFTIDHFIQKLHTARKILVLTGAGVSTSLGIPDFRS-SEGFYS--KIKHLGL 289
SIRT4 ----------KRLLVMTGAGISTESGIPDYRSEKVGLYA----RTDRR 88
SIRT6 ----------SSVVFHTGAGISTASGIPDFRG---------- 66
SIRT7 ----------KYLVVYTGAGISTAASIPDYRG---------- 121
SIRT5 ----------KHIVIISGAGVSAESGVPTFRG-AGGYWR--KWQAQDL 85
SIRT2 PYPEAIFEISYFKKHPEPFFALAKELYPGQFKPTICHYFMRLLKDKGLLLRCYTQNIDTL 172
SIRT3 PYPEAIFELPFFFHNPKPFFTLAKELYPGNYKPNVTHYFLRLLHDKGLLLRLYTQNIDGL 233
SIRT1 PDPQAMFDIEYFRKDPRPFFKFAKEIYPGQFQPSLCHKFIALSDKEGKLLRNYTQNIDTL 350
Sir2p DDPQDVFNYNIFMHDPSVFYNIANMVLPPEKIYSPLHSFIKMLQMKGKLLRNYTQNIDNL 349
SIRT4 PIQHGDFVRSAPIRQRYWARNFVGWPQFSSHQPNPAHWALSTWEKLGKLYWLVTQNVDAL 148
SIRT6 --PHGVWTMEERGLAPKFDTTFESAR------PTQTHMALVQLERVGLLRFLVSQNVDGL 118
SIRT7 --PNGVWTLLQKGRS-------VSAADLSEAEPTLTHMSITRLHEQKLVQHVVSQNCDGL 172
SIRT5 ATPLAFAHNPSRVWEFYHYRREVMGSKEPNAGHRAIAECETRLGKQGRRVVVITQNIDEL 145
SIRT2 ERIAGLEQEDLVEAHGTFYTSHCVSASCRHEYPLSWMKEKIFSEVTPKCEDCQS------ 226
SIRT3 ERVSGIPASKLVEAHGTFASATCT--VCQRPFPGEDIRADVMADRVPRCPVCTG------ 285
SIRT1 EQVAGIQR--IIQCHGSFATASCL--ICKYKVDCEAVRGDIFNQVVPRCPRCPAD----- 401
Sir2p ESYAGISTDKLVQCHGSFATATCV--TCHWNLPGERIFNKIRNLELPLCPYCYKKRREYF 407
SIRT4 HTKAGSRR--LTELHGCMDRVLCL--DCGEQTPRGVLQERFQVLNPTWSAEAHGLAPD-- 202
SIRT6 HVRSGFPRDKLAELHGNMFVEECA--KCKTQYVRDTVVGTMGLKATGRLCTVAKARG--- 173
SIRT7 HLRSGLPRTAISELHGNMYIEVCT--SCVPNREYVRVFDVTERTALHRHQTGRTCHK--- 227
SIRT5 HRKAGTKN--LLEIHGSLFKTRCTSCGVVAENYKSPICPALSGKGAPEPGTQDASIP--- 200
SIRT2 ----------LVKPDIVFFGES---LPARFFSCMQSDFLKV 254
SIRT3 ----------VVKPDIVFFGEP---LPQRFLLHVV-DFPMA 312
SIRT1 ----------EPLAIMKPEIVFFGEN---LPEQFHRAMKYDKDEV 433
Sir2p PEGYNNKVGVAASQGSMSERPPYILNSYGVLKPDITFFGEA---LPNKFHKSIREDILEC 464
SIRT4 ------GDVFLSEEQVRSFQVPTCVQCGGHLKPDVVFFGDT---VNPDKVDFVHKRVKEA 253
SIRT6 ----------LRACRGELRDTILDWEDS---LPDRDLALADEASRNA 207
SIRT7 ----------CGTQLRDTIVHFGERGTLGQPLNWEAATEAASRA 261
SIRT5 ----------VEKLPRCEEAGCGGLLRPHVVWFGEN---LDPAILEEVDRELAHC 242


**FIGURE 3.1. Multiple alignment between the 7 human sirtuins (SIRT1-7) and Sir2p of *S. cerevisiae*, the founding member of sirtuin protein family.**

*Blue box: sirtuin core domain; residues underscored in yellow: coding SNPs. Nucleotides: red= small + hydrophobic (incl.aromatic - Y) (AVFPMILW); blue= acidic (DE); magenta= basic (RHK); Green= Hydroxyl + Amine + Basic + Q (STYHCNGQ). "*" identical residues, ":" conserved residues, "." semi-conserved residues in all sequences in the alignment.*

***SNP5*** SIRT1 *Glu→Lys.*

*NP_036370.21* = Homo sapiens

*NP_062786.1* = Mus musculus

*NP_52345464* = Gallus gallus

*NP_010242.1* = Saccharomyces cerevisiae

```
gi|7657575|ref|NP_036370.2|          IPHEVPQILINREPLPHLHFDVELLGDCDVIINELCHRLGGEYAKLCCNP 504
gi|9790229|ref|NP_062786.1|          IPHEVPQILINREPLPHLHFDVELLGDCDVIINELCHRLGGEYAKLCCNP 496
gi|52345464|ref|NP_001004767.1       IPHEVPQILINREPLPHLHFDVELLGDCDVIISELCQRLGSEYTKLCYNS 515
gi|6320163|ref|NP_010242.1|          VPSHVPQVLINRDPVKHAEFDLSLLGYCDDIAAMVAQKCGWTIPHKKWND 535
                                      :* .***:****:*: * .**:.*** ** *   :.:: *   .:   *

gi|7657575|ref|NP_036370.2|          VKLSEITEKPPRTQKELAYLS-ELPPTPLHVSEDSSSPERTSPPDSSVIV 553
gi|9790229|ref|NP_062786.1|          VKLSEITEKPPRPQKELVHLS-ELPPTPLHISEDSSSPERTVPQDSSVIA 545
gi|52345464|ref|NP_001004767.1       VKLSEITEKPPRMHKELEMHSSELPPTPLDISEDSGSPEQMTPPGTSVVP 565
gi|6320163|ref|NP_010242.1|          LKNKNFKCQ--EKDKGVYVVTSDEHPKTL---------------------- 562
                                      :* .::. :  . .* :   : :  *..*

gi|7657575|ref|NP_036370.2|          TLLDQAAKSND-DLDVSESKGCMEEKPQEVQTSR-NVESIAEQMENPD-L 600
gi|9790229|ref|NP_062786.1|          TLVDQATNNNVNDLEVSES-SCVEEKPQEVQTSR-NVENIN--VENPD-F 590
gi|52345464|ref|NP_001004767.1       SEHAAECKVENSDPASETKGICTEEKLQDTQASSENPENPASELMNSETM 615
gi|6320163|ref|NP_010242.1|          ------------------------------------------------
```

***SNP14*** SIRT3 *Pro→His*

*NP_036371.1* = Homo sapiens

*NP_071878* = Mus musculus

*XP_420920.2* = Danio rerio

*NP_001073642* = Gallus gallus

```
gi|6912660|ref|NP_036371.1|          ELYPGNYKPNVTHYFLRLLHDKGLLLRLYTQNIDGLERVSGIPASKLVEA 247
gi|11967963|ref|NP_071878.1|         ELYPGHYRPNVTHYFLRLLHDKELLLRLYTQNIDGLERASGIPASKLVEA 105
gi|118091076|ref|XP_420920.2|        ELYPGNYRPNYAHYFLRLLHDKGLLLRLYTQNIDGLERVAGIPPDRLVEA 194
gi|122114557|ref|NP_001073643.       ELYPGNYQPNLTHYFIRMLHDKEQLLRMYTQNIDGLERMAGIPPKMLVEA 210
                                      *****:*:** :***:*:****  ***:********** :***.. ****

gi|6912660|ref|NP_036371.1|          HGTFASATCTVCQRPFPGEDIRADVMADRVPRCPVCTGVVKPDIVFFGEP 297
gi|11967963|ref|NP_071878.1|         HGTFVTATCTVCRRSFPGEDIWADVMADRVPRCAVCTGVVKPDIVFFGEQ 155
gi|118091076|ref|XP_420920.2|        HGTFATATCTVCRRKFPGEDFRGDVMADKVPHCRVCTGIVKPDIVFFGEE 244
gi|122114557|ref|NP_001073643.       HGTFATATCTVCRRDYKGEELRDDIMAGTVPKCPTCKGIIKPDIVFFGEE 260
                                      ****.:******:* : **::  *:**. **:* .*.*::*********

gi|6912660|ref|NP_036371.1|          LPQRFLLHVVDFPMADLLLILGTSLEVEPFASLTEAVRSSVPRLLINRDL 347
gi|11967963|ref|NP_071878.1|         LPARFLLHMADFALADLLLILGTSLEVEPFASLSEAVQKSVPRLLINRDL 205
gi|118091076|ref|XP_420920.2|        LPQRFFLHMTDFPMADLLFVIGTSLEVEPFASLAGAVRNSVPRVLINRDL 294
gi|122114557|ref|NP_001073643.       LPQHFFTYLTDFPIADLLIVMGTSLEVEPFASLAGAVRGSVPRLLINRDL 310
                                      ** :*: ::.**.:****:::************: **: ****:******
```

**FIGURE 3.2. Multiple alignment among ortholog sirtuins.**

*Red boxes identify the position of the residue of interest.*

### 3.3.3. SNP FREQUENCIES

The heterozygote frequencies of each variant were calculated for the entire screening sample (i.e. the number of samples with an altered dHPLC profile/total samples). For previously known SNPs, as a form of validation we compared the frequencies obtained in the control group with the reported distributions in other geographically related population datasets available. The SNPs identified in our study involved ones that were highly frequent but there were also rare substitutions present in only one of the subjects screened which may more likely be rare mutations rather than polymorphisms. SNP frequency was also calculated in CT and AD groups separately where 6 SNPs (SNPs 4, 7, 10, 11, 15 and 18) revealed suggestive differences in the genotype distributions observed between AD and CT (table 3.5).

| SNP (NCBI code) | SNP n (%) total | SNP n (%) AD | SNP n (%) CT | Genotypic distribution (%) 11 12 22 *Source population* |
|---|---|---|---|---|
| **SNP 1 (rs2236318)** | 48 (50) | 27 (56) | 21 (44) | 23 40 37 *EGP CEPH-PANEL** |
| **SNP 2 (rs10823103)** | 47 (49) | 25 (52) | 22 (46) | 6.9 45.1 48 *TSI§* |
| **SNP 3 (rs7896005)** | 42 (44) | 19 (40) | 23 (48) | 10.1 42.4 47.5 *TSI§* |
| **SNP 4 (rs2273773)** | 8 (8) | 6 (13) | 2 (4) | 0 12.7 87.3 *TSI§* |
| **SNP 5 (rs116040871)** | 1 (1) | 1 (2) | 0 (0) | NA |
| **SNP 6** | 1 (1) | 0 (0) | 1 (2) | - |
| **SNP 7** | 4 (4) | 0 (0) | 4 (8) | - |
| **SNP 8** | 3 (3) | 0 (0) | 3 (6) | - |
| **SNP 9** | 1 (1) | 1 (2) | 0 (0) | - |
| **SNP 10 (rs11879010)** | 12 (13) | 9 (19) | 3 (6) | NA |
| **SNP 11 (rs45496398)** | 7 (7) | 7 (15) | 0 (0) | NA |
| **SNP 12 (rs11246020)** | 33 (34) | 16 (33) | 17 (35) | 4.9 39.2 55.9 *TSI§* |
| **SNP 13 (rs547025)** | 10 (10) | 4 (8) | 6 (13) | NA |
| **SNP 14 (rs61748606)** | 1 (1) | 1 (2) | 0 (0) | NA |
| **SNP 15** | 47 (49) | 19 (40) | 28 (58) | - |
| **SNP 16 (rs511744)** | 44 (46) | 23 (48) | 21 (44) | 7.8 49 43.1 *TSI§* |
| **SNP 17** | 1 (1) | 0 (0) | 1 (2) | - |
| **SNP 18 (rs2261612)** | 32 (33) | 10 (21) | 22 (46) | 11.8 36.3 52 *TSI§* |
| **SNP 19** | 1 (1) | 0 (0) | 1 (2) | - |
| **SNP 20 (rs3734674)** | 46 (48) | 24 (50) | 22 (46) | NA |
| **SNP 21 (rs34162626)** | 1 (1) | 1 (2) | 0 (0) | 0 3 97 *CEU§* |
| **SNP 22 (rs34786277)** | 1 (1) | 0 (0) | 1 (2) | 0 3 97 AGI ASP PANEL* |
| **SNP 23 (rs352493)** | 2 (2) | 1 (2) | 1 (2) | 1 12.7 86.3 *TSI** |
| **SNP 24 (rs11554579)** | 2 (2) | 2 (4) | 0 (0) | NA |
| **SNP 25** | 1 (1) | 0 (0) | 1 (2) | - |
| **SNP 26** | 1 (1) | 1 (2) | 0 (0) | - |
| **SNP 27 (rs7246235)** | 10 (10) | 6 (13) | 4 (8) | 0 1.7 98.3 *CEU** |
| **SNP 28** | 4 (4) | 2 (4) | 2 (4) | - |
| **SNP 29** | 1 (1) | 0 (0) | 1 (2) | - |

**TABLE 3.5. Heterozygote frequency of the SNPs identified in the the dHPLC screening and corresponding genotype distributions where available from NCBI.**

*Abbreviations: NA, not available. Source population from NCBI* (http://www.ncbi.nlm.nih.gov/projects/SNP/snp_ind.cgi?ind_id=239) or HapMap§ (http://www.broadinstitute.org/~debakker/p3.html).*

# 3.4. DISCUSSION

The dHPLC screening study aimed to investigate levels of sirtuin genetic variation. The screening study revealed 29 SNPs residing in coding and small intronic (non-coding) flanking regions across the various *SIRT* genes studied. Notably, this approach revealed 11 novel SNPs which have not yet been reported. On the other hand, we did not detect in our screening sample several other reported SNPs which have a low frequency. However, we are confident that our overall method of polymorphism identification was effective since 1) we were able to identify the most frequent SNPs reported in the assessed gene portions, and 2) we confirmed the effective absence of nucleotide substitutions in a pool of samples with single peak dHPLC profile. Hence, our approach was useful to characterize sirtuin genetic variation of our sample population avoiding 1) the need of evaluating all the annoted SNPs known to date and 2) having significantly larger direct sequencing costs (which were still current at the moment we conducted the analysis).

From this study, 11 of the 29 SNPs identified resided in the protein-coding regions (cSNPs). 3 cSNPs were silent changes (scSNPs) already been reported in NCBI dbSNP: *SIRT1* L332L rs2273773, *SIRT6* F24F rs34786277, and *SIRT6* R76R rs11554579. Although silent SNPs do not affect the amino acid sequence, they deserve attention because they could alter translational efficiency as a consequence of codon usage bias. To this concern, at least in the case of SNP4 *SIRT1* L332L, it seems that the codon change occurred is not detrimental. In fact, referring to codon usage in *Homo sapiens,* leucin is more frequently encoded for by CTG (41%) rather than TTG (13%) which is the canonical codon at 332 position in *SIRT1*. However scSNPs, altering the mRNA secondary structure, could affect mRNA stability, translation and even protein structure. For example, it was demonstrated that scSNPs can lead to the synthesis of protein product with the same amino acid sequence but different structural and functional properties (Komar, 2007). A final

reason for considering these scSNPs is that even if in themselves they contribute no known biological effects, they may still serve as markers for association with disease through associations (by linkage disequilibrium) they may have with other adjacent SNPs which may mediate phenotype-associated affects.

The remaining 8 cSNPs were also found to affect changes to protein sequence, which are non-synonymous coding SNPs – nscSNPs. In particular 7 cSNPs were missense substitutions leading to a change in the relevant amino acid codons, and 1 cSNP was a 'nonsense' substitution giving rise to a "STOP" codon. Overall, with the exception of *SIRT5* R10* and *SIRT5* E305G, all of the other nscSNPs reside within the sirtuin conserved core domain (blue box in figure 3.1). Among nscSNPs, conservative missense substitutions (i.e. the canonical amino acid is changed with a novel one with similar biochemical properties), are *SIRT3* V208I, *SIRT6* S46N, *SIRT6* R121H and *SIRT7* A99V These substitutions lie in non-conserved positions within the sirtuin core domain (denoted by * in figure 3.1). However, *SIRT6* S46N is of particular interest because it is seven residues upstream the GAGIS motif and therefore could alter the microenvironment of the catalytic site.

Other missense substitutions were *SIRT1* E536K, *SIRT3* P262H and *SIRT5* E305G. In the case of *SIRT1* E536K, a negatively charged amino acid is substituted with a positively charged one, whereas in the *SIRT5* E305G change, a hydrophobic residue replaces a positively charged amino acid. For *SIRT3* P262H, a proline substitutes a positively charged amino acid presumably conferring rigidity to the structure. These amino acid substitutions could affect sirtuin protein function.

To begin to explore this possibility we performed multiple alignment between paralogue or orthologue sirtuins. Multiple alignment between human paralogue sirtuins highlighted the

more important residues for sirtuin family, such as the consensus GAG[I/V]S where serine is reported to be fundamental for sirtuin catalytic activity, where the sirtuin catalytic conserved domain was reported to reside. None of the identified SNPs apparently resided in conserved positions fundamental for sirtuin enzymatic activity (figure 3.1). However, multiple alignment between orthologue sirtuins showed an high conservation rate. *SIRT1* E536K and *SIRT3* P262H are located in conserved positions that appear to be important for the specific sirtuin class which might for example be of relevance for substrate interaction (figure 3.2). However, to avoid being overly speculative, the best means to try to clarify these questions would be to conduct appropriate functional studies which fell beyond the scope of this thesis.

The interesting substitution found in *SIRT5* was that of the introduction of a TGA (STOP codon) in place of the normal CGA codon. The is presumed to cause the truncation of SIRT5 translation after the $10^{th}$ amino acid residue position. Since this substitution was found to be heterozygotic in the subject carrying this mutation and as a result they could have only one functional *SIRT5* allele. However a detailed medical history was not available to identify if there were any unusual phenotypic aspects that might be related to this. Yet, this again would have a considerable degree of speculation which could be perhaps better unpicked through relevant functional work to ascertain the important of *SIRT5* and whether there was sufficient redundancy in its function such that a single copy would have been sufficient for normal activity.

Of the 18 SNPs identified by dHPLC which resided in the flanking intronic portions included in the analysis, none of ncSNPs apparently seem to cause aberrant splicing since they lie outside the splice site consensus sequences. Overall, we observed a higher number of variants in the *SIRT1*, *SIRT2*, *SIRT3* and *SIRT6* genes while few SNPs were found in *SIRT4*, *SIRT5* and *SIRT7*. No relationship between this difference in SNP frequency among

sirtuins and their putative phylogenetic evolution can be noticed. For example, SIRT6 and SIRT7 both belonging to Class IV (cfr. phylogenetic tree in section 1.2.1.1, figure 1.8) are extremely different in the number of variants. Furthermore, there was a high range of frequencies for the identified allelic variants. There were substitutions present in only 1 subject (~1%) which were more probably rare mutations rather than common polymorphisms, there were also variants present at low to moderate levels (under 25%) and more common variants (up to 50% frequency in the population). The more frequent polymorphisms occurred within *SIRT1*, *SIRT3* and *SIRT5* genes; instead *SIRT2*, *SIRT4*, *SIRT6* and *SIRT7* were characterized by variants with a frequency lower than 10%.

Overall, the most common variants in the population were mostly intronic. Indeed, in introns there are a lot of variants which usually have low or questionable functional importance. This is the reason why we decided to exclude intronic regions from our analysis and focus our attention on gene-coding portions. The majority of the protein-coding variants identified had a frequency lower than 10%, given the exception of SNP12 which in our screening sample was present in heterozygote form in 33% of cases. The remaining coding SNPs were low frequency variants, mostly likely to be rare mutations rather than polymorphisms, since they were found only in one subject. For most of the variants reported (5 out of 7) these constituted missense substitutions however this screen did not detect the majority of the cSNPs reported in dbSNP. This might be explained by the fact that our approach was set up to highlight more common variants whereas missense cSNPs are more likely to be rare mutations rather than polymorphisms since they alter the amino acid sequence but have also been reported in other ethnic groups which may not be as closely related to our population. However, we were able to identify rs11246020, which is highly frequent in the Caucasian population.

Of the the 29 identified SNPs, 11 were novel SNPs and the remaining 18 were already recorded in the NCBI SNP database (http://www.ncbi.nlm.nih.gov/SNP). The newly discovered SNPs were perhaps unsurprisingly mostly low frequency polymorphisms whereas those already known were generally more frequent. Furthermore, the more common variants were represented at comparable levels in both CT and AD groups of our screening sample with the only exceptions being SNPs 15 and 18 which were differently distributed between the two groups. Amongst the lower frequency variants, we found interesting differences in distribution between the AD and CT groups for SNPs 4, 7, 10, and 11. Potentially of most relevance from these is SNP4 because it is a cSNP, even if does not alter the amino acid sequence. Overall, only simple descriptive analysis was performed on the frequency data obtained from the screening study, since we designed dHPLC screening as a rapid qualitative approach only able to detect SNPs in heterozygosis and focused on a relatively small cohort (i.e. 48 subjects per group of interest). The differences found, however, deserved more investigation and as such a quantitative case-control approach (the main topic of chapter 4) was designed and conducted to clarify if following more rigourous testing in larger sample sizes there remained any evidence of associations between these SNPs and AD.

# *CHAPTER 4. CASE-CONTROL GENETIC ASSOCIATION STUDY OF SIRTUIN VARIANTS IN ALZHEIMER DISEASE*

# 4.1. SYNOPSIS

A case-control study was performed to investigate the genotype and allele distribution of several genetic variants in the sirtuin genes in an initial sample of 219 cases and 343 controls. With this sample size, the study was powered to highlight even small associations with AD (OR ~ 1.3). Based on GWAs studies reported in literature, it has been suggested that it would be unlikely to identify any further genetic variants that would have an association with odds ratio (OR) higher than 1.5 for a complex disease like AD (Ku et al., 2010).

For this study of the sirtuin genes, 34 SNPs residing on the sirtuin genes were selected according to different criteria. First, and for the majority of SNPs we selected them using a tagSNP approach to assess the genetic variation of the gene regions with high linkage disequilibrium (LD). We also included 6 SNPs which were felt to be of interest from the pilot dHPLC screening (cfr. chapter 3). Genotyping of SNPs was performed using Sequenom MassARRAY$^{TM}$ platform, in collaboration with Saarland University, Germany. The sample population included in this initial case-control study was also genotyped for *APOE* gene by RT-PCR. Overall, evidence of a marginal association between AD and rs10410544 SNP in the *SIRT2* gene (p= 0.05) was found. This association was found to be stronger in the *APOE* ε4 non-carriers, than before stratification by *APOE* genotype and was actually absent in the *APOE* ε4 carriers.

The preliminary result obtained was then further investigated in an independent replication sample of 316 cases and 298 controls. A similar pattern of association was found in the replication study but which on this occasion did not reach the nominal statistical significance. However, following the combination of the initial and the replication cohorts, in order to increase the power of the analysis, evidence of association between the rs10410544 SNP and AD in the whole sample (p= 0.03) was found. Furthermore, this

association was only present in non-*APOE* ε4 carriers (OR=1.29, 95% CI 1.04-1.59, p= 0.01) and not in *APOE* ε4 carriers (p= 0.43). Overall, we found evidence that rs10410544 T allele in the *SIRT2* gene may be a new risk factor for AD which acts independent of *APOE* ε4.

# 4.2. MATERIALS AND METHODS

## 4.2.1. SAMPLE POPULATION

The subjects included in the initial and replication case-control studies were recruited from unrelated clinical centres. A total of 561 subjects were included in the initial case-control study. The population selected was composed by 219 AD and 343 CT samples. Blood samples from LOAD patients were collected from two clinical centres: the "Luigi Sacco" hospital in Milan (Italy) and the "Beata Vergine" hospital in Mendrisio (Italian-speaking canton of Switzerland). Controls were recruited from "S. Antonio Abate" hospital in Gallarate (Italy). The three centres were within a distance of 50 km. A total of 614 subjects were also selected for the case-control replication study: 316 AD and 298 CT. For all subjects blood samples were collected from "Centro S.Giovanni di Dio-Fatebenefratelli" hospital in Brescia (Italy).

The summary demographic characteristics of the cases and controls used in the initial and replication studies are summarized in table 4.1. In both studies, AD and CT subjects were gender-matched ($p > 0.5$ Student t-test). Moreover, AD patients showed a MMSE score significantly lower than CT subjects ($p < 0.01$ Student t-test), evidence of AD cognitive decline. In the initial case-control study, controls were older than cases ($p < 0.01$ Student t-test) since they were included after a 3 years follow-up evaluation to exclude any possible neurological disorder.

| | Diagnose (No) | Gender M (%) | Mean age (years ± SD) | Mean MMSE (score ± SD) |
|---|---|---|---|---|
| **Initial case-control study** | CT (343) | 119 (34.8) | 86.8 ± 4.0 | 25.6 ± 3.2 |
| | AD (219) | 63 (28.8) | 77.5 ± 7.8* | 19.3 ± 3.8* |
| **Replication study** | CT (298) | 135 (45) | 70.76 ± 8.22 | 26.4 ± 5.3 |
| | AD (316) | 127 (40) | 71.64 ± 9.10 | 16.88 ± 4.8* |

**TABLE 4.1. Demographics of the cohorts selected for the initial case-control study and the replication study.**

*AD: Alzheimer's disease patients; CT: healthy controls; M: males; SD: standard deviation; MMSE: Mini Mental State Examination; *p< 0.01 vs. CT Student t-test.*

### 4.2.2. SIRTUIN SNP SELECTION

The SNPs selected for the case-control association study are summarized in table 4.2. In most of the cases only SNPs were examined since they are the most frequent form of variants in the human genome. Furthermore, common polymorphisms were preferred rather than rare variants because they are more likely to explain a common disease like AD (Schork et al., 2009). With the intention of covering the majority of genetic variation across the 7 sirtuin genes, 25 SNPs were chosen based on the genotype data available from the International HapMap Project (HMP) (http://hapmap.org/).

The HMP validated the millions of SNPs that were identified during and after the completion of the human Genome Project, and then characterized their correlation and measured their extent of linkage disequilibrium (LD) patterns in populations of European,

Asian and African ancestry. Thus far HMP have resulted in the validation and characterization of the LD patterns of more than 4 million SNPs. In doing this the HMP has shown that the existence of LD significantly reduces the number of SNPs that need to be genotyped in GWAs (e.g. tagSNPs tag entire LD blocks). Currently, HMP is in the process of repeating the validation exercises in an increased number of DNA samples (i.e. from the 270 and 4 representative populations) to 1301 samples from 11 different human populations.

For this project 13 sirtuin gene SNPs were selected from a tagSNP approach which was performed by querying the HapMap Genome Browser plug-in: *tag SNP picker* track (release 27 PhaseII+III, Feb09, on NCBI B36 assembly, dbSNP b126), configuring the *tagger multimarker* method and adopting a $R^2$ cut off of 0.8 and a MAF cut off of 0.2. The HapMap TSI panel was selected as reference population. The TSI ('Toscani in Italia') dataset is composed by 117 unrelated subjects resident in Tuscany (Centre of Italy). http://hapmap.ncbi.nlm.nih.gov/. A further 6 SNPs were also included in the study; these SNPs were deemed the most interesting ones from the dHPLC screening analysis (i.e. those with the highest frequency that displayed an apparenent difference in SNP frequency between AD and CT which was greater than 8% in heterozygosity). Moreover, in some instances, SNP position was taken into account to attempt to give some coverage to regions of sirtuin genes with low LD coverage.

| Gene/ chr n° | SNP | ID NCBI | Chromosome position | Exon/ Intron | NT change | Choice criteria |
|---|---|---|---|---|---|---|
| *SIRT1/* 10 | 1 | rs7896005 | 69651125 | IVS III | A>G | tagSNP |
| | 2 | rs2273773 | 69666598 | Exon V | T>C | dHPLC |
| | 3 | rs16924945 | 69674347 | IVS VIII | A>G | positional |
| | 4 | rs7897909 | 69676434 | 3'UTR | G>A | positional |
| *SIRT2/* 19 | 5 | rs2015 | 39369369 | 3'UTR | A>C | tagSNP |
| | 6 | rs11880757 | 39375632 | IVS VIII | C>T | positional |
| | 7 | rs11879010 | 39379855 | IVS VII | G>A | dHPLC |
| | 8 | rs11667030 | 39380030 | IVS VII | C>T | tagSNP |
| | 9 | rs10410544 | 39385532 | IVS II | T>C | tagSNP |
| *SIRT3/* 11 | 10 | rs3825075 | 217140 | IVS VI | G>A | tagSNP |
| | 11 | NA | 224004 | IVS V | G>A | dHPLC |
| | 12 | rs536715 | 230368 | IVS IV | G>A | positional |
| | 13 | rs4980329 | 232598 | IVS III | G>A | tagSNP |
| *SIRT4/* 12 | 14 | rs12307919 | 120741668 | Exon I | C>T | positional |
| | 15 | rs7137625 | 120746377 | IVS II | C>T | positional |
| | 16 | rs2261612 | 120750239 | IVS III | A>G | dHPLC/tagSNP |
| *SIRT5/* 6 | 17 | rs9382227 | 13579084 | IVS I | G>T | tagSNP |
| | 18 | rs2804919 | 13585142 | IVS III | G>A | tagSNP |
| | 19 | rs9370232 | 13589873 | IVS IV | G>C | tagSNP |
| | 20 | rs4712047 | 13590185 | IVS IV | A>G | tagSNP |
| | 21 | rs2253217 | 13600459 | IVS VIII | A>G | tagSNP |
| | 22 | rs2841517 | 13610188 | IVS IX | G>A | tagSNP |
| *SIRT6/* 19 | 23 | rs350846 | 4174398 | 3' UTR | G>C | positional |
| | 24 | rs107251 | 4176085 | IVS IV | C>T | positional |
| | 25 | rs350844 | 4177051 | IVS IV | G>A | positional |
| | 26 | rs352492 | 4179636 | IVS II | C>T | positional |
| | 27 | rs352493 | 4180836 | Exon II | T>C | dHPLC |
| | 28 | rs4807546 | 4182060 | IVS I | T>C | positional |
| *SIRT7/* 17 | 29 | NA | 79870250 | IVS II | C>T | dHPLC |
| | 30 | NA | 79870325 | Exon III | C>T | dHPLC |
| | 31 | rs11559052 | 79873326 | Exon V | A>T | positional |
| | 32 | rs34241371 | 79872527/8 | Exon VI | del/C | positional |
| | 33 | rs1879568 | 79872129 | IVS VII | G>A | positional |
| | 34 | rs36043502 | 79870835/6 | IVS IX | del/G | positional |

**TABLE 4.2. List of the SNPs included in the case-control study.**

*Abbreviations: chr n°, chromosome number; ID, IDentifier; NT, NucleoTide; IVS, Intronic Variant Sequence; del, deletion.*

*List of the SNPs genotyped with the corresponding NCBI's reference SNP number, chromosome positions according to genome build 37.2 (cfr. Table A.1. for chromosome reference sequences), intron/exon position within the gene and kind of substitution. In the last column it is reported the criteria of inclusion: tagging SNP (tagSNP), SNP chosen from the dHPLC study topic of chapter 3 or SNP chosen for their position.*

### 4.2.3. DATA QUALITY CONTROLS

SNP genotyping in the initial case-control study was carried on by Sequenom MassARRAY™ (Sequenom Inc.) MALDI-TOF system, in collaboration with dr. Mayhaus from Saarland University, Germany.

After genotype data was collected, several different quality control (QC) cut-offs were adopted. SNPs with genotype information lower than 90% (suggestive of difficulties in genotyping) were removed from the analysis and samples with a consistently low call rate (those who were genotyped unsuccessfully in more than 10% of the SNPs that passed the first QC) were eliminated (poor sample quality). Furthermore, to try to reduce the impact of genotyping errors, 1) Hardy-Weinberg equilibrium was taken into account for all SNPs and we excluded those SNPs whose genotype distributions was not in Hardy-Weinberg equilibrium (both in AD and CT group) ($p< 0.05$). For reference the included SNP genotype and allele frequency distributions were assessed for comparability between the cohorts studied here and the corresponding available data from the HapMap TSI panel to ensure that there were no obvious discrepancies which might be indicative of genotyping problems.

### 4.2.4. SNP GENOTYPING

The subjects included in the case-control studies: 561 in the initial study and 614 in the replication one, were all genotyped for the commonest polymorphisms in the *APOE* gene (ε2, ε3, ε4) by RT-PCR using two pre-designed TaqMan® SNP genotyping Allelic Discrimination assays (Applied Biosystems). Only rs10410544 SNP which went through to the replication study for further investigation from the initial case-control study where Sequenom was used was determined using a pre-designed TaqMan® Allelic Discrimination Assays (Applied Biosystems).

### 4.2.5. EXPRESSION QUANTITATIVE TRAIT LOCUS ANALYSIS

Expression Quantitative Trait Locus (eQTL) analysis for rs10410544 SNP was performed querying the eQTL browser (http://eqtl.uchicago.edu/cgi-bin/gbrowse/eqtl/).

### 4.2.6. STATISTICAL ANALYSIS

Demographic data were compared between cases and controls using the Student t-test.

The allele frequencies and the distribution of genotypes were compared using Pearson's goodness-of-fit $\chi^2$ test (df= 1 and df= 2 respectively). Likewise, the deviation from Hardy-Weinberg equilibrium was evaluated by $\chi^2$ test (df= 1).

A *priori* power analysis was performed with *G power* software v. 3.0 (http://www.psycho.uni-duesseldorf.de/abteilungen/aap/gpower3) to ascertain a useful sample size for the analysis of sirtuin variants and association with AD. The sample size was based on the assumption of being able to detect an association between a 'disease allele' and an outcome variable (i.e. presence of AD) with an effect size of 0.14 (corresponding to an OR of 1.3) (Chinn, 2000), with 1 degree of freedom $\chi^2$-test. The power ($\beta$) of detecting the association was set at 0.8 and the alpha-error ($\alpha$) at 0.05.

Univariate logistic regression analysis was performed to investigate a correlation between each genotyped SNP and AD susceptibility. ORs were calculated with 95% confidence intervals (CI). Multivariate logistic regression was used to assess the ORs adjusted for the effects of a number of potential confounders (i.e. gender, age and *APOE* genotype).

Pairwise LD between SNPs located on a same gene was evaluated with the HaploView program v. 4.2 (freely available at http://www.broad.mit.edu/mpg/haploview/) starting from our genotype data or from data available from the HapMap Project. Haplotypes were inferred with the PHASE v. 2.1 software using a coalescent process with recombination. The reconstructed haplotypes were tested for association with the disease outcome with

1000 permutations. Haplotypes below 0.05 frequency were excluded from the statistical analysis. For all analyses a p-value $< 0.05$ was considered to be significant.

# 4.3. RESULTS

The *a priori* power analysis suggested that at least 401 subjects, with the case:control ratio set to be 0.4:0.6, would have a power of 0.8 to detect associations with an OR of 1.3 between the SNPs investigated and AD. Given this results, we included 219 cases and 343 controls in the initial case-control study. The study design in this manner had an effective power of 0.91 and 0.65 to detect an association with an OR of 1.3 and 1.2 respectively.

### 4.3.1. *APOE* ε4 DISTRIBUTION

For all cases and controls and for the purposes of allowing for necessary stratification of sirtuin SNP data in due course we investigated the allele distributions of *APOE* main variants (ε2, ε3, ε4) both in the initial case-control sample population and in the replication cohort. We found a significantly different distribution of *APOE* ε4 allele between cases and controls (table 4.3, $p< 0.001$). The AD cases were nearly 6 fold more likely to carry an ε4 allele than controls (OR= 5.77 95% CI 3.75–8.86, OR= 5.34 95% CI 3.65-7.81 in the case-control sample and in the replication sample, respectively, $p< 0.0001$).

| | APOE *GENOTYPE* | | | | |
|---|---|---|---|---|---|
| | *AD CASES (%)* | | *CONTROLS (%)* | | *OR (95% CI)* |
| | *ε4 –* | *ε4 +* | *ε4 -* | *ε4 +* | *p-value* |
| ***Initial case-control study*** | *116 (55.5)* | *93 (44.5)* | *288 (87.8)* | *40 (12.2)* | *5.77 (3.75–8.86) p< 0.001* |
| ***Replication study*** | *155 (49.5)* | *159 (50.6)* | *250 (83.9)* | *48 (16.1)* | *5.34 (3.65-7.81) p< 0.001* |
| ***Total sample*** | *271 (51.8)* | *252 (48.2)* | *538 (85.9)* | *88 (14.1)* | *5.68 (4.28-7.54) p< 0.001* |

**TABLE 4.3. *APOE* ε4 distribution between cases and controls.**

*Subjects were divided on the basis of* APOE *genotype into* APOE *ε4 carriers and non carriers (ε4+ and ε4- respectively).*

## 4.3.2. IMPACT OF QUALITY CONTROL FILTERS ON THE INITIAL CASE-CONTROL STUDY DATA

Genotyping by Sequenom platform produced raw data to which quality controls filters were applied as previously described. In the first instance, 5 out of the 34 SNPs investigated (rs11559052, rs34241371, rs36043502, SNP11, SNP 29) were removed from the statistical analysis since they failed to be genotyped in more than 10% of the samples. Furthermore, 21 out of the 561 samples genotyped were excluded for not consistently being amplified for at least 10% of the remaining 29 SNPs and the corresponding subjects were removed from the study (9 cases and 12 controls). A further 7 SNPs (rs1879568, rs7137625, rs7897909, rs11880757, rs12307919, rs16924945, SNP30) out of the remaining 29 successfully genotyped SNPs were found to be monomorphic (i.e. having

only one genotype). Statistical analysis was the performed on the remaining 22 SNPs. All of these SNPs were found to be in Hardy-Weinberg Equilibrium, both in cases and controls ($p > 0.05$). Moreover, the genotype and allele frequencies in the studied population were similar to those of the TSI reference population taken from HapMap ($p > 0.05$) which was reassuring since the two populations are closely related both geographically and historically.

### 4.3.3. SINGLE MARKER ANALYSIS

The distributions of SIRT alleles and genotypes is displayed in table 4.4. Overall, 21 of the 22 SNPs for wich the statistical analysis was performed, were not found significantly different between cases and controls in genotype and allele frequencies. The only exception was rs10410544 SNP in the *SIRT2* gene where the T allele was present more in ADs than in CTs at a level that was borderline significant. From this it was observed that the AD cases were nearly 1.3 fold more likely to carry a T allele than controls (OR, 1.27 95% CI 0.99–1.64, $p = 0.05$). This allelic difference appeared to be driven mainly by an excess of TT homozygotes and a reduction in CC genotypes that were more frequent in AD cases than in controls. Conversely, no difference in the heterozygote frequency was found. Indeed, comparing the prevalence of the different genotypes between the AD and CT groups, we found that the OR for the CG genotype compared to the two homozygous groups was 1.14 (95% CI 0.77-1.69, $p = 0.53$) and that for the TT genotype compared to the other genotypes was 1.73 (95% CI 1.03-2.91, $p = 0.03$).

| | SNP ID NCBI | Genotype | % genotype CT | % genotype AD | $\chi^2$ [p-value] df=2 | Allele | % allele CT | % allele AD | $\chi^2$ [p-value] df=1 |
|---|---|---|---|---|---|---|---|---|---|
| SIRT1 | SNP1 rs7896005 | G//G | 46.41 | 44.65 | 0.26 [0.87] | G | 66.92 | 66.28 | 0.04 [0.82] |
| | | A//G | 41.02 | 43.26 | | A | 33.08 | 33.72 | |
| | | A//A | 12.57 | 12.09 | | | | | |
| | SNP2 rs2273773 | T//T | 84.87 | 86.51 | 1.8 [0.39] | T | 91.54 | 93.02 | 0.64 [0.42] |
| | | T//C | 13.35 | 13.02 | | C | 8.46 | 6.98 | |
| | | C//C | 1.78 | 0.47 | | | | | |
| SIRT2 | SNP5 rs2015 | A//A | 26.39 | 32.11 | 2.12 [0.34] | A | 51.75 | 55.50 | 1.65 [0.19] |
| | | A//C | 50.73 | 46.79 | | C | 48.24 | 44.49 | |
| | | C//C | 22.87 | 21.10 | | | | | |
| | SNP 7 rs11879010 | G//G | 83.82 | 85.32 | 1.92 [0.38] | G | 91.91 | 92.43 | 0.08 [0.76] |
| | | A//G | 16.18 | 14.22 | | A | 8.09 | 7.57 | |
| | | A//A | 0.00 | 0.46 | | | | | |
| | SNP 8 rs11667030 | C//C | 36.58 | 39.17 | 0.61 [0.73] | C | 60.62 | 61.52 | 0.09 [0.76] |
| | | C//T | 48.08 | 44.70 | | T | 39.38 | 38.48 | |
| | | T//T | 15.34 | 16.13 | | | | | |
| | SNP 9 rs10410544 | C//C | 35.93 | 31.13 | 4.2 [0.12] | C | 61.23 | 55.66 | 3.73 [0.05] |
| | | C//T | 50.60 | 49.06 | | T | 38.77 | 44.33 | |
| | | T//T | 13.47 | 19.81 | | | | | |
| SIRT3 | SNP 10 rs3825075 | G//G | 47.76 | 44.13 | 0.71 [0.69] | G | 69.25 | 66.90 | 0.62 [0.43] |
| | | A//G | 42.99 | 45.54 | | A | 30.75 | 33.10 | |
| | | A//A | 9.25 | 10.33 | | | | | |
| | SNP 12 rs536715 | G//G | 80.88 | 75.70 | 3.43 [0.17] | G | 89.85 | 87.62 | 1.34 [0.24] |
| | | A//G | 17.94 | 23.83 | | A | 10.15 | 12.38 | |
| | | A//A | 1.18 | 0.47 | | | | | |
| | SNP 13 rs4980329 | G//G | 59.12 | 52.56 | 3.00 [0.22] | G | 76.62 | 73.72 | 1.29 [0.25] |
| | | A//G | 35.00 | 42.33 | | A | 23.38 | 26.28 | |
| | | A//A | 5.88 | 5.12 | | | | | |
| SIRT4 | SNP 16 rs2261612 | G//G | 51.35 | 53.45 | 0.26 [0.87] | G | 71.6 | 73.04 | 0.14 [0.70] |
| | | A//G | 40.54 | 39.17 | | A | 28.3 | 26.96 | |
| | | A//A | 8.10 | 7.37 | | | | | |

**Table 4.4. Genotype and allele frequency of the investigated SNPs in the initial case-control population (continue in the next page).**

| | SNP ID NCBI | Genotype | % genotype CT | % genotype AD | $\chi^2$ [p-value] df=2 | Allele | % allele CT | % allele AD | $\chi^2$ [p-value] df=1 |
|---|---|---|---|---|---|---|---|---|---|
| SIRT5 | SNP 17 rs9382227 | G//G | 49.36 | 50.00 | 0.80 [0.66] | G | 69.39 | 70.92 | 0.25 [0.61] |
| | | G//T | 40.06 | 41.85 | | T | 30.61 | 29.08 | |
| | | T//T | 10.58 | 8.15 | | | | | |
| | SNP 18 rs2804919 | G//G | 53.43 | 49.30 | 1.41 [0.49] | G | 71.79 | 70.19 | 0.32 [0.56] |
| | | A//G | 36.72 | 41.78 | | A | 28.21 | 29.81 | |
| | | A//A | 9.85 | 8.92 | | | | | |
| | SNP 19 rs9370232 | G//G | 64.56 | 61.57 | 1.66 [0.43] | G | 78.68 | 78.01 | 0.09 [0.76] |
| | | C//G | 28.23 | 32.87 | | C | 21.32 | 21.99 | |
| | | C//C | 7.21 | 5.56 | | | | | |
| | SNP 20 rs4712047 | A//A | 33.14 | 36.28 | 0.76 [0.59] | A | 56.80 | 58.14 | 0.18 [0,67] |
| | | A//G | 47.34 | 43.72 | | G | 43.20 | 41.86 | |
| | | G//G | 19.53 | 20.00 | | | | | |
| | SNP 21 rs2253217 | A//A | 45.65 | 45.12 | 3.51 [0.17] | A | 66.52 | 68.60 | 0.44 [0.50] |
| | | A//G | 41.74 | 46.98 | | G | 33.48 | 31.40 | |
| | | G//G | 12.61 | 7.91 | | | | | |
| | SNP 22 rs2841517 | G//G | 31.27 | 37.38 | 3.79 [0.14] | G | 57.23 | 59.11 | 0.36 [0.54] |
| | | A//G | 51.92 | 43.46 | | A | 42.77 | 40.89 | |
| | | A//A | 16.81 | 19.16 | | | | | |
| SIRT6 | SNP 23 rs350846 | G//G | 81.74 | 81.69 | 0.71 [0.69] | G | 89.97 | 90.38 | 0.03 [0.84] |
| | | C//G | 16.47 | 17.37 | | C | 10.03 | 9.62 | |
| | | C//C | 1.80 | 0.94 | | | | | |
| | SNP 24 rs107251 | C//C | 81.60 | 82.33 | 0.66 [0.71] | C | 89.91 | 90.70 | 0.19 [0.65] |
| | | C//T | 16.62 | 16.74 | | T | 10.09 | 9.30 | |
| | | T//T | 1.78 | 0.93 | | | | | |
| | SNP 25 rs350844 | G//G | 80.94 | 81.19 | 0.69 [0.70] | G | 89.00 | 89.68 | 0.12 [0.72] |
| | | A//G | 16.13 | 16.97 | | A | 11.00 | 10.32 | |
| | | A//A | 2.93 | 1.83 | | | | | |
| | SNP 26 rs352492 | C//C | 89.88 | 88.37 | 0.42 [0.81] | C | 94.64 | 93.95 | 0.42 [0.81] |
| | | C//T | 9.52 | 11.16 | | T | 5.36 | 6.05 | |
| | | T//T | 0.60 | 0.47 | | | | | |
| | SNP 27 rs352493 | T//T | 90.24 | 89.35 | 0.19 [0.90] | T | 94.82 | 94.44 | 0.07 [0.78] |
| | | C//T | 9.17 | 10.19 | | C | 5.18 | 5.56 | |
| | | C//C | 0.59 | 0.46 | | | | | |
| | SNP 28 rs4807546 | T//T | 81.79 | 83.26 | 0.73 [0.69] | T | 90.00 | 91.16 | 0.41 [0.52] |
| | | C//T | 16.42 | 15.81 | | C | 10.00 | 8.84 | |
| | | C//C | 1.79 | 0.93 | | | | | |

**TABLE 4.4. Genotype and allele frequency of the investigated SNPs in the initial case-control population.**

A multivariate logistic regression model was built to calculate the OR for rs10410544 SNP adjusted for confounders. Age, ε4 allele of *APOE* and gender were taken into account. The resultant adjusted OR was 1.35 (95% CI 0.96-1.90, p= 0.08).

We also stratified the initial study sample data for AD major risk factor *APOE* ε4 allele and found that the association between AD and the T allele of rs10410544 SNP was not evident in *APOE* ε4 carriers (OR= 1.57, 95% CI 0.90-2.75; p= 0.10) but was present in *APOE* ε4 non-carriers (OR= 1.36, 95% CI 1.00-1.86; p= 0.04) (table 4.5).

| ***SIRT2*** ***rs10410544*** | ***APOE* ε4 -** | | | ***APOE* ε4 +** | | |
|---|---|---|---|---|---|---|
| **Allele** | **CNT** | **AD** | **$\chi^2$ (p-value)** | **CNT** | **AD** | **$\chi^2$ (p-value)** |
| **C** | 60.31 | 52.60 | 4.83 (**0.04**) | 68.75 | 58.24 | 2.59 (0.10) |
| **T** | 39.69 | 47.39 | 1.36 [1.00-1.86] | 31.25 | 41.76 | 1.57 [0.90-2.75] |

**TABLE 4.5. Allele frequency of rs10410544 SNP in *APOE* ε4- and ε4+ carriers in the case-control sample.**

To attempt to replicate verify a previously published association between *SIRT1* polymorphisms and AD in females older than 65 years (Helisalmi et al., 2008), we stratified our sample according to gender. In particular, we focused our attention on *SIRT1* rs2273773 since the same polymorphism for which the previous association was reported. We found no difference neither in the genotype nor in the allele frequency of this SNP between female cases and controls (table 4.7).

| Total sample | Mean age (years ± SD) | n° F (% of total sample) n° F > 65 | % genotype | | % allele | | OR (95% CI) p-value |
|---|---|---|---|---|---|---|---|
| CT (463) | 69.6 ± 5.1 | 278 (60.0) **222** | **T//T** | 74 | **T** | 86 | **1.517** (1.05-2.19) p< **0.05** |
| | | | **C//T** | 23 | **C** | 14 | |
| | | | **C//C** | 3 | | | |
| AD (326) | 72.1 ± 6.9 | 221 (69.0) **187** | **T//T** | 63 | **T** | 80 | |
| | | | **C//T** | 34 | **C** | 20 | |
| | | | **C//C** | 3 | | | |

**TABLE 4.6. Genotype and allele frequency of rs2273773 polymorphism in females older than 65 years of age in Helisalmi et al. study.**

*Abbreviations: n°, number; F, females.*

*Demographics of the Finnish sample population in Helisalmi et al. study and genotype and allele frequencies of rs2273773 in females older than 65 years of age.*

| | Genotype | % genotype CT | % genotype AD | $\chi^2$ [p-value] | Allele | % allele CT | % allele AD | $\chi^2$ [p-value] |
|---|---|---|---|---|---|---|---|---|
| **SIRT1 Rs2273773** | T//T | 83.41 | 86.28 | 4.318 [0.11] | T | 90 | 93 | 1.82 [0.17] |
| | C//T | 13.82 | 13.72 | | C | 10 | 7 | |
| | C//C | 2.76 | 0 | | | | | |

**TABLE 4.7. Genotype and allele frequency of rs2273773 polymorphism in females older than 65 years of age in the case-control study.**

### 4.3.4. HAPLOTYPE ANALYSIS

Although most of the SNPs selected for this study were chosen as tagSNP of different LD blocks (i.e. with low LD between each other), some strong pairwise LD were found, represented in figure 4.2 by red boxes. In particular, a strong LD was found between the two markers investigated of the *SIRT1* gene that were 5Kb distant from each other. Moreover, SIRT6 showed a unique LD block according to the HaploView program, consisting of all six markers genotyped. On the contrary, no sufficient information were available to build up an LD map for *SIRT4* and *SIRT7* genes. Finally, SIRT2, SIRT3 and SIRT5 showed an high LD between two nearby markers. Particularly interesting is the case of SIRT5 where an high LD was found between two markers distant 9 Kb.

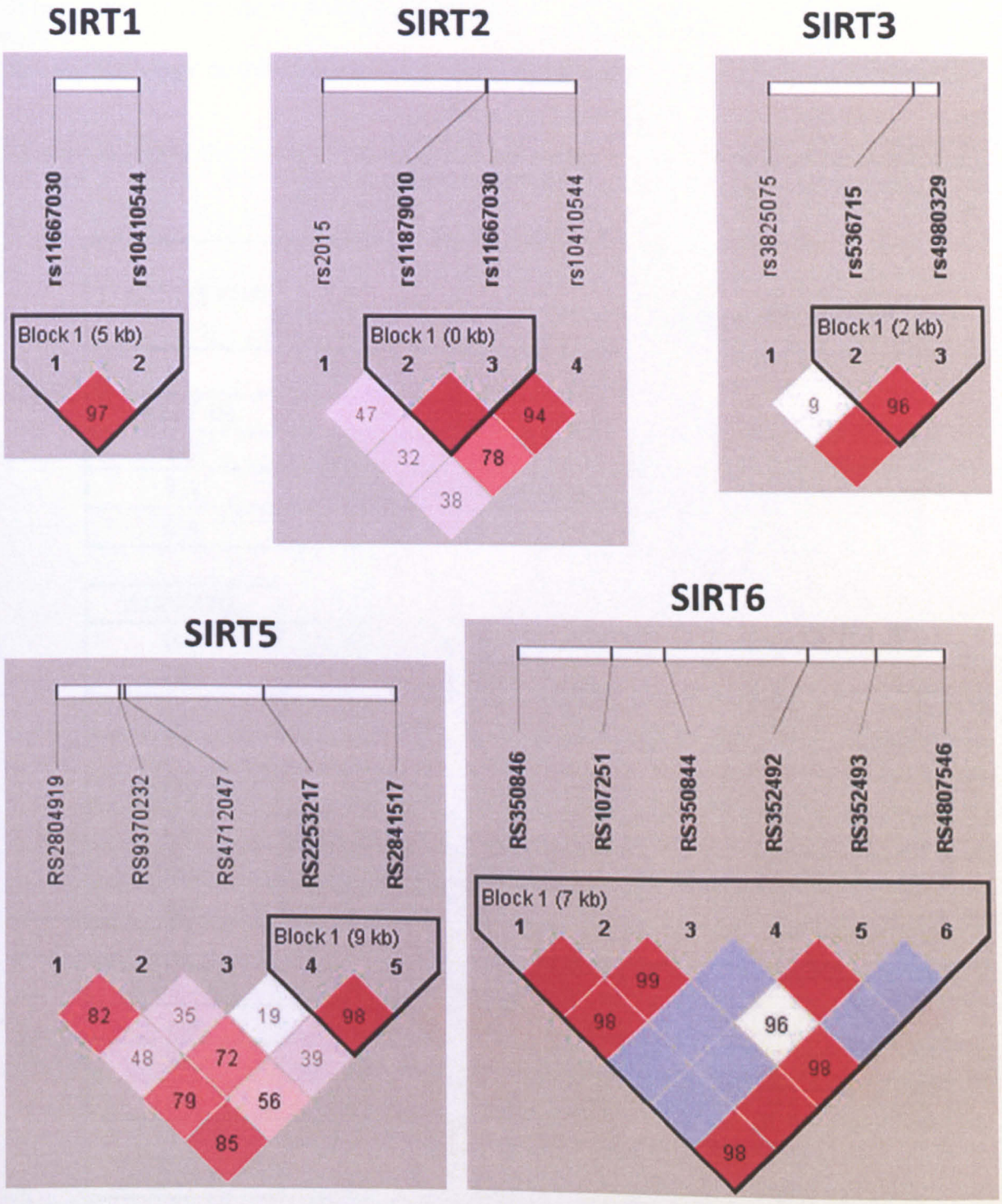


**FIGURE 4.1. Pairwise linkage disequilibrium (LD) between SIRT markers.**

*Graphs showing the genotyped SNPs according to the position along the gene and their pairwise LD pattern as measured by D' values. Red colour is suggestive of high D'. The identified LD blocks (defined by the confidence interval algorithm). are highlighted by black boxes.*

When we estimated the haplotype frequencies in the different haplotype blocks, we found that the haplotype distributions did not significantly differ between cases and controls.

| HAPLOTYPE | CT | AD | $\chi^2$ | P-VALUE (1000 permutations) |
|---|---|---|---|---|
| ***SIRT1* B1** | | | | |
| **TG** | 0.67 | 0.66 | 0.01 | 1 |
| **TA** | 0.25 | 0.27 | 0.40 | 0.99 |
| **CA** | 0.08 | 0.07 | 1.01 | 0.64 |
| ***SIRT2* B1** | | | | |
| **GC** | 0.52 | 0.54 | 0.69 | 0.68 |
| **GT** | 0.4 | 0.38 | 0.46 | 0.77 |
| **AC** | 0.08 | 0.8 | 0.09 | 0.94 |
| ***SIRT3* B1** | | | | |
| **GG** | 0.63 | 0.62 | 0.53 | 0.76 |
| **GA** | 0.27 | 0.26 | 0.07 | 0.96 |
| **AG** | 0.1 | 0.12 | 2.32 | 0.27 |
| ***SIRT5* B1** | | | | |
| **AA** | 0.43 | 0.41 | 0.37 | 0.81 |
| **GG** | 0.33 | 0.31 | 0.29 | 0.85 |
| **AG** | 0.24 | 0.28 | 1.93 | 0.36 |
| ***SIRT6* B1** | | | | |
| **GCGCTT** | 0.84 | 0.84 | 0.03 | 1.00 |
| **CTACTC** | 0.10 | 0.10 | 0.36 | 0.90 |
| **GCGTCT** | 0.05 | 0.05 | 0.02 | 1.00 |

**TABLE 4.8. Estimated haplotype frequencies of SIRT LD blocks.**

*Abbreviations: B1, block 1*

### 4.3.5. REPLICATION STUDY

Given the suggestive evidence of association from the initial case-control study for rs10410544 we sought to investigate it further in an independent sample, genotyping 316 cases and 298 controls. In this replication sample we observed the same tendency of a lower CC genotype in AD patients compared to CTs. However, this time the TT genotype was not as over-represented as was seen in the initial case-control cohort and overall the T allele was higher in cases than in controls but not to the extent of being statistically significant (OR was 1.15, 95% CI 0.92-1.45, p= 0.2).

| | Genotype | % genotype CT | % genotype AD | $\chi^2$ [p-value] df=2 | Allele | % allele CT | % allele AD | $\chi^2$ [p-value] df=1 |
|---|---|---|---|---|---|---|---|---|
| **SIRT2 Rs10410544** | C//C | 38.25 | 32.59 | 2.15 [0.34] | T | 61.9 | 58.3 | 1.59 [0.20] |
| | C//T | 47.31 | 51.58 | | C | 38.0 | 41.6 | |
| | T//T | 14.42 | 15.82 | | | | | |

**TABLE 4.9. Genotype and allele frequency of rs10410544 polymorphism in *SIRT2* gene in the replication study.**

Combining the initial and replication case-control populations, so as to increase the sample size, we again found a significant difference in the allele frequency of *SIRT2* rs10410544 between AD and CT (table 4.10). Here the T-allele carriers of *SIRT2* rs10410544 had an OR of 1.20 (95% CI 1.01-1.41, p= 0.03). We corrected the raw OR for gender, age and

*APOE* ε4 allele, and we found that the association between *SIRT2* rs10410544 T allele and AD was confirmed OR= 1.23 (95% CI 1.02-1.5, p= 0.02).

| | Genotype | % genotype CT | % genotype AD | $\chi^2$ [p-value] df=2 | Allele | % allele CT | % allele AD | $\chi^2$ [p-value] df=1 |
|---|---|---|---|---|---|---|---|---|
| **SIRT2 rs10410544** | C//C | 37.22 | 32.00 | 4.7 [0.09] | T | 61.5 | 57.2 | 4.6 [0.03] |
| | C//T | 48.72 | 50.48 | | C | 38.4 | 42.7 | |
| | T//T | 14.06 | 17.52 | | | | | |

**TABLE 4.10. Genotype and allele frequency of rs10410544 polymorphism in *SIRT2* in the two studies combined.**

Stratifying the *SIRT2* rs10410544 data by *APOE* ε4 status, the association between rs10410544 T allele and AD was present in *APOE* ε4 non-carriers only (df= 1, *APOE* ε4 non-carriers $\chi2$= 5.78, p= 0.01; *APOE* ε4 carriers $\chi2$= 0.70, p= 0.39) (table 4.11). Furthermore, among AD lacking *APOE* ε4 allele, *SIRT2* rs10410544 T allele carriers had a higher risk of developing AD of ~ 1.3 in comparison to C allele carriers (OR= 1.29, 95% CI 1.04-1.59, p= 0.01) - even higher than in the total unstratified AD sample.

| SIRT2 rs10410544 | *APOE* ε4 - | | | *APOE* ε4 + | | |
|---|---|---|---|---|---|---|
| **Allele** | **CNT (%)** | **AD (%)** | **$\chi^2$ (p-value) OR [95% CI]** | **CNT (%)** | **AD (%)** | **$\chi^2$ (p-value) OR [95% CI]** |
| **C** | 61.4 | 55.2 | 5.78 (**0.01**) | 62.0 | 58.4 | 0.7 (0.39) |
| **T** | 38.5 | 44.7 | 1.29 [1.04-1.59] | 37.9 | 41.5 | 1.16 [0.81-1.65] |

**TABLE 4.11. Allele frequency of rs10410544 polymorphism in *APOE* ε4- and ε4+ carriers in the two studies combined.**

### 4.3.6. EXPRESSION QUANTITATIVE TRAIT LOCUS ANALYSIS

To highlight a potential functional role for rs10410544 SNP, it was assessed whether this variant could regulate the transcript levels of other genes. Taking advantage of a public available eQTL browser, rs10410544 SNP was found to regulate in *cis* the transcript levels of the mitochondrial seryl-tRNA synthethase (*SARS2*) (score = 6.28) in lymphoblastoid cell lines from the HapMap CEU population (60 unrelated Utah residents with ancestry from Northern and Western Europe) (Stranger et al., 2005).

# 4.4. DISCUSSION

We performed a case-control association study to assess the impact of sirtuin common polymorphisms on LOAD risk. We adopted a tagSNP approach, which is a powerful and cost effective method to measure genetic variation within gene regions with high LD (Stram, 2004). Overall, our approach was useful to reduce the number of SNPs that needed to be tested without it detrimentally effecting having a good level of coverage of sirtuin gene variation.

This approach did miss some regions with low LD and\or variants with low minor allele frequency (MAF). Interestingly, in accordance with data reported in dbSNP database from NCBI, *SIRT7* was found to be monomorphic for all of the variants studied. In contrast to *SIRT7*, we confirmed the strong LD of *SIRT1*, where the variation could be summarized by a single SNP (e.g in our case rs7896005). Also *SIRT6* revealed a unique LD block in our sample population. This LD block was not revealed querying HapMap tagSNP browser, since we set the minor allele frequency (MAF) cut off at 0.2, and *SIRT6* SNPs all have a MAF of about 0.1.

Based on previously reported GWAs, the identification of any genetic susceptibility factors was not expected to yield an OR greater than 1.5 for AD (Ku et al., 2010). Thus, this study was powered so as to highlight even weak associations between the SNPs investigated and AD which might have an OR~ 1.3). In this, we were able to confirm the association between AD and *APOE* ε4 allele, already reported in literature also for the Italian population (Scacchi et al., 1999; Sorbi et al., 1994). Moreover, we found a lack of association between *SIRT1* variation and AD, as previously reported (Morgan et al., 2007; Helisalmi et al., 2008). Also we did not reproduce the gender-based association found by Helisalmi et al., between rs2273773 SNP (included in our study) and AD in the subgroup

of women older than 65 years. The lack of association in our sample suggests that the result reported in the previous work, as also argued by the author, may have been a false positive association due to stratification by gender and age. Indeed, applying the Bonferroni correction for the number of tests performed, the association reported was lost (Helisalmi et al., 2008).

Unlike SIRT1, the other sirtuins have been less studied in the context of AD. However, emerging data are highlighting the role of sirtuins in neurodegenerative diseases. For the first time, we investigated the potential impact of SNPs in the *SIRT2-7* genes in modulating AD susceptibility. We found evidence of a new association between rs10410544 SNP in *SIRT2* and AD in a population with Caucasian ancestors. This association was found in the initial case-control study with marginal statistical significance ($p= 0.05$). Although not confirmed in the separate replication analysis, the association was again present and stronger after combining the two study samples. The combination was possible because the two sample sets were geographically related. The *post hoc* analysis revealed that our sample size, in both studies separately, had a power of about 0.65 to detect associations with an OR around 1.2. Instead, combining the two studies we had a power higher than 0.90 to find the reported association. This could explain why we did not find the association in the replication study.

Overall, even if with a small effect size, allele T of the rs10410544 SNP might contribute to explain a percentage of SAD susceptibility. The small risk modulation identified (OR ~ 1.2) is consistent with previously reported data suggesting that, apart from *APOE* ε4, only associations with this magnitude are likely to be discovered in relation to AD. However, it is possible that our finding is a statistical false positive. Indeed, the observed association would not survive the Bonferroni's correction for multiple testing particularly given the current sample size. Furthermore, this eventuality is supported by the lack of any

associations between AD and the SNPs near *SIRT2* in a number of recent large GWAs. Otherwise, another reason why this association was not found in previous GWAs could depend on the fact that, despite thousands of samples, the GWAs are still underpowered to identify OR of this entity. Moreover, since this polymorphism does not lie in a conserved LD block, it is not represented in several commercial arrays (e.g. Illumina 500 K). However, imputation methods and GWAs meta-analysis studies are overcoming these limitations.

Noteworthy, this novel association does not arise from a false positive association due to an higher prevalence of *APOE* ε4 in the case group since the association was still present in *APOE* ε4 non-carrier subjects after stratification. Moreover, the association was not present in *APOE* ε4 carriers. This feature could be of interest in depicting a genetic risk profile in *APOE ε4* non-carrier subjects, where no evident genetic factors are playing a predisposing role. Another explanation is that the sample size in *APOE ε4* subjects is not sufficient to highlight the association.

*SIRT2* rs10410544 is an intronic variant, so whether it has a functional role is difficult to interpret. For example, in several cases, intronic variants could have a functional importance because their location may coincide with some regulatory elements (Wang et al., 2008), either already known or yet to be characterized, such as enhancers, insulators, transcription factor binding sites and sequences encoding for microRNA. To assess whether this intronic region might modulate the transcription rate of other genes, we queried an eQTL browser and we found that rs10410544 SNP is an eQTL acting in *cis* for *SARS2* gene, in the HapMap-CEU population (Stranger et al., 2005). This evidence is not easily linkable to AD, since *SARS2* gene encodes the mitochondrial seryl-tRNA synthethase. However, it was recently reported that a homozygous coding point mutation in *SARS2* (Asp390Gly) was responsible for a severe multisystemic mitochondrial

cytopathy of infancy, so this gene has a pathogenic potential that in the context of aging might lead to different clinical syndromes (Belostotsky et al., 2011). Nonetheless, for now given this data, *SIRT2* rs10410544 SNP could mediate effects over the transcription levels of other not yet investigated genes. Alternatively, and perhaps more likely, since we selected this SNP guided by LD information, this SNP could be the surrogate marker tagging for a more relevant variant that is important in AD.

In summary, we found no differences in gene variations in the *SIRT1* and *SIRTs 3-7* between AD and CT to support any roles of their corresponding proteins in the pathogenesis of AD. However we found evidence of a new association that deserves more attention and independent replications. This association, which links *SIRT2* and AD, may help clarify some of the molecular mechanisms underlying AD etiology.

# *SECTION B: IN VIVO STUDIES*

# *CHAPTER 5: ENVIRONMENTAL ENRICHMENT IN APP23 MOUSE MODEL OF ALZHEIMER'S DISEASE*

## I. Mouse models of AD

Given the high prevalence and poor prognosis of the AD, the development of animal models that mimic certain aspects of the disease has been a research priority to understand AD-like pathogenic mechanisms and to develop and test therapeutic strategies (Götz and Ittner, 2008).

The majority of transgenic mouse models of AD were generated based on information gathered from familial forms of the disease, which is far less common than sporadic disease and which is largely indistinguishable from a clinical and histopathological point of view. At the present time, transgenic models overexpressing the amyloid precursor protein (*APP*) and/or presenilins (*PSEN1, PSEN2*) harbouring one or more mutations that have been found in familial AD are available (table 5.1). These mice develop age-dependent AD-like pathology including amyloid deposits in the brain parenchyma. However, these models fail to develop detectable NFTs and consistent neuronal loss (Götz and Ittner, 2008). On the other hand, mouse models expressing human Microtubule-Associated Protein Tau (MAPT) gene with mutations found in FTD (Ballatore et al., 2007) develop both neurofibrillary tangles and neuronal loss in the absence of amyloid plaques. Triple transgenic model (3xTg-AD), harbouring three mutated transgenes: *PSEN1* (M146V), *APP* (K670M/N671L) and *MAPT* (P301L), have been generated trying to recapitulate both amyloid and tangle-related features. This model accumulates intraneuronal Aβ and subsequently forms amyloid plaques and MAPT lesions in an age-dependent fashion. These mice also develop age-dependent synaptic dysfunctions, including long-term potentiation deficits and memory deficits that correlate with the accumulation of intraneuronal Aβ (Oddo et al., 2003). However, these mice do not recapitulate all human

AD traits, for example they do not display neuronal loss and more recently the models have not been shown to be as reliable as previously suggested (Ferrington et al., 2011). Altogether the current mouse models, although not fully replicating the whole spectrum of AD-like pathologies, have provided valuable insights into disease mechanisms as well as opportunities to test therapeutic approaches.

| Mouse model | Gene (mutation) | Intraneuronal Aβ | Parenchymal Aβ plaques | Hyperphos-phorylated Tau | Neurofi-brillary tangles | Neuronal loss | Synaptic loss | CAA |
|---|---|---|---|---|---|---|---|---|
| PDAPP | APP (V717F) | - | Yes | Yes | No | No | Yes | - |
| Tg2576 | APP (K670N/M671L) | Yes | Yes | - | - | No | No | - |
| TgCRND8 | APP (K670N/M671L, V717F) | - | Yes | - | No | No | - | - |
| APP/PS1 | APP (K670N/M671L), PS1 (M146L) | - | Yes | - | - | - | - | - |
| APP23 | APP (K670N/M671L) | - | Yes | Yes | No | Little | Yes | Yes |
| Tg-SwDI | APP (E693Q, D694N) | - | Yes | - | - | - | - | Yes |
| APPDutch | APP (E693Q) | - | Little | - | - | - | - | Yes |
| APPDutch/PS1 | APP (E693Q), PS1 (G384A) | - | Yes | - | - | - | - | Little |
| hAPP-Arc | APP (E693G, K670N/M671L, V717F) | - | Yes | - | - | - | - | Little |
| Tg-ArcSwe | APP (E693G, K670N/M671L) | Yes | Yes | - | - | - | - | Yes |
| APPArc | APP (E693G) | - | Yes | - | - | - | - | Yes |
| TAPP | APP (K670N/M671L), Tau (P301L) | - | Yes | - | Yes | - | - | - |
| 3xTg-AD | APP (K670N/M671L), Tau (P301L), PS1 (M146V) | Yes | Yes | Yes | Yes | - | No | - |
| $APP_{SL}$/PS1 | APP (K670N/M671L, V717I), PS1 (M146L) | Yes | Yes | - | - | Yes | Yes | - |
| APP/PS1KI | APP (K670N/M671L, V717I), PS1 (M233T/L235P) | Yes | Yes | - | - | Yes | Yes | - |
| 5xFAD | APP (K670N/M671L, I716V, V717I), PS1 (M146L/L286V) | Yes | Yes | - | - | Yes | Yes | - |

**TABLE 5.1. Neuropathological features of the main transgenic mouse models of AD.**

*Table from* (Schaeffer et al., 2011).

*Dash (-) = not reported.*

*In the black box the human-like AD neuropathological features of APP23 (the experimental model used in this thesis) are highlighted.*

## II. Environmental enrichment in AD

The current lack of preventative and long term-acting therapies for AD provides a strong incentive for the ongoing search for more effective interventions. Besides the large amount of studies assessing novel 'disease-modifying' drugs, the efficacy of non-pharmacological treatments in delaying or preventing the onset of AD is also being examined. Non-pharmacological treatments are supported from epidemiological evidence that several lifestyle habits are risk factors for AD (diet, sedentary lifestyle, etc.). In contrast, people who have an healthy lifestyle (e.g. increased physical, mental and social activity) are less likely to develop an age-related dementia in later life (Abbott et al., 2004; Weuve et al., 2004; Friedland et al., 2001; Wilson et al., 2002).

Some lifestyle habits can be reproduced to some extent in the laboratory with animal models to allow more careful study. Housing mice in larger cages equipped with different interactive objects (i.e. tunnels, nesting material, toys and running wheels) is reported to enhance sensory, cognitive, motor and social stimulation with respect to standard housing conditions (van Praag et al., 2000). During the last decade, a large number of studies using transgenic mouse models of neurodegenerative disorders have strongly supported the beneficial effect of an enriched environment (Nithianantharajah and Hannan, 2006).

In AD mouse models, the "Environmental Enrichment" paradigm (EE) was shown to impact a variety of processes related to AD pathogenesis. For example, EE altered the enzymatic activity of the Aβ-degrading endopeptidase, neprilysin (Lazarov et al., 2005), decreased Aβ1–42/Aβ1–40 ratio (Mirochnic et al., 2009), altered expression of genes related to Aβ sequestration (Costa et al., 2007), and Aβ receptor/transporter molecules (Herring et al., 2008). Furthermore, EE was recently shown to induce changes in levels of hyperphosphorylated tau and oligomeric Aβ, the precursors of hallmark plaques and NFTs (Hu et al., 2010).

Moreover, EE was shown to increase the expression of neurotrophic factors, such as BDNF and NT-3 (Wolf et al., 2006; Berardi et al., 2007), growth factors, such as NGF (Levi et al., 2003; Berardi et al., 2007), increased synaptic proteins (Cracchiolo et al., 2007; Levi et al., 2003) and expression of various molecules associated with synaptic plasticity, neurogenesis, dendritic branching and axonal transport (Costa et al., 2007; Herring et al., 2009; Hu et al., 2010).

However, some controversial points still remain. In fact, varying outcomes have been reported for EE depending on the AD-like mouse model, the age of the mice, the duration of exposure and the type of the intervention used (Nithianantharajah and Hannan, 2006). For example, EE has been shown in different studies to have opposing and even null effects on Aβ plaque related pathology (Lazarov et al., 2005) (Arendash et al., 2004) (Jankowsky et al., 2003). Moreover, different effects of EE on mice cognitive performance have been observed: some studies have shown improvements (Levi et al., 2003) and others have reported no change (Görtz et al., 2008).

Finally, controversial results were reported about EE-induced cellular plasticity and neurogenesis. In some cases, EE was shown to effectively increase proliferation and/or the number of mature new-born hippocampal neurons (Wolf et al., 2006; Herring et al., 2009; Mirochnic et al., 2009; Hu et al., 2010). Others have shown that while enrichment can increase the rate of neural progenitor proliferation, it does not affect an impairment in survival of neural progenitor cells, thus resulting in fewer new neurons being generated in the hippocampus of AD mouse models (Wen et al., 2004; Catlow et al., 2009). In contrast, there is also evidence for a lack of hippocampal plasticity and deficiency in enrichment-induced proliferation (Choi et al., 2008) and/or neurogenesis in the dentate gyrus (Cotel et al., 2010).

Overall, EE is an attractive and promising approach that may provide therapeutic benefits and as such deserves more attention and further investigations.

## III. Sirtuin involvement in environmental paradigms.

Sirtuins have an important role in modulating metabolic processes in response to environmental changes. Sirtuins have been related largely to calorie restriction (CR), a protocol already proved to be beneficial in counteracting ageing and age-related diseases [topic of chapter 1.2.2.1.]. More recently, there as been growing evidence that this protein family is implicated in physical activity (PA). Exercise slows the deleterious effects of ageing in rats by increasing SIRT1 levels and activity in skeletal muscle (Suwa et al., 2008; Koltai et al., 2010) and heart (Ferrara et al., 2008). Moreover, PA was also shown to reduces SIRT6 levels in rat muscles (Koltai et al., 2010). Furthermore, endurance exercise in humans counteracted observed decreases in SIRT3 levels in muscle tissue from aged people with a sedentary lifestyle (Lanza et al., 2008). However, despite the suggested beneficial effects to the brain observed with environmental paradigm, few studies have analysed the level of sirtuins in the brain tissue after exposure to external stimula such as CR and PA (Kelly, 2010; Steiner et al., 2011). It is noteworthy that environmental paradigms such as CR, PA and EE were proposed to share common pathways able to counteract ageing and age-related diseases (Mattson et al., 2002).

# 5.1. SYNOPSIS

The overall aim of the work presented in this chapter was to set up a protocol of long lasting environmental enrichment (EE) in adult mice and assess whether this protocol was able to counteract the cognitive decline and the progressive pathological changes that normally occur in APP23 AD-like mouse model. In this context, the involvement of sirtuins was investigated by assessing mRNA and protein levels.

To achieve these goals, APP23 TG mice were moved to EE cages (TG-EEs) starting form 2-3 months of age. TG-EEs were compared to TG mice housed in standard cages (TG-SHs) and wild-type littermates in the two housing conditions (WT-EEs and WT-SHs) were also included as reference groups. At 6-7 months of age mice were tested for behavioural performance with Morris Water Maze (MWM) and visual Object Recognition Test (vORT) and then sacrificed at 8 months of age for biochemical analyses (8-10 mice per group) or at 18 months of age for plaque load assessment (4 mice per group).

At 6-7 months TG-SHs displayed an impaired behavioural performance in Morris Water Maze (MWM) test and visual Object Recognition Test (vORT) which reflected disturbance to spatial and recognition memory, respectively. EE was able to significantly restore mice behavioural performance in the TG mice. Moreover EE, although not affecting the expression of total soluble APP and its processing in 8-month-old mice, partially counteracted Aβ deposition in 18-month-old TG mice. In contrast, Aβ production was apparently not affected by EE. Finally, the application of an EE protocol did not modulate sirtuin mRNA and protein levels nor in WT neither in TG mice.

# 5.2. MATERIALS AND METHODS

## 5.2.1. EXPERIMENTAL SCHEME

All the experiments presented in this chapter were performed on heterozygous male APP23 mice and male wild-type littermates. Four groups were defined (n = 12-14 mice per group): TG housed in standard condition (TG-SHs), TG housed in enriched cages (TG-EEs), WT in standard cages (WT-SHs) and WT enriched cages (WT-EEs).

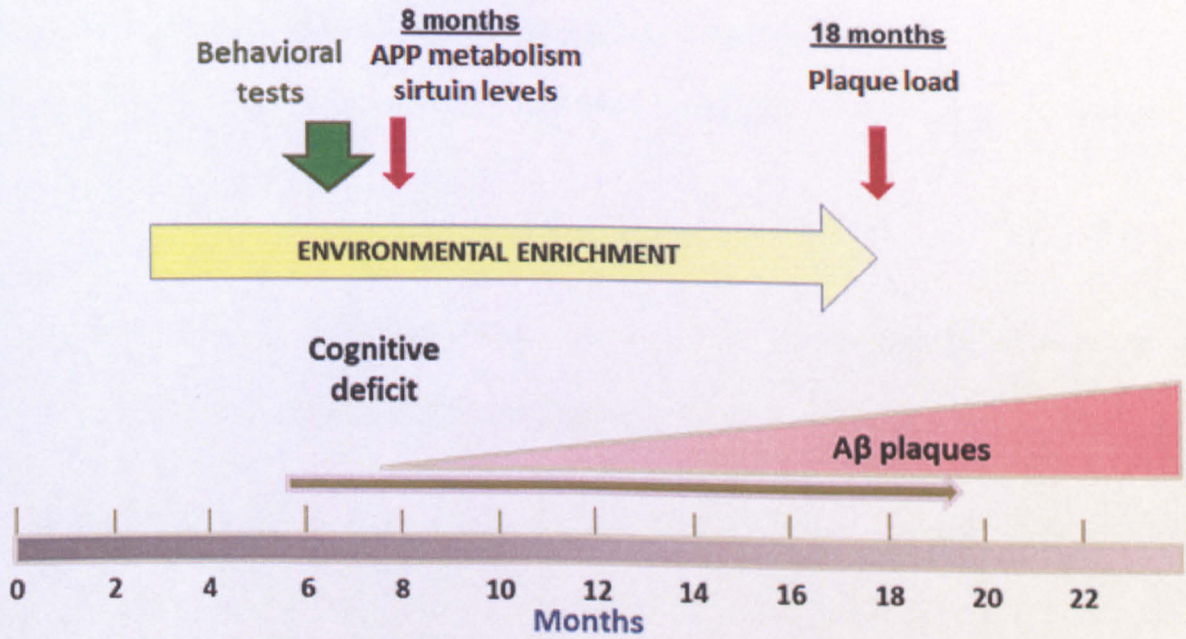


**FIGURE 5.1. Experimental scheme of the adopted environmental enrichment protocol.**

*Mice were weaned at 1 month of age and housed in standard cages. At 2-3 months of age, mice were randomly assigned to either enriched or standard cages. Enrichment lasted till the end of the experiment. Mice were assessed for behavioural performance at 6-7 months of age and then sacrificed for biochemical analysis n= 8-10. Another group was carried on till 18 months to assess plaque load n= 4.*

### 5.2.2. STATISTICAL ANALYSIS

All the analyses reported in this chapter were performed with GraphPad Prism® v. 5.0.
The acquisition session in MWM test was analysed using a repeated measures two-way ANOVA with groups as between-subjects factor and trials as within subjects factor followed by Bonferroni's *post hoc* test.

MWM probe trial, vORT exploration time and discrimination indexes, BDNF mRNA, and sirtuin mRNA and protein levels were analysed using a two-way ANOVA with genotype as between-subjects factor and housing condition as within subjects factor followed by Bonferroni's *post hoc* test. To directly compare TG-SHs and TG-EEs performance one-way ANOVA was adopted followed by Tukey's *post hoc* test.
TG-SHs and TG-EEs were directly compared with Student's t-test for all the parameters assessed concerning APP metabolism.

Two-tailed levels of significance were used in all the above mentioned analyses and $P<0.05$ was considered statistically significant.

# 5.3. RESULTS

## 5.3.1. EFFECT OF ENVIRONMENTAL ENRICHMENT ON BEHAVIORAL PERFORMANCE

To investigate whether TG mice behavioural performance compared to the WT counterpart was influenced by EE, 6/7-month-old mice housed for 4 months in SH or EE cages were tested with Morris Water Maze (MWM) and visual Object Recognition Test (vORT).

### *5.3.1.1. Morris Water Maze*

During the acquisition phase of the MWM experiment, the escape latencies of the trained mice decreased as a function of the number of days of training ($F_{days(df=9,480)}$= 9.99, P< 0.0001; two-way RM-ANOVA). The statistical analysis showed a significant difference between the four experimental groups assessed ($F_{groups\ (df=\ 3,480)}$= 9.03, P< 0.0001; two-way RM-ANOVA). Globally all groups improved their performance as a function of days of training. Indeed, no statistically significant interaction effect was visible (days of training x groups: $F_{int\ (df=\ 27,480)}$= 0.62, p= 0.93; two-way RM-ANOVA). However, TG-SHs mice performed worse in MWM training task compared to WT-SHs mice at each day of training (cfr. figure 5.2.). This visible tendency reached the statistical significance only at day 6 (P< 0.05; Bonferroni's *post hoc* test). Conversely, TG-EEs performed more similarly to WT mice, although never reaching statistically significant differences compared to TG-SHs.

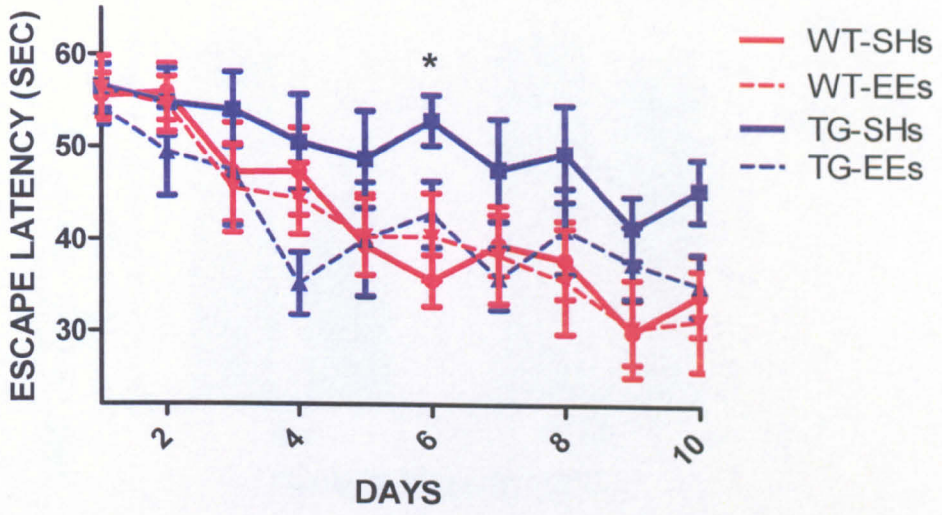


**FIGURE 5.2. MWM learning curves.**

*Escape latency of 6/7-month-old WT-SHs, WT-EEs, TG-SHs and TG-EEs during days of training. Each data point represents mean (± SEM) summed results of four daily trials. *P< 0.05 TG-SHs vs WT-SHs; Bonferroni's post hoc test.*

During the probe trial at day 11, 24 h after the last training session, the percentage of time spent in the target quadrant was influenced both by genotype and housing condition ($F_{genotype\ (df=\ 1,32)}= 12.79$, $P< 0.01$ and $F_{housing\ (df=\ 1,32)}= 4.17$, $P< 0.05$; two-way ANOVA). Moreover, two-way ANOVA showed that genotype effect on escape latency was influenced by housing condition ($F_{int\ (df=\ 1,32)}= 4.17$, $P< 0.05$; two-way ANOVA). Indeed, as shown in figure 5.3 TG-SHs mice spent less time in the correct quadrant than WT-SHs ($P< 0.001$ TG-SHs vs WT-SHs; Bonferroni's *post hoc* test) while no significant difference was visible between TG-EEs and WT-EEs (n.s. TG-EEs vs WT-EEs; Bonferroni's *post hoc* test). Moreover, Tukey's *post hoc* test revealed a significant difference between TG-SHs and TG-EEs ($P< 0.05$ Tukey's *post hoc* test).

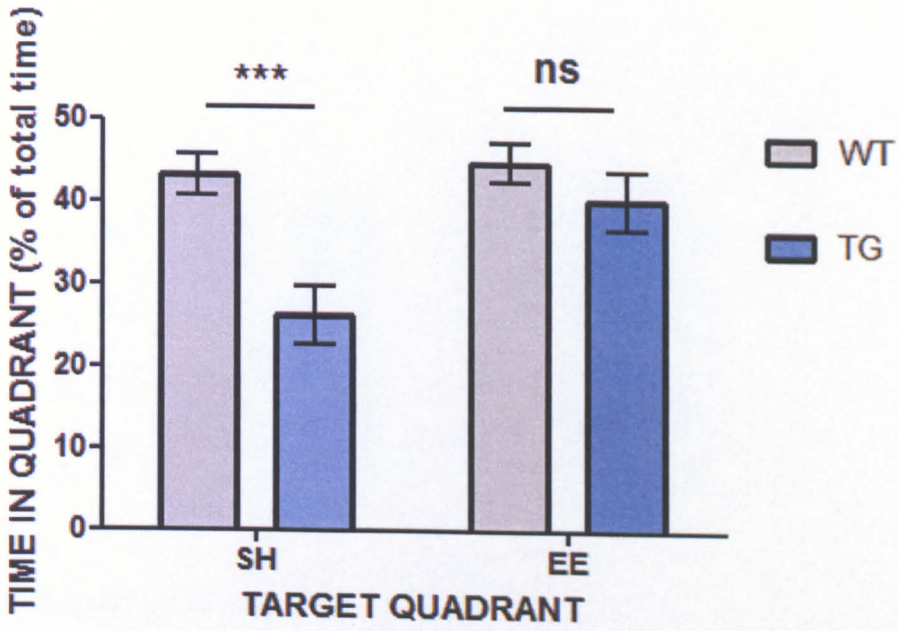


**FIGURE 5.3. MWM test probe.**

*Proportion of time spent in the target quadrant by 6/7-month-old WT-SHs, WT-EEs, TG-SHs and TG-EEs during MWM test probe with 24 h retention time. Bar graph indicates mean ± SEM.* $^{***}P< 0.001$ *TG-SHs vs WT-SHs; . ns. TG-EEs vs WT-EEs; Bonferroni's post hoc test.*

### *5.3.1.2. Object Recognition Test (vORT)*

During the training trial (familiarization phase) of vORT, the total exploration time was not affected either by genotype and housing condition nor by the interaction of the two parameters ($F_{genotype\ (df= 1,32)}= 0.24$, $P> 0.05$; $F_{housing\ (df= 1,32)}= 0.01$, $P> 0.05$; and $F_{int\ (df= 1,32)}= 0.01$, $P> 0.05$; Two-way ANOVA; figure 5.4).

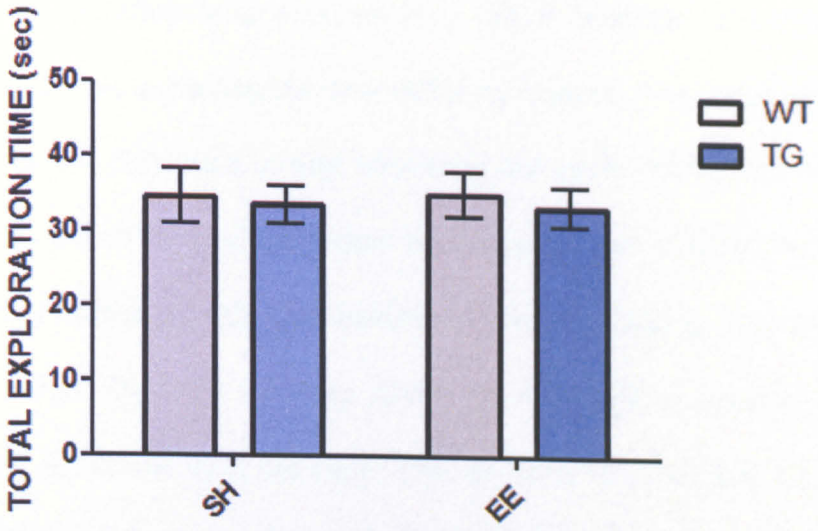


**FIGURE 5.4. Exploration time in the training trial**

*Total time spent exploring the two identical objects. Bar graph indicates mean ± SEM.*

In the familiarization phase none of the experimental group exhibited a preference in exploring one of the identical objects revealed by the discrimination index ($F_{genotype\ (df=\ 1,32)}= 0.05$, $P> 0.05$; $F_{housing\ (df=\ 1,32)}= 0.05$, $P> 0.05$; and $F_{int\ (df=\ 1,32)}= 2.01$; $P> 0.05$; Two-way ANOVA; figure 5.5).

.

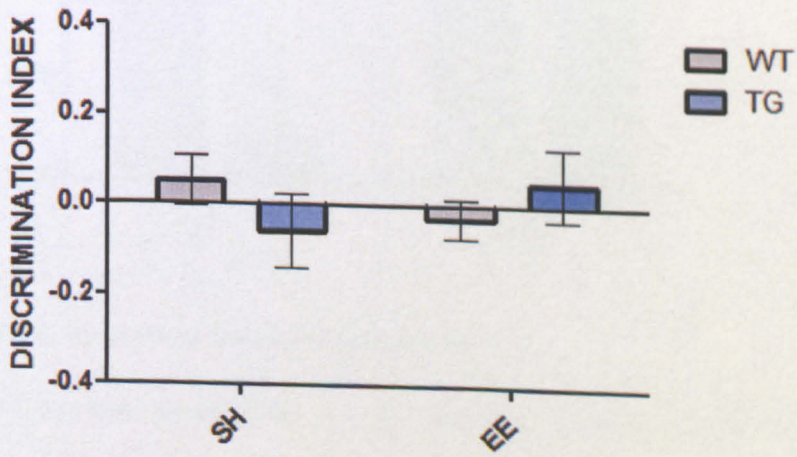


**FIGURE 5.5. Discrimination Index in the familiarization phase**

*The discrimination index was measured as the time spent exploring the left object minus the right object divided for the total exploration time. Bar graph indicates mean ± SEM.*

In the test probe assessing long-term memory (24 h retention time), the four groups exhibited different time exploring the two different objects. A discrimination index (DI) was calculated as the difference in time exploring the novel object and the familiar one, expressed as the ratio of the total time spent exploring the two objects. Both genotype and housing condition influenced this discrimination index ($F_{genotype\ (df=\ 1,32)}= 16.23$; $P< 0.001$, $F_{housing\ (df=\ 1,32)}= 4.31$; $P< 0.05$; two-way ANOVA). Genotype x housing interaction was only marginally significant ($F_{int\ (df=\ 1,32)}= 394$; $p= 0.055$). However, *post hoc* analysis revealed that TG-SHs mice had a DI lower than WT-SHs ($P< 0.001$ TG-SHs vs WT-SHs; Bonferroni's *post hoc* test) while no significant difference was visible between TG-EEs and WT-EEs (n.s. TG-EEs vs WT-EEs; Bonferroni's *post hoc* test). Moreover, Tukey's *post hoc* test revealed a significant difference between TG-SHs and TG-EEs ($P< 0.05$).

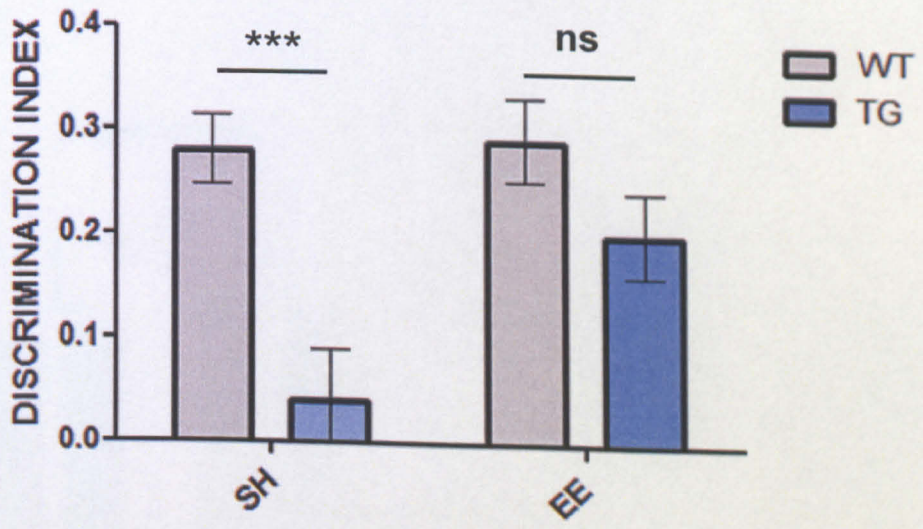


**FIGURE 5.6. Discrimination Index in the probe test**

*Long-term (24 h) discrimination index for the novel object in 8 month-old mice. Bar graph indicates mean ± SEM. ***P< 0.001 TG-SHs vs WT-SHs; ns= not significant. TG-EEs vs WT-EEs; Bonferroni's post hoc test.*

### 5.3.2. BDNF mRNA LEVELS

BDNF mRNA levels were investigated to verify the effectiveness of the adopted EE protocol since a large body of evidence show that environmental paradigms like EE and PA increase BDNF levels (Neeper et al., 1996; Wolf et al., 2006).

In 8-month-old mice no effect of genotype on BDNF was found both in hippocampus (hp) and cortex (cx) ($Fhp_{genotype\ (df=\ 1,32)}= 0.04$, $P> 0.05$; $Fcx_{genotype\ (df=\ 1,32)}= 0.00$, $P> 0.05$). Conversely, EE increased BDNF levels as shown in figure 5.7 for these brain areas. The EE effect was highly significant in the cortex as revealed by two-way ANOVA ($Fcx_{housing\ (df=\ 1,32)}= 12.88$, $P< 0.01$; $Fhp_{housing\ (df=\ 1,32)}= 6.64$, $p<0.05$). Noteworthy, there was no evidence of an interaction between EE and genotype which influenced either hippocampal or cortical BDNF levels ($Fhp_{genotype\ (df=\ 1,32)}= 0.01$, $P> 0.05$; $Fcx_{genotype\ (df=\ 1,32)}= 0.10$, $P> 0.05$).

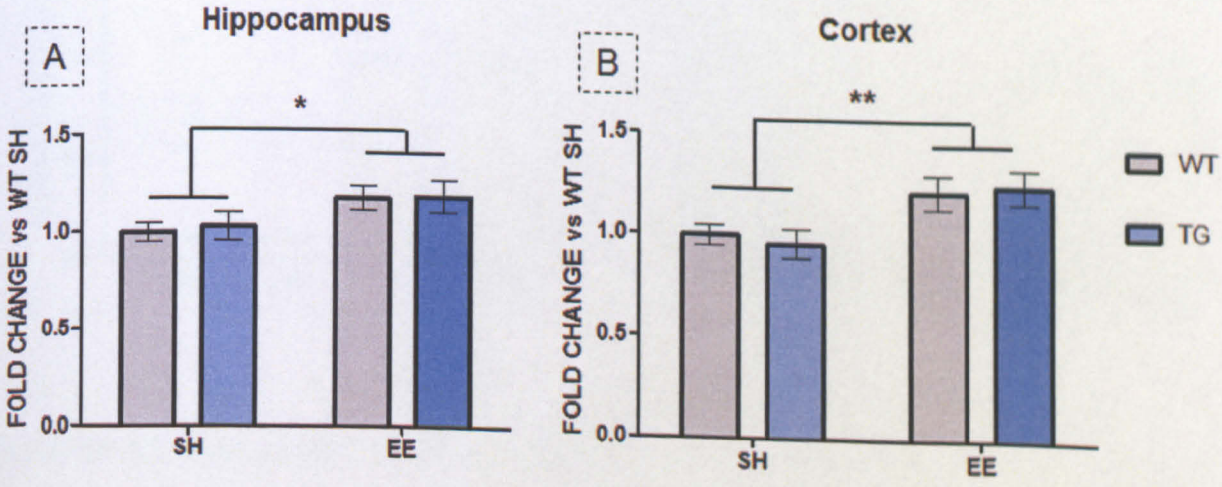


**FIGURE 5.7. BDNF mRNA levels**

*Murine BDNF mRNA levels in A. hippocampus and B. cortex of 8-month-old mice were assessed by RT-PCR referring to α-actin as endogenous gene. The results are reported as mean fold change vs WT-SHs and are represented as mean ± SEM.*

## 5.3.3. APP METABOLISM

### *5.3.3.1 Total APP levels and APP processing*

At 8 months, TG mice showed an overexpression of total APP compared to WT mice in hippocampus and cortex, revealed by WB using 22C11 antibody which recognizes both human and murine APP. The increased levels of APP in both brain regions of TG mice were not influenced by EE (P> 0.05 TG-SHs vs TG-EEs, Student's t-test).

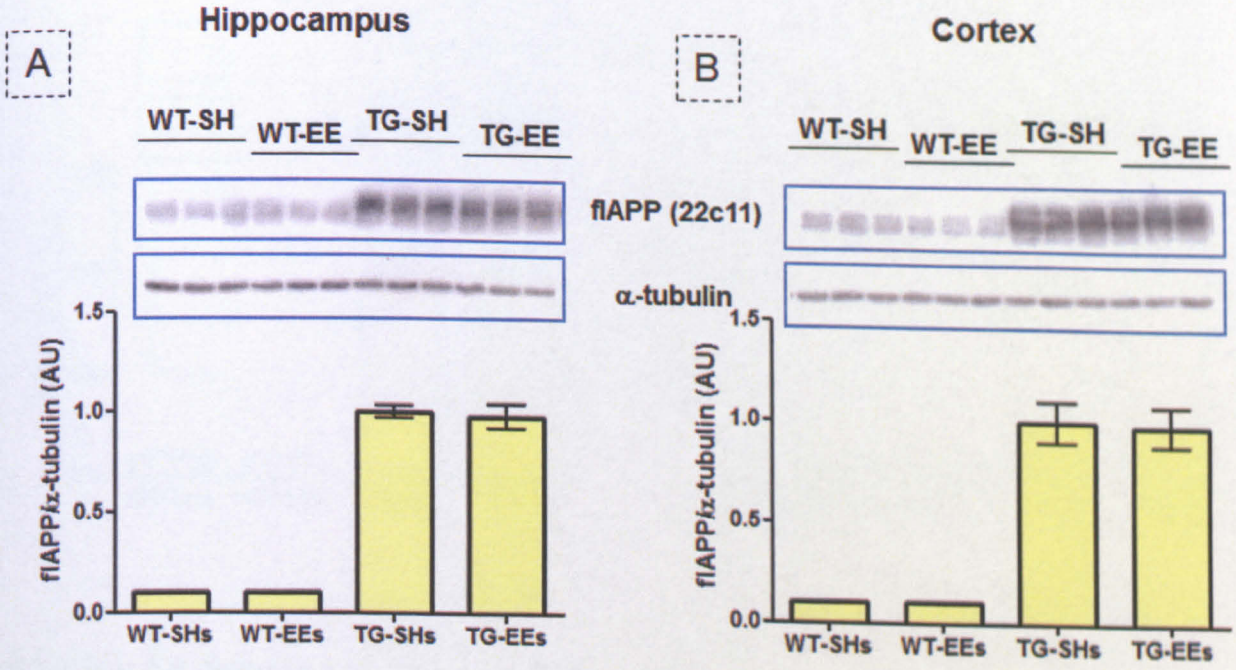


**FIGURE 5.8. Full length APP protein levels**

*APP protein levels in A. hippocampus and B. cortex of 8-month-old mice assessed by WB with 22C11 antibody normalized for murine α-tubulin. The related densitometric quantifications are shown below. The results are expressed using TG-SHs as reference group [set at 1, arbitrary units (AU)] and are represented as mean ± SEM.*

To investigate whether EE could affect APP cleavage by α-secretase, the enrichment in α-APP was assessed in hippocampal and cortical brain lysates by WB using 6E10 antibody, whose epitope is not present in the sAPPβ fragment released after β-secretase cleavage (Qin et al., 2006b). In parallel to the overexpression of full length APP, TG mice also showed the overproduction of soluble α-APP compared to WT mice. EE did not affect α-APP levels in TG mice both in the hippocampus and cortex ($p > 0.05$, Student's t-test).

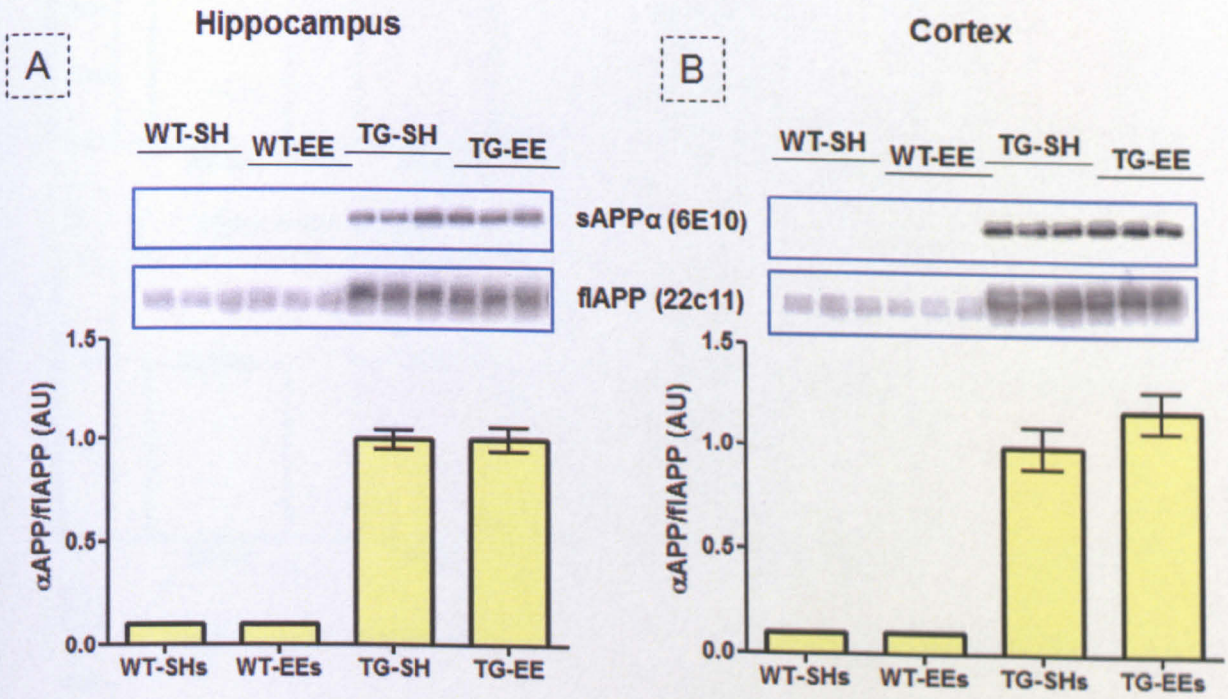


**FIGURE 5.9. Soluble α-APP protein levels**

*α-APP protein levels in A. hippocampus and B. cortex of 8-month-old mice assessed by WB with 6E10 antibody normalized for full length APP stained with 22C11 antibody. The related densitometric quantifications are shown in the histogram below. The results are expressed using TG-SHs as reference group [set at 1, arbitrary units (AU)] and are represented as mean ± SEM.*

To assess whether EE could affect the production of Aβ40 and Aβ42 peptides by β- and γ-secretases, Aβ40 and Aβ42 were measured in hippocampal and cortical lysates from 8-month-old TG mice by ELISA assays. No difference was visible comparing TG-SHs and TG-EEs either measuring Aβ40 and Aβ42 or Aβ42/ Aβ40 ratio.

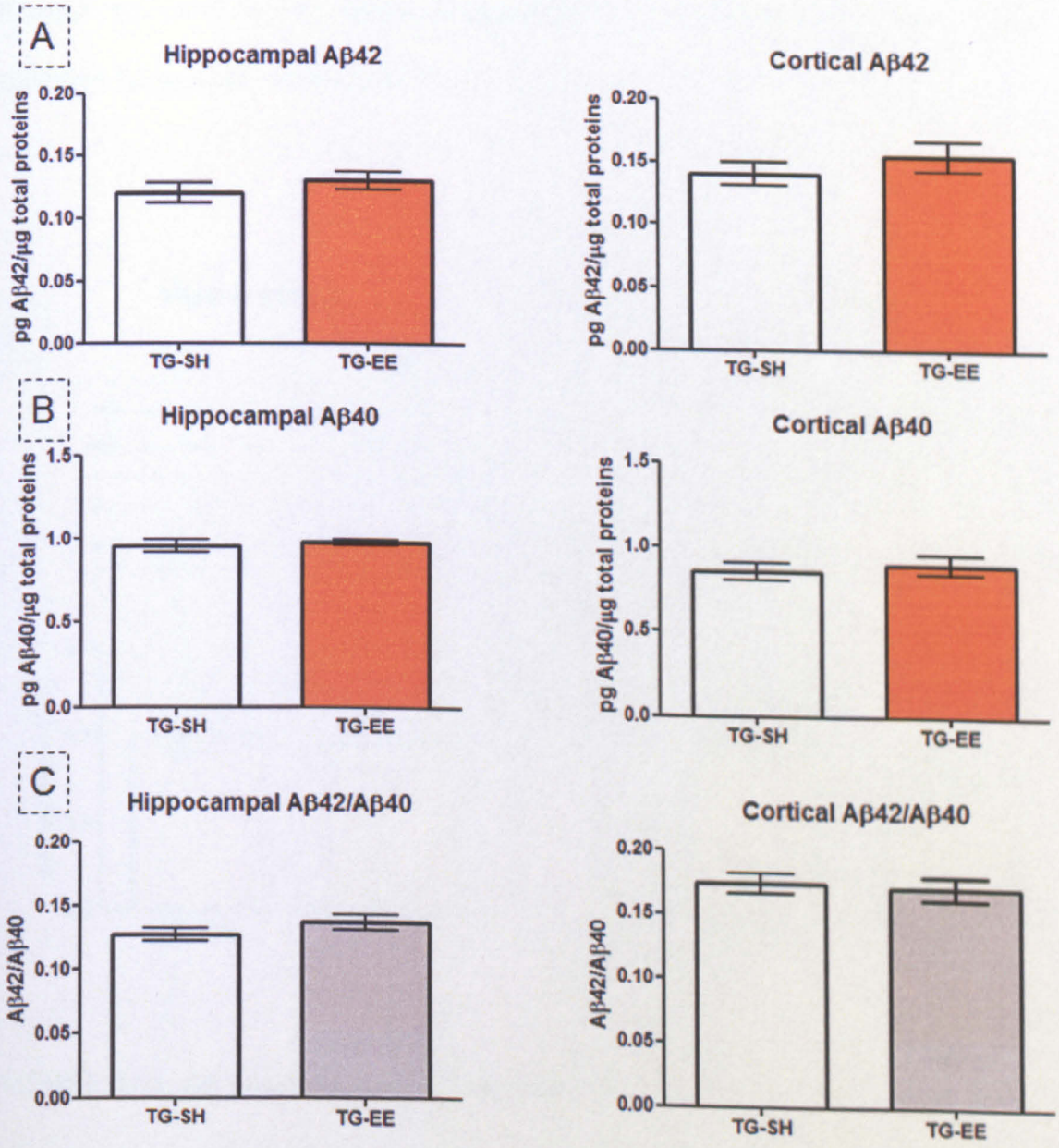


**FIGURE 5.10. Hippocampal and cortical Aβ42, Aβ40 and Aβ42/Aβ40 ratio**

*Hippocampal and cortical A. Aβ42, B. Aβ40 and C. Aβ42/Aβ40 ratio of 8-month-old TG mice housed in SH or EE conditions measured by ELISA assay. Results are expressed as pg of peptide/µg of total proteins assessed by BCA protein quantification ± SEM.*

### *5.3.3.2. Aβ oligomer formation*

To address whether EE could modulate the production of Aβ oligomers, hippocampal and cortical lysates from 8-month-old TG mice were analysed by Slot Blot with A11 antibody. TG mice showed an intense staining with A11 antibody revealing the presence of oligomeric species. EE did not significantly counteract Aβ oligomer production. However, although not reaching the statisical significance, a small decrease in A11 signal was registered for cortical lysates (p= 0.15).

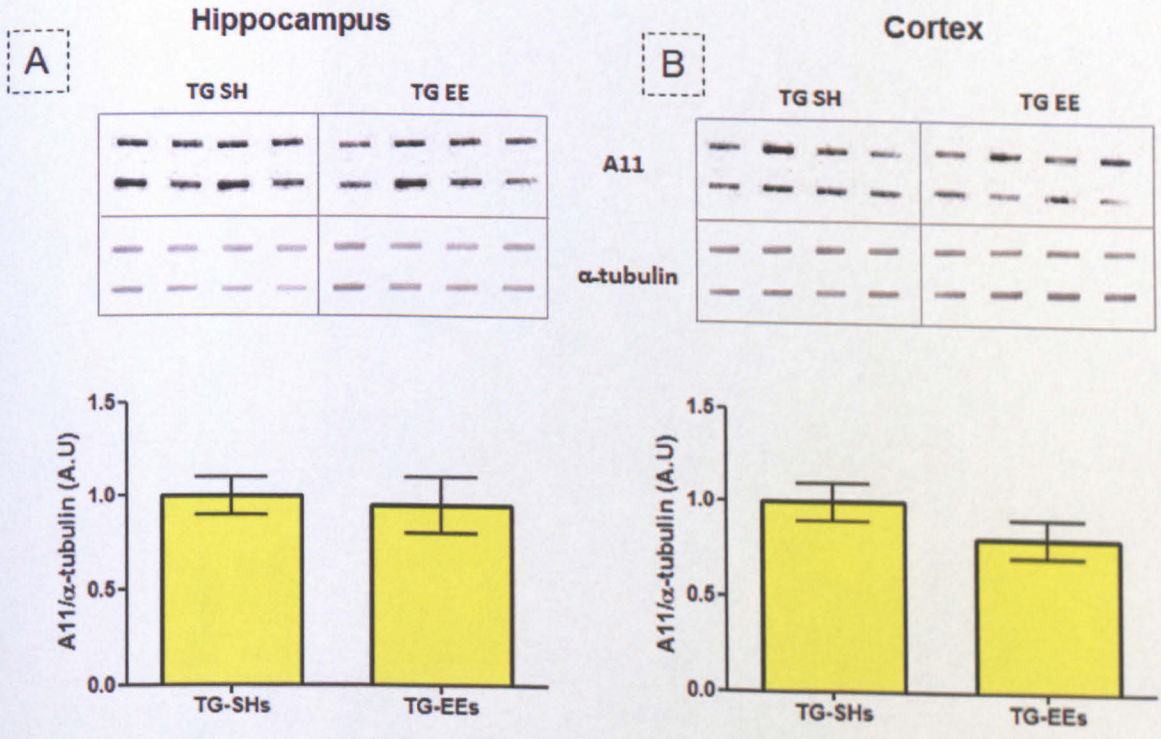


**FIGURE 5.11. Aβ oligomers in 8-month-old mice**

*Aβ oligomers in A. hippocampus and B. cortex of 8-month-old mice assessed by Slot Blot with A11 antibody normalized for murine α-tubulin. Densitometric quantifications are reported below. The results are expressed chosing TG-SHs as reference group and are represented as mean ± SEM.*

### *5.3.3.3. Plaque load in 18-month-old APP23 mice*

To investigate whether EE could counteract Aβ extracellular deposition in plaques, sagittal brain section from 18-month-old WT and TG mice were stained with 6E10 antibody. A consistent number of plaques was evident in several brain areas of TG mice, including neocortex and hippocampus while plaques were absent in the WT littermates of the same age. Notably, a reduction of plaque number and total area covered by plaques was registered in TG-EEs compared to TG-SHs mice.

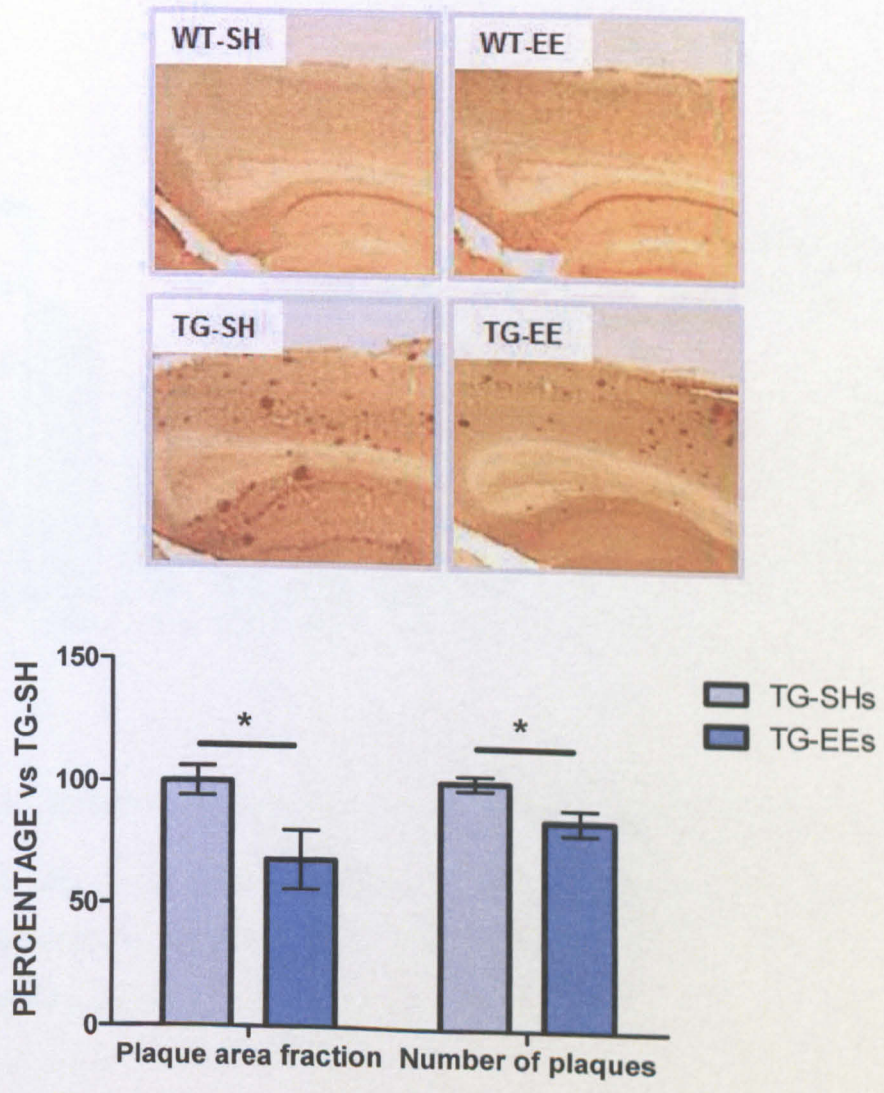


**FIGURE 5.12. Aβ plaques in 18-month-old mice.**

*Immunohistochemistry with DAB using 6E10 antibody on sagittal brain slices. Plaques were counted in cortex and hippocampus and the area covered by them was quantified. Results are espressed as the percentage of TG-SHs ± SEM. *P< 0.05, Student's t-test.*

### 5.3.4. SIRTUINS LEVELS IN THE BRAIN OF APP23 MICE

The expression of all 7 SIRT genes was evaluated in adult WT mouse brain by comparative RT-PCR measuring the ΔCt values relative to that for murine α-actin. The result revealed interesting differences of expression between the 7 SIRT genes in mouse brain. In particular, *SIRT2* is the sirtuin with the highest expression in adult mouse brain, while *SIRT4* has the lowest expression level. Finally, the expression profile of the 7 SIRT genes was quite similar in hippocampus and cortex given the exception of SIRT3 gene that is more expressed in the cortex compared to the hippocampus (ΔCthp-ΔCtcx= 1.5).

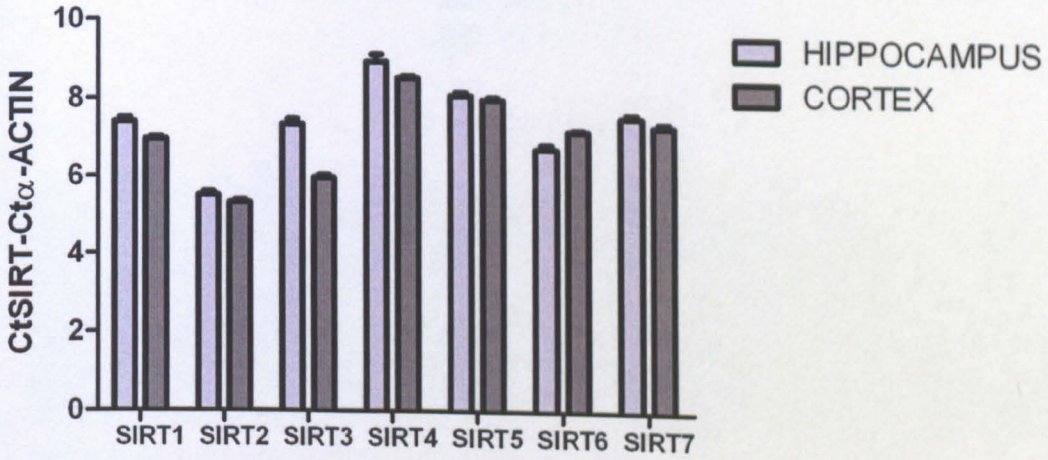


**FIGURE 5.13. Relative expression of the murin SIRT genes in mouse brain.**

*Hippocampus and cortex from 8-month-old WT mice were examined for the expression of the 7 SIRT genes by the comparative RT-PCR assay. The expression levels are represented as ΔCt ($Ct_{SIRT}$-$Ct_{\alpha\text{-}ACTIN}$).*

### 5.3.5. EXPRESSION OF SIRT GENES AND PROTEINS IN APP23 MICE UNDER ENVIRONMENTAL ENRICHMENT

To evaluate whether the expression of SIRT genes were influenced by the presence of the transgene in APP23 mice, or by EE or by the interaction of the two factors, the expression of SIRT genes was investigated in 8-month-old mice belonging to WT-SHs, WT-EEs, TG-SHs and TG-EEs groups by comparative RT-PCR. Overall, no significant differences were observed comparing the four groups by two-way ANOVA either in the hippocampus and the cortex.

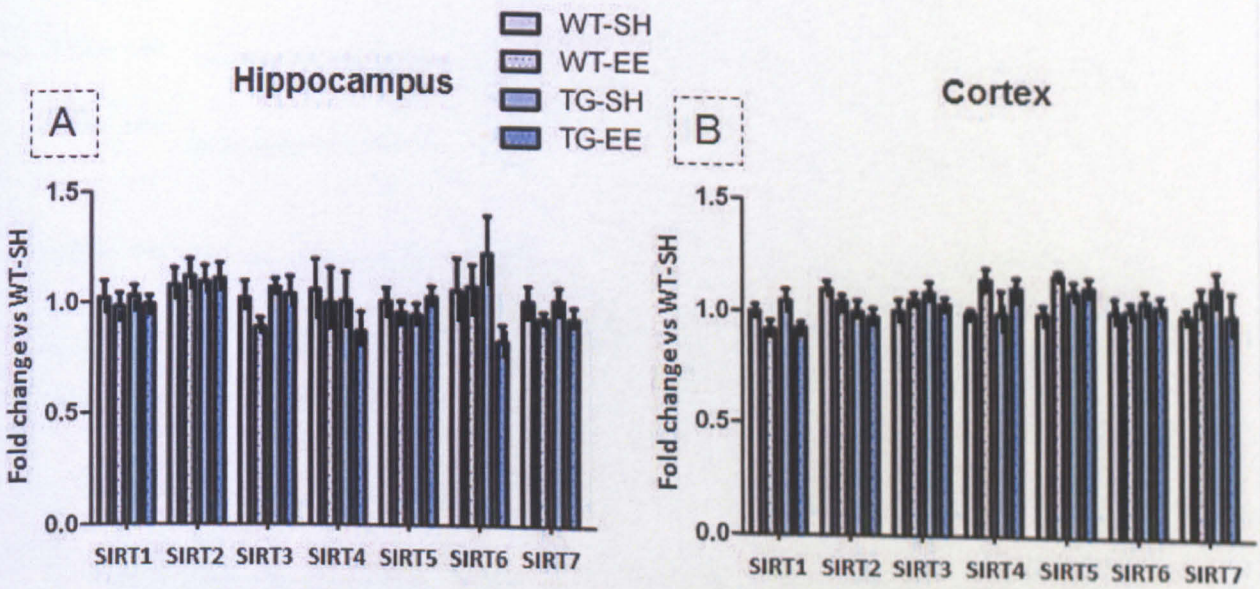


**FIGURE 5.14. Expression of SIRT genes under EE in APP23 mice.**

*Hippocampus and cortex from 8-month-old WT mice were examined for the expression of the 7 SIRT genes by the comparative RT-PCR assay in hippocampus and cortex. Data were normalized on the murine endogenous gene α-ACTIN and WT-SHs group was used as calibrator. Results are expressed ± SEM.*

To explore whether there were any post-translational effects, sirtuin protein levels were also assessed by WB. In particular, SIRT1 and SIRT2 showed multi-bands corresponding to different isoforms and these were quantified together (figure 5.15) and separately (not

shown). Similarly to mRNA levels, no significant differences were observed comparing the SIRT protein levels in the four animal groups by two-way ANOVA either in the hippocampus and the cortex.

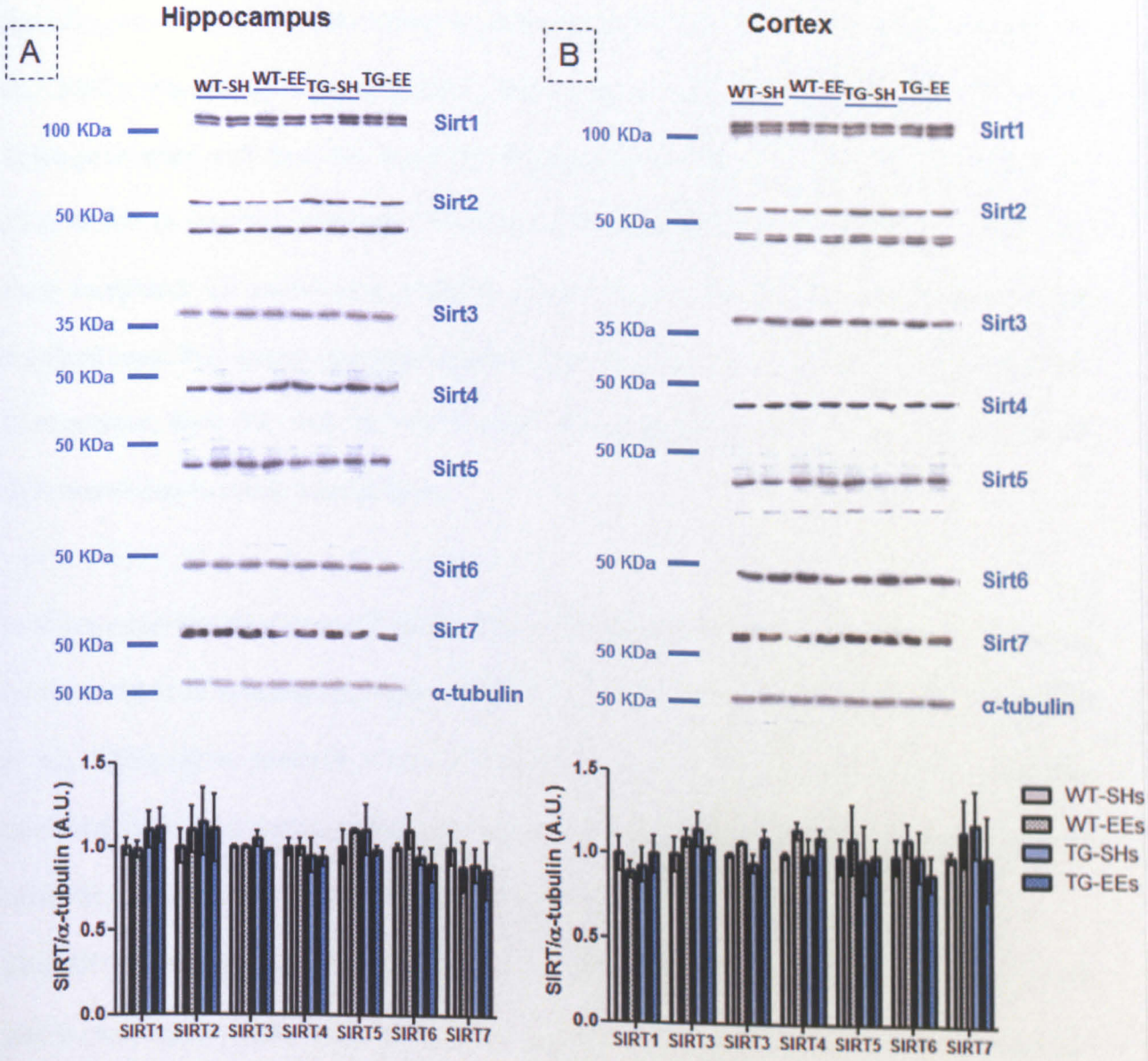


**FIGURE 5.15. Expression of Sirt proteins under EE in APP23 mice.**

*Sirt protein levels in A. hippocampus and B. cortex of 8-month-old mice assessed by WB normalized for α-tubulin. The related densitometric quantifications are shown below. The results are expressed using WT-SHs as reference group and are represented as mean ± SEM.*

# 5.4. DISCUSSION

The work described in this chapter describes the application of an EE protocol to test whether this paradigm could ameliorate AD-like pathology in the APP23 mouse model.

An EE protocol with an early onset, similarly to Lazarov et al. was employed (Lazarov et al., 2005), mimicking a preventative rather than a therapeutic protocol in TG mice. Transgenic mice and their wild-type littermates were assigned to EE (TG-EEs and WT-EEs) or left in standard housing (TG-SHs and WT-SHs) at 2-3 months of age until they were sacrificed. EE mice were housed in cages that were double the dimension of the standard ones. This larger size was required because of the space occupied by the objects. Furthermore, both EE and SH mice were all caged in groups of 3-4 mice to avoid differences due to social interactions.

In these experiments only male mice were used. No increase in aggressiveness measured by the number of wounds was registererd. Our result, supported by other groups (Lazarov et al., 2005), is in contrast with some reports suggesting that EE in males increases territorial behaviour causing stress for subordinate animals and resulting in an increased variability and stress as a confounding variable (Mirochnic et al., 2009).

The APP23 mouse model was chosen since it reflected several aspects of AD pathology and it was characterised by a slow onset and course of the disease. Indeed, it has been argued that EE is not able to counteract pathological manifestations in more severe models, such as APP/PS1KI (Cotel et al., 2010).

After 4 months of EE, mice were tested with two different behavioural tests: MWM and vORT. At this stage, APP23 mice already display cognitive impairment in performing MWM task (Van Dam et al., 2003). MWM allows the testing of both learning and memory, two features affected in human AD patients. Learning, or memory acquisition, is reflected in escape latency curves, whereas a probe trial is used to assess storage and retrieval after 24 h retention time. Mice were trained for the MWM task for ten days with four-trials on each day and escape latencies recorded. During the acquisition phase of the MWM experiment, all mice improved their performance in reaching the hidden platform. TG-SHs showed the worst learning curve, registering higher escape latencies at each day of training. However, only at day 6 the performance of TG-SHs was significantly different from WT-SHs. Moreover, despite the apparent trends, TG-SHs and TG-EEs performances were never significantly different. The presence of a learning deficit in TG-SHs was confirmed during the probe trial, as TG-SHs spent significantly less time in the target quadrant than WT-SHs did. Moreover EE significantly recovered mice from learning impairment registered at 24 h from the last training section.

vORT revealed a long-term recognition memory impairment in TG-SHs. This contrasted with WT-SHs who showed a net preference for the novel object, TG-SHs were not able to discriminate between the novel and the familiar object [i.e. Descrimination Index (DI) ≅ 0]. The EE paradigm counteracted this impairment. Indeed, TG-EEs showed a DI for the novel object not statistically different from their wild-type counterpart. TG-EEs' preference for the novel object relied on a difference in long-term memory retention. Indeed, as revealed in the familiarization phase of vORT task, the training paradigm did not introduce any artifactual bias (e.g. due to a preference in the object position within the arena). Moreover, the restored performance in TG-EEs was not the result of a different

exploration habit of mice housed in enriched conditions. Indeed, total exploration time in the familiarization phase was similar in the four experimental groups.

Overall, MWM and vORT revealed that cognitive impairment in TG mice can be reversed by exposing mice to an enriched environment. Conversely, EE paradigm did not improve learning and memory performance in WT mice revealed with this test.

*Effects of EE on gene transcription and AD-like hallmarks in APP23*

The EE paradigm, similar to physical stimulation, was shown to increase BDNF mRNA levels in different experimental AD-like mouse model including APP23 (Wolf et al., 2006). In the present study, BDNF mRNA level was assessed in the hippocampus and cortex of the 8-month-old mice previously tested with the behavioural test battery. TG-SHs had stable BDNF levels compared to WT-SHs. This result, already reported in literature (Wolf et al., 2006) is different to what has been observed in other AD-like mouse models (e.g. CRND8 (Peng et al., 2009)) where a decreased BDNF level in TG mice was linked to synaptic and cellular loss. In APP23, EE increased BDNF mRNA levels in a genotype-independent manner. This result, in line with previously published data (Wolf et al., 2006), further confirmed the effect of the adopted EE protocol. Moreover, the increased BDNF mRNA levels observed in WT-EEs also highlighted the effectiveness of EE protocol in WT mice, even if no improvement in behavioural performance was registered with behavioural tests.

The memory impairment observed in APP23 TG mice is related to the appearance of AD hallmarks in the cortex and hippocampus (Sturchler-Pierrat et al., 1997). The ability of EE to reverse cognitive imparment in TG mice could therefore possibly affect these biological markers. APP23 mice are characterised by a 7-fold increase in APP levels, and this

PAGE
NUMBERING
AS
ORIGINAL

overexpression, together with the expression of the "Swedish" mutation, is the triggering event that leads to the AD-like manifestations in APP23.

First, APP total protein levels were assessed by WB and no difference was shown between TG-SHs and TG-EEs. Second, because the overexpression of APPswe causes a disproportionate shift from normal APP physiological and pathological cleavage, APP processing was also evaluated. Soluble αAPP was therefore assessed as a marker of the physiological APP processing and levels of Aβ40 and Aβ42 as markers of the pathological cleavage of APP in 8-month-old mice. Both sets of analyses revealed no effect of EE on APP processing. EE also did not affect the Aβ42/Aβ40 ratio, which has been proposed as a reliable indicator of neurochemical dementia diagnosis (Weih et al., 2007).

Aβ40 and expecially Aβ42 are aggregation-prone peptides. To assess whether EE could alter Aβ peptide nucleation and growth, levels of Aβ oligomers and Aβ plaques were assessed. Oligomers were recently proposed to be the real toxic species while Aβ plaques, although having a controversial pathological relevance, are noteworthy because they are suggested to be an end point of APP metabolism.

To detect Aβ oligomers in 8-month-old mice, Slot Blots were performed using A11 antibody. This antibody was reported to selectively recognize prefibrillar intermediates larger than tetramers for many amyloid peptides (Kayed et al., 2003). No significant difference in A11 levels was observed between TG-SHs and TG-EEs, despite a small apparent decrease in cortex that may warrant further investigation. At 18-months of age, APP23 were also assessed for plaque deposition. At this age, APP23 were reported to have consistent plaque deposition (Balducci et al., 2010). The immunohistochemical analysis with the anti-Aβ 6E10 antibody of sagittal brain slices from TG mice showed a robust plaque deposition, whilst there were no plaques in WT mice. Notably, compared to TG-

overexpression, together with the expression of the "Swedish" mutation, is the triggering event that leads to the AD-like manifestations in APP23.

First, APP total protein levels were assessed by WB and no difference was shown between TG-SHs and TG-EEs. Second, because the overexpression of APPswe causes a disproportionate shift from normal APP physiological and pathological cleavage, APP processing was also evaluated. Soluble αAPP was therefore assessed as a marker of the physiological APP processing and levels of Aβ40 and Aβ42 as markers of the pathological cleavage of APP in 8-month-old mice. Both sets of analyses revealed no effect of EE on APP processing. EE also did not affect the Aβ42/Aβ40 ratio, which has been proposed as a reliable indicator of neurochemical dementia diagnosis (Weih et al., 2007).

Aβ40 and expecially Aβ42 are aggregation-prone peptides. To assess whether EE could alter Aβ peptide nucleation and growth, levels of Aβ oligomers and Aβ plaques were assessed. Oligomers were recently proposed to be the real toxic species while Aβ plaques, although having a controversial pathological relevance, are noteworthy because they are suggested to be an end point of APP metabolism.

To detect Aβ oligomers in 8-month-old mice, Slot Blots were performed using A11 antibody. This antibody was reported to selectively recognize prefibrillar intermediates larger than tetramers for many amyloid peptides (Kayed et al., 2003). No significant difference in A11 levels was observed between TG-SHs and TG-EEs, despite a small apparent decrease in cortex that may warrant further investigation. At 18-months of age, APP23 were also assessed for plaque deposition. At this age, APP23 were reported to have consistent plaque deposition (Balducci et al., 2010). The immunohistochemical analysis with the anti-Aβ 6E10 antibody of sagittal brain slices from TG mice showed a robust plaque deposition, whilst there were no plaques in WT mice. Notably, compared to TG-

SHs, TG-EEs showed a reduction of both plaque number and the total area covered by plaques. This result is in line with that reported by other groups with similar early onset EE protocols (Lazarov et al., 2005; Adlard et al., 2005; Berardi et al., 2007). However, this result is different from two studies in APP23 mice published by Kempermann's group (Mirochnic et al., 2009; Wolf et al., 2006): Wolf et al. performed a long-lasting protocol by exposing mice to 11 months of EE (starting at 2 months of age), while Mirochnic et al. perfomed a short-lasting protocol (~ 1 month starting at 18 months). In both studies no change in plaque load was visible, but the differences reported could relate to the gender of the mice studied. In fact, these two studies used female mice, whereas males were involved in the present work and in literature consistent observations of gender-specific differences in Aβ deposition are reported independently from EE (Wang et al., 2003; Schäfer et al., 2007). Furthermore, consistently with the results collected in the present study, Lazarov et al. registered a decrease in plaque load in male mice under EE, although in a different transgenic model (Lazarov et al., 2005).

*EE effect on sirtuins*

Sirtuin expression levels in 8-month-old mice were also assessed. First, the relative sirtuin gene expression was investigated in the cortex and hippocampus of WT mice. The seven murine sirtuins were all expressed in the cortex and hippocampus similar to that seen in human brain (Michishita et al., 2005). However, the gene expression characterization in the mice study here revealed that sirtuins have differential expression patterns within the brain. In particular, SIRT2 is the sirtuin with the highest expression, suggesting a key role of this gene in the brain, while SIRT4 is the sirtuin with the lowest expression level. Finally, no differences were visible comparing sirtuins in the cortex and hippocampus except for SIRT3 which is expressed more in the cortex. This difference deserves more attention. Indeed, it could highlight a prominent role of SIRT3 in the cortex.

It was also investigated whether transgene or housing condition or the interaction of the two parameters could affect sirtuin levels. Indeed, there were few but promising evidence that sirtuins could be related with both physical and mental stimulation. However, both mRNA and protein assessment failed to show any significant differences in sirtuin levels in the four experimental groups assessed. In particular this result did not confirm a previous work, where in a different TG mouse model of AD an increase in SIRT1 levels was reported in transgenic mice compared to controls (Kim et al., 2007).

*Summary*

Overall, the present study showed that it is possible to counteract the progression of cognitive decline and reduce some AD-like pathological hallmarks in the APP23 mouse model of AD by exposing animals to EE. Moreover, preliminary indications suggest that, unlike other environmental paradigms, such as CR, EE does not modulate sirtuin expression levels in the brain.

# *SECTION C: IN VITRO STUDIES*

# *CHAPTER 6: ROLE OF SIRT1 ACTIVATION BY RESVERATROL IN IN VITRO MODELS LINKED TO ALZHEIMER'S DISEASE ETIOPATHOGENESIS*

# SECTION C: BACKGROUND

Oxidative stress is a common feature of many neurodegenerative disorders, including AD (Keating, 2008). The brain in AD appears to accumulate more oxidative damage than normal brain and exhibits an increased susceptibility to oxidative stress (Axelsen et al., 2011).

Oxidative stress is a recognised phenomenon early in the pathogenesis of AD, and environmental and lifestyle-related risk factors for AD (e.g. aluminum exposure, smoking, high calorie intake, lack of exercise, and lack of intellectual activities) were associated with an increase in the production of reactive oxygen species and/or a decrease in endogenous antioxidant defences (Nunomura et al., 2006). In contrast, more health conscious lifestyles such as calorie restriction, exercise, and intellectual activity have been shown to promote neuronal survival through an enhancement of endogenous antioxidant defences in experimental animal models (Mattson et al., 2002).

Calorie restriction (CR - i.e. restriction of calorie intake while avoiding malnutrition) is a novel paradigm that was shown to increase the resistance of neurons to intracellular and extracellular stresses and consequently was proven to be beneficial in different models of neurodegenerative diseases, such as AD (Schroeder et al., 2010). Since a CR protocol is not easily applied to humans, there has been interest in attempting to mimick CR beneficial effects with drugs. A body of evidence highlighted the existence of a conserved evolutionary pathtway for CR that seemed to involve the members of the sirtuin protein family (Haigis and Sinclair, 2010). In particular, SIRT1 may have a significant role in CR-mediated reduction in stress signaling and enhanced mitochondrial performance (Morris et al., 2011). As such, the sirtuin activator resveratrol (RES) has been proposed as a candidate CR mimetic (Barger et al., 2008).

RES is a naturally occurring phytocompound, found in red wine, that has been proved beneficial against cardiovascular diseases and cancer (Bradamante S, Barenghi L, 2004; Aggarwal and Shishodia, 2006) and is protective in a variety of experimental paradigms of neurodegeneration (Anekonda, 2006). Although the data about the role of RES to activate SIRT1 is still conflicting (Hu et al., 2011), several studies reported that RES is able to promote neuroprotective effects both *in vitro* and *in vivo*, and this capacity is counteracted by blocking SIRT1 pharmacologically or genetically (Baur, 2010).

SIRT1 (SIRT1, NM_012238, NP_036370) is the most investigated member of the sirtuin protein family. SIRT1 regulates a diverse array of cellular functions related to mammal senescence, including metabolism, gene transcription, DNA repair and cellular stress response. Recently, SIRT1 has also been implicated in neurodegeneration. A neuroprotective role of SIRT1 was suggested in models of Huntington's disease (Parker et al., 2005), AD (Chen et al., 2005b; Qin et al., 2006b) and amyotrophic lateral sclerosis (Kim et al., 2007)

Despite the growing number of studies, the role of SIRT1 in neurodegeneration is still poorly understood. Therefore, the overall aim of this chapter was to better elucidate the role of SIRT1 activation by RES in pathogenic mechanisms linked to AD etiology in a neuroblastoma cell line.

# 6.1. SYNOPSIS

The first aim was to investigate the neuroprotective role of SIRT1 activation by RES against oxidative stress, a common feature of many neurodegenerative diseases, including AD (Keating, 2008). To achieve this goal, an *in vitro* model which involved challenging the neuroblastoma cell line SK-N-BE(2) with hydrogen peroxide ($H_2O_2$) was set up. SIRT1 enzymatic activity was increased by RES (SIRT1 activator) and decreased by sirtinol (SIRT1 inhibitor), and cell viability was assessed. To further elucidate the involvement of SIRT1, its transcriptional levels were also downregulated by a siRNA approach.
This *in vitro* model of oxidative challenge, allowed the exploration of the potential involvement of SIRT1-related mechanisms in countreracting oxidative stress. From this, SIRT1 involvement in depleting ROS production under oxidative stress was assessed and, for the first time, allowed the study of SIRT1 involvement in oxidative stress-mediated autophagy.

The second aim of the work presented in this chapter was to assay the neuroprotective role of RES treatment against aggregation prone-protein Aβ42. To achieve this, SK-N-BE(2) were exposed to Aβ42 and subsequent cell viability was assessed. In this model we investigated the impact of using the same treatments as before by modulating SIRT1 by RES and sirtinol.

In summary, this chapter describes studies that show how SIRT1 activation by RES counteracted oxidative stress-induced cell death in SK-N-BE(2). Indeed, pre-treatment of SK-N-BE(2) cells with RES increased their viability despite being challenged with $H_2O_2$, whilst both sirtinol and SIRT1 gene-silencing reversed this protective effect. Moreover, under oxidative stress conditions, SIRT1 was involved in RES-mediated depletion of

intracellular ROS. Furthermore, SIRT1 was shown to have a role in $H_2O_2$-induced autophagy, although this did not appear to be responsible for the observed RES-induced neuroprotection. Finally, RES counteracted cell toxicity and ROS production in SK-N-BE(2) cells exposed to Aβ42. However, this time RES-mediated protection was not mediated by SIRT1 activation but possibly derived from a interaction with Aβ fibrils.

# 6.2. MATERIALS AND METHODS

All the experiments presented in this chapter were conducted in undifferentiated SK-N-BE(2) cells. The main results were subsequently confirmed with similar observations in SK-N-BE(2) cells differentiated by retinoic acid (cfr. chapter 2.4.1).

All the statistical analyses were performed with GraphPad Prism®.

## 6.2.1. CELL SEEDING

For the experiments described in this chapter, cells were counted with a Burker chamber and seeded in the appropriate multi-well at the desired concentration.

| Application | Differentiation with RA | N° wells/plate dimensions/well | Cell number/ volume of medium |
|---|---|---|---|
| Cell viability (CV) | - | 96 (6.4 mm) (Ø) | 30'000/200 µL |
| | + | 48 (10 mm) (Ø) | 20'000/200 µL |
| Immunocytochemistry (IC) | - | 8 (9.4 x 10.7 x 6.8 mm) (w x l x h) | 50'000/200 µL |
| | + | | 20'000/200 µL |
| Western Blotting (WB) | - | 24 (16 mm) (Ø) | 150'000/400 µL |
| | + | 12 (22 mm) (Ø) | 80'000/500 µL |
| Real Time-PCR RT-PCR | - | 12 (22 mm) (Ø) | 300'000/500 µL |
| | + | 6 (35 mm) (Ø) | 300'000/800 µL |

**TABLE 6.1. Seeding conditions used in the experiments performed.**

*RA: retinoic acid; Ø: diameter,*

## 6.2.2. CELL TREATMENTS

### Oxidative-stress challenge

To model the effects of oxidative stress on SK-N-BE(2) cells, a dose-response curve was plotted using $H_2O_2$. Cells were exposed to increasing doses of $H_2O_2$, ranging from 25 μM to 100 μM for 24 h, and then cell viability was assessed. The following experiments with $H_2O_2$ were run with 75 μM $H_2O_2$.

To challenge cells with $H_2O_2$, fresh dilutions were prepared in DMEM at 100x the final concentrations desired and then added to the medium at 1:100.

### Aβ42 challenge

Before use, Aβ42 peptide was dissolved in 0.01 M NaOH to a final concentration of 440 μM. Working dilutions were made in DMEM medium and Aβ42 was added to the cell at the desired concentration. Cells were incubated with Aβ42 for 24 h. For the dose-response experiment cells were exposed to increasing doses of $H_2O_2$ ranging from 5 μM to 20 μM. For the following experiments the final concentration of 10 μM $H_2O_2$ was chosen.

### Modulation of SIRT1 activity

RES (i.e. SIRT1 activator) and sirtinol (i.e. SIRT1 inhibitor) were dissolved in DMSO at the stock concentration of 20 mM. Working dilutions were made in DMEM medium and added to the corresponding well. For the experiments designed to set up RES and sirtinol treatments, cells were exposed to increasing doses (ranging from 2.5 μM to 15 μM) of the two drugs for 24 h. For the following experiments cells were exposed to sirtinol and/or RES at 2.5 μM and 7.5 μM, respectively.

**RES protection against toxic challenges**

To investigate whether RES was able to protect cells from $H_2O_2$- or Aβ-induced cell death, SK-N-BE(2) cells were treated with two different experimental schedules:

1) Cells were treated with RES 7.5 μM, after 4 h they were exposed to the toxic challenge and after further 24 h their viability was assessed.

2) RES 7.5 μM was given twenty and 4 h before the toxic challenge and after further 24 h cell viability was assessed.

To confirm SIRT1 involvement in RES protection, sirtinol 2.5 μM was given 2 h before each RES treatment.

**SIRT1 downregulation**

SK-N-BE(2) cells were seeded in multi-well plates (for the number of cells seeded cfr. WB and RT-PCR applications in table 6.1) and grown overnight. The next day, the medium was replaced with freshly prepared complete medium and a pre-designed double-strand small-interfering RNA (siRNA) against SIRT1 mRNA sequence (sense: 5'-GCCUCACAUGCAAGCUCUAtt-3', antisense: 5'-UAGAGCUUGCAUGUGAGGCtc-3') (Ambion) was added in 50 μL serum-free Optimem (Invitrogen) (final concentration: 300 nM) using SilentFect liposome formulation (siRNA lipid vehicle) (Bio-Rad Laboratories). The medium was not changed for 72 h from siRNA addition. To prove SIRT1 specific down-regulation, a siRNA negative control (CT-) with no match to any known human transcribed sequence was used.

# 6.3. RESULTS

## 6.3.1. $H_2O_2$ AND RES TREATMENT SET UP

To construct a model of oxidative stress, SK-N-BE(2) cells were treated with $H_2O_2$. Exposure for 24 h to increasing doses of $H_2O_2$, ranging from 25 to 100 μM, induced a dose-dependent decrease of cell viability in SK-N-BE(2) cells (figure 6.1). The dose of 75 μM, that reduced cell viability by about 50%, was chosen for the subsequent experiments.

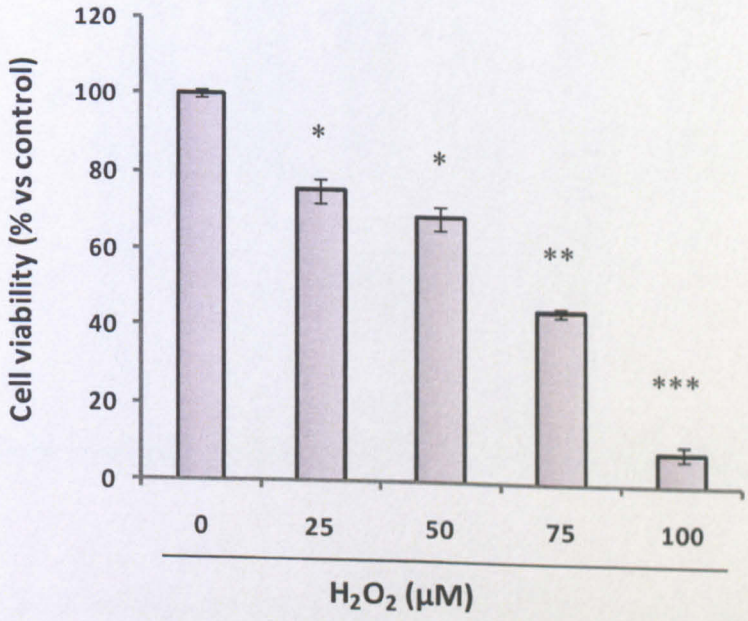


**FIGURE 6.1. Dose response relationship between $H_2O_2$ concentration and SK-N-BE(2) viability.**

*SK-N-BE(2) cells were exposed to increasing doses of $H_2O_2$ for 24 h, then cell viability was assessed. Viability of control cells was set at 100%, and viability with respect to the control is presented. Bar graph indicates the mean ± SEM (n=4). *: $p< 0.05$, **: $p< 0.01$, ***: $p< 0.001$; one-way ANOVA followed by Dunnett's post hoc test versus control (untreated cells).*

To evaluate the intrinsic toxicity of RES in SK-N-BE(2), cells were incubated with increasing doses of the molecule. Exposure for 24 h to RES, ranging from 2.5 to 10 μM, did not affect cell viability in SK-N-BE(2) cells. RES was slightly toxic starting from 10 μM (figure 6.2). The following experiments were run using 7.5 μM RES.

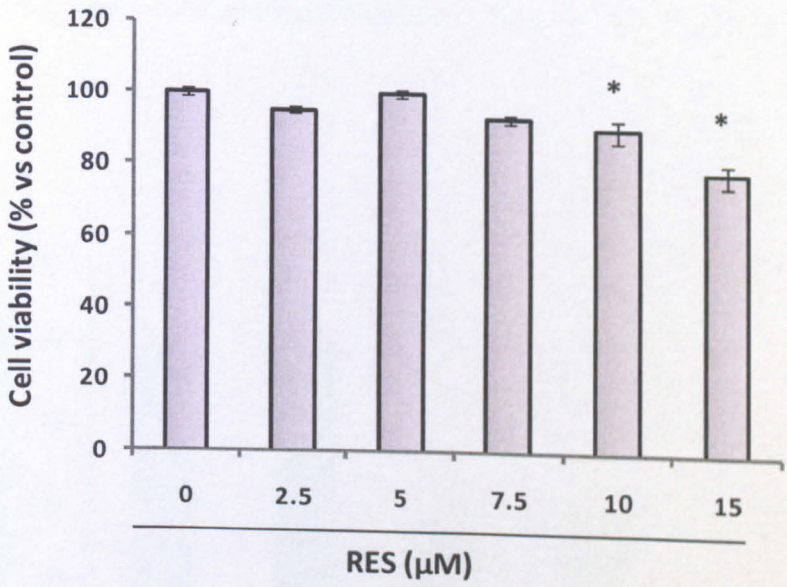


**FIGURE 6.2. Dose response relationship between RES concentration and SK-N-BE(2) viability.**

*SK-N-BE(2) cells were exposed to increasing doses of RES for 24 h, then cell viability was assessed. Viability of control cells was set at 100%, and viability with respect to the control is presented. Bar graph indicates the mean ± SEM (n=4). *: $p<0.05$; one-way ANOVA followed by Dunnetts's post hoc test versus control (cells treated with vehicle = 0.05% DMSO).*

### 6.3.2. RES PRE-TREATMENT COUNTERACTS CELL DEATH INDUCED BY OXIDATIVE STRESS

To investigate whether RES was able to protect cells from $H_2O_2$ exposure, SK-N-BE(2) were pre-treated with RES 7.5 µM 4 h before $H_2O_2$ challenge. This treatment did not counteract cell death caused by 75 µM $H_2O_2$ (figure 6.3.). Given this result, an overnight pre-treatment with RES was designed. To ensure a better bioavailability of RES, the drug was supplemented after an overnight incubation (15 h) with a further 7.5 µM of RES.

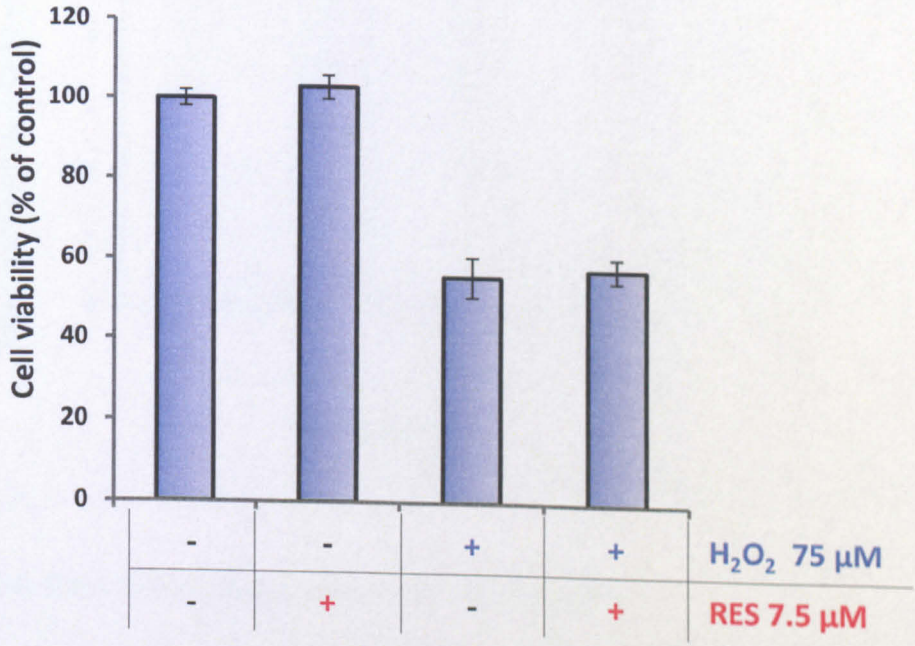


**FIGURE 6.3. RES pre-treatment 4 h before oxidative challenge is uneffective**

*SK-N-BE(2) were pre-treated with RES 7.5 µM 4 h before treatment with $H_2O_2$ 75 µM for further 24 h. Cells viability is expressed as percentage of the control (cells treated with vehicle = 0.05% DMSO). Bar graph indicates the mean ± SEM (n=4).*

To confirm RES uptake by SK-N-BE(2), and to estimate RES bioavailability over time, cells were treated with RES as described above and the subsequent intracellular levels of

RES was measured at different time-points relevant for the following experiments (figure 6.4). RES was taken-up by SK-N-BE(2) cells and its concentration decreased over time. However, after 44 h RES intracellular content was still appreciable and around 60% to that seen at the second time-point (16 h).

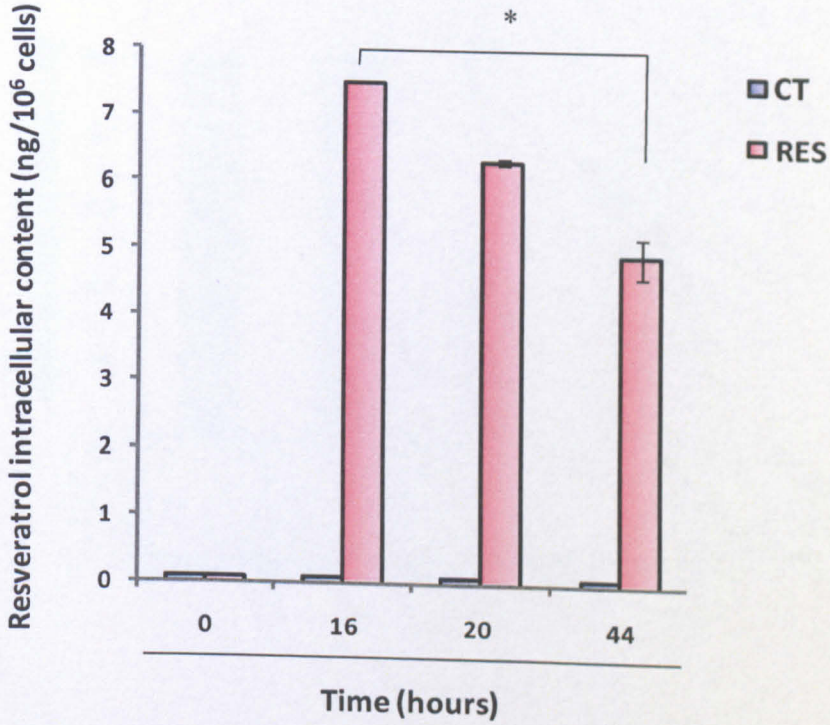


**FIGURE 6.4. RES intracellular uptake in SK-N-BE(2)**

*RES 7.5 μM was added at time 0 and 16 h later. RES was quantified by mass spectrometry at time point: 0, 16, 20 and 44 h. Each time-point was in triplicate and normalized to $10^6$ cells. *: $p<0.05$, one-way ANOVA followed by Tukey's test.*

The next experiment aimed to assess whether RES had a neuroprotective role in counteracting $H_2O_2$-induced cell death, SK-N-BE(2) cells were pre-treated with RES 7.5 μM 20 and 4 h before exposure to $H_2O_2$ for 24 h. Notably, a double-treatment protocol of RES did not affect cell viability. Conversely, this treatment significantly reduced the extent of cell death caused by $H_2O_2$ (cell viability was increased by about 30%) (figure 6.5).

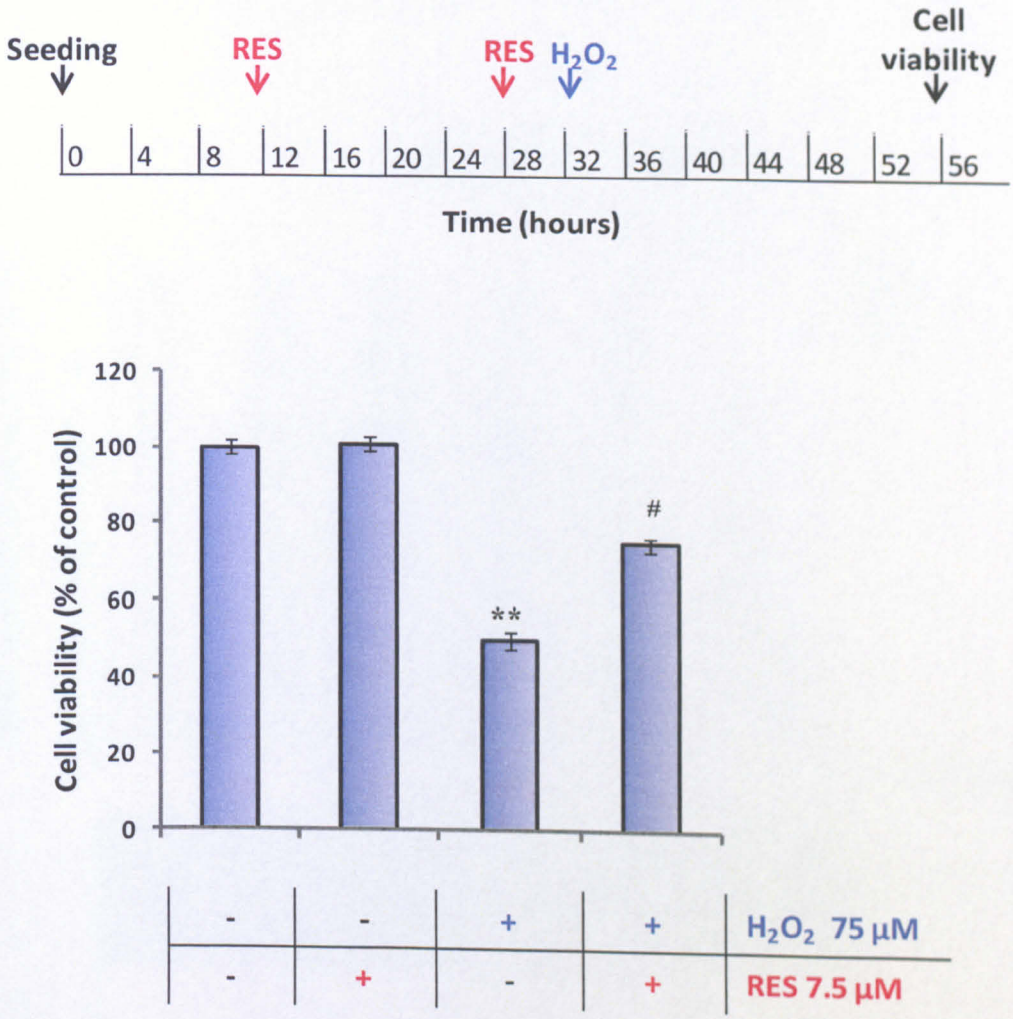


**FIGURE 6.5. RES prevents $H_2O_2$-induced toxicity in SK-N-BE(2).**

*SK-N-BE(2) were pre-treated with RES 7.5 µM 20 and 4 h before treatment with $H_2O_2$ 75 µM for a further 24 h. Cells viability is expressed as percentage of the control (cells treated with vehicle = 0.1% DMSO). Bar graph indicates the mean ± SEM (n=4). **$p < 0.01$ versus control; #$p < 0.01$ $H_2O_2$ x RES, Two-way ANOVA.*

To exclude whether RES had a pro-apoptotic effect, apoptosis was checked in our model by Hoechst 33342 staining (figure 6.6.). The double treatment with RES 7.5 µM did not increase the percentage of apoptotic nuclei, even in the presence of oxidative stress triggered by $H_2O_2$ 75 µM. Following higher doses of RES (i.e. double treatment with 15 µM) apoptotic nuclei were not detected. In contrast the introduction of $H_2O_2$ 75 µM in

addition to RES 15 μM significantly increased the number of fragmented nuclei in SK-N-BE(2) cells (24%, $p < 0.001$, Tukey's Test).

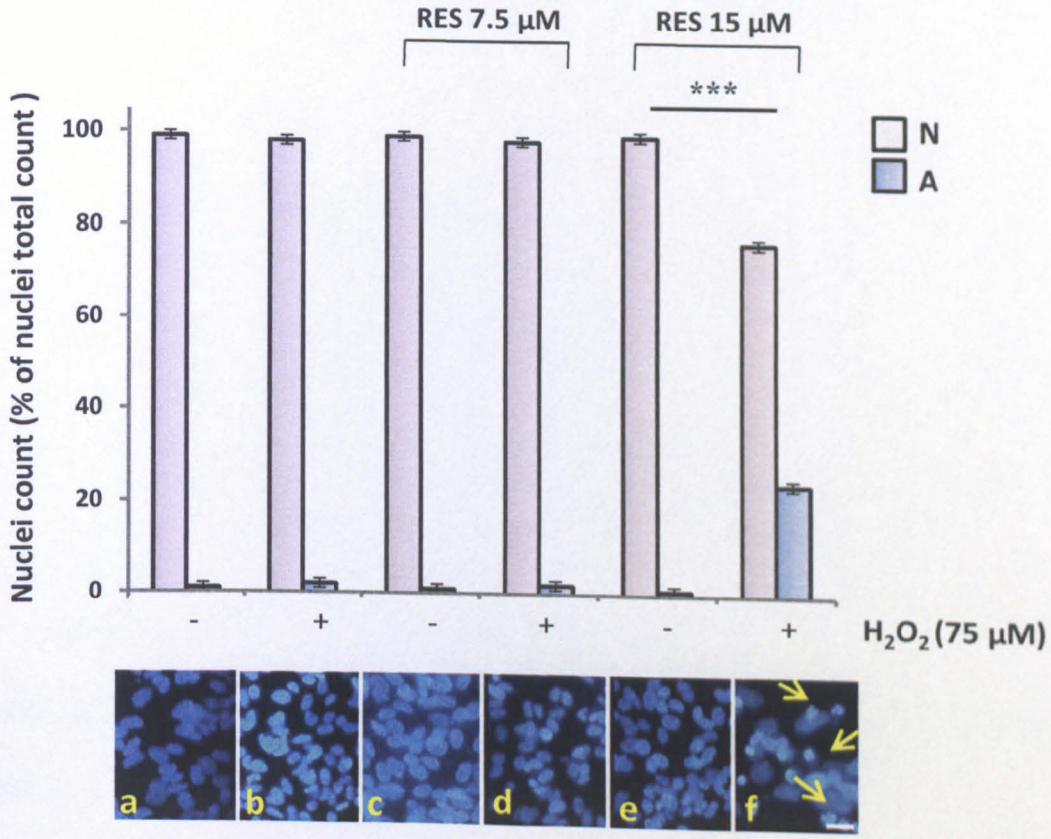


**FIGURE 6.6. Percentage of apoptotic nuclei stained with Hoechst 33342 in SK-N-BE(2) cells treated with RES and $H_2O_2$.**

*Normal nuclei (N) and apoptotic nuclei (A) were counted and plotted as percentage of nuclei total count. Bar graph indicates the mean ± SEM (n=4 replicates, 10 field counted for each replicate), ***$p < 0.001$, RES 15 μM + $H_2O_2$ 75 μM vs. RES 15 μM alone, Tukey's test. The insert below the histogram shows Hoechst 33342 stained nuclei under UV light. The arrows point to fragmented nuclei (magnification: 20X, scale bar: 15 μm).*

To test whether RES-mediated neuroprotection against $H_2O_2$, was actually due to the activation of SIRT1 by RES, SIRT1 was inhibited by sirtinol.

Sirtinol toxicity was first assessed in SK-N-BE(2) by exposing cells to increasing doses of the molecules for 24 h. Sirtinol was toxic starting from 5 μM (figure 6.7). The dose of 2.5 μM sirtinol was chosen for the subsequent experiment.

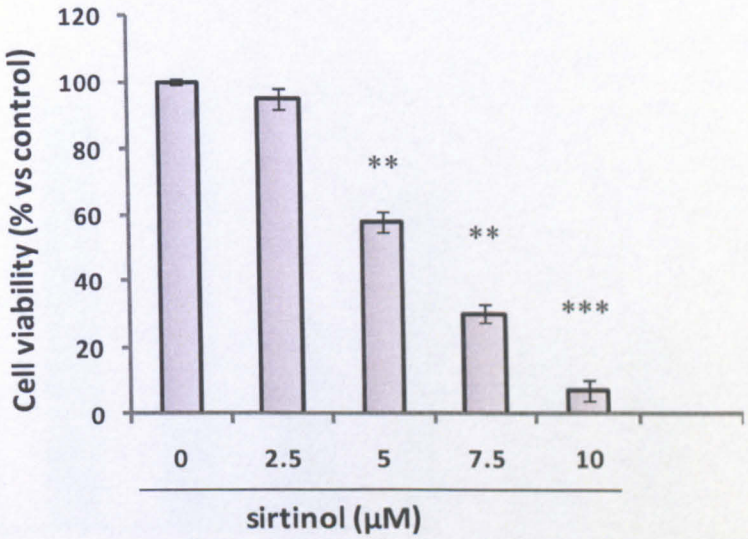


**FIGURE 6.7. Dose response effects of increasing doses of sirtinol on SK-N-BE(2) viability.**

*SK-N-BE(2) cells were exposed to increasing doses of sirtinol 24 h, then cell viability was assessed. Viability of control cells was set at 100%, and viability with respect to the control is presented. Bar graph indicates the mean ± SEM (n=4). **: $p<0.01$, ***: $p<0.001$; one-way ANOVA followed by Dunnetts's post hoc test versus control (cells treated with vehicle = 0.05% DMSO).*

To assess sirtinol ability to reverse RES protection, cells were pre-treated with sirtinol 2 h before each RES treatment. Despite there being evidence of some sirtinol-mediated toxicity at micromolar concentrations, the double-treatment with the molecule at 2.5 μM did not significantly affect cell viability (column 3 figure 6.8). When SK-N-BE(2) cells that were exposed to $H_2O_2$ in the presence of RES having been pre-treated with sirtinol, the protective RES-mediated effect was no longer detectable (column 7 figure 6.8).

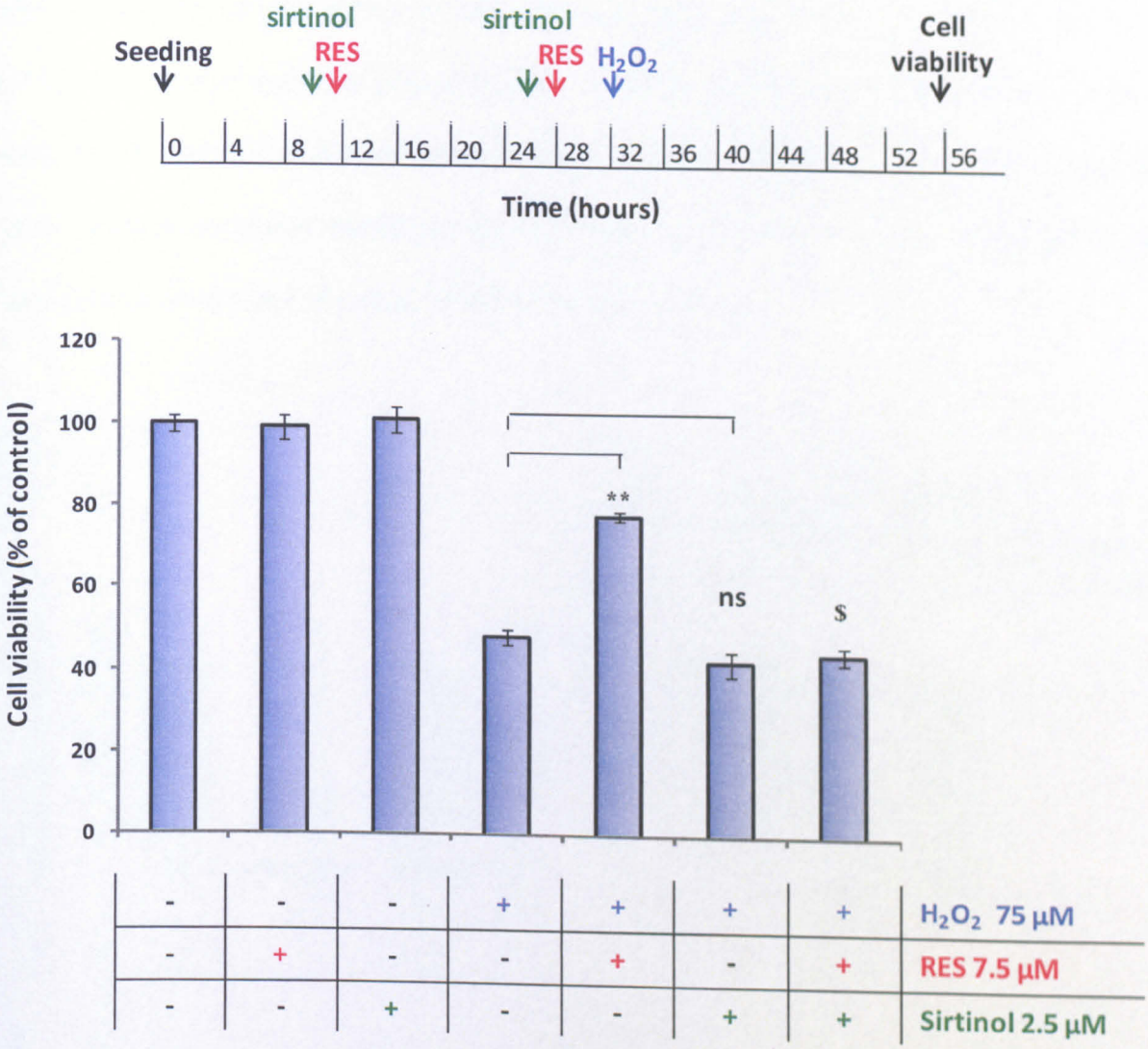


**FIGURE 6.8. Sirtinol conteracts RES-mediated protection against $H_2O_2$-induced toxicity.**

*SK-N-BE(2) cells were pre-treated with sirtinol 2 h before each RES treatment followed by $H_2O_2$ challenge as summarized in the panel above the graph. Cells viability is expressed as a percentage of the control (cells treated with vehicle = 0.2% DMSO). Bar graph indicates the mean ± SEM (n=4). Statistical analysis was performed by 2-way ANOVA ($H_2O_2$ alone as reference group) **$p < 0.01$ RES effect; ns: sirtinol effect, $ $p < 0.01$ sirtinol x RES at $H_2O_2$ 75 µM.*

To confirm whether SIRT1 was inolved in RES-mediated protection, SIRT1 expression was transiently downregulated in SK-N-BE(2) by adding 300 nM siRNA for 72 h. A reduction of SIRT1 mRNA of about 70% was measured by RT-PCR, using β-actin as

internal standard (figure 6.9A). A corresponding reduction was verified by WB using α-tubulin as internal standard (figure 6.9B). To check for the specificity of the silencing strategy, SK-N-BE(2) cells were incubated with a siRNA negative control (CT-). Using the same time/concentration conditions as were used for the *SIRT1* silencing by siRNA, no reduction of SIRT1 was found by mRNA/protein levels.

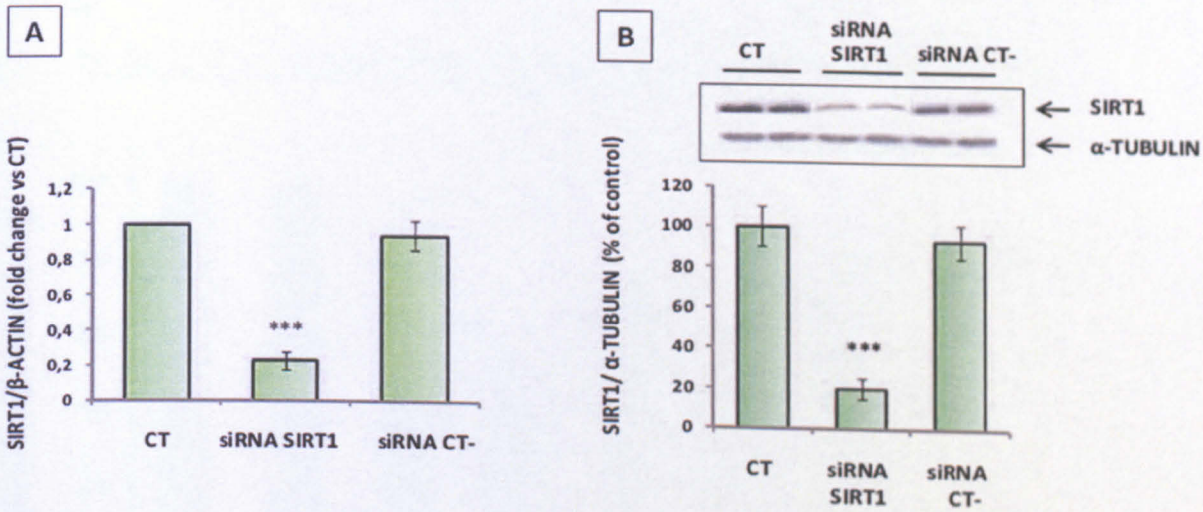


**FIGURE 6.9. Effects of SIRT1 silencing in SK-N-BE(2) cells.**

*SK-N-BE(2)cells were transfected by liposome treatment with 300 nM siRNA against SIRT1 or 300 nM siRNA negative control. 72 h after cell transfection, SIRT1 mRNA expression levels [A] were analyzed using quantitative RT-PCR and were normalized to β-actin expression as a standard. SIRT1 protein levels [B] were determined by WB and were normalized to α-tubulin. The relative densitometric values expressed as % of the control group are shown below. Bar graph indicates the mean ± SEM (n=3). ***: $p<0.001$; one-way ANOVA followed by Dunnetts's post hoc test versus control (cells treated with vehicle = 0.2 μL liposome).*

Under circumstances where SIRT1 is silenced, RES-mediated protection against $H_2O_2$ was assessed. As expected, the group challenged by oxidative stress but pre-incubated with RES was protected from cell damage. Whereas, when cells were silenced for SIRT1 and then exposed to $H_2O_2$ in the presence of RES, there was no difference to the cells which

were solely exposed to $H_2O_2$. In contrast, RES protection was not counteracted by the presence of a siRNA negative control (figure 6.10). Notably, SIRT1 silencing alone was not toxic and did not increase $H_2O_2$ toxicity.

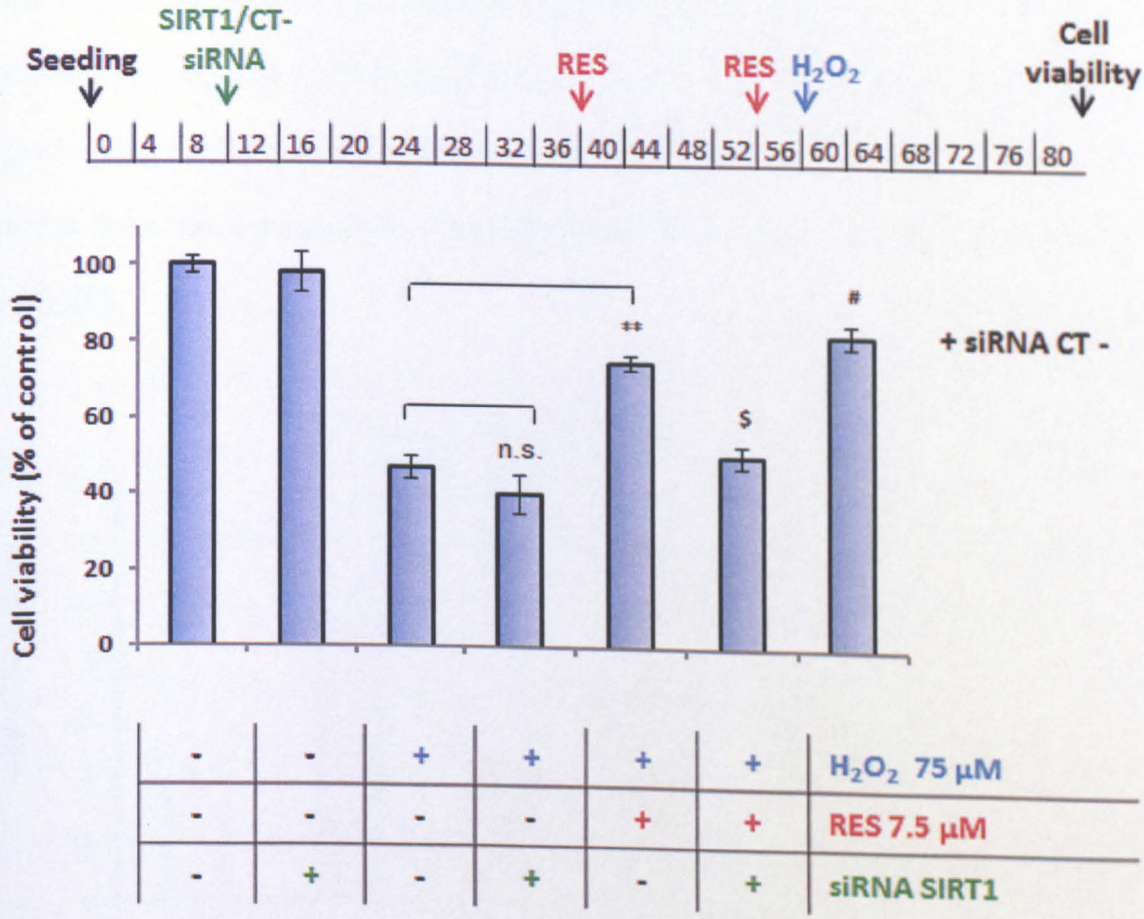


**FIGURE 6.10. SIRT1 silencing prevents RES-mediated protection of SK-N-BE(2) against oxidative challenge.**

*SK-N-BE(2) cells were transfected by liposome treatment with 300 nM siRNA against SIRT1 or 300 nM siRNA negative control. Under conditions of SIRT1 silencing, RES double treatment followed by $H_2O_2$ challenge was performed as summarized in the panel above the graph. Cells viability is expressed as the percentage of the control (cells treated with vehicle = 0.2 µL liposomes). Bar graph indicates the mean ± SEM (n=4). Statistical analysis was performed by 2-way ANOVA ($H_2O_2$ alone as reference group) $^{**}p < 0.01$ RES effect; ns: siRNA SIRT1, $ $p < 0.01$ siRNA SIRT1 x RES at $H_2O_2$ 75 µM. # n.s siRNA CT- x RES at $H_2O_2$ 75 µM.*

### 6.3.3. SIRT1 INVOLVEMENT IN ROS PRODUCTION

To attempt to elucidate the basis of SIRT1 involvement in counteracting $H_2O_2$ toxicity, intracellular ROS were measured using DCFH-DA, a well-established compound to detect and quantify intracellular ROS (Rizzardini et al., 2003) (cfr. chapter 2.4.4). When cells were exposed to $H_2O_2$ for 24 h, ROS increased in comparison to untreated cells, while RES pre-treatment reduced ROS to basal levels (figure 6.11). Furthermore, when SIRT1 was downregulated, RES pre-treatment was no longer able to restore ROS to basal level, even though there was a suggestion of a reduction of ROS level in comparison to $H_2O_2$ alone ($p= 0.08$).

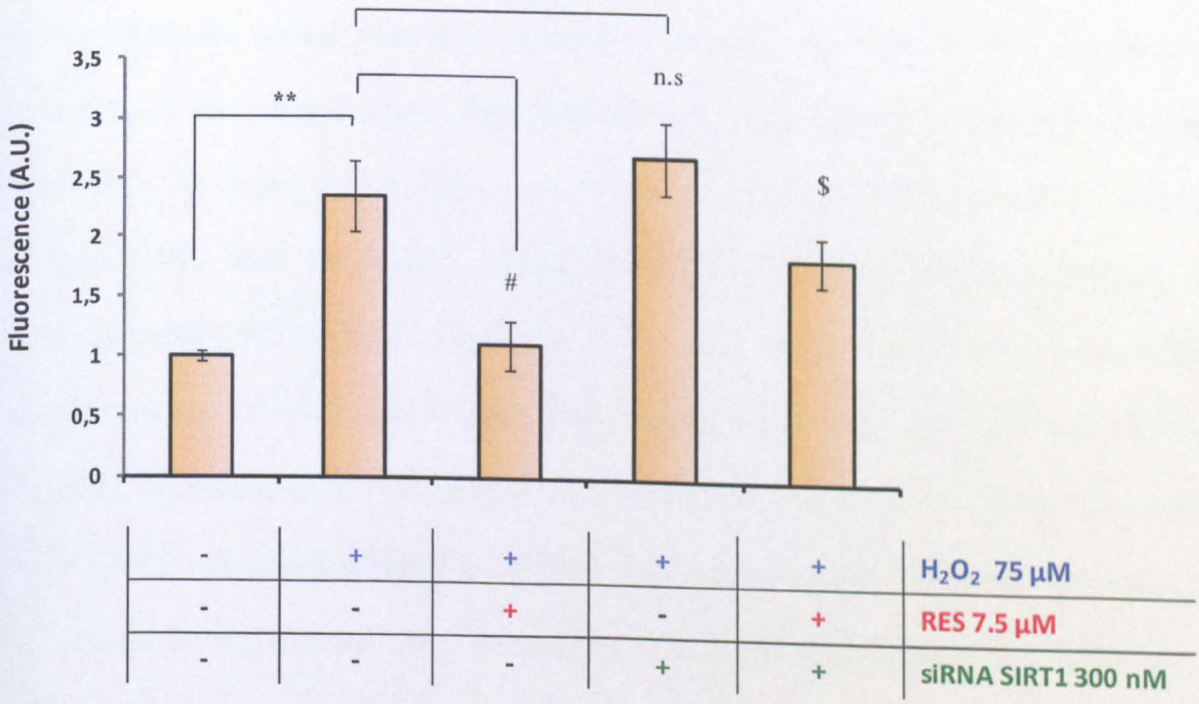


**FIGURE 6.11. SIRT1 silencing prevents RES-mediated decrease of ROS in SK-N-BE(2) cells.**

*SK-N-BE(2) cells were treated as in figure 6.10. 1 h before $H_2O_2$ challenge, cells were pre-loaded with DCFH-DA. At the end of the experiment fluorescence was recorded and expressed as arbitrary units (A.U.). Bar graph indicates the mean ± SEM (n=4), **p<0.01; one-way ANOVA followed by Student's t-test; #p < 0.01 RES effect, ns: siRNA SIRT1, and $ p < 0.01 siRNA SIRT1 x RES at $H_2O_2$ 75 µM, two-way ANOVA.*

### 6.3.4. SIRT1 INVOLVEMENT IN AUTOPHAGY UNDER OXIDATIVE STRESS

The potential role of SIRT1 in autophagy was investigated under conditions of oxidative stress. SK-N-BE(2) cells were silenced for *SIRT1* and then challenged with $H_2O_2$ for 24 h, as described above. At the end of the exposure to oxidative stress, the formation of autophagosomes was assessed using an antibody against the microtubule-associated protein 1 light chain 3 (LC3) by immunocytochemistry (IC) and WB. Newly synthesized LC3 is converted into the cytoplasmic form LC3-I. During autophagy, LC3 I is processed and recruited to the autophagosomes, where LC3 II is generated by site specific proteolysis. The amount of LC3-II is correlated with the extent of autophagosome formation (Kabeya et al., 2000).

SK-N-BE(2) cells treated with $H_2O_2$ showed an increase in autophagosome formation in comparison to the control group, highlighted by the higher number of bright green spots observed by IC (figure 6.12A). Under conditions of oxidative challenge, SIRT1 silencing by transfection with the siRNA against SIRT1 partially prevented the increase of autophagosomes that remained unaffected when cells where transfected with a siRNA negative control (CT-) (figure 6.12A). Consistently, under $H_2O_2$ exposure, the ratio of LC3-II/LC3-I measured by WB analysis increased compared to untreated cells. Moreover, when SIRT1 was downregulated by siRNA, LC3-II/LC3-I ratio decreased compared to cells exposed to $H_2O_2$ alone, while it remained unchanged in presence of a siRNA negative control (CT-).

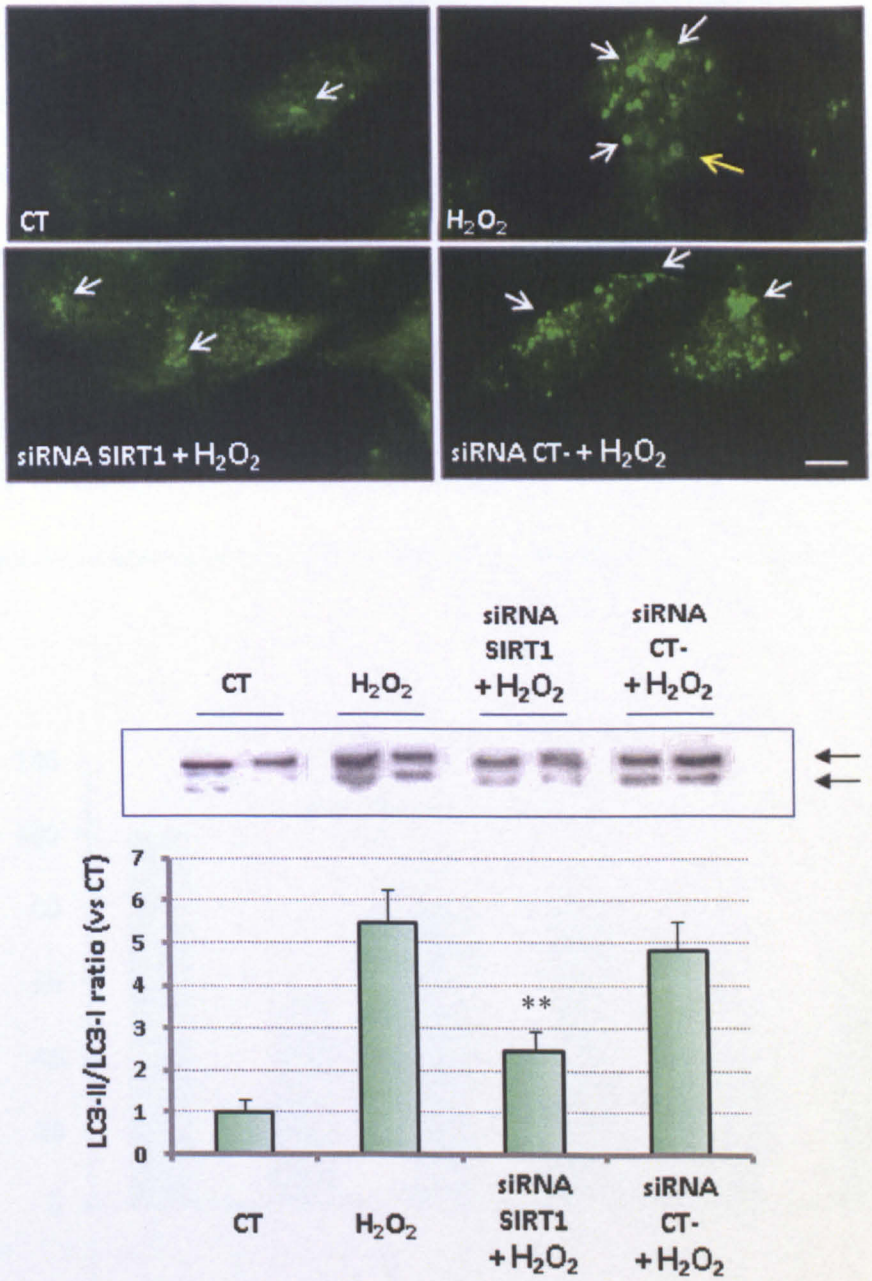


**FIGURE 6.12. SIRT1 silencing attenuates autophagy after oxidative stress**

*SK-N-BE(2) cells were transfected by liposome treatment with 300 nM siRNA against SIRT1 or 300 nM siRNA negative control. 48 h after transfection, cells were exposed to 75 μM $H_2O_2$ for further 24 h. At the end of the experiment, autophagosome formation was assessed with LC3 antibody. A] Immunocytochemistry. The arrows highlight LC3 bright spots reactivity (magnification: 40X, scale bar: 10 μM). B] WB. Cell lysates were loaded on 16% polyacrylamide gel. Immunostaining with the antibody against LC3 revealed two bands at 19 and 17 kDa corresponding to LC3-I and LC3-II, respectively. The graph shows the densitometric quantification of LC3-II/LC3-I ratio. Bar graph indicates the mean ± SEM (n=4), $^{**}p < 0.01$ siRNA SIRT1 x $H_2O_2$, two-way ANOVA.*

In order to elucidate the involvement of autophagy in RES-mediated neuroprotection, autophagy was inhibited after treating SK-N-BE(2) cells with 3-Methyladenine [3-MA, specific inhibitor of autophagic/lysosomal protein degradation (Seglen and Gordon, 1982)] at a concentration of 10 mM. RES double treatment was performed as above and 3-MA 10 mM was also added 1 h before oxidative challenge that continued for a further 24 h. As shown in figure 6.13, 3-MA treatment alone was toxic and increased $H_2O_2$ toxicity. Within this context, RES pre-treatment was able to counteract both $H_2O_2$ toxicity and $H_2O_2$ toxicity in combination with 3-MA (with respect to the corresponding controls).

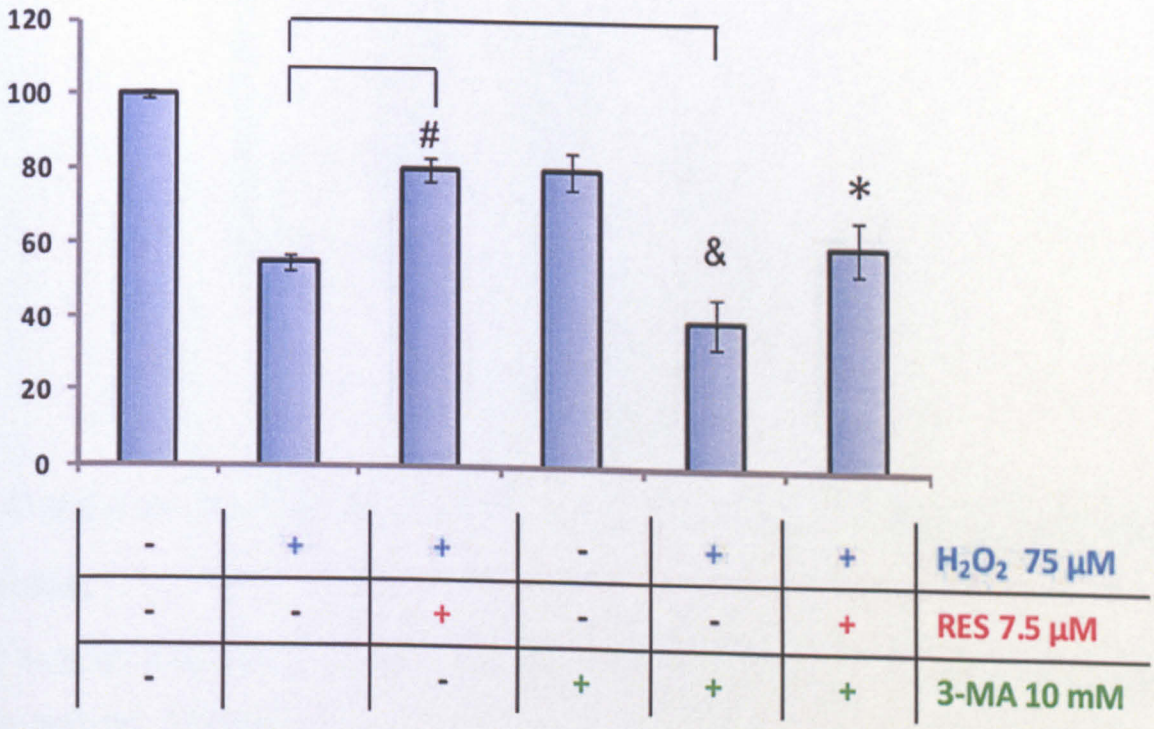


**FIGURE 6.13. RES-mediated neuroprotection is not mediated by autophagy**

*SK-N-BE(2) cells were pre-treated with RES as descibed above and 1 h before $H_2O_2$ challenge cells were exposed to 3-MA. Cells viability is expressed as a percentage of the control (cells treated with vehicle = 0.1% DMSO). Bar graph indicates the mean ± SEM (n=4). Statistical analysis was performed by 2-way ANOVA ($H_2O_2$ alone as reference group) #P< 0.01 RES effect; &P<0.05 3-MA effect;* P<0.05 3-MA x RES x $H_2O_2$ vs 3-MA x $H_2O_2$ Tukey's post hoc test.*

### 6.3.6. RES TREATMENT PREVENTS CELL DEATH TRIGGERED BY Aβ42

The potential preventative effect of RES was evaluated in SK-N-BE(2) cells challenged with Aβ42. First SK-N-BE(2) cells were treated with increasing doses of Aβ42 for 24 h. The dose of 10 μM Aβ42 that reduced cell viability by about 50% was chosen for the following experiments.

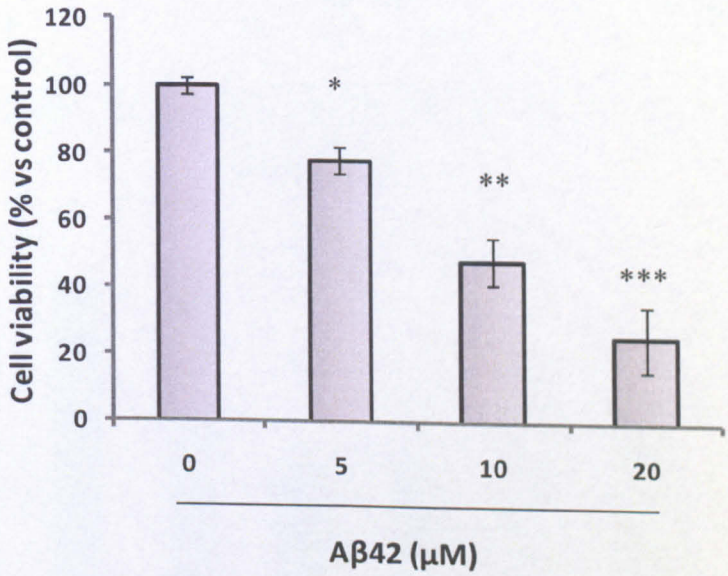


**FIGURE 6.14. Dose response effects of increasing doses of Aβ42 on SK-N-BE(2) viability.**

*SK-N-BE(2) cells were exposed to increasing doses of Aβ42 for 24 h, then cell viability was assessed. Viability of control cells was set at 100%, and viability with respect to the control is presented. Bar graph indicates the mean ± SEM (n=4). *: p<0.05; **: p<0.01, ***: p<0.001; one-way ANOVA followed by Dunnetts's post hoc test versus control (cells treated with vehicle = 2% NaOH 0.01 M).*

Then, SK-N-BE(2) cells were pre-treated with RES 7.5 μM (20 and 4 h before the toxic challange) and then exposed to Aβ42 for a further 24 h. Cells pre-treated with RES were

less susceptible to Aβ toxicity (figure 6.15). Indeed, a reduction of about 30% in cell mortality was registered in this treatment group compared to Aβ42 alone group.

To assess if RES-mediated protection was elicited by SIRT1 in this context the SIRT inhibitor sirtinol was used. Unexpectedly, when cells were exposed to sirtinol 2 h before each RES addition, the protective effect was still present (though slightly less).

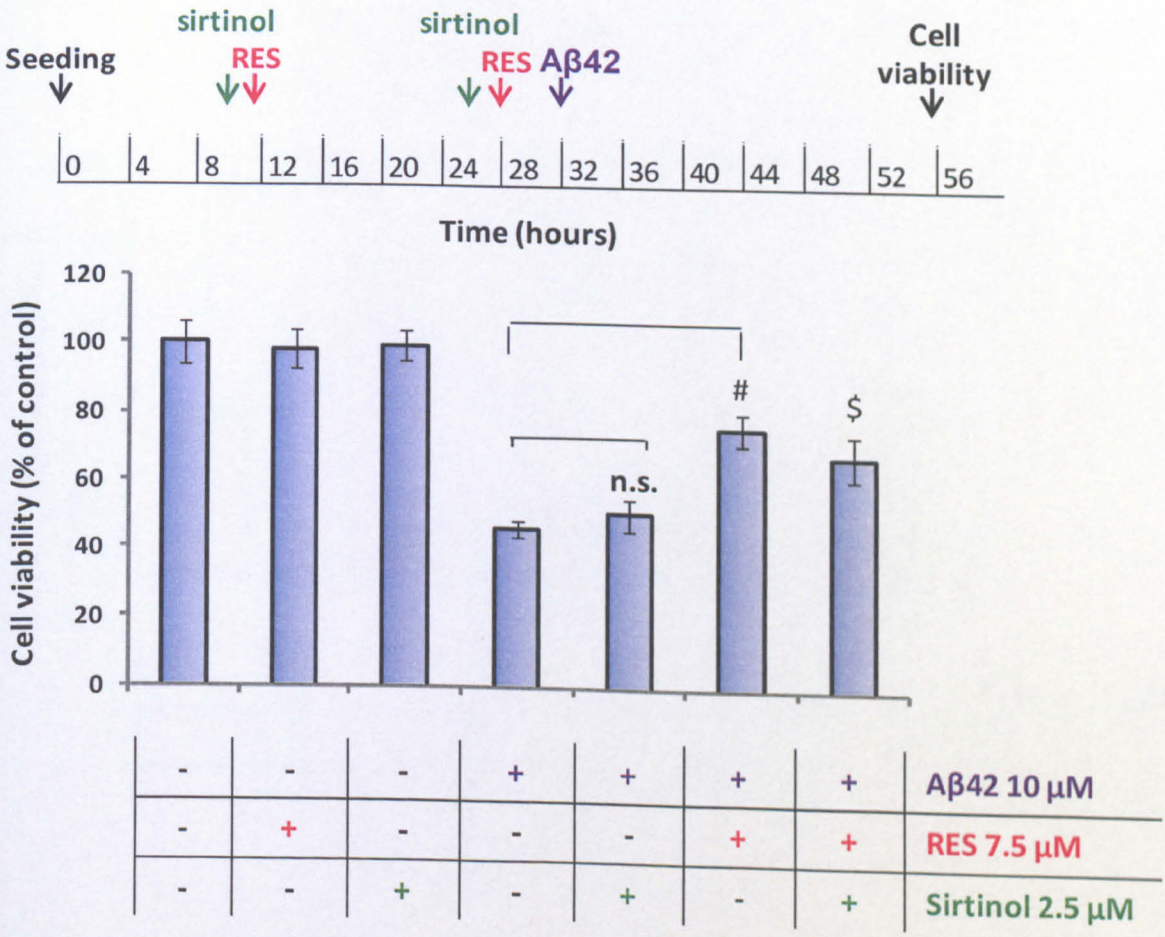


**FIGURE 6.15. RES is associated with reduced cell toxicity arising from exposure of SK-N-BE(2) cells to aggregation-prone protein Aβ42.**

*SK-N-BE(2) cells were pre-treated with sirtinol 2 h before each RES treatment followed by Aβ42 challenge as summarized in the panel above the graph. Cell viability is expressed as a percentage of the control (cells treated with vehicle = 2% NaOH 0.01 M and 0.2% DMSO). Bar graph indicates the mean ± SEM (n=4). Statistical analysis was performed by 2-way ANOVA (Aβ42 alone as reference group) #p < 0.01 RES effect; ns: sirtinol effect, $ n.s. sirtinol x RES at Aβ42 10 μM.*

To better elucidate the RES-mediated protective mechanism against Aβ42 exposure, intracellular levels of ROS were measured. Under conditions of Aβ42 exposure, levels of ROS increased similarly to those observed following exposure to $H_2O_2$. Once again, increases in ROS were counteracted by RES pre-treatment. Notably, SIRT1 inhibition by sirtinol treatment did not reverse increases in ROS.

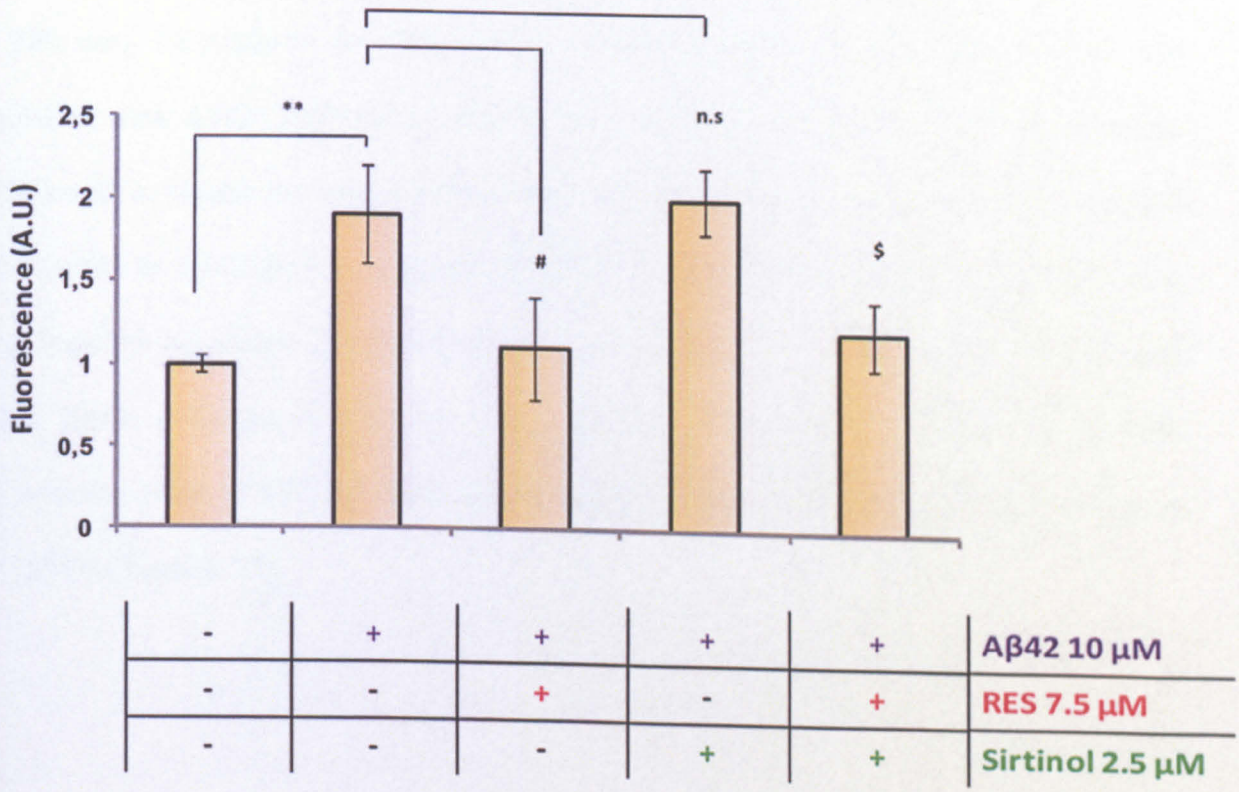


**FIGURE 6.16. RES treatment counteracts ROS generation following Aβ42 in a SIRT1-independent way.**

*SK-N-BE(2) cells were treated as in figure 6.14. 1 h before $H_2O_2$ challenge, cells were pre-loaded with DCFH-DA. At the end of the experiment fluorescence was recorded and expressed as arbitrary units (A.U.). The bar graph indicates the mean ± SEM (n=4). **p<0.01; one-way ANOVA followed by Student's t-test; #p < 0.01 RES effect, ns: sirtinol, and $ n.s. sirtinol x RES at Aβ42 10 µM, two-way ANOVA.*

Given these results, it was postulated that the observed RES effects might be mediated independent of SIRT1. To this concern, a direct effect of RES on Aβ42 fibrils was assessed. To achieve this, a fluorimetric binding assay was performed which took advantage of the intrinsic fluorescence of RES (excitation wavelength of 320 nm). With this technique RES was shown to bind Aβ42. In fact, following the binding of RES to Aβ42 its emission spectrum dramatically changed as highlighted in figure 6.17 by the red arrow (emission wavelength at which the highest peak was registered shifted from 400 nm to 380 nm). To evaluate the dissociating property of RES on Aβ42 fibrils, RES was incubated with Aβ42 fibrils for 24 h or 10 min and then measured at 320 nm excitation wavelength to assess the ratio between free RES (supernatant, emission at 400 nm) and RES bound to Aβ42 (pellet, emission at 380 nm) separated by centrifugation. RES alone was found to be almost completely free in the supernatant, while after incubation with Aβ42 fibrils a fluorescence signal was found in the insoluble pellet fraction. A weak dissociating effect of RES on Aβ42 fibrils was found after 24 h (around 20% dissociation, $p= 0.045$) (figure 6.17).

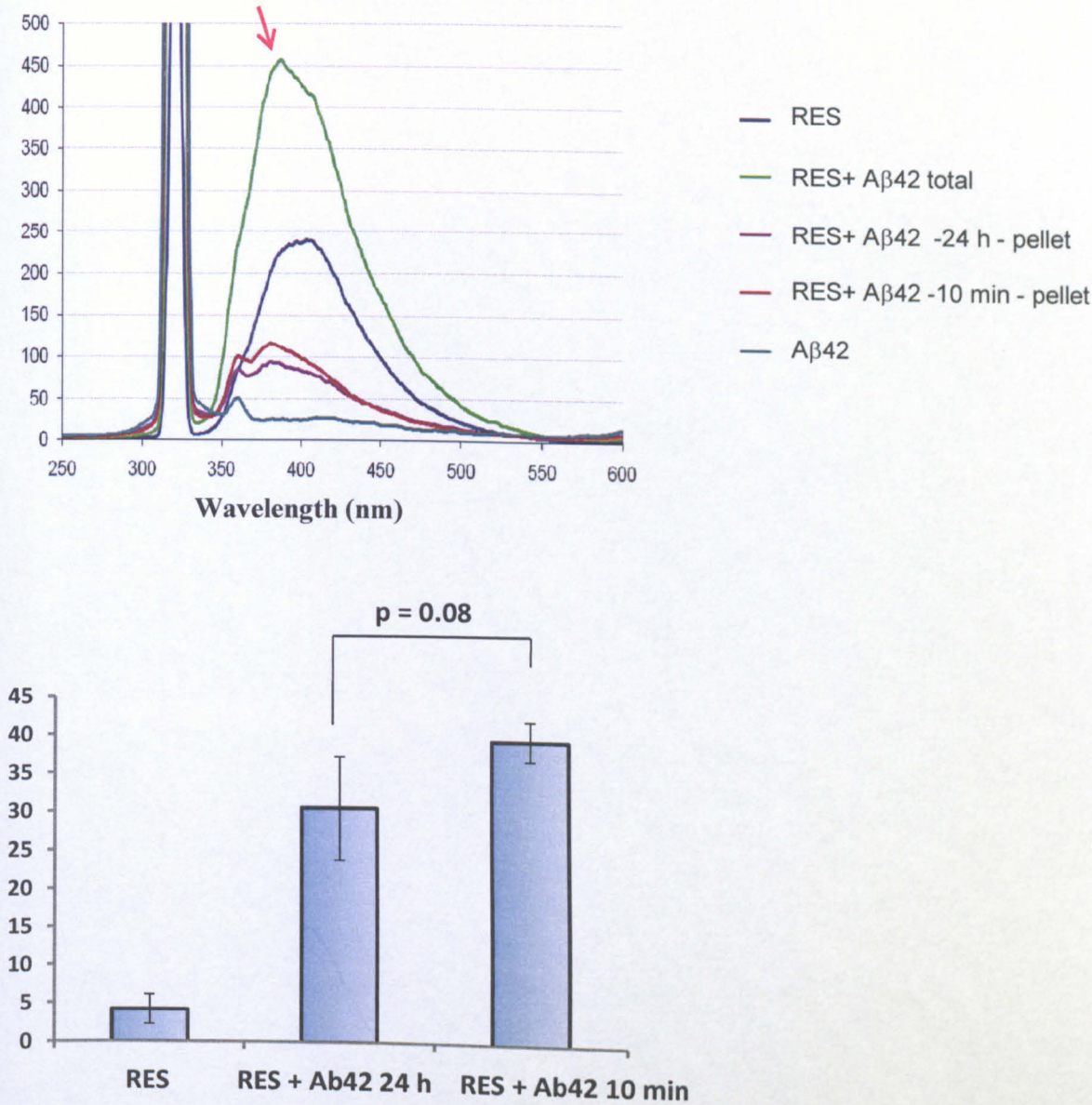


**FIGURE 6.17. RES binds and weakly dissociates Aβ42 fibrils after 24 h.**

*A. Fluorescence emission recording of RES, Aβ42 and RES+Aβ42 at excitation wavelength of 320 nm. B. Evaluation of RES dissociating property on Aβ42 fibrils performed by incubating RES + Aβ42 fibrils for 24 h or 10 min and then measuring at 320 nm the ratio between free RES (supernatant, emission at 400 nm) and RES bound to Aβ42 (pellet, emission at 380 nm) separated by centrifugation. Each group was run in quadruplicate. Bar graph indicates the mean ± SEM (n=4).*

To test the ability of RES to counteract Aβ42 aggregation, Aβ42 oligomers and protofibrils formation was monitored over time by atomic force microscopy (AFM). By comparing Aβ42 incubated with RES to Aβ42 alone, it was shown that the presence of RES delayed

the formation of Aβ42 oligomers and protofibrils for up to 6 h (figure 6.18), while at 24 h fibril dimension and density in absence or presence of RES were similar (not shown).

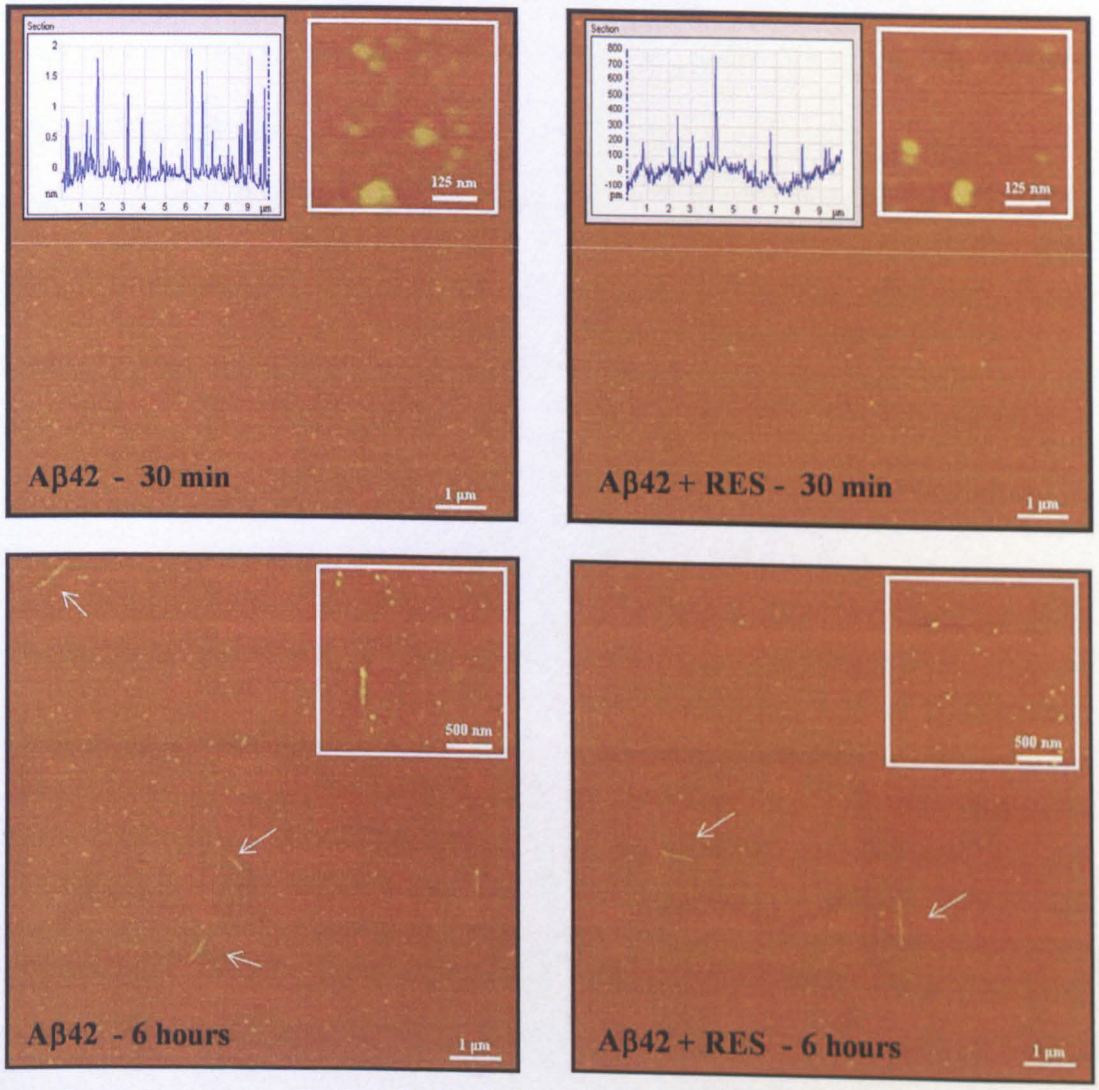


**FIGURE 6.18. RES can delay Aβ42 fibril formation.**

*Aβ42 was incubated at 37 °C for increasing time intervals (0.5, 6 and 24 h) in absence or presence of RES (1:1.5 ratio). One aliquot was then diluted to 1 µM with PBS 10 mM, pH 7.4 and incubated for 0.5 min on a freshly cleaved Muscovite mica disk. After the incubation time, the disk was washed with water and dried under gentle nitrogen stream and assessed with AFM. The graphs in the insert show an example of the dimension distribution of Aβ42 pre-fibrillar stage (Y-axis scale nm – left vs. pm –right). The arrows point to Aβ42 filamentous aggregates.*

# 6.4. DISCUSSION

The work summarized in this chapter first explored the question whether RES was beneficial in counteracting oxidative stress that is triggered by $H_2O_2$, and whether this protective action was dependent on SIRT1. To this aim, an *in vitro* model of oxidative stress was developed in the human neuroblastoma cell line SK-N-BE(2) by exposing cells to $H_2O_2$. Cell exposure for 24 h to increasing doses of $H_2O_2$ led to a dose-dependent reduction of cell viability. The final concentration of 75 μM $H_2O_2$, that reduced cell viability of about 50%, was chosen for the experiments presented in this chapter. In this *in vitro* model set up, the induction of oxidative stress was confirmed by an increase in intracellular ROS registered with the DCFH-DA probe. Notably, this increase in ROS did not activate apoptosis in SK-N-BE(2) cells measured with nuclear fragmentation assessed by staining cells with Hoescht 33342.

To investigate the role of SIRT1 against oxidative stress, SIRT1 activity was increased by RES and decreased by sirtinol in our cell-based model. RES and sirtinol concentration ranges were chosen according to those previously described in the literature (Chong and Maiese, 2008) and were finalised by pilot dose-response experiments. Moreover, since RES given 2 h before $H_2O_2$ was not able to protect cells from $H_2O_2$–mediated toxicity, a longer pre-treatment scheme was adopted. RES was given as an overnight pre-treatment and refreshed the day after for an additional 4 h. Then cells were challenged with $H_2O_2$ treatment. Within this double pre-treatment schedule, RES uptake by SK-N-BE(2) cells and its stability over time were assessed by mass spectrometry.

RES is a pleiotropic molecule reported to exert protective properties at low concentrations (few μMs) and to induce apoptosis at higher concentrations (Mukherjee et al., 2010). To

this concern, the pro-apoptotic effect of RES was assessed in our *in vitro* model. RES did not induce apoptosis at the final concentration chosen (7.5 μM) neither alone nor in combination with $H_2O_2$. Conversely, a higher concentration of RES (15 μM) although only in combination with $H_2O_2$, increased by 20% the percentage of apoptotic nuclei.

Notably, double pre-treatment with RES 7.5 μM was able to increase cell viabiliy by about 30% in SK-N-BE(2) cells challenge with $H_2O_2$ thus suggesting that RES at this concentration exerted neuroprotective effects. RES is a phytocompound that was reported to exert an antioxidant activity (Frankel et al., 1993). To assess this point the ability of RES to counteract $H_2O_2$-mediated increase in ROS species was evaluated. Interestingly, RES pre-treatment restored ROS basal levels under conditions of $H_2O_2$ exposure. To evaluate whether the observed RES neuroprotective effect observed was due to its general antioxidant properties or to SIRT1 activation by RES, SIRT1 enzymatic activity was inhibited with sirtinol, and cell viability was assessed under oxidative stress. Interestingly, RES antioxidant property using cell viability as a surrogate marker was affected by sirtinol treatment thereby suggesting the involvement of SIRT1.

To attempt to verify the actual involvement of SIRT1 and exclude the potential activation\inhibition of other sirtuins by RES and sirtinol, SIRT1 gene expression was downregulated by transfecting cells with siRNA. This yielded consistent findings to those observed with sirtinol, where transient downregulation of SIRT1 prevented RES-associated antioxidant properties as determined according by cell viability.

Overall, these data suggest that the protection induced by RES was mediated through SIRT1 activation. Notably, the ability of RES to decrease ROS was significantly affected by *SIRT1* silencing thus suggesting that SIRT1 could have a role in counteracting ROS, but since it was not completely reversed, it also possible that RES direct antioxidant action contributed to cell protection.

Another interesting result was the effect of oxidative stress and *SIRT1* silencing on autophagy. The relevance of the autophagic pathway under oxidative stress remains unclear. Indeed, basal levels of autophagic degradation of cell components (i.e., organelles, cytosolic proteins) occur in nearly all cell types as a means to maintain cellular homeostasis. Additionally, autophagy rapidly increases during periods of cellular starvation as a means to generate the necessary nutrients to sustain cell survival. However, excessive autophagy results in degradation of essential cell constituents, ultimately resulting in cell death. Determinants of whether autophagy promotes cell survival or cell death depend upon the severity and degree of stress in the cellular environment (Essick and Sam, 2010). SIRT1 involvement in autophagy has already been reported under nutrient starvation (Lee et al., 2008) as well as autophagosome formation after oxidative stress challenge (Pyo et al., 2008). Here this study has shown for the first time that SIRT1 may have a role in autophagosome formation under oxidative stress. Indeed, SIRT1 silencing partially counteracted $H_2O_2$-induced autophagy activation. However, the decrease in autophagy registered under $H_2O_2$ exposure in cells silenced for SIRT1 did not affect cell viability. This result, which is in contrast to the toxic effect reported by Seo et al. following SIRT1 silencing in a neuroblastoma cell line (Seo et al., 2010) could be caused by the incomplete silencing of SIRT1 in current cell model used here. Furthermore, this could also partially explain the high sirtinol toxicity registered in SK-N-BE(2) cells, although there was no evidence that the observed RES protective effect was related to autophagy. Indeed, RES-mediated protection against $H_2O_2$ was insensitive to the inhibitor of authophagy 3-MA.

Finally, the work presented in this chapter also evaluated the impact of RES as a neuroprotectent against Aβ42. Exposure of cells to Aβ42 triggered cell death and increased intracellular ROS in a similar manner as $H_2O_2$ treatment. This result is consistent with

previously published data showing that Aβ protein causes $H_2O_2$ and lipid peroxides to accumulate in cells (Behl et al., 1994). RES treatment was found to counteract cell death triggered by Aβ42 treatment and rescued ROS to basal levels (Jang et al., 2007). However, sirtinol did not totally reverse RES neuroprotective action, suggesting that other mechanisms independent of SIRT1 could also have been involved. For example, recently RES was shown to act as a ROS scavenger against the toxicity induced by Aβ-metal complexes (Granzotto and Zatta, 2011).

This study showed that RES could partly prevent Aβ toxicity by direct interaction with Aβ fibrils, as already reported (Ahn et al., 2007; Rivière et al., 2007). Moreover, a weak RES destabilization effect on Aβ fibrils but also an antifibrillogenic RES action that delayed Aβ42 oligomers and fibrils formation was found. This double effect can partly explain how RES provided some protection against Aβ42 toxicity. Indeed, it has been consistently reported recently that a subset of Aβ conformers (soluble prefibrillar oligomers, fibrillar intermediates, and fibrils) elicit RES to dramatically remodel their structure, whereas non-toxic oligomers and monomers do not. Moreover, RES remodels soluble oligomers and both fibrillar conformers into aggregated species that possess biochemical properties not found in the original conformers (Ladiwala et al., 2010).

Overall, in this cell model RES protected cells from Aβ42 toxicity independently from SIRT1 action but acting partly through the modifications of Aβ42 fibril formation and stability as well as by reducing intracellular Aβ42-dependent ROS generation. Other protective mechanisms such as RES-mediated activation of proteasomes after Aβ challenge could also be involved (Marambaud et al., 2005) or via alternate pathways not requiring SIRT1 activation as suggested by Pfister et al. (Pfister et al., 2008).

# *CHAPTER 7: FINAL REMARKS AND FUTURE STUDIES*

A large body of evidence has underscored the potential relevance of members of the sirtuin family (SIRT1-SIRT7) in pathogenic mechanisms leading to AD. In particular, SIRT1 was shown to counteract two important features of AD: APP metabolism and tauopathy. Indeed, several studies showed that SIRT1 shifts APP metabolism towards the non-amyloidogenic pathway through α-secretase upregulation (Qin et al., 2006a, 2006b; Donmez et al., 2010) and more recently SIRT1 was shown to deacetylate tau thus promoting its degradation and counteracting tauopathy (Min et al., 2010). Furthermore SIRT1 was proposed to be involved in collateral pathways relevant for AD, for example in response to oxidative stress, apoptosis, axonopathy (Haigis and Sinclair, 2010). For the other six sirtuins (SIRT2-SIRT7) no direct evidence was available about their role in AD but there exists numerous data relating the involvement of sirtuins in cell survival and stress response in neurodegenerative contexts (Haigis and Sinclair, 2010).

The importance of sirtuins in AD was first suggested in relation to calorie restriction (CR), a dietary regimen known to delay or even prevent age-related diseases such as AD (Baur, 2010). Several studies had already shown that the beneficial effect of CR on longevity was mediated by sirtuins in simple organisms. As such, the existence of an evolutionary conserved pathway fired by CR and involving members of the sirtuin family was proposed (Baur, 2010). Notably, some members of the sirtuin family were also shown to be modulated under other beneficial environmental paradigms such as PA (Koltai et al., 2010; Ferrara et al., 2008; Suwa et al., 2008). However, a systematic analysis of sirtuin modulation under these other paradigms was not yet performed especially in pathological contexts such as AD.

Given these preliminary remarks, the experiments described in this thesis were aimed to investigate the involvement of all 7 known sirtuins in modulating AD susceptibility through a translational research design. This involved the use of human genetic association studies, the use of *in vivo* modeling to explore the involvement of this protein family in an

environmental enrichment (EE) paradigm, a non-pharmacological treatment proved to be beneficial in neurodegenerative contexts and explored possible mechanisms for SIRT1 in AD through its pharmacological activation in *in vitro* models of AD.

The genetic section of this thesis (chapter 3 and 4) was aimed to 1] conduct a analysis of sirtuin genes by denaturing high performance liquid chromatography (dHPLC) with a view to identify gene variants that might be associated with AD susceptibility and 2] to test the extent of the association between common sirtuin gene variants (previously known and newly identified) and AD risk.

In achieving the first aim 29 SNPs were identified in a screening cohort of 48 AD patients and 48 controls. Eleven of these were novel SNPs which have not yet been reported while the remaining ones were already recorded in the NCBI SNP database. Despite being only a pilot study and using small numbers, it already suggested that some SNPs might be differently distributed between AD and CT. In particular, *SIRT1* and *SIRT2* were characterized by several SNPs appearing to be different found in the two groups. In most cases these variants were intronic given the exception of SNP4 (rs2273773), a silent SNP lying on exon V of *SIRT1*. These SNPs, although lacking an obvious functional importance, could still serve as genetic markers for association with AD through their genetic association with other adjacent SNPs which may be more disease relevant. As such, these SNPs were included in a more formal case-control genetic association study aimed to collect more evidence of whether there might be a true genetic association between genetic variants laying on SIRT genes and AD susceptibility.

In this second stage of the genetic study, beside previously identified SNPs, other intronic variants, laying in sirtuin portions not included in the dHPLC study, were selected so as to retain sirtuin variability in gene regions with high linkage disequilibrium (i.e. using a tagSNPs approach) (Stram, 2004). Thirty-four SNPs across all the 7 SIRT genes were assayed. This study replicated previous studies of *SIRT1* where no associations with AD

risk were found (Morgan et al., 2007; Helisalmi et al., 2008). There was marginally significant evidence of a new association between rs10410544 SNP in *SIRT2* and AD from the initial case-control study (p= 0.05). Furthermore, although this was not confirmed in the separate replication analysis, there remained evidence of association after combining the two study samples. This combination increased the power of the analysis [power (β)> 0.90] and was possible because the two sample sets were geographically related and the combined sample yielded an OR ~ 1.2 (95% CI 1.02-1.5, p= 0.02). Overall, this is a small effect size, although it remains possible that allele T of the rs10410544 SNP might make a small contribution to SAD susceptibility. The small effect size is consistent with previously reported data suggesting that, apart from *APOE* ε4, only associations of this magnitude are likely to be discovered in relation to AD. However, to confirm this association, further studies will be planned to validate it in larger sample sets. Furthermore, also given the interesting heterozygote distribution comparing AD and CT found in the dHPLC study of SNPs rs11879010 and rs45496398 in *SIRT2* gene, a higher-density genotyping of *SIRT2* might be worthwhile, particularly because as it transpired from this study, the tagging approach used was later found not to give good coverage to some regions with low LD.

Finally, given the wide role of sirtuins in neurodegeneration/neuroprotection in general, and specifically the detrimental role of SIRT2 in Parkinson's disease, it may be worthwhile exploring the impact of this polymorphism as a susceptibility factor for other neurodegenerative diseases.

The *in vivo* section of this thesis described the application of an EE protocol to APP23 mice and addressed the question whether this paradigm could delay the onset and progression of AD-like pathology. In this context the modulation of sirtuins was also evaluated.

After 4 months of EE, TG mice revealed an improvement of performance in two different memory tasks: MWM and vORT. Overall, these tests showed that the normal levels of cognitive impairment expected in TG mice at 6-7 months of age, when compared to TG-SHs mice, was reversed by EE. Conversely, the EE paradigm did not further improve learning and memory performance in WT mice. However, EE was shown to induce molecular changes in WT mice as shown by increased BDNF mRNA levels that were registered in 8-month-old mice were independent of genotype. This, highlighted the effectiveness of this EE protocol also in WT mice and prompts the need to further explore the effect of EE from the presence of the transgene. In particular, to evaluate the relevance of BDNF modulation in the pathogenic context of APP23 it would be worth to evaluate the outcome of the application of the EE protocol in transgenic APP23 mice crossbred with BDNF-/- mice.

Moreover, given the improvement in performance in these tests measuring hippocampus-dependent memory and the increase in BDNF that is linked to long term potentiation (LTP), LTP could be assessed in TG mice housed in the two different housing conditions. Interestingly, despite the noted changes to pathology, EE did not appear to elicit any molecular changes relevant to the AD-phenotype in the APP23 TG mice such as APP overexpression and its metabolism, or in Aβ oligomer production. However, given the now widely recognized acceptance of central role of oligomers in AD, considered to be the real toxic species, further studies would require a greater attention to these in the future. In particular, an ultrastructural analysis of intracellular Aβ oligomers in synaptic compartments will be performed. Moreover, it will also be assessed whether EE could reverse the hippocampal postsynaptic alterations registered in APP23 such as in the trafficking of synaptic NMDA receptor subunits NR2A and NR2B shown by our laboratory in APP23 TG mice (Balducci et al., 2010). Eventual differences could explain the restored behavioural performance otherwise not fully elucidated by the data collected till now. Anyway, despite no difference was registered in APP metabolism in 8-month-old

mice, a marked decrease in plaque deposition in 18-month-old TG mice was observed in TG-EEs compared to TG-SHs. This evidence should be further elucidated for example by investigating the levels and activity of enzymes capable of degrading Aβ such as neprilysin and insulin-degrading enzyme (Miners et al., 2008). Furthermore it could be worth of note to measure the accumulation of Aβ within cerebral blood vessels since APP23 develop a marqued cerebral amyloid angiopathy (Sturchler-Pierrat et al., 1997).

Finally sirtuin expression levels in 8-month-old mice were assessed. Both the presence of the transgene and/or housing conditions did not affect sirtuin levels. These findings would suggest that the EE paradigm provides benefits that are independent of or removed from the involvement of sirtuins. Although, it might be worth assessing whether EE modulates sirtuins in other peripheral tissues (e.g. skeletal muscle) which may identify changes already suggested in the literature in relation to sirtuins and physical stimulation.

Overall, the present study showed that it is possible to attenuate the progression of cognitive decline and reduce some AD-like pathological hallmarks in the APP23 mouse model of AD by using EE. Moreover, preliminary indications suggest that, unlike other environmental paradigms, such as CR or physical activity, EE does not modulate sirtuin expression levels in the brain.

In the last section of this thesis the role of SIRT1 pharmacological activation by resveratrol (RES) was evaluated in *in vitro* models using SK-N-BE(2) recapitulating two different detrimental features of AD pathology, i.e. oxidative stress and exposure to Aβ42. In the first part of the *in vitro* section, RES was shown to be neuroprotective against oxidative stress through the activation of SIRT1, since both pharmacological inhibition of SIRT1 and its silencing affected RES neuroprotection. Moreover, RES counteracted resultant ROS increases under oxidative stress and this effect was significantly affected by *SIRT1* silencing suggesting that SIRT1 could be involved. This is consistent with findings in a different model where SIRT1 was protective against Aβ-induced ROS production

(Savaskan et al., 2003). Another interesting finding was the novel observation that SIRT1 may be involved in autophagosome formation under oxidative stress. However, the relevance of the autophagic pathway under oxidative stress still requires more work since this mechanism was insensitive to the inhibitor of authophagy 3-MA. All these findings highlighted a role for SIRT1 in counteracting oxidative stress that could pass through different intracellular mechanisms, all giving their contribution.

The potential neuroprotective effect of RES action against Aβ42 was also shown, however, this appeared to be independent of SIRT1 since sirtinol did not reverse RES-mediated neuroprotective actions nor did it affect the ability of RES to decrease ROS production following Aβ42 challenge. All these results suggested that other mechanisms independent of SIRT1 may be involved which could include direct molecular destabilizing interactions between RES and various species of Aβ fibrils. It may still be worthwhile to investigate the neuroprotective role of SIRT1 in relation to its activation with drugs not structurally related with RES. In particular, SRT1720, a more potent activator of SIRT1 now commercially available could be tested. Another interesting aspect to take into account concerns the neuroprotective role of SIRT1 independently from its activation as suggested by Pfister .

In conclusion, the present thesis identified that *SIRT2* variation may confer some small risk or disease modifying effect for AD. It also confirmed the neuroprotective role of SIRT1 activation by RES, proposing ROS clearance and autophagy as potential mechanisms that deserve further studies in relation to SIRT1. Finally this thesis has given further evidence that EE could be beneficial in an AD-like mouse model, but does not mediate its benefits through modifications of sirtuin expression levels in the brain.

# *APPENDIX*

| *GENE/ PROTEIN* | *CHR N°* | *CHROMOSOME REF SEQ* [#] | *mRNA . REF SEQ* | *PROTEIN REF SEQ* | PROTEIN LENGTH |
|---|---|---|---|---|---|
| ***SIRT1/*** **SIRT1** | 10 | NC_000010.10 | NM_012238.4* | NP_036370.2* | 747 aa |
| | | | NM_001142498.1 | NP_001135970.1 | 452 aa |
| ***SIRT2/*** **SIRT2** | 19 | NC_000019.9 | NM_012237.3* | NP_036369.2* | 389 aa |
| | | | NM_030593.2 | NP_085096.1 | 352 aa |
| | | | NM_001193286.1 | NP_001180215.1 | 234 aa |
| ***SIRT3/*** **SIRT3** | 11 | NC_000011.9 | NM_012239.5* | NP_036371.1* | 399 aa |
| | | | NM_001017524.2 | NP_001017524.1 | 257 aa |
| ***SIRT4/*** **SIRT4** | 12 | NC_000012.11 | NM_012240.2* | NP_036372.1* | 314 aa |
| ***SIRT5/*** **SIRT5** | 6 | NC_000006.11 | NM_012241.3* | NP_036373.1* | 310 aa |
| | | | NM_031244.2 | NP_112534.1 | 299 aa |
| | | | NM_001193267.1 | NP_001180196.1 | 292 aa |
| ***SIRT6/*** **SIRT6** | 19 | NC_000019.9 | NM_016539.2* | NP_057623.2* | 355 aa |
| | | | NM_001193285.1 | NP_001180214.1 | 328 aa |
| ***SIRT7/*** **SIRT7** | 17 | NC_000017.10 | NM_016538.2* | NP_057622.1* | 400 aa |

**TABLE A.1. NCBI Entrez reference sequences of human sirtuins.**

*Abbreviations: CHR N°, chromosome number; REF SEQ, reference sequence; aa, amino acid.*

[#] *Chromosome reference sequences according to genome build 37.2*

* *Full length transcripts and proteins.*

| *GENE/ PROTEIN* | *CHR N°* | *CHROMOSOME REF SEQ* [#] | *mRNA REF SEQ* | *PROTEIN REF SEQ* | **PROTEIN LENGTH** |
|---|---|---|---|---|---|
| ***SIRT1/*** **SIRT1** | 10 | NC_000076.5 | NM_019812.2* | NP_062786.1* | 737 aa |
| | | | NM_001159589.1 | NP_001153061.1 | 698 aa |
| | | | NM_001159590.1 | NP_001153062.1 | 576 aa |
| ***SIRT2/*** **SIRT2** | 7 | NC_000073.5 | NM_022432.4* | NP_071877.3* | 389 aa |
| | | | NM_001122765.1 | NP_001116237.1 | 352 aa |
| | | | NM_001122766.1 | NP_001116238.1 | 319 aa |
| ***SIRT3/*** **SIRT3** | 7 | NC_000073.5 | NM_001177804.1* | NP_001171275.1* | 334 aa |
| | | | NM_001127351.1 | NP_001120823.1 | 257 aa |
| ***SIRT4/*** **SIRT4** | 5 | NC_000071.5 | NM_001167691.1* | NP_001161163.1* | 333 aa |
| ***SIRT5/*** **SIRT5** | 13 | NC_000079.5 | NM_178848.3* | NP_849179.1* | 310 aa |
| ***SIRT6/*** **SIRT6** | 10 | NC_000076.5 | NM_181586.3* | NP_853617.1* | 334 aa |
| | | | NM_001163430.1 | NP_001156902.1 | 294 aa |
| ***SIRT7/*** **SIRT7** | 11 | NC_000077.5 | NM_153056.2* | NP_694696.2* | 402 aa |

**TABLE A.2. NCBI Entrez reference sequences of murine sirtuins.**

*Abbreviations: CHR N°, chromosome number; REF SEQ, reference sequence; aa, amino acid.*

[#] *Reference Assembly: MGSCv37-C57BL/6J*

* *Full length transcripts and proteins.*

| Gene | A | Exon | Forward primer (5'→3') | Reverse primer (3'→5') | Size (bp) | $T_{annealing}$ (°C) | $T_{melting}$ (°C) in DHPLC |
|---|---|---|---|---|---|---|---|
| *SIRT1* | 1 | I | gccagagaggcagttgga | atctcctcctccctctcccc | 501 | 64,9-57,9 | 66,7 |
| | 2 | II | aaccgttcatacattttaggtgc | ggtttgtttgttttgagacagagtt | 253 | 57,1 | 58,2 |
| | 3 | III | aaaaccctcacagaatgctaactc | cttatgccttttccaagtaggaa | 404 | 57,8 | 55,5 |
| | 4 | IV | ttggcctgacttaaaaattcc | gtgaatgctgctactgtggc | 516 | 59,8-52,8 | 56,4 |
| | 5 | V | gcatccatctagatactttaaaatgc | ctgactgccatcgagaagtg | 379 | 58,6 | 57,0 |
| | 6 | VI | cttaaaccctcttaacatttgtg | ggaagaaaatagttagcatttggg | 321 | 56,0 | 56,0 |
| | 7 | VII | tgttgactatttctaacttgggc | gtcatgggttgtgggtctgt | 317 | 58,0 | 57,6 |
| | 8 | VIII | cccttgttggatttttgcat | tggaagaaaaaccacaggaag | 418 | 54,4 | 56,5 |
| | 9 | VIII | cccacacctcttcatgtttc | cggcaggttaatcgataggg | 421 | 58,3 | 57,0 |
| | 10 | IX | agagctggaacccacacttc | gtatcttcaatcagctgttggtca | 669 | 59,1 | 58,0 |
| *SIRT2* | 11 | I | ggacacagtggttggtgacg | cagccctcagaatcccactc | 216 | 61,3 | 56,5 |
| | 12 | II | cttaatcgttctccccactgtaac | agtgtgggatgtggaacaagtc | 177 | 60,2 | 61,3 |
| | 13 | III | cttttccccaaacctggtatc | tacatactttggatgtcactcctga | 249 | 58,4 | 61,0 |
| | 14 | IV | ggccttgtgcctttagatgt | aaggtttcaataaatggttcaagtg | 327 | 56,5 | 63,7 |
| | 15 | V | gtcatatggtgcataagttcctctc | tataccatactaaccctcccaggac | 183 | 61,6 | 59,6 |
| | 16 | VI | cctgggagggttagtatggtataga | tgaaatagctgatctcaaagatgg | 159 | 63,1-56,1 | 59,9 |
| | 17 | VII | tgagatcagctatttcaaggtttgt | cacccatgtacttaatggctacata | 299 | 58,3 | 62,5 |
| | 18 | VIII | taaaacagtcacagtgcctagaaca | ctctgctgaggacaccatgc | 233 | 60,2 | 64,3 |
| | 19 | IX | cctccatctctccctctagaaca | ctaagctggatgaaaggtgagg | 155 | 61,0 | 60,6 |
| | 20 | X | tcttactgccttctctttcttcc | acctctgtctctctgaacagtgc | 220 | 64,3-57,3 | 61,3 |
| | 21 | XI | ccccatgtcactgtctctgtc | gtatgcagtcagtaagtggccc | 110 | 61,7 | 62,1 |
| | 22 | XII | cagggaggtttgctgctg | cctcatcagcaagtaggttgg | 170 | 59 | 63,9 |
| | 23 | XIII | ctccctcatcagcaagtaggtt | cctctcacccttttcctcagag | 218 | 60,9 | 63,5 |
| | 24 | XIV | aagtcacagagctaggatacaaacc | agatgagaggagcaggcagg | 264 | 61,1 | 63,3 |
| | 25 | XV | aaggcagatgagaggagcag | acagtgacctttgacttctgtgac | 243 | 59,9 | 63,7 |
| | 26 | XVI | tgacctttgacttctgtgacctt | ccagtgacagctgcatctcc | 203 | 63,9-56,9 | 63,2 |

| | | | | | | | |
|---|---|---|---|---|---|---|---|
| *SIRT3* | 27 | I | tccggaggactccttggact | aaatacctcgaaaagaagaaactgg | 316 | 63,4-56,4 | 67,5 |
| | 28 | II | ctatctgtttcctttgctgctgt | gactgtgggcagtacctgaagt | 245 | 64,2-57,2 | 59,0 |
| | 29 | III | gcccagtttattccacttcc | aggaagaagcataagcgataggt | 451 | 57,9 | 61,4 |
| | 30 | IV | aagttgtgctcttggccttg | cttttccagatcaccccaac | 232 | 57,2 | 63,0 |
| | 31 | V | tccttttacagggtgttgcag | ccatgagatgactcctgtaccc | 291 | 63,8-56,8 | 62,3 |
| | 32 | VI | ctgtggcatgaaacatcctg | aggtggaccataccctagagc | 348 | 63,4-56,4 | 61,5 |
| | 33 | VII | ctgtttgaacagagatctgct | gaggtcttgtcagaattggga | 167 | 56,7 | 58,2 |
| *SIRT4* | 34 | I | aaccaccccagtttctcaca | caacacacgggtttgcgttc | 580 | 58,3 | 60,9 |
| | 35 | II | cgtctctgacagctttgtgc | tctctccaggactcccaatc | 419 | 59,3 | 60,8 |
| | 36 | III | ggagagacaccctgtttgg | caagtgaaagtccctgttgg | 277 | 58,1 | 58,1 |
| *SIRT5* | 37 | I | gcctcaagcattagaactacagaca | gaaagtcctacacttcgagaggaat | 221 | 60,8 | 59,7 |
| | 38 | II | aaatgtccaaactgtacactggatt | agtttccagaacattaaaagcctct | 215 | 57,5 | 57,1 |
| | 39 | III | ctcactcctgcctcctctcc | attcagggaaccagctttaaaac | 299 | 62,7-55,7 | 63,0 |
| | 40 | IV | tggagaaggttgctcttgattatac | aaatgtgaggaaattgaacattcat | 229 | 60,7-53,7 | 55,3 |
| | 41 | V | gccaggcaaatatacaaactgag | gtgttccaggttaccaaaacaaa | 194 | 57,6 | 54,0 |
| | 42 | VI | cttaaggatcccattcttccag | tttatgtctagtggtgggtcatg | 156 | 58,3 | 60,9 |
| | 43 | VII | atctccgtgtacttgccttgtag | agattcaggtactgggataccct | 154 | 60,2 | 61,9 |
| | 44 | VIII | cttgctgaagtagggcattcatt | cttatgggtggtgagctgagtac | 236 | 64,3-57,3 | 58,2 |
| *SIRT6* | 45 | I | agtcgaggatgtcggtgaatta | ctcccattgtctagcctcagtg | 189 | 64,0-57,0 | 69,2 |
| | 46 | II | acttgggggaactgttttgac | ctgcacaatcacagacctgaagt | 192 | 59,0 | 63,9 |
| | 47 | III | gtctcttttctgttcccctctc | atagaaccaggaaaaggggactc | 331 | 60,2 | 66,2 |
| | 48 | IV | atcaagcctcttcctgctcttc | agagacccagagggtatggg | 176 | 60,6 | 62,5 |
| | 49 | V | ctagaaacagtgcgagagtcacc | actctcctcagcttcctcattg | 244 | 61,0 | 66,1 |
| | 50 | VI | actctcctcagcttcctcattg | gacgacagcagaaacacagc | 170 | 59,6 | 66,7 |
| | 51 | VII | cacagatggcctaggtgtgaac | ctcagacacctacgtgcttggt | 231 | 61,8 | 66,7 |
| | 52 | VIII | accaagcacgtaggtgtctgag | gtgagaccacgagagaaaaagaa | 487 | 64,2-57,2 | 65,3 |

| | | | | | | | |
|---|---|---|---|---|---|---|---|
| *SIRT7* | 53 | I | gaagcggaagagcaggtctc | ctgcagctccgttaccaggtc | 287 | 62,4 | 69,0 |
| | 54 | II | cggacctggtaacggagctg | gcctgtgtagacgaccaagtatt | 268 | 65,8-58,8 | 70,4 |
| | 55 | III | gtgaccaccctggcgtctt | tggagctcatactccgtcct | 176 | 60,2 | 66,0 |
| | 56 | IV | ccttttgacttggcttacctttt | caaggtgaggagagctggag | 186 | 63,0-56.0 | 63,7 |
| | 57 | V | agtgtggacactgcttcagaaag | gctcttaccagcttctgctcat | 215 | 60,1 | 65,5 |
| | 58 | VI | ggtactgacctccccaccac | gcaggactgctcacttcaatgta | 177 | 65,8-58,8 | 64,2 |
| | 59 | VII | ttgcctctaggtctgtacctcct | ctcggttcactcattgtgtcat | 279 | 64,1-57,1 | 65,2 |
| | 60 | VIII | tacagacttgtcccttgtgtgtg | taagacccagatctaaggacgtg | 175 | 60,2 | 63,0 |
| | 61 | IX | gctgttactctcactcggcttt | ctcacgagagaagacagacaagg | 214 | 61,0 | 66,3 |
| | 62 | X | ctttccctttttggcaggtg | aaaatgtcatccccaaagagttc | 327 | 57,0 | 63,5 |

**TABLE A.3. List of the primers and analysis settings for dHPLC study**

*Abbreviations: Amplicon (A)*

*List of primer sequences, size of the amplified products, annealing temperature in PCR and dHPLC melting temperature.*

| Gene | NCBI ref seq (NM) | TaqMan® Assay ID_ |
|---|---|---|
| **mSIRT1** | All | Mm00490758 |
| **mSIRT2** | NM_022432.4*<br>NM_001122765.1 | Mm00452114 |
| **mSIRT3** | All | Mm00452129 |
| **mSIRT4** | All | Mm01201915 |
| **mSIRT5** | All | Mm00663721 |
| **mSIRT6** | NM_181586.3 | Mm00725029 |
| **mSIRT7** | All | Mm00461895 |
| **mβ-ACTIN** | NM_007393.1 | 4352933E |
| **mBDNF** | All | Mm04230607 |
| **hSIRT1** | All | Hs01009006 |
| **hβ-ACTIN** | NM_001101.2 | 4333762T |

**TABLE A.4. RT-PCR TaqMan® gene expression assays**

*Abbreviations: m, murine; h, human. NCBI reference sequences are listed in table A.2.*

# PAGE NUMBERING AS ORIGINAL

# *BIBLIOGRAPHY*


Abbott, R. D., White, L. R., Ross, G. W., Masaki, K. H., Curb, J. D., and Petrovitch, H. (2004). Walking and dementia in physically capable elderly men. JAMA 292, 1447–1453.

Adlard, P. A., Perreau, V. M., Pop, V., and Cotman, C. W. (2005). Voluntary exercise decreases amyloid load in a transgenic model of Alzheimer's disease. J Neurosci 25, 4217–4221.

Aggarwal, B. B., and Shishodia, S. (2006). Molecular targets of dietary agents for prevention and therapy of cancer. Biochem Pharmacol 71, 1397–1421.

Ahn, J. S., Lee, J.-H., Kim, J.-H., and Paik, S. R. (2007). Novel method for quantitative determination of amyloid fibrils of alpha-synuclein and amyloid beta/A4 protein by using resveratrol. Anal Biochem 367, 259–265.

Ahuja, N., Schwer, B., Carobbio, S., Waltregny, D., North, B. J., Castronovo, V., Maechler, P., and Verdin, E. (2007). Regulation of insulin secretion by SIRT4, a mitochondrial ADP-ribosyltransferase. J Biol Chem 282, 33583–33592.

Alcendor, R. R., Gao, S., Zhai, P., Zablocki, D., Holle, E., Yu, X., Tian, B., Wagner, T., Vatner, S. F., and Sadoshima, J. (2007). Sirt1 regulates aging and resistance to oxidative stress in the heart. Circ Res 100, 1512–1521.

Alhazzazi, T. Y., Kamarajan, P., Verdin, E., and Kapila, Y. L. (2011). SIRT3 and cancer: Tumor promoter or suppressor? BBA 1816, 80–88.

Alonso, A., Zaidi, T., Novak, M., Grundke-Iqbal, I., and Iqbal, K. (2001). Hyperphosphorylation induces self-assembly of tau into tangles of paired helical filaments/straight filaments. PNAS 98, 6923–6928.

Aluise, C. D., Sowell, R. A., and Butterfield, D. A. (2008). Peptides and proteins in plasma and cerebrospinal fluid as biomarkers for the prediction, diagnosis, and monitoring of therapeutic efficacy of Alzheimer's disease. BBA 1782, 549–558.

Alzheimer's Disease International (2009). World Alzheimer Report 2009 (London).

Ames, D. J., Bhathal, P. S., Davies, B. M., and Fraser, J. R. (1988). Hepatotoxicity of tetrahydroaminoacridine. Lancet 1, 887.

Anekonda, T. S. (2006). Resveratrol--a boon for treating Alzheimer's disease? Brain Res Rev 52, 316–326.

Anstey, K. J., Lipnicki, D. M., and Low, L.-F. (2008). Cholesterol as a risk factor for dementia and cognitive decline: a systematic review of prospective studies with meta-analysis. Am J Geriatr Psychiatry 16, 343–354.

Anstey, K. J., Mack, H. A., and Cherbuin, N. (2009). Alcohol consumption as a risk factor for dementia and cognitive decline: meta-analysis of prospective studies. Am J Geriatr Psychiatry 17, 542–555.

Araki, T., Sasaki, Y., and Milbrandt, J. (2004). Increased nuclear NAD biosynthesis and SIRT1 activation prevent axonal degeneration. Science 305, 1010–1013.

Arendash, G. W., Garcia, M. F., Costa, D. A., Cracchiolo, J. R., Wefes, I. M., and Potter, H. (2004). Environmental enrichment improves cognition in aged Alzheimer's transgenic mice despite stable beta-amyloid deposition. Neuroreport 15, 1751–1754.

Areosa, S. A., Sherriff, F., and McShane, R. (2005). Memantine for dementia. Cochrane Database Syst Rev (Online), CD003154.

Axelsen, P. H., Komatsu, H., and Murray, I. V. J. (2011). Oxidative stress and cell membranes in the pathogenesis of Alzheimer's disease. Physiology 26, 54–69.

Balducci, C., Tonini, R., Zianni, E., Nazzaro, C., Fiordaliso, F., Salio, M., Vismara, L., Gardoni, F., Di Luca, M., Carli, M., et al. (2010). Cognitive deficits associated with alteration of synaptic metaplasticity precede plaque deposition in AβPP23 transgenic mice. JAD 21, 1367–1381.

Ballatore, C., Lee, V. M.-Y., and Trojanowski, J. Q. (2007). Tau-mediated neurodegeneration in Alzheimer's disease and related disorders. Nat Rev Neurosci 8, 663–672.

Bao, J., Scott, I., Lu, Z., Pang, L., Dimond, C. C., Gius, D., and Sack, M. N. (2010). SIRT3 is regulated by nutrient excess and modulates hepatic susceptibility to lipotoxicity. Free Rad Biol Med 49, 1230–1237.

Barger, J. L., Kayo, T., Vann, J. M., Arias, E. B., Wang, J., Hacker, T. A., Wang, Y., Raederstorff, D., Morrow, J. D., Leeuwenburgh, C., et al. (2008). A low dose of dietary resveratrol partially mimics caloric restriction and retards aging parameters in mice. PLoS One 3, e2264.

Barker, W. W., Luis, C. A., Kashuba, A., Luis, M., Harwood, D. G., Loewenstein, D., Waters, C., Jimison, P., Shepherd, E., Sevush, S., et al. (2002). Relative frequencies of Alzheimer disease, Lewy body, vascular and frontotemporal dementia, and hippocampal sclerosis in the State of Florida Brain Bank. ADAD 16, 203–212.

Bartus, R. T., Dean, R. L., Beer, B., and Lippa, A. S. (1982). The cholinergic hypothesis of geriatric memory dysfunction. Science 217, 408–414.

Baur, J. A. (2010). Resveratrol, sirtuins, and the promise of a DR mimetic. Mech Ageing Dev 131, 261–269.

Baur, J. A., Pearson, K. J., Price, N. L., Jamieson, H. A., Lerin, C., Kalra, A., Prabhu, V. V., Allard, J. S., Lopez-Lluch, G., Lewis, K., et al. (2006). Resveratrol improves health and survival of mice on a high-calorie diet. Nature 444, 337–342.

Beal, M. F. (1998). Mitochondrial dysfunction in neurodegenerative diseases. BBA 1366, 211–223.

Behl, C., Davis, J. B., Lesley, R., and Schubert, D. (1994). Hydrogen peroxide mediates amyloid beta protein toxicity. Cell 77, 817–827.

Bellizzi, D., Rose, G., Cavalcante, P., Covello, G., Dato, S., De Rango, F., Greco, V., Maggiolini, M., Feraco, E., Mari, V., et al. (2005). A novel VNTR enhancer within the SIRT3 gene, a human homologue of SIR2, is associated with survival at oldest ages. Genomics 85, 258–263.

Belostotsky, R., Ben-Shalom, E., Rinat, C., Becker-Cohen, R., Feinstein, S., Zeligson, S., Segel, R., Elpeleg, O., Nassar, S., and Frishberg, Y. (2011). Mutations in the mitochondrial seryl-tRNA synthetase cause hyperuricemia, pulmonary hypertension, renal failure in infancy and alkalosis, HUPRA syndrome. Am J Hum Genet 88, 193–200.

Benigni, A., Corna, D., Zoja, C., Sonzogni, A., Latini, R., Salio, M., Conti, S., Rottoli, D., Longaretti, L., Cassis, P., et al. (2009). Disruption of the Ang II type 1 receptor promotes longevity in mice. J Clin Invest 119, 524–530.

Berardi, N., Braschi, C., Capsoni, S., Cattaneo, A., and Maffei, L. (2007). Environmental enrichment delays the onset of memory deficits and reduces neuropathological hallmarks in a mouse model of Alzheimer-like neurodegeneration. JAD 11, 359–370.

Bertram, L. (2011). Alzheimer's genetics in the GWAS era: a continuing story of "replications and refutations". Curr Neurol Neurosci Rep 11, 246–253.

Bertram, L., Blacker, D., Mullin, K., Keeney, D., Jones, J., Basu, S., Yhu, S., McInnis, M. G., Go, R. C., Vekrellis, K., et al. (2000). Evidence for genetic linkage of Alzheimer's disease to chromosome 10q. Science 290, 2302–2303.

Bertram, L., Lill, C. M., and Tanzi, R. E. (2010). The genetics of Alzheimer disease: back to the future. Neuron 68, 270–281.

Beydoun, M. A., Beydoun, H. A., and Wang, Y. (2008). Obesity and central obesity as risk factors for incident dementia and its subtypes: a systematic review and meta-analysis. Obesity Rev 9, 204–218.

Blander, G., and Guarente, L. (2004). The Sir2 family of protein deacetylases. Annu Rev Biochem 73, 417–435.

Blennow, K., de Leon, M. J., and Zetterberg, H. (2006). Alzheimer's disease. Lancet 368, 387–403.

Blum, C. A., Ellis, J. L., Loh, C., Ng, P. Y., Perni, R. B., and Stein, R. L. (2010). SIRT1 Modulation as a Novel Approach to the Treatment of Diseases of Aging. J Med Chem 54, 417-32.

Bordone, L., Cohen, D., Robinson, A., Motta, M. C., van Veen, E., Czopik, A., Steele, A. D., Crowe, H., Marmor, S., Luo, J., et al. (2007). SIRT1 transgenic mice show phenotypes resembling calorie restriction. Aging cell 6, 759–767.

Bordone, L., Motta, M. C., Picard, F., Robinson, A., Jhala, U. S., Apfeld, J., McDonagh, T., Lemieux, M., McBurney, M., Szilvasi, A., et al. (2006). Sirt1 regulates insulin secretion by repressing UCP2 in pancreatic beta cells. PLoS Biol 4, e31.

Brachmann, C. B., Sherman, J. M., Devine, S. E., Cameron, E. E., Pillus, L., and Boeke, J. D. (1995). The SIR2 gene family, conserved from bacteria to humans, functions in silencing, cell cycle progression, and chromosome stability. Genes Dev 9, 2888–2902.

Bradamante S, Barenghi L, V. A. (2004). Cardiovascular protective effects of resveratrol. Cardiovasc Drug Rev 22, 169–188.

Bryk, M., Banerjee, M., Murphy, M., Knudsen, K. E., Garfinkel, D. J., and Curcio, M. J. (1997). Transcriptional silencing of Ty1 elements in the RDN1 locus of yeast. Genes Dev 11, 255–269.

Carlson, M. C., Helms, M. J., Steffens, D. C., Burke, J. R., Potter, G. G., and Plassman, B. L. (2008). Midlife activity predicts risk of dementia in older male twin pairs. Alzheimer's & dementia 4, 324–331.

Catlow, B. J., Rowe, A. R., Clearwater, C. R., Mamcarz, M., Arendash, G. W., and Sanchez-Ramos, J. (2009). Effects of environmental enrichment and physical activity on neurogenesis in transgenic PS1/APP mice. Brain Res 1256, 173–179.

Chen, D., Bruno, J., Easlon, E., Lin, S.-J., Cheng, H.-L., Alt, F. W., and Guarente, L. (2008). Tissue-specific regulation of SIRT1 by calorie restriction. Genes Dev 22, 1753–1757.

Chen, D., Steele, A. D., Lindquist, S., and Guarente, L. (2005a). Increase in activity during calorie restriction requires Sirt1. Science 310, 1641.

Chen, J., Zhou, Y., Mueller-Steiner, S., Chen, L.-F., Kwon, H., Yi, S., Mucke, L., and Gan, L. (2005b). SIRT1 protects against microglia-dependent amyloid-beta toxicity through inhibiting NF-kappaB signaling. J Biol Chem 280, 40364–40374.

Chinn, S. (2000). A simple method for converting an odds ratio to effect size for use in meta-analysis. Stat Med 19, 3127–3131.

Choi, S. H., Veeraraghavalu, K., Lazarov, O., Marler, S., Ransohoff, R. M., Ramirez, J. M., and Sisodia, S. S. (2008). Non-cell-autonomous effects of presenilin 1 variants on enrichment-mediated hippocampal progenitor cell proliferation and differentiation. Neuron 59, 568–580.

Chong, Z. Z., and Maiese, K. (2008). Enhanced tolerance against early and late apoptotic oxidative stress in mammalian neurons through nicotinamidase and sirtuin mediated pathways. Curr Neurovasc Res 5, 159–170.

Cimen, H., Han, M.-J., Yang, Y., Tong, Q., Koc, H., and Koc, E. C. (2010). Regulation of succinate dehydrogenase activity by SIRT3 in mammalian mitochondria. Biochemistry 49, 304–311.

Citron, M., Oltersdorf, T., Haass, C., McConlogue, L., Hung, A. Y., Seubert, P., Vigo-Pelfrey, C., Lieberburg, I., and Selkoe, D. J. (1992). Mutation of the beta-amyloid precursor protein in familial Alzheimer's disease increases beta-protein production. Nature 360, 672–674.

Cole, G. M., Lim, G. P., Yang, F., Teter, B., Begum, A., Ma, Q., Harris-White, M. E., and Frautschy, S. A. (2005). Prevention of Alzheimer's disease: Omega-3 fatty acid and phenolic anti-oxidant interventions. Neurobiol Aging 26 Suppl 1, 133–136.

Colman, R. J., Anderson, R. M., Johnson, S. C., Kastman, E. K., Kosmatka, K. J., Beasley, T. M., Allison, D. B., Cruzen, C., Simmons, H. A., Kemnitz, J. W., et al. (2009). Caloric restriction delays disease onset and mortality in rhesus monkeys. Science 325, 201–204.

Corder, E. H., Saunders, A. M., Strittmatter, W. J., Schmechel, D. E., Gaskell, P. C., Small, G. W., Roses, A. D., Haines, J. L., and Pericak-Vance, M. A. (1993). Gene dose of apolipoprotein E type 4 allele and the risk of Alzheimer's disease in late onset families. Science 261, 921–923.

Costa, D. A., Cracchiolo, J. R., Bachstetter, A. D., Hughes, T. F., Bales, K. R., Paul, S. M., Mervis, R. F., Arendash, G. W., and Potter, H. (2007). Enrichment improves cognition in AD mice by amyloid-related and unrelated mechanisms. Neurobiol Aging 28, 831–844.

Cotel, M.-C., Jawhar, S., Christensen, D. Z., Bayer, T. A., and Wirths, O. (2010). Environmental enrichment fails to rescue working memory deficits, neuron loss, and neurogenesis in APP/PS1KI mice. Neurobiol Aging 285, 41517-24

Coyle, J. T., Price, D. L., and DeLong, M. R. (1983). Alzheimer's disease: a disorder of cortical cholinergic innervation. Science 219, 1184–1190.

Cracchiolo, J. R., Mori, T., Nazian, S. J., Tan, J., Potter, H., and Arendash, G. W. (2007). Enhanced cognitive activity--over and above social or physical activity--is required to protect Alzheimer's mice against cognitive impairment, reduce Abeta deposition, and increase synaptic immunoreactivity. Neurobiol Learn Mem 88, 277–294.

Crowe, M., Andel, R., Pedersen, N. L., Johansson, B., and Gatz, M. (2003). Does participation in leisure activities lead to reduced risk of Alzheimer's disease? A prospective study of Swedish twins. J gerontol 58, P249–P255.

Dai, Q., Borenstein, A. R., Wu, Y., Jackson, J. C., and Larson, E. B. (2006). Fruit and vegetable juices and Alzheimer's disease: the Kame Project. AM J Med 119, 751–759.

Van Dam, D., D'Hooge, R., Staufenbiel, M., Van Ginneken, C., Van Meir, F., and De Deyn, P. P. (2003). Age-dependent cognitive decline in the APP23 model precedes amyloid deposition. Eur J Neurosci 17, 388–396.

Delabar, J. M., Goldgaber, D., Lamour, Y., Nicole, A., Huret, J. L., de Grouchy, J., Brown, P., Gajdusek, D. C., and Sinet, P. M. (1987). Beta amyloid gene duplication in Alzheimer's disease and karyotypically normal Down syndrome. Science 235, 1390–1392.

Dirks, A. J., and Leeuwenburgh, C. (2006). Caloric restriction in humans: potential pitfalls and health concerns. Mech Ageing Dev 127, 1–7.

Donmez, G., Wang, D., Cohen, D. E., and Guarente, L. (2010). SIRT1 Suppresses β-Amyloid Production by Activating the α-Secretase Gene ADAM10. Cell 142, 320–332.

Dryden, S. C., Nahhas, F. A., Nowak, J. E., Goustin, A.-S., and Tainsky, M. A. (2003). Role for human SIRT2 NAD-dependent deacetylase activity in control of mitotic exit in the cell cycle. MCB 23, 3173–3185.

Dubois, B., Feldman, H. H., Jacova, C., DeKosky, S. T., Barberger-Gateau, P., Cummings, J., Delacourte, A., Galasko, D., Gauthier, S., and Jicha, G. (2007). Research criteria for the diagnosis of Alzheimer's disease: revising the NINCDS–ADRDA criteria. Lancet Neurol 6, 734–746.

Duff, K., Kuret, J., and Congdon, E. E. (2010). Disaggregation of tau as a therapeutic approach to tauopathies. Curr Alzheimer Res 7, 235–240.

Essick, E. E., and Sam, F. (2010). Oxidative stress and autophagy in cardiac disease, neurological disorders, aging and cancer. Oxid Med Cell Longev 3, 168–177.

Fabrizio, P., Gattazzo, C., Battistella, L., Wei, M., Cheng, C., McGrew, K., and Longo, V. D. (2005). Sir2 blocks extreme life-span extension. Cell 123, 655–667.

Fan, W., and Luo, J. (2010). SIRT1 regulates UV-induced DNA repair through deacetylating XPA. Mol Cell 39, 247–258.

Farlow, M. R., He, Y., Tekin, S., Xu, J., Lane, R., and Charles, H. C. (2004). Impact of APOE in mild cognitive impairment. Neurology 63, 1898–1901.

Feige, J. N., Lagouge, M., Canto, C., Strehle, A., Houten, S. M., Milne, J. C., Lambert, P. D., Mataki, C., Elliott, P. J., and Auwerx, J. (2008). Specific SIRT1 activation mimics low energy levels and protects against diet-induced metabolic disorders by enhancing fat oxidation. Cell Metab 8, 347–358.

Fernández, J. A., Rojo, L., Kuljis, R. O., and Maccioni, R. B. (2008). The damage signals hypothesis of Alzheimer's disease pathogenesis. JAD 14, 329–333.

Ferrara, N., Rinaldi, B., Corbi, G., Conti, V., Stiuso, P., Boccuti, S., Rengo, G., Rossi, F., and Filippelli, A. (2008). Exercise training promotes SIRT1 activity in aged rats. Rejuvenation Res 11, 139–150.

Ferreira, S. T., Vieira, M. N. N., and De Felice, F. G. (2007). Soluble protein oligomers as emerging toxins in Alzheimer's and other amyloid diseases. IUBMB 59, 332–345.

Ferri, C. P., Prince, M., Brayne, C., Brodaty, H., Fratiglioni, L., Ganguli, M., Hall, K., Hasegawa, K., Hendrie, H., and Huang, Y. (2006). Global prevalence of dementia: a Delphi consensus study. Lancet 366, 2112–2117.

Ferrington, L., Miners, J. S., Palmer, L. E., Bond, S. M., Povey, J. E., Kelly, P. A., Love, S., Horsburgh, K. J., and Kehoe, P. G. (2011). Angiotensin II-inhibiting drugs have no effect on intraneuronal Aβ or oligomeric Aβ levels in a triple transgenic mouse model of Alzheimer's disease. Am J Transl Res 3, 197–208.

Fontana, L., Partridge, L., and Longo, V. D. (2010). Extending healthy life span--from yeast to humans. Science 328, 321–326.

Ford, E., Voit, R., Liszt, G., Magin, C., Grummt, I., and Guarente, L. (2006). Mammalian Sir2 homolog SIRT7 is an activator of RNA polymerase I transcription. Genes Dev 20, 1075–1080.

Fotuhi, M., Mohassel, P., and Yaffe, K. (2009). Fish consumption, long-chain omega-3 fatty acids and risk of cognitive decline or Alzheimer disease: a complex association. Nature clinical practice. Neurology 5, 140–152.

Frankel, E. N., Waterhouse, A. L., and Kinsella, J. E. (1993). Inhibition of human LDL oxidation by resveratrol. Lancet 341, 1103–1104.

Fratiglioni, L., Paillard-Borg, S., and Winblad, B. (2004). An active and socially integrated lifestyle in late life might protect against dementia. Lancet Neurol 3, 343–353.

Fratiglioni, L., and Wang, H.-X. (2007). Brain reserve hypothesis in dementia. JAD 12, 11–22.

Frescas, D., Valenti, L., and Accili, D. (2005). Nuclear trapping of the forkhead transcription factor FoxO1 via Sirt-dependent deacetylation promotes expression of glucogenetic genes. J Biol Chem 280, 20589–20595.

Friedland, R. P., Fritsch, T., Smyth, K. A., Koss, E., Lerner, A. J., Chen, C. H., Petot, G. J., and Debanne, S. M. (2001). Patients with Alzheimer's disease have reduced activities in midlife compared with healthy control-group members. PNAS 98, 3440–3445.

Frye, R. A. (2000). Phylogenetic classification of prokaryotic and eukaryotic Sir2-like proteins. Biochem Biophys Res Comm 273, 793–798.

Féart, C., Samieri, C., Rondeau, V., Amieva, H., Portet, F., Dartigues, J.-F., Scarmeas, N., and Barberger-Gateau, P. (2009). Adherence to a Mediterranean diet, cognitive decline, and risk of dementia. JAMA 302, 638–648.

Gatz, M., Reynolds, C. A., Fratiglioni, L., Johansson, B., Mortimer, J. A., Berg, S., Fiske, A., and Pedersen, N. L. (2006). Role of genes and environments for explaining Alzheimer disease. Arch Gen Psychiatry 63, 168–174.

Gerhart-Hines, Z., Rodgers, J. T., Bare, O., Lerin, C., Kim, S.-H., Mostoslavsky, R., Alt, F. W., Wu, Z., and Puigserver, P. (2007). Metabolic control of muscle mitochondrial function and fatty acid oxidation through SIRT1/PGC-1alpha. EMBO J 26, 1913–1923.

Geula, C. (1998). Abnormalities of neural circuitry in Alzheimer's disease: hippocampus and cortical cholinergic innervation. Neurology 51, 18–29

Ghoshal, N., García-Sierra, F., Wuu, J., Leurgans, S., Bennett, D. A., Berry, R. W., and Binder, L. I. (2002). Tau conformational changes correspond to impairments of episodic memory in mild cognitive impairment and Alzheimer's disease. Exp Neurol 177, 475–493.

Glass, C. K., Saijo, K., Winner, B., Marchetto, M. C., and Gage, F. H. (2010). Mechanisms underlying inflammation in neurodegeneration. Cell 140, 918–934.

Glenner, G. G., and Wong, C. W. (1984). Alzheimer's disease: initial report of the purification and characterization of a novel cerebrovascular amyloid protein. Biochem Biophys Res Comm 120, 885–890.

Goate, A., Chartier-Harlin, M. C., Mullan, M., Brown, J., Crawford, F., Fidani, L., Giuffra, L., Haynes, A., Irving, N., and James, L. (1991). Segregation of a missense mutation in the amyloid precursor protein gene with familial Alzheimer's disease. Nature 349, 704–706.

Gong, C.-X., and Iqbal, K. (2008). Hyperphosphorylation of microtubule-associated protein tau: a promising therapeutic target for Alzheimer disease. Curr Med Chem 15, 2321–2328.

Gottschling, D. E., Aparicio, O. M., Billington, B. L., and Zakian, V. A. (1990). Position effect at S. cerevisiae telomeres: reversible repression of Pol II transcription. Cell 63, 751–762.

Granzotto, A., and Zatta, P. (2011). Resveratrol Acts Not through Anti-Aggregative Pathways but Mainly via Its Scavenging Properties against Aβ and Aβ-Metal Complexes Toxicity. PLoS One 6, e21565.

Green, R. C., Cupples, L. A., Go, R., Benke, K. S., Edeki, T., Griffith, P. A., Williams, M., Hipps, Y., Graff-Radford, N., Bachman, D., et al. (2002). Risk of dementia among

white and African American relatives of patients with Alzheimer disease. JAMA 287, 329–336.

Grob, A., Roussel, P., Wright, J. E., McStay, B., Hernandez-Verdun, D., and Sirri, V. (2009). Involvement of SIRT7 in resumption of rDNA transcription at the exit from mitosis. J Cell Sci 122, 489–498.

Grundke-Iqbal, I., Iqbal, K., Tung, Y. C., Quinlan, M., Wisniewski, H. M., and Binder, L. I. (1986). Abnormal phosphorylation of the microtubule-associated protein tau (tau) in Alzheimer cytoskeletal pathology. PNAS 83, 4913–4917.

Görtz, N., Lewejohann, L., Tomm, M., Ambrée, O., Keyvani, K., Paulus, W., and Sachser, N. (2008). Effects of environmental enrichment on exploration, anxiety, and memory in female TgCRND8 Alzheimer mice. Behav Brain Res 191, 43–48.

Götz, J., and Ittner, L. M. (2008). Animal models of Alzheimer's disease and frontotemporal dementia. Nat Rev Neurosci 9, 532–544.

Haass, C., Hung, A. Y., Selkoe, D. J., and Teplow, D. B. (1994). Mutations associated with a locus for familial Alzheimer's disease result in alternative processing of amyloid beta-protein precursor. J Biol Chem 269, 17741–17748.

Haigis, M. C., Mostoslavsky, R., Haigis, K. M., Fahie, K., Christodoulou, D. C., Murphy, A. J., Valenzuela, D. M., Yancopoulos, G. D., Karow, M., Blander, G., et al. (2006). SIRT4 inhibits glutamate dehydrogenase and opposes the effects of calorie restriction in pancreatic beta cells. Cell 126, 941–954.

Haigis, M. C., and Sinclair, D. A. (2010). Mammalian sirtuins: biological insights and disease relevance. Annu Rev Pathol 5, 253–295.

Hamer, M., and Chida, Y. (2009). Physical activity and risk of neurodegenerative disease: a systematic review of prospective evidence. Psychol Med 39, 3–11.

Han, M.-K., Song, E.-K., Guo, Y., Ou, X., Mantel, C., and Broxmeyer, H. E. (2008). SIRT1 regulates apoptosis and Nanog expression in mouse embryonic stem cells by controlling p53 subcellular localization. Cell Stem Cell 2, 241–251.

Hardy, J., and Selkoe, D. J. (2002). The amyloid hypothesis of Alzheimer's disease: progress and problems on the road to therapeutics. Science 297, 353–356.

Helisalmi, S., Vepsäläinen, S., Hiltunen, M., Koivisto, A. M., Salminen, A., Laakso, M., and Soininen, H. (2008). Genetic study between SIRT1, PPARD, PGC-1alpha genes and Alzheimer's disease. J Neurol 255, 668–673.

Heneka, M. T., and O'Banion, M. K. (2007). Inflammatory processes in Alzheimer's disease. J Neuroimmunol 184, 69–91.

Hernick, M., and Fierke, C. A. (2005). Zinc hydrolases: the mechanisms of zinc-dependent deacetylases. ABB 433, 71–84.

Herring, A., Ambrée, O., Tomm, M., Habermann, H., Sachser, N., Paulus, W., and Keyvani, K. (2009). Environmental enrichment enhances cellular plasticity in transgenic mice with Alzheimer-like pathology. Exp Neurol 216, 184–192.

Herring, A., Yasin, H., Ambrée, O., Sachser, N., Paulus, W., and Keyvani, K. (2008). Environmental enrichment counteracts Alzheimer's neurovascular dysfunction in TgCRND8 mice. Brain Pathol 18, 32–39.

Herrup, K. (2010). Reimagining Alzheimer's Disease--An Age-Based Hypothesis. J Neurosci 30, 16755–16762.

Hirschey, M. D., Shimazu, T., Goetzman, E., Jing, E., Schwer, B., Lombard, D. B., Grueter, C. A., Harris, C., Biddinger, S., Ilkayeva, O. R., et al. (2010). SIRT3 regulates mitochondrial fatty-acid oxidation by reversible enzyme deacetylation. Nature 464, 121–125.

Hollingworth, P., Harold, D., Sims, R., Gerrish, A., Lambert, J.-C., Carrasquillo, M. M., Abraham, R., Hamshere, M. L., Pahwa, J. S., Moskvina, V., et al. (2011). Common variants at ABCA7, MS4A6A/MS4A4E, EPHA1, CD33 and CD2AP are associated with Alzheimer's disease. Nat Genet 43, 429–435.

Holtzman, D. M., Morris, J. C., and Goate, A. M. (2011). Alzheimer's disease: the challenge of the second century. Sci Transl Med 3, 77sr1.

Howitz, K. T., Bitterman, K. J., Cohen, H. Y., Lamming, D. W., Lavu, S., Wood, J. G., Zipkin, R. E., Chung, P., Kisielewski, A., Zhang, L.-L., et al. (2003). Small molecule activators of sirtuins extend Saccharomyces cerevisiae lifespan. Nature 425, 191–196.

Hu, Y., Liu, J., Wang, J., and Liu, Q. (2011). The controversial links among calorie restriction, SIRT1, and resveratrol. Free Rad Biol Med.

Hu, Y.-S., Xu, P., Pigino, G., Brady, S. T., Larson, J., and Lazarov, O. (2010). Complex environment experience rescues impaired neurogenesis, enhances synaptic plasticity, and attenuates neuropathology in familial Alzheimer's disease-linked APPswe/PS1DeltaE9 mice. FASEB J 24, 1667–1681.

Hynd, M. R., Scott, H. L., and Dodd, P. R. (2004). Glutamate-mediated excitotoxicity and neurodegeneration in Alzheimer's disease. Neurochem Int 45, 583–595.

Iqbal, K., Alonso, A. del C., Chen, S., Chohan, M. O., El-Akkad, E., Gong, C.-X., Khatoon, S., Li, B., Liu, F., Rahman, A., et al. (2005). Tau pathology in Alzheimer disease and other tauopathies. BBA 1739, 198–210.

Iqbal, K., Grundke-Iqbal, I., Zaidi, T., Merz, P. A., Wen, G. Y., Shaikh, S. S., Wisniewski, H. M., Alafuzoff, I., and Winblad, B. (1986). Defective brain microtubule assembly in Alzheimer's disease. Lancet 2, 421–426.

Iqbal, K., Liu, F., Gong, C.-X., Alonso, A. D. C., and Grundke-Iqbal, I. (2009). Mechanisms of tau-induced neurodegeneration. Acta Neuropathol 118, 53–69.

Iqbal, K., Liu, F., Gong, C.-X., and Grundke-Iqbal, I. (2010). Tau in Alzheimer disease and related tauopathies. Curr Alzheimer Res 7, 656–664.

Isik, A. T. (2010). Late onset Alzheimer's disease in older people. J Clin Inter Aging 5, 307–311.

Jang, M. H., Piao, X. L., Kim, H. Y., Cho, E. J., Baek, S. H., Kwon, S. W., and Park, J. H. (2007). Resveratrol oligomers from Vitis amurensis attenuate beta-amyloid-induced oxidative stress in PC12 cells. BPB 30, 1130–1134.

Jankowsky, J. L., Xu, G., Fromholt, D., Gonzales, V., and Borchelt, D. R. (2003). Environmental enrichment exacerbates amyloid plaque formation in a transgenic mouse model of Alzheimer disease. J Neuropathol Exp Neurol 62, 1220–1227.

Jellinger, K. A. (2008). The pathology of "vascular dementia": a critical update. JAD 14, 107–123.

Jeong, J., Juhn, K., Lee, H., Kim, S.-H., Min, B.-H., Lee, K.-M., Cho, M.-H., Park, G.-H., and Lee, K.-H. (2007). SIRT1 promotes DNA repair activity and deacetylation of Ku70. Exp Mol Med 39, 8–13.

Jing, E., Gesta, S., and Kahn, C. R. (2007). SIRT2 regulates adipocyte differentiation through FoxO1 acetylation/deacetylation. Cell Metab 6, 105–114.

Julien, C., Tremblay, C., Emond, V., Lebbadi, M., Salem, N., Bennett, D. A., and Calon, F. (2009). Sirtuin 1 reduction parallels the accumulation of tau in Alzheimer disease. J Neuropathol Exp Neurol 68, 48–58.

Kabeya, Y., Mizushima, N., Ueno, T., Yamamoto, A., Kirisako, T., Noda, T., Kominami, E., Ohsumi, Y., and Yoshimori, T. (2000). LC3, a mammalian homologue of yeast Apg8p, is localized in autophagosome membranes after processing. EMBO J 19, 5720–5728.

Kaeberlein, M., McVey, M., and Guarente, L. (1999). The SIR2/3/4 complex and SIR2 alone promote longevity in Saccharomyces cerevisiae by two different mechanisms. Genes Dev 13, 2570–2580.

Kanfi, Y., Peshti, V., Gil, R., Naiman, S., Nahum, L., Levin, E., Kronfeld-Schor, N., and Cohen, H. Y. (2010). SIRT6 protects against pathological damage caused by diet-induced obesity. Aging cell 9, 162–173.

Kang, J., Lemaire, H. G., Unterbeck, A., Salbaum, J. M., Masters, C. L., Grzeschik, K. H., Multhaup, G., Beyreuther, K., and Müller-Hill, B. (1987). The precursor of Alzheimer's disease amyloid A4 protein resembles a cell-surface receptor. Nature 325, 733–736.

Kawahara, T. L. A., Michishita, E., Adler, A. S., Damian, M., Berber, E., Lin, M., McCord, R. A., Ongaigui, K. C. L., Boxer, L. D., Chang, H. Y., et al. (2009). SIRT6 links histone H3 lysine 9 deacetylation to NF-kappaB-dependent gene expression and organismal life span. Cell 136, 62–74.

Kayed, R., Head, E., Thompson, J. L., McIntire, T. M., Milton, S. C., Cotman, C. W., and Glabe, C. G. (2003). Common structure of soluble amyloid oligomers implies common mechanism of pathogenesis. Science 300, 486–489.

Keating, D. J. (2008). Mitochondrial dysfunction, oxidative stress, regulation of exocytosis and their relevance to neurodegenerative diseases. J Nerochem 104, 298–305.

Kehoe, P. G., Miners, S., and Love, S. (2009). Angiotensins in Alzheimer's disease - friend or foe? TINS 32, 619–628.

Kelly, G. (2010). A review of the sirtuin system, its clinical implications, and the potential role of dietary activators like resveratrol: part 1. Alt Med Rev 15, 245–263.

Kemper, J. K., Xiao, Z., Ponugoti, B., Miao, J., Fang, S., Kanamaluru, D., Tsang, S., Wu, S.-Y., Chiang, C.-M., and Veenstra, T. D. (2009). FXR acetylation is normally dynamically regulated by p300 and SIRT1 but constitutively elevated in metabolic disease states. Cell Metab 10, 392–404.

Kim, D., Nguyen, M. D., Dobbin, M. M., Fischer, A., Sananbenesi, F., Rodgers, J. T., Delalle, I., Baur, J. A., Sui, G., Armour, S. M., et al. (2007). SIRT1 deacetylase protects against neurodegeneration in models for Alzheimer's disease and amyotrophic lateral sclerosis. EMBO J 26, 3169–3179.

Kim, H.-S., Xiao, C., Wang, R.-H., Lahusen, T., Xu, X., Vassilopoulos, A., Vazquez-Ortiz, G., Jeong, W.-I., Park, O., Ki, S. H., et al. (2010). Hepatic-Specific Disruption of SIRT6 in Mice Results in Fatty Liver Formation Due to Enhanced Glycolysis and Triglyceride Synthesis. Cell Metab 12, 224–236.

Kim, J.-M., Stewart, R., Kim, S.-W., Shin, I.-S., Yang, S.-J., Shin, H.-Y., and Yoon, J.-S. (2008). Changes in folate, vitamin B12 and homocysteine associated with incident dementia. J Neurol Neurosurg Psychiatry 79, 864–868.

Kim, W., and Hecht, M. H. (2005). Sequence determinants of enhanced amyloidogenicity of Alzheimer A{beta}42 peptide relative to A{beta}40. J Biol Chem 280, 35069–35076.

Klar, A. J., Fogel, S., and Macleod, K. (1979). MAR1-a Regulator of the HMa and HMalpha Loci in Saccharomyces cerevisiae. Genetics 93, 37–50.

Kleim, J. A., Jones, T. A., and Schallert, T. (2003). Motor enrichment and the induction of plasticity before or after brain injury. Neurochem Res 28, 1757–1769.

Koltai, E., Szabo, Z., Atalay, M., Boldogh, I., Naito, H., Goto, S., Nyakas, C., and Radak, Z. (2010). Exercise alters SIRT1, SIRT6, NAD and NAMPT levels in skeletal muscle of aged rats. Mech Ageing Dev 131, 21–28.

Komar, A. A. (2007). Silent SNPs: impact on gene function and phenotype. Pharmacogenomics 8, 1075–1080.

Kong, X., Wang, R., Xue, Y., Liu, X., Zhang, H., Chen, Y., Fang, F., and Chang, Y. (2010). Sirtuin 3, a New Target of PGC-1alpha, Plays an Important Role in the Suppression of ROS and Mitochondrial Biogenesis. PLoS One 5, e11707.

Kosik, K. S., Joachim, C. L., and Selkoe, D. J. (1986). Microtubule-associated protein tau (tau) is a major antigenic component of paired helical filaments in Alzheimer disease. PNAS 83, 4044–4048.

Ku, C. S., Loy, E. Y., Pawitan, Y., and Chia, K. S. (2010). The pursuit of genome-wide association studies: where are we now? J Hum Genet 55, 195–206.

Kuningas, M., Putters, M., Westendorp, R. G. J., Slagboom, P. E., and van Heemst, D. (2007). SIRT1 gene, age-related diseases, and mortality: the Leiden 85-plus study. J Gerontol 62, 960–965.

Kurz, A., Altland, K., Lautenschlager, N., Zimmer, R., Busch, R., Gerundt, I., Lauter, H., and Müller, U. (1996). Apolipoprotein E type 4 allele and Alzheimer's disease: effect on age at onset and relative risk in different age groups. J Neurol 243, 452–456.

Köpke, E., Tung, Y. C., Shaikh, S., Alonso, A. C., Iqbal, K., and Grundke-Iqbal, I. (1993). Microtubule-associated protein tau. Abnormal phosphorylation of a non-paired helical filament pool in Alzheimer disease. J Biol Chem 268, 24374–24384.

Ladiwala, A. R. A., Lin, J. C., Bale, S. S., Marcelino-Cruz, A. M., Bhattacharya, M., Dordick, J. S., and Tessier, P. M. (2010). Resveratrol selectively remodels soluble oligomers and fibrils of amyloid Abeta into off-pathway conformers. J Biol Chem 285, 24228–24237.

Lambert, M. P., Barlow, A. K., Chromy, B. A., Edwards, C., Freed, R., Liosatos, M., Morgan, T. E., Rozovsky, I., Trommer, B., Viola, K. L., et al. (1998). Diffusible, nonfibrillar ligands derived from Abeta1-42 are potent central nervous system neurotoxins. PNAS 95, 6448–6453.

Lanza, I. R., Short, D. K., Short, K. R., Raghavakaimal, S., Basu, R., Joyner, M. J., McConnell, J. P., and Nair, K. S. (2008). Endurance exercise as a countermeasure for aging. Diabetes 57, 2933–2942.

Lazarov, O., Robinson, J., Tang, Y.-P., Hairston, I. S., Korade-Mirnics, Z., Lee, V. M.-Y., Hersh, L. B., Sapolsky, R. M., Mirnics, K., and Sisodia, S. S. (2005). Environmental enrichment reduces Abeta levels and amyloid deposition in transgenic mice. Cell 120, 701–713.

Lee, I. H., Cao, L., Mostoslavsky, R., Lombard, D. B., Liu, J., Bruns, N. E., Tsokos, M., Alt, F. W., and Finkel, T. (2008). A role for the NAD-dependent deacetylase Sirt1 in the regulation of autophagy. PNAS 105, 3374–3379.

Lee, J.-H., Song, M.-Y., Song, E.-K., Kim, E.-K., Moon, W. S., Han, M.-K., Park, J.-W., Kwon, K.-B., and Park, B.-H. (2009). Overexpression of SIRT1 protects pancreatic beta-cells against cytokine toxicity by suppressing the nuclear factor-kappaB signaling pathway. Diabetes 58, 344–351.

Lee, V. M., Balin, B. J., Otvos, L., and Trojanowski, J. Q. (1991). A68: a major subunit of paired helical filaments and derivatized forms of normal Tau. Science 251, 675–678.

Lee, Y., Back, J. H., Kim, J., Kim, S.-H., Na, D. L., Cheong, H.-K., Hong, C. H., and Kim, Y. G. (2010). Systematic review of health behavioral risks and cognitive health in older adults. IPA 22, 174–187.

Levi, O., Jongen-Relo, A. L., Feldon, J., Roses, A. D., and Michaelson, D. M. (2003). ApoE4 impairs hippocampal plasticity isoform-specifically and blocks the environmental stimulation of synaptogenesis and memory. Neurobiol Dis 13, 273–282.

Levy, E., Carman, M. D., Fernandez-Madrid, I. J., Power, M. D., Lieberburg, I., van Duinen, S. G., Bots, G. T., Luyendijk, W., and Frangione, B. (1990). Mutation of the Alzheimer's disease amyloid gene in hereditary cerebral hemorrhage, Dutch type. Science 248, 1124–1126.

Levy-Lahad, E., Wasco, W., Poorkaj, P., Romano, D. M., Oshima, J., Pettingell, W. H., Yu, C. E., Jondro, P. D., Schmidt, S. D., and Wang, K. (1995). Candidate gene for the chromosome 1 familial Alzheimer's disease locus. Science 269, 973–977.

Li, F., and Tsien, J. Z. (2009). Memory and the NMDA receptors. N Engl J Med 361, 302–303.

Li, L., Zhang, X., Yang, D., Luo, G., Chen, S., and Le, W. (2009). Hypoxia increases Abeta generation by altering beta- and gamma-cleavage of APP. Neurobiol Aging 30, 1091–1098.

Li, X., Zhang, S., Blander, G., Tse, J. G., Krieger, M., and Guarente, L. (2007). SIRT1 deacetylates and positively regulates the nuclear receptor LXR. Mol Cell 28, 91–106.

Lippa, C. F., Saunders, A. M., Smith, T. W., Swearer, J. M., Drachman, D. A., Ghetti, B., Nee, L., Pulaski-Salo, D., Dickson, D., Robitaille, Y., et al. (1996). Familial and sporadic Alzheimer's disease: neuropathology cannot exclude a final common pathway. Neurology 46, 406–412.

Livak, K. J., and Schmittgen, T. D. (2001). Analysis of relative gene expression data using real-time quantitative PCR and the 2(-Delta Delta C(T)) Method. Methods 25, 402–408.

Loane, D. J., Pocivavsek, A., Moussa, C. E.-H., Thompson, R., Matsuoka, Y., Faden, A. I., Rebeck, G. W., and Burns, M. P. (2009). Amyloid precursor protein secretases as therapeutic targets for traumatic brain injury. Nat Med 15, 377–379.

Lombard, D. B., Alt, F. W., Cheng, H.-L., Bunkenborg, J., Streeper, R. S., Mostoslavsky, R., Kim, J., Yancopoulos, G., Valenzuela, D., Murphy, A., et al. (2007). Mammalian Sir2 homolog SIRT3 regulates global mitochondrial lysine acetylation. MCB 27, 8807–8814.

Lu, F.-P., Lin, K.-P., and Kuo, H.-K. (2009). Diabetes and the risk of multi-system aging phenotypes: a systematic review and meta-analysis. PloS one 4, e4144.

Luchsinger, J. A., Tang, M.-X., Shea, S., and Mayeux, R. (2002). Caloric intake and the risk of Alzheimer disease. Arch Neurol 59, 1258–1263.

Luthi-Carter, R., Taylor, D. M., Pallos, J., Lambert, E., Amore, A., Parker, A., Moffitt, H., Smith, D. L., Runne, H., Gokce, O., et al. (2010). SIRT2 inhibition achieves neuroprotection by decreasing sterol biosynthesis. PNAS 107, 7927–7932.

Maccioni, R. B., Lavados, M., Guillón, M., Mujica, C., Bosch, R., Farías, G., and Fuentes, P. (2006). Anomalously phosphorylated tau and Abeta fragments in the CSF correlates with cognitive impairment in MCI subjects. Neurobiol Aging 27, 237–244.

Macias, M., Dwornik, A., Ziemlinska, E., Fehr, S., Schachner, M., Czarkowska-Bauch, J., and Skup, M. (2007). Locomotor exercise alters expression of pro-brain-derived neurotrophic factor, brain-derived neurotrophic factor and its receptor TrkB in the spinal cord of adult rats. Eur J Neurosci 25, 2425–2444.

Mangialasche, F., Solomon, A., Winblad, B., Mecocci, P., and Kivipelto, M. (2010). Alzheimer's disease: clinical trials and drug development. Lancet Neurol 9, 702–716.

Marambaud, P., Zhao, H., and Davies, P. (2005). Resveratrol promotes clearance of Alzheimer's disease amyloid-beta peptides. J Biol Chem 280, 37377–37382.

Masters, C. L., Simms, G., Weinman, N. A., Multhaup, G., McDonald, B. L., and Beyreuther, K. (1985). Amyloid plaque core protein in Alzheimer disease and Down syndrome. PNAS 82, 4245–4249.

Mattson, M. P., Chan, S. L., and Duan, W. (2002). Modification of brain aging and neurodegenerative disorders by genes, diet, and behavior. Physiol Rev 82, 637–672.

McBurney, M. W., Yang, X., Jardine, K., Hixon, M., Boekelheide, K., Webb, J. R., Lansdorp, P. M., and Lemieux, M. (2003). The mammalian SIR2alpha protein has a role in embryogenesis and gametogenesis. MCB 23, 38–54.

McCord, R. A., Michishita, E., Hong, T., Berber, E., Boxer, L. D., Kusumoto, R., Guan, S., Shi, X., Gozani, O., Burlingame, A. L., et al. (2009). SIRT6 stabilizes DNA-dependent protein kinase at chromatin for DNA double-strand break repair. Aging 1, 109–121.

McGeer, P. L., and McGeer, E. G. (1996). Anti-inflammatory drugs in the fight against Alzheimer's disease. Ann N Y Acad Sci 777, 213–220.

McKenzie, K. J., McLellan, D. R., Gentleman, S. M., Maxwell, W. L., Gennarelli, T. A., and Graham, D. I. (1996). Is beta-APP a marker of axonal damage in short-surviving head injury? Acta Neuropathol 92, 608–613.

McKhann, G., Drachman, D., Folstein, M., Katzman, R., Price, D., and Stadlan, E. M. (1984). Clinical diagnosis of Alzheimer's disease: report of the NINCDS-ADRDA Work Group under the auspices of Department of Health and Human Services Task Force on Alzheimer's Disease. Neurology 34, 939–944.

Menéndez, M. (2005). Down syndrome, Alzheimer's disease and seizures. Brain Dev 27, 246–252.

Michan, S., Li, Y., Chou, M. M.-H., Parrella, E., Ge, H., Long, J. M., Allard, J. S., Lewis, K., Miller, M., Xu, W., et al. (2010). SIRT1 Is Essential for Normal Cognitive Function and Synaptic Plasticity. J Neurosci 30, 9695–9707.

Michan, S., and Sinclair, D. (2007). Sirtuins in mammals: insights into their biological function. Biochem J 404, 1–13.

Michishita, E., McCord, R. A., Berber, E., Kioi, M., Padilla-Nash, H., Damian, M., Cheung, P., Kusumoto, R., Kawahara, T. L. A., Barrett, J. C., et al. (2008). SIRT6 is a histone H3 lysine 9 deacetylase that modulates telomeric chromatin. Nature 452, 492–496.

Michishita, E., Park, J. Y., Burneskis, J. M., Barrett, J. C., and Horikawa, I. (2005). Evolutionarily conserved and nonconserved cellular localizations and functions of human SIRT proteins. Mol Biol Cell 16, 4623–4635.

Milne, J. C., Lambert, P. D., Schenk, S., Carney, D. P., Smith, J. J., Gagne, D. J., Jin, L., Boss, O., Perni, R. B., Vu, C. B., et al. (2007). Small molecule activators of SIRT1 as therapeutics for the treatment of type 2 diabetes. Nature 450, 712–716.

Min, S.-W., Cho, S.-H., Zhou, Y., Schroeder, S., Haroutunian, V., Seeley, W. W., Huang, E. J., Shen, Y., Masliah, E., Mukherjee, C., et al. (2010). Acetylation of Tau Inhibits Its Degradation and Contributes to Tauopathy. Neuron 67, 953–966.

Miners J.-S., Baig S., Palmer J., Palmer L.-E., Kehoe P.-G., Love S. (2008). Abeta-degrading enzymes in Alzheimer's disease. Brain Pathol 18, 240-52.

Mirochnic, S., Wolf, S., Staufenbiel, M., and Kempermann, G. (2009). Age effects on the regulation of adult hippocampal neurogenesis by physical activity and environmental enrichment in the APP23 mouse model of Alzheimer disease. Hippocampus 19, 1008–1018.

de la Monte, S. M., and Wands, J. R. (2008). Alzheimer's disease is type 3 diabetes-evidence reviewed. J Diab Sci Tech 2, 1101–1113.

Morgan, A. R., Turic, D., Jehu, L., Hamilton, G., Hollingworth, P., Moskvina, V., Jones, L., Lovestone, S., Brayne, C., Rubinsztein, D. C., et al. (2007). Association studies of 23 positional/functional candidate genes on chromosome 10 in late-onset Alzheimer's disease. Am J Med Genet 144, 762–770.

Morris, K. C., Lin, H. W., Thompson, J. W., and Perez-Pinzon, M. A. (2011). Pathways for ischemic cytoprotection: role of sirtuins in caloric restriction, resveratrol, and ischemic preconditioning. J Cer Blood Flow Metab 31, 1003–1019.

Morris, R., and Mucke, L. (2006). Alzheimer's disease: A needle from the haystack. Nature 440, 284–285.

Mostoslavsky, R., Chua, K. F., Lombard, D. B., Pang, W. W., Fischer, M. R., Gellon, L., Liu, P., Mostoslavsky, G., Franco, S., Murphy, M. M., et al. (2006). Genomic instability and aging-like phenotype in the absence of mammalian SIRT6. Cell 124, 315–329.

Mukherjee, S., Dudley, J. I., and Das, D. K. (2010). Dose-dependency of resveratrol in providing health benefits. Dose Response 8, 478–500.

Mullan, M., Crawford, F., Axelman, K., Houlden, H., Lilius, L., Winblad, B., and Lannfelt, L. (1992). A pathogenic mutation for probable Alzheimer's disease in the APP gene at the N-terminus of beta-amyloid. Nat Genet 1, 345–347.

Murray, I. V. J., Proza, J. F., Sohrabji, F., and Lawler, J. M. (2011). Vascular and metabolic dysfunction in Alzheimer's disease: a review. Exp Biol Med 236, 772–782.

Möller, H. J., and Graeber, M. B. (1998). The case described by Alois Alzheimer in 1911. Historical and conceptual perspectives based on the clinical record and neurohistological sections. Eur Arch Psy Clin Neurosci 248, 111–122.

Naj, A. C., Jun, G., Beecham, G. W., Wang, L.-S., Vardarajan, B. N., Buros, J., Gallins, P. J., Buxbaum, J. D., Jarvik, G. P., Crane, P. K., et al. (2011). Common variants at MS4A4/MS4A6E, CD2AP, CD33 and EPHA1 are associated with late-onset Alzheimer's disease. Nat Genet 43, 436–441.

Nakagawa, T., Lomb, D. J., Haigis, M. C., and Guarente, L. (2009). SIRT5 Deacetylates carbamoyl phosphate synthetase 1 and regulates the urea cycle. Cell 137, 560–570.

Napper, A. D., Hixon, J., McDonagh, T., Keavey, K., Pons, J.-F., Barker, J., Yau, W. T., Amouzegh, P., Flegg, A., Hamelin, E., et al. (2005). Discovery of indoles as potent and selective inhibitors of the deacetylase SIRT1. J Med Chem 48, 8045–8054.

Nasrin, N., Kaushik, V. K., Fortier, E., Wall, D., Pearson, K. J., de Cabo, R., and Bordone, L. (2009). JNK1 phosphorylates SIRT1 and promotes its enzymatic activity. PLoS One 4, e8414.

Nasrin, N., Wu, X., Fortier, E., Feng, Y., Bare', O. C., Chen, S., Ren, X., Wu, Z., Streeper, R. S., and Bordone, L. (2010). SIRT4 regulates fatty acid oxidation and mitochondrial gene expression in liver and muscle cells. J Biol Chem 285, 31995–32002.

Neeper, S. A., Gómez-Pinilla, F., Choi, J., and Cotman, C. W. (1996). Physical activity increases mRNA for brain-derived neurotrophic factor and nerve growth factor in rat brain. Brain Res 726, 49–56.

Nilsberth, C., Westlind-Danielsson, A., Eckman, C. B., Condron, M. M., Axelman, K., Forsell, C., Stenh, C., Luthman, J., Teplow, D. B., Younkin, S. G., et al. (2001). The "Arctic" APP mutation (E693G) causes Alzheimer's disease by enhanced Abeta protofibril formation. Nat Neurosci 4, 887–893.

Nithianantharajah, J., and Hannan, A. J. (2006). Enriched environments, experience-dependent plasticity and disorders of the nervous system. Nat Rev Neurosci 7, 697–709.

North, B. J., and Verdin, E. (2007). Interphase nucleo-cytoplasmic shuttling and localization of SIRT2 during mitosis. PLoS One 2, e784.

North, B. J., and Verdin, E. (2004). Sirtuins: Sir2-related NAD-dependent protein deacetylases. Genome Biol 5, 224.

Nunomura, A., Castellani, R. J., Zhu, X., Moreira, P. I., Perry, G., and Smith, M. A. (2006). Involvement of oxidative stress in Alzheimer disease. J Neuropathol Exp Neurol 65, 631–641.

Oddo, S., Caccamo, A., Shepherd, J. D., Murphy, M. P., Golde, T. E., Kayed, R., Metherate, R., Mattson, M. P., Akbari, Y., and LaFerla, F. M. (2003). Triple-transgenic model of Alzheimer's disease with plaques and tangles: intracellular Abeta and synaptic dysfunction. Neuron 39, 409–421.

Ogoh, S., and Ainslie, P. N. (2009). Regulatory mechanisms of cerebral blood flow during exercise: new concepts. Ex Sport Sci Rev 37, 123–129.

Ogura, M., Nakamura, Y., Tanaka, D., Zhuang, X., Fujita, Y., Obara, A., Hamasaki, A., Hosokawa, M., and Inagaki, N. (2010). Overexpression of SIRT5 confirms its involvement in deacetylation and activation of carbamoyl phosphate synthetase 1. Biochem Biophys Res Comm 393, 73–78.

Olson, M. I., and Shaw, C. M. (1969). Presenile dementia and Alzheimer's disease in mongolism. Brain 92, 147–156.

Outeiro, T. F., Kontopoulos, E., Altmann, S. M., Kufareva, I., Strathearn, K. E., Amore, A. M., Volk, C. B., Maxwell, M. M., Rochet, J.-C., McLean, P. J., et al. (2007). Sirtuin 2 inhibitors rescue alpha-synuclein-mediated toxicity in models of Parkinson's disease. Science 317, 516–519.

Pandithage, R., Lilischkis, R., Harting, K., Wolf, A., Jedamzik, B., Lüscher-Firzlaff, J., Vervoorts, J., Lasonder, E., Kremmer, E., Knöll, B., et al. (2008). The regulation of SIRT2 function by cyclin-dependent kinases affects cell motility. J Cell Biol 180, 915–929.

Parker, J. A., Arango, M., Abderrahmane, S., Lambert, E., Tourette, C., Catoire, H., and Néri, C. (2005). Resveratrol rescues mutant polyglutamine cytotoxicity in nematode and mammalian neurons. Nat Genet 37, 349–350.

Pearson, K. J., Baur, J. A., Lewis, K. N., Peshkin, L., Price, N. L., Labinskyy, N., Swindell, W. R., Kamara, D., Minor, R. K., Perez, E., et al. (2008). Resveratrol delays age-related deterioration and mimics transcriptional aspects of dietary restriction without extending life span. Cell Metab 8, 157–168.

Pendlebury, S. T., and Rothwell, P. M. (2009). Prevalence, incidence, and factors associated with pre-stroke and post-stroke dementia: a systematic review and meta-analysis. Lancet Neurol 8, 1006–1018.

Peng, S., Garzon, D. J., Marchese, M., Klein, W., Ginsberg, S. D., Francis, B. M., Mount, H. T. J., Mufson, E. J., Salehi, A., and Fahnestock, M. (2009). Decreased brain-derived neurotrophic factor depends on amyloid aggregation state in transgenic mouse models of Alzheimer's disease. J Neurosci 29, 9321–9329.

Petersen, R. C. (2004). Mild cognitive impairment as a diagnostic entity. J Int Med 256, 183–194.

Peterson, C., Ratan, R. R., Shelanski, M. L., and Goldman, J. E. (1986). Cytosolic free calcium and cell spreading decrease in fibroblasts from aged and Alzheimer donors. PNAS 83, 7999–8001.

Pfister, J. A., Ma, C., Morrison, B. E., and D'Mello, S. R. (2008). Opposing effects of sirtuins on neuronal survival: SIRT1-mediated neuroprotection is independent of its deacetylase activity. PLoS One 3, e4090.

Pfluger, P. T., Herranz, D., Velasco-Miguel, S., Serrano, M., and Tschöp, M. H. (2008). Sirt1 protects against high-fat diet-induced metabolic damage. PNAS 105, 9793–9798.

Picard, F., Kurtev, M., Chung, N., Topark-Ngarm, A., Senawong, T., Machado De Oliveira, R., Leid, M., McBurney, M. W., and Guarente, L. (2004). Sirt1 promotes fat mobilization in white adipocytes by repressing PPAR-gamma. Nature 429, 771–776.

Poirier, J., Davignon, J., Bouthillier, D., Kogan, S., Bertrand, P., and Gauthier, S. (1993). Apolipoprotein E polymorphism and Alzheimer's disease. Lancet 342, 697–699.

Ponugoti, B., Kim, D.-H., Xiao, Z., Smith, Z., Miao, J., Zang, M., Wu, S.-Y., Chiang, C.-M., Veenstra, T. D., and Kemper, J. K. (2010). SIRT1 deacetylates and inhibits SREBP-1C activity in regulation of hepatic lipid metabolism. J Biol Chem 285, 33959–33970.

van Praag, H., Kempermann, G., and Gage, F. H. (2000). Neural consequences of environmental enrichment. Nat Rev Neurosci 1, 191–198.

Purushotham, A., Schug, T. T., Xu, Q., Surapureddi, S., Guo, X., and Li, X. (2009). Hepatocyte-specific deletion of SIRT1 alters fatty acid metabolism and results in hepatic steatosis and inflammation. Cell Metab 9, 327–338.

Pyo, J.-O., Nah, J., Kim, H.-J., Lee, H.-J., Heo, J., Lee, H., and Jung, Y.-K. (2008). Compensatory activation of ERK1/2 in Atg5-deficient mouse embryo fibroblasts suppresses oxidative stress-induced cell death. Autophagy 4, 315–321.

Qiao, L., and Shao, J. (2006). SIRT1 regulates adiponectin gene expression through Foxo1-C/enhancer-binding protein alpha transcriptional complex. J Biol Chem 281, 39915–39924.

Qin, W., Chachich, M., Lane, M., Roth, G., Bryant, M., de Cabo, R., Ottinger, M. A., Mattison, J., Ingram, D., Gandy, S., et al. (2006a). Calorie restriction attenuates Alzheimer's disease type brain amyloidosis in Squirrel monkeys (Saimiri sciureus). JAD 10, 417–422.

Qin, W., Yang, T., Ho, L., Zhao, Z., Wang, J., Chen, L., Zhao, W., Thiyagarajan, M., MacGrogan, D., Rodgers, J. T., et al. (2006b). Neuronal SIRT1 activation as a novel mechanism underlying the prevention of Alzheimer disease amyloid neuropathology by calorie restriction. J Biol Chem 281, 21745–21754.

Qin, W., Zhao, W., Ho, L., Wang, J., Walsh, K., Gandy, S., and Pasinetti, G. M. (2008). Regulation of forkhead transcription factor FoxO3a contributes to calorie restriction-induced prevention of Alzheimer's disease-type amyloid neuropathology and spatial memory deterioration. Ann N Y Acad Sci 1147, 335–347.

Qiu, C., Winblad, B., and Fratiglioni, L. (2005). The age-dependent relation of blood pressure to cognitive function and dementia. Lancet Neurol 4, 487–499.

Quistorff, B., Secher, N. H., and Van Lieshout, J. J. (2008). Lactate fuels the human brain during exercise. FASEB J 22, 3443–3449.

Radak, Z., Hart, N., Sarga, L., Koltai, E., Atalay, M., Ohno, H., and Boldogh, I. (2010). Exercise plays a preventive role against Alzheimer's disease. JAD 20, 777–783.

Radák, Z., Kaneko, T., Tahara, S., Nakamoto, H., Pucsok, J., Sasvári, M., Nyakas, C., and Goto, S. (2001). Regular exercise improves cognitive function and decreases oxidative damage in rat brain. Neurochem Int 38, 17–23.

Raff, M. C., Whitmore, A. V., and Finn, J. T. (2002). Axonal self-destruction and neurodegeneration. Science 296, 868–871.

Rasbach, K. A., and Schnellmann, R. G. (2008). Isoflavones promote mitochondrial biogenesis. JPET 325, 536–543.

Rego, A. C., and Oliveira, C. R. (2003). Mitochondrial dysfunction and reactive oxygen species in excitotoxicity and apoptosis: implications for the pathogenesis of neurodegenerative diseases. Neurochem Res 28, 1563–1574.

Reiling, E., van Vliet-Ostaptchouk, J. V., van 't Riet, E., van Haeften, T. W., Arp, P. A., Hansen, T., Kremer, D., Groenewoud, M. J., van Hove, E. C., Romijn, J. A., et al. (2009). Genetic association analysis of 13 nuclear-encoded mitochondrial candidate genes with type II diabetes mellitus: the DAMAGE study. EJHG 17, 1056–1062.

Rimm, E. B., Williams, P., Fosher, K., Criqui, M., and Stampfer, M. J. (1999). Moderate alcohol intake and lower risk of coronary heart disease: meta-analysis of effects on lipids and haemostatic factors. BMJ 319, 1523–1528.

Rine, J., and Herskowitz, I. (1987). Four genes responsible for a position effect on expression from HML and HMR in Saccharomyces cerevisiae. Genetics 116, 9–22.

Rivière, C., Richard, T., Quentin, L., Krisa, S., Mérillon, J.-M., and Monti, J.-P. (2007). Inhibitory activity of stilbenes on Alzheimer's beta-amyloid fibrils in vitro. Bio Med Chem 15, 1160–1167.

Rizzardini, M., Lupi, M., Bernasconi, S., Mangolini, A., and Cantoni, L. (2003). Mitochondrial dysfunction and death in motor neurons exposed to the glutathione-depleting agent ethacrynic acid. J Neurol Sci 207, 51–58.

Rodgers, J. T., Lerin, C., Haas, W., Gygi, S. P., Spiegelman, B. M., and Puigserver, P. (2005). Nutrient control of glucose homeostasis through a complex of PGC-1alpha and SIRT1. Nature 434, 113–118.

Rogina, B., and Helfand, S. L. (2004). Sir2 mediates longevity in the fly through a pathway related to calorie restriction. PNAS 101, 15998–16003.

Rose, G., Dato, S., Altomare, K., Bellizzi, D., Garasto, S., Greco, V., Passarino, G., Feraco, E., Mari, V., Barbi, C., et al. (2003). Variability of the SIRT3 gene, human silent information regulator Sir2 homologue, and survivorship in the elderly. Exp Gerontol 38, 1065–1070.

Rountree, S. D., Chan, W., Pavlik, V. N., Darby, E. J., Siddiqui, S., and Doody, R. S. (2009). Persistent treatment with cholinesterase inhibitors and/or memantine slows clinical progression of Alzheimer disease. Alzheimers Res Ther 1, 7.

Salminen, A., Huuskonen, J., Ojala, J., Kauppinen, A., Kaarniranta, K., and Suuronen, T. (2008). Activation of innate immunity system during aging: NF-kB signaling is the molecular culprit of inflamm-aging. Ageing Res Rev 7, 83–105.

Salmona, M., Morbin, M., Massignan, T., Colombo, L., Mazzoleni, G., Capobianco, R., Diomede, L., Thaler, F., Mollica, L., Musco, G., et al. (2003). Structural properties of Gerstmann-Straussler-Scheinker disease amyloid protein. J Biol Chem 278, 48146–48153.

Sasaki, T., Maier, B., Koclega, K. D., Chruszcz, M., Gluba, W., Stukenberg, P. T., Minor, W., and Scrable, H. (2008). Phosphorylation regulates SIRT1 function. PLoS One 3, e4020.

Saunders, A. M., Strittmatter, W. J., Schmechel, D., George-Hyslop, P. H., Pericak-Vance, M. A., Joo, S. H., Rosi, B. L., Gusella, J. F., Crapper-MacLachlan, D. R., and Alberts, M. J. (1993). Association of apolipoprotein E allele epsilon 4 with late-onset familial and sporadic Alzheimer's disease. Neurology 43, 1467–1472.

Sauve, A. A. (2010). Sirtuin chemical mechanisms. BBA 1804, 1591–1603.

Savaskan, E., Olivieri, G., Meier, F., Seifritz, E., Wirz-Justice, A., and Müller-Spahn, F. (2003). Red wine ingredient resveratrol protects from beta-amyloid neurotoxicity. Gerontology 49, 380–383.

Scacchi, R., Gambina, G., Ruggeri, M., Martini, M. C., Ferrari, G., Silvestri, M., Schiavon, R., and Corbo, R. M. (1999). Plasma levels of apolipoprotein E and genetic markers in elderly patients with Alzheimer's disease. Neurosci Lett 259, 33–36.

Scarmeas, N., Stern, Y., Tang, M.-X., Mayeux, R., and Luchsinger, J. A. (2006). Mediterranean diet and risk for Alzheimer's disease. Ann Neurol 59, 912–921.

Schaeffer, E. L., Figueiro, M., and Gattaz, W. F. (2011). Insights into Alzheimer disease pathogenesis from studies in transgenic animal models. Clinics 66, 45–54.

Scheuner, D., Eckman, C., Jensen, M., Song, X., Citron, M., Suzuki, N., Bird, T. D., Hardy, J., Hutton, M., Kukull, W., et al. (1996). Secreted amyloid beta-protein similar to that in the senile plaques of Alzheimer's disease is increased in vivo by the presenilin 1 and 2 and APP mutations linked to familial Alzheimer's disease. Nat Med 2, 864–870.

Schlicker, C., Gertz, M., Papatheodorou, P., Kachholz, B., Becker, C. F. W., and Steegborn, C. (2008). Substrates and regulation mechanisms for the human mitochondrial sirtuins Sirt3 and Sirt5. J Mol Biol 382, 790–801.

Schork, N. J., Murray, S. S., Frazer, K. A., and Topol, E. J. (2009). Common vs. rare allele hypotheses for complex diseases. Curr Opin Genet Dev 19, 212–219.

Schroeder, J. E., Richardson, J. C., and Virley, D. J. (2010). Dietary manipulation and caloric restriction in the development of mouse models relevant to neurological diseases. BBA 1802, 840–846.

Schäfer, S., Wirths, O., Multhaup, G., and Bayer, T. A. (2007). Gender dependent APP processing in a transgenic mouse model of Alzheimer's disease. J Neural Transm 114, 387–394.

Seglen, P. O., and Gordon, P. B. (1982). 3-Methyladenine: specific inhibitor of autophagic/lysosomal protein degradation in isolated rat hepatocytes. PNAS 79, 1889–1892.

Seo, J.-S., Moon, M.-H., Jeong, J.-K., Seol, J.-W., Lee, Y.-J., Park, B.-H., and Park, S.-Y. (2010). SIRT1, a histone deacetylase, regulates prion protein-induced neuronal cell death. Neurobiol Aging.

Sequeira, J., Boily, G., Bazinet, S., Saliba, S., He, X., Jardine, K., Kennedy, C., Staines, W., Rousseaux, C., Mueller, R., et al. (2008). sirt1-null mice develop an autoimmune-like condition. Exp Cell Res 314, 3069–3074.

Sherman, J. M., Stone, E. M., Freeman-Cook, L. L., Brachmann, C. B., Boeke, J. D., and Pillus, L. (1999). The conserved core of a human SIR2 homologue functions in yeast silencing. Mol Biol Cell 10, 3045–3059.

Sherrington, R., Rogaev, E. I., Liang, Y., Rogaeva, E. A., Levesque, G., Ikeda, M., Chi, H., Lin, C., Li, G., Holman, K., et al. (1995). Cloning of a gene bearing missense mutations in early-onset familial Alzheimer's disease. Nature 375, 754–760.

Shi, T., Wang, F., Stieren, E., and Tong, Q. (2005). SIRT3, a mitochondrial sirtuin deacetylase, regulates mitochondrial function and thermogenesis in brown adipocytes. J Biol Chem 280, 13560–13567.

Sinclair, D. A., and Guarente, L. (2006). Unlocking the secrets of longevity genes. Sci Am 294, 48–51, 54–57.

Smith, E. E., and Greenberg, S. M. (2009). Beta-amyloid, blood vessels, and brain function. Stroke 40, 2601–2606.

Smith, J. S., and Boeke, J. D. (1997). An unusual form of transcriptional silencing in yeast ribosomal DNA. Genes Dev 11, 241–254.

Song, R., Xu, W., Chen, Y., Li, Z., Zeng, Y., and Fu, Y. (2011). The expression of Sirtuins 1 and 4 in peripheral blood leukocytes from patients with type 2 diabetes. EJH 55, e10.

Sorbi, S., Nacmias, B., Forleo, P., Latorraca, S., Gobbini, I., Bracco, L., Piacentini, S., and Amaducci, L. (1994). ApoE allele frequencies in Italian sporadic and familial Alzheimer's disease. Neurosci Lett 177, 100–102.

Steiner, J. L., Murphy, E. A., McClellan, J. L., Carmichael, M. D., and Davis, J. M. (2011). Exercise Training Increases Mitochondrial Biogenesis in the Brain. J Appl Physiol. Epub ahead of print.

Stern, Y., Gurland, B., Tatemichi, T. K., Tang, M. X., Wilder, D., and Mayeux, R. (1994). Influence of education and occupation on the incidence of Alzheimer's disease. JAMA 271, 1004–1010.

Stram, D. O. (2004). Tag SNP selection for association studies. Genet Epidemiol 27, 365–374.

Stranger, B. E., Forrest, M. S., Clark, A. G., Minichiello, M. J., Deutsch, S., Lyle, R., Hunt, S., Kahl, B., Antonarakis, S. E., Tavaré, S., et al. (2005). Genome-wide associations of gene expression variation in humans. PLoS genetics 1, e78.

Sturchler-Pierrat, C., Abramowski, D., Duke, M., Wiederhold, K. H., Mistl, C., Rothacher, S., Ledermann, B., Bürki, K., Frey, P., Paganetti, P. A., et al. (1997). Two amyloid precursor protein transgenic mouse models with Alzheimer disease-like pathology. PNAS 94, 13287–13292.

Sullivan, P. G., Rabchevsky, A. G., Waldmeier, P. C., and Springer, J. E. (2005). Mitochondrial permeability transition in CNS trauma: cause or effect of neuronal cell death? J Neurosci Res 79, 231–239.

Sundaresan, N. R., Gupta, M., Kim, G., Rajamohan, S. B., Isbatan, A., and Gupta, M. P. (2009). Sirt3 blocks the cardiac hypertrophic response by augmenting Foxo3a-dependent antioxidant defense mechanisms in mice. J Clin Invest 119, 2758–2771.

Sundström, A., Nilsson, L.-G., Cruts, M., Adolfsson, R., Van Broeckhoven, C., and Nyberg, L. (2007). Increased risk of dementia following mild head injury for carriers but not for non-carriers of the APOE epsilon4 allele. IPA 19, 159–165.

Suwa, M., Nakano, H., Radak, Z., and Kumagai, S. (2008). Endurance exercise increases the SIRT1 and peroxisome proliferator-activated receptor gamma coactivator-1alpha protein expressions in rat skeletal muscle. Metabolism 57, 986–998.

Suzuki, T., Asaba, T., Imai, E., Tsumoto, H., Nakagawa, H., and Miyata, N. (2009). Identification of a cell-active non-peptide sirtuin inhibitor containing N-thioacetyl lysine. Bio Med Chem Lett 19, 5670–5672.

Takasugi, N., Tomita, T., Hayashi, I., Tsuruoka, M., Niimura, M., Takahashi, Y., Thinakaran, G., and Iwatsubo, T. (2003). The role of presenilin cofactors in the gamma-secretase complex. Nature 422, 438–441.

Tang, B. L., and Chua, C. E. L. (2008). SIRT2, tubulin deacetylation, and oligodendroglia differentiation. Cell Mot. Cytoskeleton 65, 179–182.

Tanner, K. G., Landry, J., Sternglanz, R., and Denu, J. M. (2000). Silent information regulator 2 family of NAD- dependent histone/protein deacetylases generates a unique product, 1-O-acetyl-ADP-ribose. PNAS 97, 14178–14182.

Tanno, M., Sakamoto, J., Miura, T., Shimamoto, K., and Horio, Y. (2007). Nucleocytoplasmic shuttling of the NAD+-dependent histone deacetylase SIRT1. J Biol Chem 282, 6823–6832.

Tariot, P. N., Farlow, M. R., Grossberg, G. T., Graham, S. M., McDonald, S., and Gergel, I. (2004). Memantine treatment in patients with moderate to severe Alzheimer disease already receiving donepezil: a randomized controlled trial. JAMA 291, 317–324.

Terry, A. V., and Buccafusco, J. J. (2003). The cholinergic hypothesis of age and Alzheimer's disease-related cognitive deficits: recent challenges and their implications for novel drug development. JPET 306, 821–827.

Tissenbaum, H. A., and Guarente, L. (2001). Increased dosage of a sir-2 gene extends lifespan in Caenorhabditis elegans. Nature 410, 227–230.

Tomiyama, T., Nagata, T., Shimada, H., Teraoka, R., Fukushima, A., Kanemitsu, H., Takuma, H., Kuwano, R., Imagawa, M., Ataka, S., et al. (2008). A new amyloid beta variant favoring oligomerization in Alzheimer's-type dementia. Ann Neurol 63, 377–387.

Tsang, A. W., and Escalante-Semerena, J. C. (1998). CobB, a new member of the SIR2 family of eucaryotic regulatory proteins, is required to compensate for the lack of nicotinate mononucleotide:5,6-dimethylbenzimidazole phosphoribosyltransferase activity in cobT mutants during cobalamin biosynthesis in Salm. J Biol Chem 273, 31788–31794.

Vakhrusheva, O., Braeuer, D., Liu, Z., Braun, T., and Bober, E. (2008a). Sirt7-dependent inhibition of cell growth and proliferation might be instrumental to mediate tissue integrity during aging. J Physiol Parmacol 59 , 201–212.

Vakhrusheva, O., Smolka, C., Gajawada, P., Kostin, S., Boettger, T., Kubin, T., Braun, T., and Bober, E. (2008b). Sirt7 increases stress resistance of cardiomyocytes and prevents apoptosis and inflammatory cardiomyopathy in mice. Circ Res 102, 703–710.

Vaquero, A., Scher, M. B., Lee, D. H., Sutton, A., Cheng, H.-L., Alt, F. W., Serrano, L., Sternglanz, R., and Reinberg, D. (2006). SirT2 is a histone deacetylase with preference for histone H4 Lys 16 during mitosis. Genes Dev 20, 1256–1261.

Vaquero, A., Scher, M., Lee, D., Erdjument-Bromage, H., Tempst, P., and Reinberg, D. (2004). Human SirT1 interacts with histone H1 and promotes formation of facultative heterochromatin. Mol Cell 16, 93–105.

Vinciguerra, M., Fulco, M., Ladurner, A., Sartorelli, V., and Rosenthal, N. (2010). SirT1 in muscle physiology and disease: lessons from mouse models. Dis Model Mech 3, 298–303.

Visser, P. J., Scheltens, P., and Verhey, F. R. J. (2005). Do MCI criteria in drug trials accurately identify subjects with predementia Alzheimer's disease? J Neurol Neurosurg Psychiatry 76, 1348–1354.

Wang, D., Hang, T., Wu, C., and Liu, W. (2005a). Identification of the major metabolites of resveratrol in rat urine by HPLC-MS/MS. J chromatogr B Analyt technol biomed life sci 829, 97–106.

Wang, F., Nguyen, M., Qin, F. X.-F., and Tong, Q. (2007). SIRT2 deacetylates FOXO3a in response to oxidative stress and caloric restriction. Aging cell 6, 505–514.

Wang, J., Ho, L., Qin, W., Rocher, A. B., Seror, I., Humala, N., Maniar, K., Dolios, G., Wang, R., Hof, P. R., et al. (2005b). Caloric restriction attenuates beta-amyloid neuropathology in a mouse model of Alzheimer's disease. FASEB J 19, 659–661.

Wang, J., Tanila, H., Puoliväli, J., Kadish, I., and van Groen, T. (2003). Gender differences in the amount and deposition of amyloidbeta in APPswe and PS1 double transgenic mice. Neurobiol Dis 14, 318–327.

Wang, L., Li, B., Lu, X., Zhao, Q., Li, Y., Ge, D., Li, H., Zhang, P., Chen, S., Chen, R., et al. (2008). A functional intronic variant in the tyrosine hydroxylase (TH) gene confers risk of essential hypertension in the Northern Chinese Han population. Clin Sci 115, 151–158.

Weih, M., Wiltfang, J., and Kornhuber, J. (2007). Non-pharmacologic prevention of Alzheimer's disease: nutritional and life-style risk factors. J Neural Transm 114, 1187–1197.

Weindruch, R. (1996). The retardation of aging by caloric restriction: studies in rodents and primates. Toxicol Pathol 24, 742–745.

Weingarten, M. D., Lockwood, A. H., Hwo, S. Y., and Kirschner, M. W. (1975). A protein factor essential for microtubule assembly. PNAS 72, 1858–1862.

Wen, P. H., Hof, P. R., Chen, X., Gluck, K., Austin, G., Younkin, S. G., Younkin, L. H., DeGasperi, R., Gama Sosa, M. A., Robakis, N. K., et al. (2004). The presenilin-1 familial Alzheimer disease mutant P117L impairs neurogenesis in the hippocampus of adult mice. Exp Neurol 188, 224–237.

Westphal, C. H., Dipp, M. A., and Guarente, L. (2007). A therapeutic role for sirtuins in diseases of aging? TIBS 32, 555–560.

Weuve, J., Kang, J. H., Manson, J. E., Breteler, M. M. B., Ware, J. H., and Grodstein, F. (2004). Physical activity, including walking, and cognitive function in older women. JAMA 292, 1454–1461.

Weyrich, P., Machicao, F., Reinhardt, J., Machann, J., Schick, F., Tschritter, O., Stefan, N., Fritsche, A., and Häring, H.-U. (2008). SIRT1 genetic variants associate with the metabolic response of Caucasians to a controlled lifestyle intervention--the TULIP Study. BMC med genet 9, 100.

Wilcock, G. K. (2003). Memantine for the treatment of dementia. Lancet Neurol 2, 503–505.

Wilson, R. S., Bennett, D. A., Bienias, J. L., Aggarwal, N. T., Mendes De Leon, C. F., Morris, M. C., Schneider, J. A., and Evans, D. A. (2002). Cognitive activity and incident AD in a population-based sample of older persons. Neurology 59, 1910–1914.

Wolf, S. A., Kronenberg, G., Lehmann, K., Blankenship, A., Overall, R., Staufenbiel, M., and Kempermann, G. (2006). Cognitive and physical activity differently modulate disease progression in the amyloid precursor protein (APP)-23 model of Alzheimer's disease. Biol Psychiatry 60, 1314–1323.

World Health Organization (2003). The World Health Report 2003: Shaping the Future (Geneva).

Yang, H., Yang, T., Baur, J. A., Perez, E., Matsui, T., Carmona, J. J., Lamming, D. W., Souza-Pinto, N. C., Bohr, V. A., Rosenzweig, A., et al. (2007a). Nutrient-sensitive mitochondrial NAD+ levels dictate cell survival. Cell 130, 1095–1107.

Yang, Y., Fu, W., Chen, J., Olashaw, N., Zhang, X., Nicosia, S. V., Bhalla, K., and Bai, W. (2007b). SIRT1 sumoylation regulates its deacetylase activity and cellular response to genotoxic stress. Nat Cell Biol 9, 1253–1262.

Yeung, F., Hoberg, J. E., Ramsey, C. S., Keller, M. D., Jones, D. R., Frye, R. A., and Mayo, M. W. (2004). Modulation of NF-kappaB-dependent transcription and cell survival by the SIRT1 deacetylase. EMBO J 23, 2369–2380.

Yu, W., Fu, Y.-C., Zhou, X.-H., Chen, C.-J., Wang, X., Lin, R.-B., and Wang, W. (2009). Effects of resveratrol on H(2)O(2)-induced apoptosis and expression of SIRTs in H9c2 cells. J Cell Biochem 107, 741–747.

Yuan, Z., Zhang, X., Sengupta, N., Lane, W. S., and Seto, E. (2007). SIRT1 regulates the function of the Nijmegen breakage syndrome protein. Mol Cell 27, 149–162.

Zakhary, S. M., Ayubcha, D., Dileo, J. N., Jose, R., Leheste, J. R., Horowitz, J. M., and Torres, G. (2010). Distribution analysis of deacetylase SIRT1 in rodent and human nervous systems. Anat Rec 293, 1024–1032.

Zhang, Y.-W., Thompson, R., Zhang, H., and Xu, H. (2011). APP Processing in Alzheimer's Disease. Mol Brain 4, 3.

Zheng, H., and Koo, E. H. (2006). The amyloid precursor protein: beyond amyloid. Mol Neurodeg 1, 5.

Zhong, L., D'Urso, A., Toiber, D., Sebastian, C., Henry, R. E., Vadysirisack, D. D., Guimaraes, A., Marinelli, B., Wikstrom, J. D., Nir, T., et al. (2010). The histone deacetylase Sirt6 regulates glucose homeostasis via Hif1alpha. Cell 140, 280–293.

Zillikens, M. C., van Meurs, J. B. J., Rivadeneira, F., Amin, N., Hofman, A., Oostra, B. A., Sijbrands, E. J. G., Witteman, J. C. M., Pols, H. A. P., van Duijn, C. M., et al. (2009a). SIRT1 genetic variation is related to BMI and risk of obesity. Diabetes 58, 2828–2834.

Zillikens, M. C., van Meurs, J. B. J., Sijbrands, E. J. G., Rivadeneira, F., Dehghan, A., van Leeuwen, J. P. T. M., Hofman, A., van Duijn, C. M., Witteman, J. C. M., Uitterlinden, A. G., et al. (2009b). SIRT1 genetic variation and mortality in type 2 diabetes: interaction with smoking and dietary niacin. Free Rad Biol Med 46, 836–841.